Contribution to the development of new bio-based thermal insulation materials made from vegetal pith and natural binders: hygrothermal performance, fire reaction and mould growth resistance

by

MARIANA PALUMBO

A thesis submitted to
Universitat Politècnica de Catalunya
In partial fulfilment of the requirements for the degree of
Doctor of Philosophy in Architecture

Thesis supervisors:
ANA M. LACASTA
JAUME AVELLANEDA

Architectural, Building construction and urbanism Technology Program
DEPARTMENT OF APPLIED PHYSICS

Barcelona, 2015

To my family

ABSTRACT

The building sector is moving towards new approaches to energy-efficient design, which include not only the improvement of the thermal performance of the building envelope but also the reduction in the embodied energy of the materials. The development of bio-based thermal insulation materials contribute to such approaches, as their use may result in a reduction of both energy demand and embodied energy, together with other beneficial environmental aspects such as the reduction in the depletion of non-renewable resources and in waste generation.

Currently, there are several commercial examples of bio-based materials, which are mostly based on industrial fibres (flax, hemp, kenaf, etc.), wood or sheep's wool. The use of food-crop by-products is less common, but might be an interesting alternative for some countries such as Spain, where industrial fibre production is very marginal. These by-products, especially cereal straw, have been used and are increasingly being used in building as reinforcement in composites, deck finishes, interior partitions or structural closures. In this research their use in building thermal insulation is proposed.

The first part of this research, is aimed at exploring the possibility of using the by-products available in Spain for the development of rigid thermal insulation boards. The availability of the raw materials is evaluated in contrast with two different forecast scenarios of demand. As a result, three widely available crop by-products (barley straw, corn pith and rice husks) are chosen to develop experimental composites using two natural binders (corn starch and sodium alginate). Both the raw materials and the six different composites produced from them are characterised. Attention is focused on the physical, thermal and hygroscopic

properties of the materials, especially their porous structure, density, thermal conductivity and diffusivity, water vapour sorption and water vapour diffusivity. In addition, the fire reaction of the composites is investigated using small-scale laboratory tests. Results are evaluated in comparison with commercially available bio-based materials and other conventional insulation materials.

The second part of this research is focused on the analysis and development of one of the six composites investigated in the first part. The composite produced from corn pith and alginate is chosen since it presents several properties (such as low density, low thermal conductivity, significant moisture adsorption, and low fire contribution) which are suitable for thermal insulation materials. On one hand, the dependence of the thermal and the hygroscopic properties of the composite on moisture content alongside its hygrothermal performance are examined. On the other, the fire reaction and the resistance to mould growth of the material is evaluated and improved with the addition of specific treatments. Finally, the hygrothermal performance of an ETIC-like (External Thermal Insulation Construction System) system incorporating the new material is evaluated and compared with mainstream materials.

RESUMEN

El sector de la construcción se interesa cada vez más por la eficiencia energética de la edificación, lo que incluye no sólo la mejora del comportamiento térmico de los cerramientos, sino también la reducción de la energía incorporada en los materiales. El desarrollo de eco-materiales aislantes térmicos puede contribuir a este fin, ya que su uso puede conllevar tanto una reducción de la demanda energética como de la energía incorporada, además de otros beneficios como la reducción del uso de recursos no renovables y de la generación de residuos.

Actualmente existen diversos eco-materiales disponibles en el mercado, la mayoría a base de fibras vegetales industriales (lino, cáñamo, kenaf, etc.), madera o lana de oveja. El uso de subproductos agrícolas es menos común, pero podría ser una alternativa interesante para países como España, donde la producción de fibra industrial es muy marginal. Estos subproductos, especialmente la paja de cereales, se han utilizado y se utilizan cada vez más en la construcción como refuerzo en materiales compuestos, acabados de cubierta, particiones interiores o cerramientos estructurales. En esta investigación se propone su uso como aislamiento térmico.

En una primera etapa de la investigación, el objetivo es explorar la posibilidad de utilizar algunos de los subproductos agrícolas disponibles en España para el desarrollo de paneles aislantes rígidos. Se ha evaluado la disponibilidad de las materias primas contrastándola con dos posibles escenarios de demanda. Tres de los subproductos disponibles (paja de cebada, médula de maíz y cascarilla de arroz) se seleccionaron para el desarrollo de materiales compuestos experimentales que se aglutinaron con dos tipos de polímeros naturales (almidón de maíz y alginato de sodio). Tanto las materias primas como los materiales compuestos fueron

caracterizados analizándose sus propiedades físicas, térmicas e higroscópicas, en concreto su estructura porosa, su densidad, su conductividad y difusividad térmicas, la sorción y la difusividad al vapor de agua de los materiales. Los resultados se contrastaron con los de otros materiales convencionales. Por otra parte, se analizó la reacción al fuego de los materiales compuestos. El compuesto basado en la médula de maíz y alginato presentó diversas propiedades favorables tales como una baja densidad y una baja conductividad térmica, una capacidad de adsorción de vapor de agua significativa y una baja contribución a la propagación del fuego, por lo que ha sido objeto de una investigación ulterior.

Por lo tanto, en una segunda etapa, se ha estudiado en más profundidad el compuesto a base de médula de maíz y alginato. Se ha analizado la dependencia de las principales propiedades térmicas e higroscópicas con el contenido de humedad del material, así como su comportamiento higrotérmico. Por otra parte, se ha tratado de mejorar su comportamiento en dos aspectos importantes: su reacción al fuego y su resistencia al ataque biótico. Para evaluar el primer aspecto se analizó principalmente el proceso de smouldering. Se observó que la incorporación de ácido bórico reduce la velocidad de avance del frente de combustión, mientras que el polifosfato de amonio es capaz de impedir el smouldering hasta ciertas temperaturas. Para la evaluación del segundo aspecto se analizó la afectación de los materiales expuestos a distintos niveles de humedad y temperatura comprobando que la cal es capaz de incrementar significativamente la resistencia al ataque biótico de los materiales. Finalmente, se ha evaluado el rendimiento higrotérmico de los Sistemas SATE que incorporan el nuevo material comparándolo con el de otros materiales convencionales.

RESUM

El sector de la construcció s'interessa cada vegada més per l'eficiència energètica de l'edificació, cosa que inclou no només la millora del comportament tèrmic dels tancaments, sinó també la reducció de l'energia incorporada en els materials. El desenvolupament d'eco-materials aïllants tèrmics pot suposar una bona contribució a aquest fi, ja que el seu ús pot comportar tant una reducció de la demanda energètica com de l'energia incorporada, a més d'altres beneficis com la reducció de l'ús de recursos no renovables i de la generació de residus.

Actualment existeixen diversos eco-materials disponibles al mercat, la majoria a base de fibres vegetals industrials (lli, cànem, kenaf, etc.), fusta o llana d'ovella. L'ús de subproductes agrícoles és menys comú, però podria ser una alternativa interessant per a països com Espanya, on la producció de fibra industrial és molt marginal. Aquests subproductes, especialment la palla de cereals, s'han utilitzat i s'utilitzen cada vegada més en la construcció com a reforç en materials compostos, acabats de coberta, façana o tancaments estructurals. En aquesta investigació es proposa el seu ús en aïllaments tèrmics.

En una primera etapa de la investigació, l'objectiu és explorar la possibilitat d'utilitzar alguns dels subproductes agrícoles disponibles a Espanya per al desenvolupament de panells aïllants rígids. S'ha avaluat la disponibilitat de les matèries primeres contrastant-la amb dos possibles escenaris de demanda. Tres dels subproductes disponibles (palla d'ordi, medul·la de blat de moro i clofolla d'arròs) s'han seleccionat per al desenvolupament de materials compostos experimentals, aglutinats amb dos tipus de polímers naturals (midó de blat de moro i alginat de sodi). Tant les matèries primeres com els materials compostos han estat

caracteritzats analitzant les seves propietats físiques, tèrmiques i higroscòpiques, en concret la seva estructura porosa, la seva densitat, la seva conductivitat i difusivitat tèrmiques, la sorció i la difusivitat al vapor d'aigua. Els resultats s'han contrastat amb els d'altres materials convencionals. D'altra banda, s'ha analitzat la reacció al foc dels materials compostos. El compost basat en la medul·la de blat de moro i alginat ha presentat diverses propietats favorables com ara una baixa densitat i una baixa conductivitat tèrmica, una capacitat d'adsorció de vapor d'aigua significativa i una baixa contribució a la propagació del foc, pel que ha estat objecte d'una investigació ulterior.

Per tant, en una segona etapa, s'ha estudiat en més profunditat el compost a base de medul·la de blat de moro i alginat. S'ha analitzat la dependència de les principals propietats tèrmiques i higroscòpiques amb el contingut d'humitat del material, així com el seu comportament higrotèrmic. D'altra banda, s'ha tractat de millorar el seu comportament en dos aspectes importants: la seva reacció al foc i la seva resistència a l'atac biòtic. Per avaluar el primer aspecte s'ha analitzat principalment el procés de smouldering. S'observa que la incorporació d'àcid bòric redueix la velocitat de propagació del front de combustió, mentre que el polifosfat d'amoni és capaç d'impedir l'smouldering fins a certes temperatures. Per a l'avaluació del segon aspecte s'ha analitzat l'afectació dels materials exposats a diferents nivells d'humitat i temperatura, i s'ha comprovat que la calç és capaç d'incrementar significativament la resistència a l'atac biòtic dels materials. Finalment, s'ha avaluat el rendiment higrotèrmic de Sistemes SATE que incorporen el nou material comparant-lo amb el d'altres materials convencionals.

ACKNOWLEDGMENTS

I am deeply grateful to my supervisors Ana M. Lacasta and Jaume Avellaneda for their support and inspiration and for giving me the freedom to define my subject of interest. Ana could not have been a better guidance in this process both professionally and personally. She has shown a huge interest in this work, being his patience and perseverance essential to push me forward whenever needed.

I would like to convey my sincere thanks to Laia Haurie and Joan Formosa for their helpful discussions and advice on their chemistry lessons regarding the bio-based materials and for their complicity on the singular experiments that we performed at the Fire Laboratory. I am also very grateful to Antonia Navarro and Marc Tous for their advice on the laboratory testing procedures and for their willingness to provide assistance at all times.

My appreciation is extended to the rest of my colleges at the GICITED research group, Joan Ramon Rosell, Inmaculada Rodriguez, Montserrat Bosch, Judith Ramirez and Joaquin Montón for all the unforgettable moments we have lived throughout these years.

I would like to express my sincere thanks to the people at the BRE-CICM of the University of Bath. Special thanks go to Pete Walker and Andy Shea who offered me the opportunity to work at the BRE-CICM and gave me their inestimable support and guidance which undoubtedly contributed to improve my work. I would like to thank Neal Holcroft, Fionn Mc Gregor and Andrew Thomson for their help and kind advice on the hygroscopicity and the mould growth resistance of bio-based

materials and the use of the DVS. All my thanks to the rest of the researchers that I met at the University of Bath for making my short-term visit so enjoyable.

I wish to express my sincere gratitude to the members of the INCAFUST, M. Pilar Giraldo, Eduard Correal and Marcel Vilches for their support on the hygrothermal testing of the insulation materials.

Thanks to Juli Bergé, Peter Homer and all the farmers without whom this thesis would have not been possible and would probably have not had any sense.

I do not want to miss this opportunity to express my gratitude to Belen, Laura and to the graduate students, Núria, Javier, Angel, Diego and Jacqueline who got involved with this work and whose energy and enthusiasm were contagious.

All my thanks to those who helped, encouraged and supported me during these past years and whose names are not mentioned here, to all my friends and my relatives, Sully, Helena and Alfonso, to whom I am forever indebted.

Finantial support from *Comisionat per a Universitats i Recerca del Departament d'Innovació, Universitats i Empresa de la Generalitat de Catalunya i del Fons Social Europeu* under a predotoral FI grant is gratefully acknowledged.

Mariana Palumbo
Barcelona, July 2015

TABLE OF CONTENTS

SYMBOLS AND ABBREVIATIONS

Symbols

A	Area
A_{BET}	Specific surface area of the adsorbent
Ba	Available crop by-products
Bf	Reincorporated crop by-products
Bt	Total crop by-products
Bu	Unavailable crop by-products (already used)
b_m	Moisture effusivity
C/N ratio	Carbon -Nitrogen content ratio
D	Diameter
$D_{by\text{-}products}$	Demand of food crop by-products
D_v	Vapour diffusion coefficient
d	Thickness
G	Water vapour flow rate
HI	harvest index
h_{ad}	Latent heat of sorption
M	The molecular weight of adsorbate
MBV	Moisture Buffering Value
MBV_{ideal}	Ideal Moisture Buffering Value

MC	Moisture content
Mloss	Mass loss fraction
Mt	Million tonnes
N	Avogadro's number
N_{ig}	Number of ignitions
P	Pressure
Pv	Vapour pressure
P_{sat}	Pressure of saturation
RPR	Residue to product ratio
Rv	Gas constant for water vapour
T	Temperature
T_{onset}	Onset temperature of combustion
t	Time
u	Moisture content
V_{ins}	Volume demand of insulation
w_m	Monolayer capacity of the material

α	Thermal diffusivity
γ	Surface tension
δ	Water vapour permeability
Δm	Average of the adsorbed and desorbed mass
Δ_p	Average water vapour pressure difference
Δ_{RH}	Difference in relative humidity
Δt_{ig}	Average duration of the ignitions
δa	Ratio of the water vapour permeability of air
ε_l	Volum
Θ	Wetting angle
λ	Thermal conductivity
μ	Water vapour diffusion resistance factor
μ_{TI}	Attenuation factor

ρ_0	Dry density
ρ_{ins}	Average density of existing insulations
ρ_v	Vapour water density
ρC_p	Product of density by heat capacity
σ_m	Diameter of a single adsorbate molecule
ϕ	Relative humidity
φ_{MAX}	Thermal lag at maximum temperature
φ_{MIN}	Thermal lag at minimum temperature

Abbreviations

A	Sodium alginate binder
AG	Sodium alginate treated specimen
AH	Aluminium hydroxide treated specimen
APP	Ammonium polyphosphate treated specimen
APPB	Ammonium polyphosphate and boric acid treated specimen
ASTM	American Society for Testing and Materials
AT_I	Immersion acetylation treated specimen
AT_V	Vapour phase acetylation treated specimen
B	Barley straw fibres
BA	Barley straw alginate specimen
BAC	Boric acid treated specimen
BAG	Boric acid and sodium alginate treated specimen
BAH	Boric acid and aluminium hydroxide treated specimen
BAPP	Boric acid and ammonium polyphosphate treated specimen
BET	Brunauer–Emmett–Teller
BRE-CICM	Building Research Establishment Centre for Innovative Construction Materials
BS	Barley straw starch specimen

C	Corn pith aggregate
CA	Corn pith alginate specimen
CS	Corn pith starch specimen
DAP	di-ammonium phosphate
DP	Degree of polymerization
DSC	Differential Scanning Calorimetry
DVS	Dynamic Vapour Sorption
EPS	expanded polystyrene
ETICS	External thermal insulation construction system
GHG	Greenhouse gases
GW	Glasswool
HFM	Heat Flow Meter
HR	Heat Release Capacity
HRR	Heat Release Rate
INCAFUST	Institut Català de la Fusta
L	Lime treated specimen
LG	Lauryl gallate treated specimen
LOI	Limiting Oxygen Index
LOI	Limiting Oxygen Index
MDI	methyl isocyanate
MT	Mimosa tannin treated sample
MW	Mineral wool specimen
MARM	Ministerio de Agricultura, Alimentación y Medioambiente
PCFC	Pyrolysis Combustion Flow Calorimetre
PF	Phenol formaldehyde
PUR/PIR	Polyurethane and polyisocyanurate
PVA	Polyvinyl acetate
pMDI	Polymethyl isocyanate
R	Rice husk aggregate
RA	Rice husk alginate specimen

RH	Relative humidity
RS	Rice husk starch specimen
S	Corn starch binder
SCTUB	Serveis Cientificotécnics Universitat de Barcelona
SE	Secondary electrons
SEM	Scanning Electron Microscopy
ST	Stearate treated specimen
STA	Simultaneous thermal analysis
SW	Stone wool
Tac	Air temperature inside the chamber
Tal	Air temperature at the laboratory
Tint	Temperature within the panel
Tsc	Surface temperature at the prototype face inside the chamber
Tsl	Surface temperature at the prototype face outside the chamber
TG	Thermogravimetric Analysis
TGA	Thermogravimetric analysis
TPHRR	Temperature at peak heat release rate
UF	Urea formaldehyde binder
WW	Wood wool specimen
WF	Wood fibre specimen
XPS	Extruded polystyrene

1. INTRODUCTION

1.1. Context of the study

Intervention in the existing building stock is a key strategy for tackling the challenges posed by the European Commission targets for reducing greenhouse gases (GHG) emissions by the years 2020 and 2050. Such targets urge member countries to reduce the internal GHG emissions by 20% in year 2020 and 80% in year 2050, with respect to their 1990 emission levels (Latif et al. 2010; Cuchí and Sweatman 2011). Specifically in Spain, it is estimated that, to meet these challenges, about 10 million dwellings should be refurbished between now and the year 2050 (Cuchí and Sweatman 2011; 2012; 2014). Existing buildings consume about 40% of EU's total annual energy consumption, mainly for heating and air conditioning. Thus, the implementation of optimized thermal insulation systems is regarded as one of the main strategies to improve their energy efficiency and reduce derived GHG emissions. Indeed, the use of thermal insulation materials in Europe has significantly increased in previous years (Papadopoulos 2005), which opens the discussion on what the impact of these materials is, not only based on energy consumption and GHG emissions, but also on further environmental issues such as indoor air quality, waste generation or depletion of natural resources.

The use of bio-based thermal insulation materials is regarded as an alternative in reducing such environmental impacts, although these materials are still only marginally used. In 2013, mineral wools and organic foams –both produced from non-renewable raw materials- accounted for about 97% of the market share in Spain

(Rockwool 2013). The renewable alternative, that is, bio-based thermal insulation materials, represented less than 3% of the market (as shown in Figure 1.1). Furthermore, most of these materials were imported, with some exceptions such as *Termofitex Lan* (sheep wool), *RMT-NITA* products (sheep's' wool, textile waste or hemp fibre), *Cannabric* products (hemp based) and *Aislanat* (cellulose). Several factors, such as regulations, lack of standardised label certifications, production costs, lack of incentives and uncertainty of policies, among others, prevent bio-based thermal insulations from having a greater presence in the market (Yates 2006; Kretschmer et al. 2012). Nevertheless, it is reasonable to forecast a growing demand for these products in the coming years, due to the increasing concern about environmental issues and changes in policies.

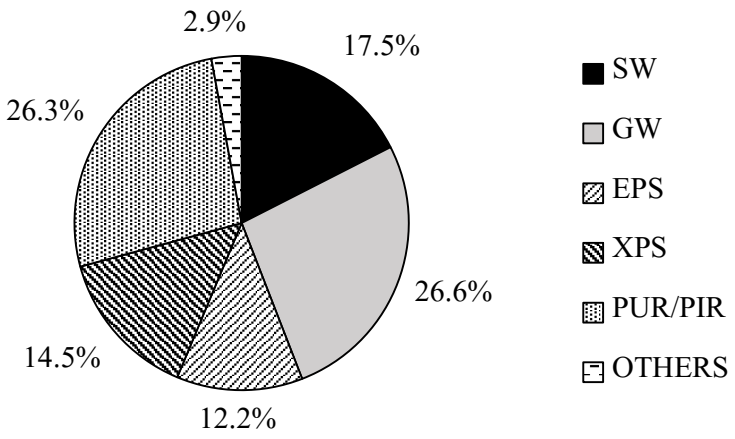

Figure 1.1. Spanish insulation market share. Stone wool (SW), glass wool (GW), expanded and extruded polystyrene (EPS and XPS), polyurethane and polyisocyanurate (PUR/PIR) and others (OTHERS). Natural insulation materials are included in this last category.

1.2. Aim of the study

This study sets out to be a small contribution to the development of new bio-based construction materials to be used in the building sector. Its aim is to explore the possibility of using existent crop by-products as raw materials for innovative material developments by proposing and investigating a new bio-based insulation board made from any of the available crop by-products. The material should present

competitive hygrothermal performance and should be completely compostable and biodegradable, with controlled fire reaction and enhanced mould resistance.

To this end, one of the objectives of this work is to analyse the availability of the different crop by-products in Spain given the demand forecast on building insulation materials.

The second objective is to characterize the most abundant crop by-products in order to determine the by-product that present the most favourable conditions to be used as a thermal insulation material in buildings.

The third objective is to analyse the technical feasibility of the proposed composite while comparing its hygrothermal performance, fire reaction and mould growth resistance with that of commercially available insulation materials. Such analysis aims also at the improvement of the material's properties achieved by the adjustment of the binder ratio or through the incorporation of biocompatible additives.

The availability of the raw materials is estimated using the currently available data, while the characterization and analysis of the technical feasibility of the materials is investigated through laboratory based experiments. The goal of the experimental work is to characterise the materials and to establish correlations between the properties of the raw materials and the performance of the composites.

Finally, the study of the performance of the proposed material in an external thermal insulation construction system (ETICS) usually used in walls for building energy refurbishment is pursued.

The hypothesis proposed are:

The availability of crop by-products in Spain is relevant to the construction industry. The exploitation of such raw materials can be made in a sustainable way without compromising soil productivity or food production.

Crop by-products naturally present advantageous hygrothermal properties for use in building thermal insulation materials.

It is possible to produce highly performant thermal insulation materials from crop by-products using small amounts of natural gums and low tech manufacturing systems.

The main drawbacks of bio-based insulation materials are fire reaction and mould growth resistance. It is possible to improve these aspects using harmless fibre pre-treatments and additives.

1.3. Scope and limitations

This thesis focuses on the design of a new bio-based material incorporating locally existing crop by-products, with low environmental impact, high compostability and an acceptable durability which is suitable for façade building insulation (for exemple, ETIC System). The analysis of the available crop by-products is limited to the Spanish territory, although the results and findings presented in this thesis are valid for other regions of the world where the same raw materials are available.

The thesis is mainly based on experimental laboratory work which is focused on the characterization, evaluation and comparison of the performance of the experimental materials proposed. The aspects investigated in the characterization are related to physical properties (mainly porosity and density), thermal properties (thermal conductivity and diffusivity), and hygroscopic properties (moisture content and water vapour permeability). The analysis of the performance of the materials is focused in three main areas: hygrothermal performance, fire reaction and mould growth resistance. It is beyond the scope of this thesis to analyse other relevant aspects such as the mechanical properties, chemical interactions between the matrix and the aggregate or the life cycle analysis of the proposed composites.

The thesis is fostered by the current scientific knowledge related to any of the three main areas mentioned above. It is beyond the scope of this thesis to propose new mathematical models or to discuss the theoretical validity of existing models.

In buildings, insulation materials are integrated into complex construction systems, the configuration of which determines the service performance of the materials, Thus, it is important not only to evaluate the performance of such materials individually, but also as part of the specific construction systems. Here, the

hygrothermal performance of an ETIC System incorporating the proposed material is evaluated. The mechanical aspects concerning the applicability of the material in such a system as well as the construction details necessary for its implementation are beyond the scope of this thesis. However, half scale samples are realized in order to qualitatively verify whether the composite is capable of supporting handling and coating.

1.4. Outline

The present document is divided into four parts dealing with (1) the background, general description of the thesis and the state of the art; (2) the methodology and raw materials used; (3) the outcomes of the experimental work and (4) the general conclusions and recommendations for future work.

Sections 1-3 present the background, general description of the thesis and the state of the art. In Section 1, the context of the study including the characteristics of the existing building stock, the regulations regarding the energy building refurbishment and the situation of the insulation marked in Spain are discussed. Thereafter, the aim, scope and outline of the present investigation are presented. Section 2 deals with the state of the art on bio-based insulation materials for buildings. The characteristics and diversity of the existing and experimental materials is commented. The three main issues addressed in this thesis are also included. The concepts related to the hygrothermal performance, fire reaction and mould growth resistance of the existing materials are discussed. Previous works conducted in these areas are presented. In section 3, the availability of crop by-products is investigated in order to assess the feasibility of their use as raw materials for bio-based thermal insulations. This is then contrasted with an estimation of the demand based on two different scenarios: a forecast based on the current market size and a forecast based on the volume of the thermal insulation hypothetically needed to fulfil the EU's targets for GHG emissions reduction by 2050.

Sections 4-5 present the methodology and the materials used. In Section 4 the experimental set-ups and procedures used in this investigation are described. Laboratory tests are organized in four main categories: (1) tests designed to the physical, thermal and hygroscopic characterization of both the raw materials and

the composites; (2) experiments aimed at the determination of the hygrothermal performance of the materials and the construction systems incorporating such materials; (3) tests focused on the analysis of fire reaction and mould growth resistance of the materials; and (4) tests evaluating the performance of construction systems incorporating the experimental materials. The raw materials are described and characterized in Section 5 in order to determine their physical, thermal and hygroscopic properties. The crop by-products used as raw materials in this thesis are three distinct of the most abundant crop by-products detected in Section 3: barley straw, corn pith and rice husk. Moreover, in this investigation two natural gums: corn starch and sodium alginate are used as binders. The chemical and gelation properties of such materials are presented and their thermal decomposition is experimentally determined.

Sections 6-8 contain the findings obtained from the experimental work. In Section 6 the procedure adopted in the manufacturing of the six different experimental composites analysed in this thesis is presented. The composites are: barley starch (BS), barley alginate (BA), corn pith starch (CS), corn pith alginate (CA), rice husk starch (RS) and rice husk alginate (RA). The results on their physical, thermal and hygroscopic characterization are presented and compared to those of the raw materials alone. The findings on the fire reaction of the different bio-based composites are also included in the analysis of the experimental composites. The corn pith alginate (CA) composite is further investigated in Section 7. Wood based insulation boards and expanded polystyrene are used for comparison. The hygrothermal performance of the corn pith – alginate materials is evaluated. The variation of its hygrothermal properties with moisture content is experimentally determined and its thermal performance analysed by dynamic tests where the environmental conditions are cyclically modified. On the other hand, the fire reaction of the material, especially the smouldering combustion, is investigated. Boric acid, aluminium hydroxide, and ammonium polyphosphate are used as fire retardants. The effect of incorporating a higher amount of sodium alginate is also investigated. Besides, the mould resistance of the material is analysed. The corn pith aggregates are pre-treated using different substances in order to improve the mould growth resistance of the corn pith alginate composite. Boric acid, lime, silicate, different kinds of stearates, tannins, acetic anhydride and lauryl gallate are tested. The formulations showing a higher mould growth resistance are further tested in order to determine their mould growth resistance profile using the isopleth

system. Larger scale specimens are incorporated into an ETIC System. The hygrothermal performance of the ensemble is evaluated through dynamic tests. The durability of the system is evaluated by its dimensional stability and water absorption after being exposed to an accelerated ageing protocol. The outcomes of these tests are presented in Section 8.

Finally, general conclusions arising from the work designed above are drawn in Section 9. The technical feasibility of the proposed material is evaluated by identifying its strengths and weaknesses. Opportunities for further research are discussed.

2. BIO-BASED INSULATION MATERIALS

2.1. Introduction

As discussed earlier, the reduction in the GHG emissions and energy use in the building sector is a key strategy for global climate change mitigation and thus, policies are being implemented in Europe to tackle this issue. Concepts such as *passive house* and *net zero emission building* are being introduced, which underlie the need to diminish the heat transfer through the building envelope if the energy used to preserve the comfort conditions at the indoor environment is to be significantly reduced.

Excluding aspects related to the design and installation such as air leakages, etc., heat transfer through a wall in a transitory regime is defined by the heat diffusion equation and depends on the thermal diffusivity of the different layers forming the wall. The thermal diffusivity (α) is a factor that indicates the speed of temperature change with time within a material, expressed in m^2/s. It is directly proportional to the thermal conductivity of the material (λ) and inversely proportional to the product of its density and its heat capacity (ρCp). Thus, in order to reduce the heat flow rate through a wall, two main strategies can be adopted: (1) the reduction of its thermal conductivity or (2) the increase in its density and heat capacity. Each strategy has different implications and is suitable for different situations and climates and are usually used in combination in buildings.

Thermal insulations are materials with a low thermal conductivity capable of retarding the rate of heat flow by conduction, convection and radiation (Al-Homoud

2005) and thus, play an important role in the implementation of the first strategy defined above. There are different types of thermal insulation materials. Depending on the principles behind their thermal performance, current and under development thermal insulation materials can be classified as (Jelle 2011):

- Air based insulation
- Vacuum/gas filled insulation
- Nanocellular insulation, such as aerogels.
- Switchable thermal insulation.
- Reflective membranes, which need to be used in combination with other insulation for it to be effective.

However, the most common ones are, by far, air based insulations. The thermal performance of these materials is based on the entrapment of still air in their internal porous structure which suppresses convective heat transfer. Thus, their thermal conductivity cannot be lower than that of still air and is typically ranged between 0.050 and 0.025 W/mK.

Two subcategories can be identified within this group of thermal insulations regarding the nature of their internal structure: (1) cellular materials, such as foamy petrol based materials -polystyrene, polyurethane, etc.-, cork boards and cellular glass; and (2) fibrous materials, such as mineral wools -glass wool or stone wool-, wood fibre boards and cellulose. In Europe, as in Spain, mineral wools and foamy petrol based materials dominate the insulation market (Papadopoulos 2007; Rockwool 2013). Comprehensive reviews on the different kinds of existing thermal insulation and their properties can be found in (Al-Homoud 2005; Papadopoulos 2007; Pfundstein et al. 2007; Bozsaky 2010; Jelle 2011).

Apart from their internal structure, air based thermal insulation materials can also be classified according to the nature of their raw materials in inorganic, petrol based, bio-based and combined materials. Thus, under this classification, the term bio-based insulation materials designates those materials derived from renewable organic biological resources. This category comprises both cellular and fibrous materials that might suffer different degrees of transformation and manufacturing

before their use. Renewable organic biological resources refers to lignocellulosic and other vegetable materials and animal materials such as fur or wool, but excludes shells, bones and other inorganic structures produced by living organisms. In this thesis, the term bio-based is restricted to materials or composites in which the renewable, organic, biological raw materials represent at least 90% of the total mass and are biodegradable.

In fact, bio-based insulation materials were the first insulation materials used in construction. Apart from the prehistoric times, when the same materials used for clothing (fur, wool, skins…) were used for shelter insulation, there are evidences of cork being used by Romans for roof insulation during the 1st century. However, it was not until the 1870s that the first cork board was produced. In contrast, petrol based plastic foams only appeared in the market in the 1940s and 1950s, causing a huge revolution (Bozsaky 2010). In recent decades, as a result of the increasing consciousness of the hazardous effects that certain insulation building materials have both on human health and on the environment, bio-based materials are being revised. Efforts are devoted to the development of high performant materials that are intended to be both technically and economically competitive.

2.2. Existing materials and experimental developments

Recent developments support the use of those natural fibres commonly employed in industry (such as wood, hemp, kenaf, cotton, flax or sheep's wool) as an alternative to petrol based products. Such fibres present a high porosity, which confers on them a naturally low bulk density and, consequently, a naturally low thermal conductivity (Domínguez-Muñoz et al. 2010). As a result of these developments, some bio-based insulation materials such as hemp wools or wood fibres are nowadays part of the mainstream market. In addition to the good hygrothermal properties of these natural materials due to their low thermal conductivity and high hygroscopicity, which may contribute to maintaining comfort in buildings (Osanyintola and Simonson 2006), their availability from renewable resources is considered as one of their main advantages compared to petrol based insulations. Moreover, they tend to be biodegradable, which contributes to the reduction of waste going to landfills, and may contribute to the development of an industry, based on closed production cycles, where the concept

of waste disappears (McDonough and Braungart 2010). On the other hand, bio-based insulation materials present several drawbacks among which moisture absorption, which produces important variations in the weight and volume of the materials, compromising their durability; low fire and mould growth resistance are the most remarkable.

Some research has been carried out as well on the use of crop by-products such as straw, stalks or husks of cereals (Madurwar et al. 2013) which are more rarely industrially used. The use of crop by-products in composites to be used in building applications, may offer an interesting alternative to existing insulation materials, especially in regions such as Spain where the production of industrial fibres is scarce compared with agricultural production. In addition, the use of food crop by-products has a positive environmental impact because it implies the revaluation of existing natural resources which:

- Are renewable annually, in contrast to wood or cork, which has longer regeneration cycles.

- Are easily accessible and do not compete in fertile land use with food production, as is the case of industrial fibres.

- Their valorisation may contribute to diversify the market for farmers (Yates 2006). Moreover, it may contribute to the use of native species that have not been modified to increase their harvest index.

- Are naturally low thermal conductors, which may mean that they do not need to be highly transformed to achieve the thermal requirements for insulation materials (Pinto et al. 2011).

All of these beneficial aspects encourage their use in building insulation. However such materials present a number of drawbacks. Apart from those common for all bio-based materials, the main drawbacks in the use of crop by-products mentioned in literature are:

- Inhomogeneity. The properties of bio-based materials may vary due to external factors such as climate, soil conditions, method of production, plant diseases, etc.

- Highly variable price, dependent on production, economic policies, the development of competing uses, etc.

- Seasonal availability.

Thereafter, all these aspects should be taken into account in the analysis of the feasibility of derived products for building applications.

Although many of the research on the use of crop by-products in building applications have been focused on the reinforcement in composites (Sobral 2004; Magniont 2010), the development of high and medium density boards (Halvarsson et al. 2010) or straw bale wall systems (De Bouter et al. 2009; Wall et al. 2012), there is an increasing interest in their use in bio-based thermal insulation materials.

Many factors influence the basic properties of these materials. As pointed out earlier, density is an important factor. The orientation of the aggregate particles in the matrix, the particle size distribution, the internal porous structure of the raw materials, the ratio and nature of the binder used or the manufacturing process are other factors that are usually investigated (Vejeliene et al. 2011a; Liu et al. 2012).

Density is an important factor not only for bio-based thermal insulation materials but for all kinds of air based insulation materials. Domínguez-Muñoz et al. (2010) presented a statistical work comparing the density and thermal conductivity of several existing insulation materials. Their research show how the thermal conductivity is lower for materials the density of which fall in a range between 30 and 100 kg/m^3, and that lower or higher density generally implies higher thermal conductivity.

In the case of bio-based materials, in general, higher density implies higher thermal conductivity, although, it allows for a reduction in the amount of binder needed (Norford et al. 1999) which might have a positive impact on thermal conductivity. Vejeliene et al. (2011b) tested specimens of binderless -tied- wheat straw insulation boards in different configurations and discovered that boards made of chopped straw (2-4 cm long) presented a lower thermal conductivity than those made with entire stalks. Density seemed to have an important impact on the latter, increasing 2.5 times when density was doubled. However, density seemed not to have any impact on thermal conductivity when straw was chopped. Entire straw at 50 kg/m^3

had similar conductivity than chopped straw packed at densities between 60 and 80 kg/m^3 (about 0,041 W/mK).

If the aggregate is of fibrous nature, fibre orientation seems to have some influence on the thermal conductivity of the final composites, as thermal conductivity is lower when fibres are orientated perpendicular to the heat flux (De Bouter et al. 2009; Vejeliene et al. 2011b). Particle size, on the other hand, do not significantly influence the thermal conductivity, provided the final density is maintained similar. According to Norford et al. (1999), the presence of fine particles might entail a reduction in the heat transmission by radiation, but this effect is probably counteracted by an increase in conduction transmittance through the solid part of the compound. In his work the author developed chopped straw boards, achieving a thermal conductivity similar to that of extruded polystyrene or mineral wool (0,038W/mK). Results pointed out that despite the presence of dust particles do not significantly affect the thermal conductivity of the material, it does interfere with the matrix, compromising its mechanical properties.

Vejeliene et al. (2011a) did some work evaluating the influence of the internal porous structure of the fibres on its thermal conductivity. They analysed the effect of the porous structure on thermal conductivity for different kinds of fibres (barley straw, reed stalks, cattail stalks and blades of grass) through scanning electron microscopy. Results indicated that the thermal conductivity was greatly affected by the porous nature of the materials. Reed specimens were found to have the smallest pores (less than 0.1 μm) and, although their density was almost 1.5 times lower than that of bent grass, they presented the highest thermal conductivity (~0.085 W/mK). Bent grass specimens were two times denser than barley straw ones but presented similar thermal conductivity (~0.06 W/mK) and similar pore sizes (from 0.1 to 1.0 μm). Cattail stalks, the interior of which is full of vegetable pith (with open porosity between 5 and 10 μm), presented the lowest density and lowest thermal conductivity among the analysed materials (61.5 kg/m^3 and 0.057W/mK).

The binder chosen is a driving factor in determining the overall properties of bio-based materials. It has great impact, for instance, on the environmental impact of the final material. In addition, the application method is also relevant, as it determines how the fibres are mixed with the binder, the drying speed and the pressure applied (Norford et al. 1999). In general, a higher proportion of binder involves a greater dimensional stability of the material, which, however, also

increases its density and its cost. A large variety of binders can be found which can be classified based on different criteria. Regarding their nature, binders can be classified as inorganic and organic. Cement, lime and other inorganic materials such as sodium silicate, are commonly used as binders at high rates, which generally increases the thermal conductivity of the final product. Cement presents a high embodied energy and a poor compatibility with lignocellulosic materials (Claramunt 2011) and thus tends to be replaced by other products (Magniont 2010). Hemp lime composites are being issue for an extensive research (Evrard 2008; Glé et al. 2011; Laurent and Gourlay 2012; Shea et al. 2012; Collet et al. 2013) which resulted in a wide range of products having reached the market during the last years (*Tradical Hemcrete, Hemp Eco Systems, The Limecrete Company,* or *Chanvribloc*, are some examples of the companies currently commercialising hemp lime products). Krus et al. (2014) used magnesite as a binder in cattail leaf based insulation boards. Magnesite accounted for 40% to 60% of the total mass. The density of the resulting composites ranged between 220 and 350 kg/m^3, and their thermal conductivity was about 0.055 W/mK. The use of inorganic binders contributes to improve both fire and mould growth resistance of the bio-based materials, but might prevent their biodegradability after their lifespan. Organic binders are also generally used. The most effective substances are those which present high molecular weights and form long molecular chains, such as polymers. Organic binders can be divided, based on the origin of their raw materials into bio-based and synthetic/petrol-based binders. Proteins and polysaccharides are examples of naturally occurring polymers while vinyls, aldehyde condensation resins and polyesters are examples of synthetic/petrol-based polymers. According to their hardening process, organic binders can also be classified into two distinct groups: thermoplastic and thermosetting binders. The first can be melted or softened with heat or solvents and set by solidification and cooling without (within certain temperature limits) undergoing chemical change. They are normally limited to indoor, non-structural applications. The second harden through an irreversible chemical change which forms moisture resistant bonds and are used for structural application in wood products (Ebnesajjad 2008). Figure 2.1 depicts different examples of each kind of binder.

Aldehyde condensation resins (phenolic, resorcinol, urea and melamine) are the synthetic adhesives most commonly used in the wood industry. Besides their low price, most of these substances present the advantage of being resistant to weather,

boiling water and bio-deterioration which make them suitable for exterior grade products. However, they emit volatile organic compounds (formaldehydes) causing important hazardous effects on humans, which makes inadvisable their use. Other alternative binders, such as methylene diphenyl diisocyanate (MDI) and polymeric MDI (pMDI) are available, but they are mainly non-compostable petrol-based substances with a high embodied energy, which causes problems of waste disposal and resource depletion. Moreover, in case of fire they can give off hazardous gases, such as hydrogen cyanide and nitrogen oxides.

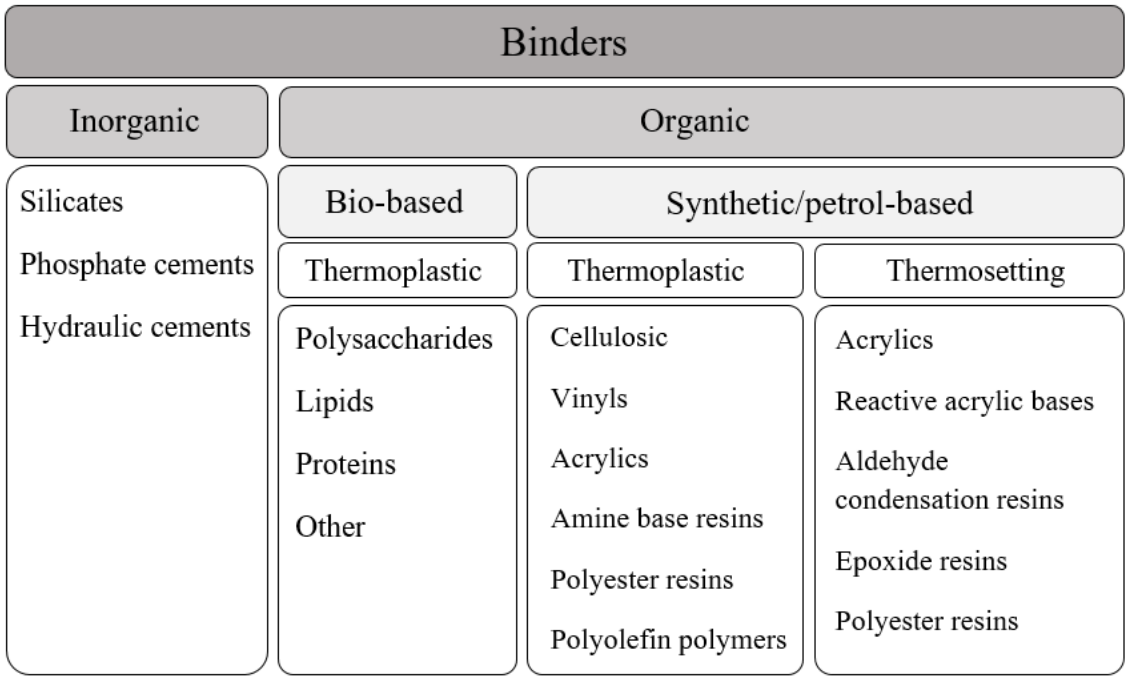

Figure 2.1. Binder classification according to the nature and origin of their raw materials.

One of the strategies to overcome these problems is to replace the conventional binders with binders based on biodegradable polymers. This alternative is being issue for intensive scientific research, especially on poly lactic acid (PLA) and soybean protein, which are, by far, the most commonly used biopolymers. Nowadays, the two main drawbacks of bio-based binders is their high production cost (which is from two to ten times higher than that of synthetic/petroleum based binders with similar properties) and their hydrophilic nature which is a disadvantage in terms of durability and reduces the range of possible applications (Dittenber and GangaRao 2012). A wide range of raw materials can be used as binders which can be classified into polysaccharides, proteins, lipids and others. In

Figure 2.2 some examples are presented. Starch-based thermoplastics are among the most affordable bio-based binders and are easy to work with. Cadena and Bula (2002) developed insulation boards based on rice husks and yucca starch. They concluded that starch was a suitable binder as it did not increase the thermal conductivity of the samples as polyvinyl acetate (PVA) did. The best mixture presented a thermal conductivity of 0.065 W/mK and a density of 195 kg/m^3. Nevertheless, the resistance in the presence of water had to be improved.

Apart from the use of bio-based binders, other interesting strategies aiming at the reduction in the material's environmental impact are the development of binderless boards. However, their production needs high pressure which increases their density and their thermal conductivity. Another interesting strategy is to use mould mycelium as a binder. The mycelium is left to grow on a crop by-product substrate until the board is formed (typically one to two weeks), after which the remaining spores are eliminated with UV radiation. A wide range of materials are being commercialised by *Ecovative Design* using this method.

It is important to note that the environmental advantages offered by bio-based materials are reduced at each stage of processing, implying that the simplest production method provides the greatest environmental benefit.

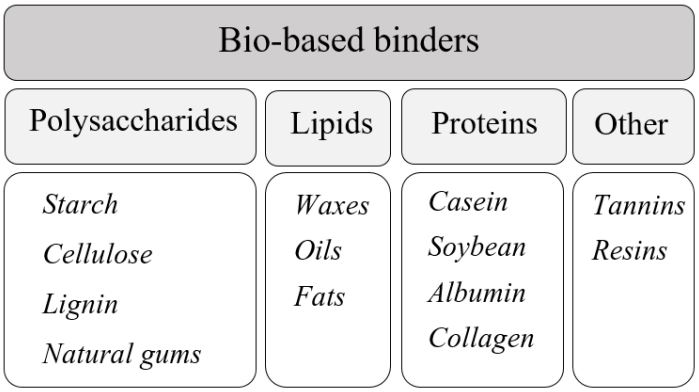

Figure 2.2. Raw materials used in bio-based binders

2.3. Hygrothermal performance of bio-based insulation materials

In terms of their hygrothermal performance, probably the most relevant property of bio-based insulation materials is their high hygroscopicity. This means that such materials have the capacity to accumulate or release moisture from their internal porous structure by adsorption or desorption from the environment (Korjenic et al. 2011). The amount of moisture accumulated is material specific and is dependent on the relative humidity and the temperature of the environment. Thus, as well as other hygroscopic materials, bio-based materials can be regarded as dynamic three-phase systems (solid, the material matrix; liquid, the water adsorbed to the surface of the material; and gas, the air and water vapour within the pores of the material) which are in constant equilibrium with the environment.

This is relevant because all the basic thermal and hygroscopic properties of materials depend on the moisture content (Jerman and Cerny 2012). Collet and Pretot (2014) found a rate variation of thermal conductivity with moisture content of about 0.0022 W/mK% for hemp lime with little differences due to density and fibre/binder ratio. Other authors reported the variation of thermal conductivity with temperature to be from one to two orders of magnitude lower than with relative humidity (Karamanos et al. 2008; Ochs et al. 2008). Thermal diffusivity is reported to be sensitive to moisture content as well. Carmeliet et al. (2004) noticed a reduction of 5 to 13% when the moisture content was doubled for brick and calcium silicate respectively. Jerman et al. (2013) reported a rate variation of water vapour permeability of 0.13 10-6 $m^2/s\%$ for different kinds of aerated concrete. Finally, heat capacity significantly increases with moisture content due to the high specific heat capacity of water (Jerman and Cerny 2012).

Moreover, a certain amount of energy is associated with the adsorption process and the phase changes of adsorbed moisture. Therefore it is clear that hygroscopicity has a direct influence on the energy performance of buildings. The extent and orientation (against or in favour of building energy efficiency) of such influence depends on each specific case and how this phenomenon is taken into account during the design and construction phases.

Thereafter, the understanding of the combined mechanisms of heat and mass transport in a porous media is essential in the quantification of the thermal building performance. Different models have been proposed to describe the dynamic

evolution of hygroscopic materials under variable environmental conditions of relative humidity and/or temperature (Mendes et al. 2003; Osanyintola 2005; Qin et al. 2009; Tran Le et al. 2010). Although there are some differences between the various models, all of them are based on the conservation of mass and energy. In their corresponding equations, there are some magnitudes (thermal conductivity, density, specific heat, water vapour permeability) that depend on relative humidity, and therefore a complete knowledge of the material hygrothermal properties is needed in order to numerically solve the equations.

As the adsorption is higher when relative humidity is increased and the excess of moisture is released when humidity is decreased, the capacity of adsorbing and desorbing moisture enables hygroscopic materials to act as a moisture buffer, thereby moderating humidity extremes in an indoor environment (Simonson et al. 2004; Osanyintola and Simonson 2006; Qin et al. 2011). This has positive effects on indoor air quality and might enable a reduction in the ventilation rate and thus, a reduction in heat loses. The moisture buffer performance of a room is the ability of the materials within the room to moderate variations in the relative humidity. In the frame of the NORDTEST Project (Rode et al. 2005) and the standard ISO 24353, a useful index, the moisture buffering value (MBV) was introduced to quantify the moisture buffer capacity of a material in conditions of surrounding humidity variation. The MBV indicates the amount of water vapour that is transported in or out of a material, during a certain period of time, after a controlled variation of environmental relative humidity. It can be determined in an experimental set up where the sample is exposed to cyclic step-changes in relative humidity between high and low values for determined periods of time.

2.3.1. Dynamical model and Moisture Buffering Value

The heat and mass transport in porous media can be modelled, under certain assumptions, by a set of one-dimensional coupled equations (Osanyintola and Simonson 2006) which account for the conservation of mass (adsorbed and gas phases) and energy:

$$\rho_l \frac{\partial \varepsilon_l}{\partial t} + \dot{m} = 0 \qquad (2.1)$$

$$\frac{\partial(\rho_v \varepsilon_g)}{\partial t} - \dot{m} = \frac{\partial}{\partial x}\left(D_v \frac{\partial \rho_v}{\partial x} \right) \qquad (2.2)$$

$$\rho C_p \frac{\partial T}{\partial t} + \dot{m} h_{ad} = \frac{\partial}{\partial x}\left(\lambda \frac{\partial T}{\partial x} \right) \qquad (2.3)$$

where t is the time and x is the spatial position along the width of the sample. In these equations $\varepsilon_l(x,t)$ and $\varepsilon_g(x,t)$ are the volume fractions of liquid and gas phases respectively, $\rho_v(x,t)$ is the vapour water density and T(x,t) is the temperature. Volume fractions are constrained by the relationship $\varepsilon_l(x,t)+\varepsilon_g(x,t)+ \varepsilon_s =1$, where ε_s is the volume fraction of the solid walls of the material. ρ_v is the liquid water density and h_{ad} is the latent heat of sorption. From each pair of local and instantaneous values of vapour density and temperature, the relative humidity ϕ can be evaluated by using thermodynamic relationships. $\phi = Pv/Psat$, where Pv is the vapour pressure and Psat is the saturation vapour pressure at temperature T. The vapour diffusion coefficient, D_v, is evaluated from the water vapour permeability δ as $D_v=\delta$ Rv T, being Rv the gas constant for water vapour. The magnitudes λ (thermal conductivity), ϕ (water vapour permeability) and ρCp (product of density with specific heat capacity of the sample) depend on the relative humidity, so they need to be re-evaluated at each time step. *m*(t,x) is the phase change rate per unit volume and can be evaluated from the moisture content, u, as

$$\dot{m} = -\rho_0 \frac{\partial u}{\partial t} \qquad (2.4)$$

where ρ_0 is the dry density of the material. Moisture content u depends on relative humidity according to its corresponding isotherm. In conclusion, in order to use Equations (1)-(4), there are four magnitudes whose dependence on relative humidity should be known: u, λ, $D_{v,}$ and ρC_p.

A theoretical description of the material moisture buffer capacity, based on the heat-moisture transfer analogy, was proposed by the NORDTEST Project (Rode et al. 2005). The so-called ideal moisture buffering value, MBV_{ideal}, indicates the quantity

of water absorbed or released by the porous materials when a periodic variation of relative humidity is directly imposed on its surface. It is introduced as:

$$MBV_{ideal} = 0.00568 \cdot p_{sat} \cdot b_m \cdot \sqrt{t_p} \qquad (2.5)$$

where Psat [Pa] is the saturation vapour pressure, t_p [s] is the time period and b_m [kg/(m^{2}Pa·s$^{1/2}$)] is the moisture effusivity given by:

$$b_m = \sqrt{\frac{\delta \cdot \rho_0 \frac{\partial u}{\partial \phi}}{p_{sat}}} \qquad (2.6)$$

The MBV is normalized per % of relative humidity variation, its units being kg/(m^2%RH). The ideal MBV is primarily a material characterization while the MBV experimentally determined is a material/environment one, differing from each other by the air surface resistance (Rode et al. 2005; Abadie and Mendonça 2009).

2.4. Fire reaction analysis of lignocellulosic materials

The behaviour of bio-based materials in case of fire is a crucial aspect that should be well-known before establishing the feasibility of their use in construction. Several authors have analysed the thermal degradation and flammability of different raw bio-based materials and composites. Alvarez and Vázquez (2004) performed a thermal analysis of cellulose derivatives/starch blends with different sisal short fibre content, and discovered that the addition of the sisal fibres produced no significant effect on the thermal degradation of the composite materials in comparison with the matrix alone. Yao et al (2008) investigated the thermal decomposition processes of 10 types of natural fibres commonly used in the polymer composite industry. These fibres included wood, bamboo, agricultural residue, and bast fibres. Dorez et al (2013) considered cellulose, hemp, flax, sugar cane and bamboo as natural fibres, and polybutylene succinate (PBS) as a polymer matrix. Differences in chemical composition, together with other factors such as

crystallinity and the degree of polymerization, are on the basis of variations in the flammability of bio-based materials. High cellulose content materials tend to be more flammable while high silica content materials present better fire properties. Lignin has been shown to positively contribute to char formation which acts as a heat barrier, protecting the interior of the material (Chapple and Anandjiwala 2010). The treatments of fibres prior to their use in composites have also been analysed in terms of possible changes in their thermal degradation properties. For example, Rana et al. (1996) used a simple solvent and catalyst acetylation method on jute fibres and found that the thermal stability of acetylated jute was higher than the untreated jute. The addition of flame retardants in lignocellulosic materials has also been widely studied (Rana et al. 1996; Lewin 2005; Yao et al. 2008; Suardana et al. 2011). These kinds of retardants include phosphorus-based ones like di-ammonium phosphate (DAP) and sulfamic acid salts such as ammonium sultamate (Lewin 2005).

The strategy commonly used to analyse thermal degradation and fire behaviour combines small-scale thermal analysis such as Thermogravimetric Analysis (TGA) and/or Differential Scanning Calorimetry (DSC) with fire reaction tests such as cone calorimetre and Limiting Oxygen Index (LOI). However, the use of a microcalorimetre known as Pyrolysis Combustion Flow Calorimetre (PCFC) is also becoming common (Patel et al. 2011; Yang and He 2011). Microscale combustion calorimetry combines thermal analysis and oxygen consumption calorimetry, thus enabling the determination of Heat Release Capacity (HR) and Heat Release Rate (HRR) of small samples. Data from the PCFC have been shown to correlate well with other established fire tests (Lyon and Walters 2004; Cogen et al. 2009) and it has been approved as an ASTM International Standard for plastics and other solid materials (ASTM D7309:2007).

In addition to flaming combustion, that take place in gas phase between the generated volatile gases and oxygen, smouldering is commonly observed in the lignocellulosic materials (Hagen et al. 2011; Hagen 2013). Smouldering is a slow, flameless form of combustion that is sustained by the exothermic surface reaction between solid fuel and oxygen. This type of combustion is characteristic of porous materials which form a solid carbonaceous char when heated, and is frequently observed in cellulosic materials (Ohlemiller and Lucca 1983; Drysdale 1998; Hagen et al. 2011). Smouldering propagation is about ten times slower than flame spread over a solid. In spite of its weak combustion characteristics, smouldering is

a significant fire hazard. The initiation and propagation of smouldering are controlled by several interrelated factors such as the surface area per unit mass of fuel, the permeability and the thermal insulation (Moussa et al. 1977; Shafizadeh and Bradbury 1979; Drysdale 1998). He et al (2009) investigated the reaction heat of agro-stalks using a Simultaneous Thermal Analyser (STA), in air, using a crucible with lid. Based on the analysis of the DSC curves, the heat from the oxidative degradation of the polymer and the heat from char oxidation were obtained from experimental data. Ohlemiller (1990) analysed both unretarded cellulosic insulation and insulation having 25 wt% of the smoulder retardant (boric acid) added on. Boric acid was unable to halt the smoulder process but it slowed its spread by about a factor of 2. Several medium-scale devises have been proposed by different authors (Ohlemiller 1990; Hagen et al. 2011; Hagen et al. 2015) to analyse the kinetics of the smouldering process.

The fire behaviour of bio-based materials can be improved with the addition of flame retardants. Flame retardants are used to impede the ignition of materials and to slow down the spread of flames during the ignition phase of a fire. They can act in different ways: (1) by a cooling effect (achieved for instance by an endothermic decomposition), where the reach of the ignition temperature is delayed; (2) by a dilution effect, where the flammable materials are mixed with non-flammable decomposition gases which impedes ignition; (3) by the prevention of the free-radical formation, which is an exothermic reaction that provides additional heat to the combustion process; or (4) by the formation of a charred layer with a high melting point (carbonization) at the surface of the substrate, which prevents the oxygen from reaching the flammable material. Regarding their mode of action and their chemical constitution, fire retardants can be classified into halogenated, organic flame retardants containing phosphorus, inorganic phosphorus compounds, inorganic metal hydroxides, boron compounds and nitrogen compounds (Leisewitz et al. 2001). In particular, flame retardants containing phosphorous promote the formation of a charred layer which hinders the progress of decomposition through oxidation (smouldering). On the other hand, boron compounds act in several combined modes and are usually used in cellulosic materials. In general, there is a lack of data regarding the toxicity and eco-toxicity of the flame retardants, although some initiatives have been carried out aiming to evaluate this issue. Leisewitz et al. (2001) presented an evaluation of 14 of the most commonly used substances,

concluding that the application of red phosphorous, ammonium polyphosphate and aluminium trihydroxide is unproblematic from a toxicological viewpoint.

2.5. Mould growth resistance of bio-based materials

Bio-based materials have been used in construction for centuries and can last many thousands of years under proper conditions (Summers et al. 2003). However, they can also degrade due to the action of microorganisms such as fungi or bacteria, which compromises their durability. The activity of such microorganisms depends on environmental factors, mainly moisture and temperature and on the substrate characteristics such as nutrient content or hygroscopicity.

Crop by-products and other bio-based materials represent a potential source of nutrients for fungi and bacteria. However, under the same environmental conditions, they are not equally affected by mould growth. Their resistance against mould growth determines their suitability for application. A number of standardized methods are available for mould growth resistance assessment, generally based on the same principles. The materials are inoculated with fungi spores and exposed for a certain period of time to favourable conditions for mould growth (90-95% RH and more than 20ºC). After that, mould growth is evaluated using different means, such as visual inspection or gravimetrically. A comprehensive comparison between several methods can be found in Johansson (2014). The above mentioned methods are usually intended to compare materials in a worst case scenario, but do not provide information on how a material will perform in a building, where moisture conditions are not as severe as in laboratory tests (Johansson 2014). In order to evaluate the mould growth resistance of building materials, the critical moisture level, defined as the limit of environmental conditions from which mould growth on a specific material is possible, is to be determined. Johansson (2014) compared a laboratory method determining the critical moisture level of different materials with on-site measurements and found that, in general, results can be extrapolated. However, the effect of magnitude and frequency of RH and temperature changes in real conditions have to be considered for accurate mould growth predictions. Other causes of discordances between laboratory and on-site results are the fungal species present and spore exposure of the materials (Johansson et al. 2012). In laboratory tests, few fungal species are present, at controlled, high concentrated doses of

spores, while on building conditions a larger number of fungal species is expected at unknown concentrations. In order to closely reproduce a real exposure situation and to prevent unknown changes to the substrate, the use of naturally occurring spores of non-sterilised nor inoculated substrates has been proposed by Thomson (2014). Johansson (2011) uses a five-point rating scale mould growth assessment based on visual inspections which has the advantage to be rapid and effective. Results are presented in figures where the rating is plotted against time. So mould growth by time can be assessed for different substrates and at different RH or temperatures, but not at simultaneous variations of both parameters. Hofbauer et al. (Hofbauer et al. 2008; Sedlbauer et al. 2011) proposed to use an isopleth system to create a material specific profile showing at which climatic conditions (temperature and relative humidity) similar mould activity takes place. These material specific graphs allow a quick and easy comparison among the different building materials and are compatible with moisture transfer modelling such as WUFI simulations (Thomson and Walker 2014). They are completed using a red-light system where the environments presenting no risk, low risk and high risk of mould growth in a specific substrate are coloured in green, orange and red respectively. Moreover, Sedlbauer (2001) proposed a simple classification of materials into three categories, regarding their mould growth resistance: Class I for poor resistant materials experiencing mould growth from 70% RH, Class II for medium resistant and Class III for the most resistant materials, which safely resist high air relative humidities (>90%). They found that bio-based materials present extremely different resistance profiles: hemp showed a rather high resistance to mould growth (similar to mineral based materials) while straw was far less resistant. The isopleth graphs of these materials presented by Sedlbauer et al. (2011) are shown in Figure 2.3.

The mould growth resistance of a material can be improved with (1) the addition of biocides, (2) the modification of the raw materials so that they are less easily attacked by enzymes or (3) the incorporation of protective coatings and paintings. Boric acid and derived salts such as borates are commonly used as biocides in some commercial insulation materials such as blowing cellulose (e.g. *Homatherm flexCL, Thermaflox* and *Isocell* cellulose insulations). Such substances have the advantage to act both as a biocide and as fire retardant and used to be considered a greener alternative to metal based fungicides, commonly used in wood preservation. However, nowadays their toxicity is under evaluation and their use is limited by the

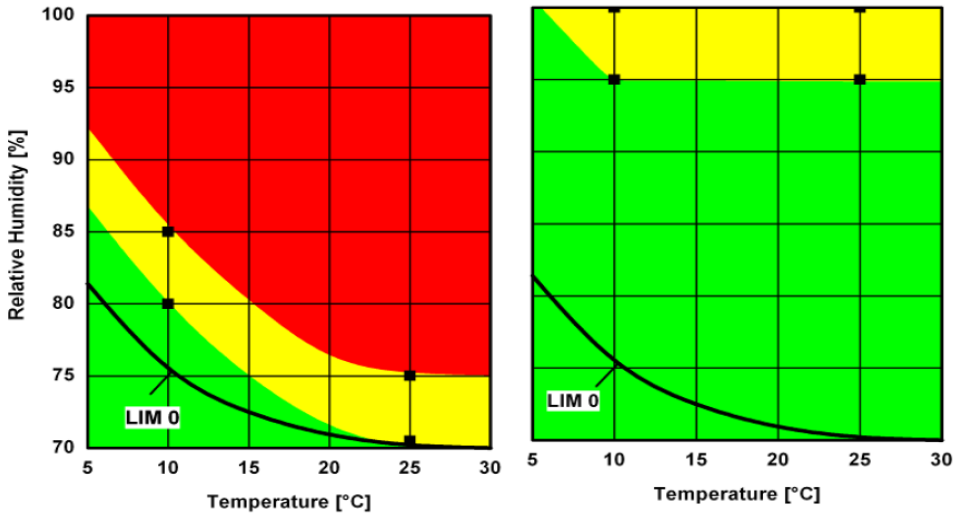

Figure 2.3. Isopleth graphs of straw (left) and hemp (right) presented by Sedlbauer et al. (2011)

European regulation, to a concentration under 5.5% (w/w) of the final products (ECHA 2010). Lesar (unpublished) compared the fungal and fire resistance of cellulose insulation boards treated with boric acid and aluminium hydroxide. The author used different percentages of both products and found that a mixture of 3% of boric acid and 6% of aluminium hydroxide gave the best results. Some studies point out that leaching over time, one of the main drawbacks of boric treatments, can be reduced with the incorporation of mimosa tannins (Thevenon et al. 2010; Liibert et al. 2011; Tondi et al. 2012). A further approach is the use of non-biocidal techniques for protection against fungi. Bio-based raw materials can be modified to change the molecular configuration of their components or reduce their hygroscopicity. Acetylation (Karr and Sun 2000; Bledzki et al. 2008) or lauryl gallate laccase mediated grafting are two examples of such treatments (Garcia-Ubasart et al. 2011; Dong et al. 2014). Moreover, raw materials can be impregnated with water repellents, such as waxes (Lesar et al. 2011) or coated with inert substances that create a physical barrier between the substrate and the biotic agents. Lime has been traditionally used in construction to prevent mould growth and is still used in agriculture as an effective fungistatic. Lime coatings generate an alkali environment (pH about 12.5) which is an adverse media for mould growth.

3. AVAILABILITY OF CROP BY-PRODUCTS

3.1. Introduction

In this chapter, the amount of available crop by-products to be used as raw materials in the production of bio-based thermal insulation boards in Spain is investigated. The results are contrasted with two different estimation scenarios of future demand of thermal insulation materials in the construction sector with the aim to determine whether the existing resources would be sufficient to meet such demand.

Crop by-products are an important portion of the total biomass yearly produced in Europe and Spain, and will still be in the near future (Panoutsou et al. 2009; Boyle et al. 2010; Hernandez and Fuertes 2011; IDAE 2011). According to Panoutsou et al. (2009), the total available biomass in the EU27 in the year 2010 was about 159 Mt, 34% of which consisted of crop by-products. The rest was scattered between forestry, wood waste biomass and industrial biomass such as solid industrial residues, black liquor or sewage sludge. Hernández and Fuertes (2011) estimated in 36.2 Mt/year the total biomass available in Spain for the period 2005-2007, 50% of which corresponded to crop by-products. Among them, the most abundant were cereals' and sunflowers' by-products (that is, straw, stalks and husks) which represented about 90% of the crop by-products yearly produced in Spain. A similar estimation was made for the period 2008-2010, following the methodology presented by Hernández and Fuertes (2011). The results show that the distribution of crop by-products is maintained, confirming that practically the totality of crop by-products produced in Spain correspond to cereals and sunflower. Thereafter, it

was decided that the estimation on the availability of crop by-products in Spain would be focused on these crops alone.

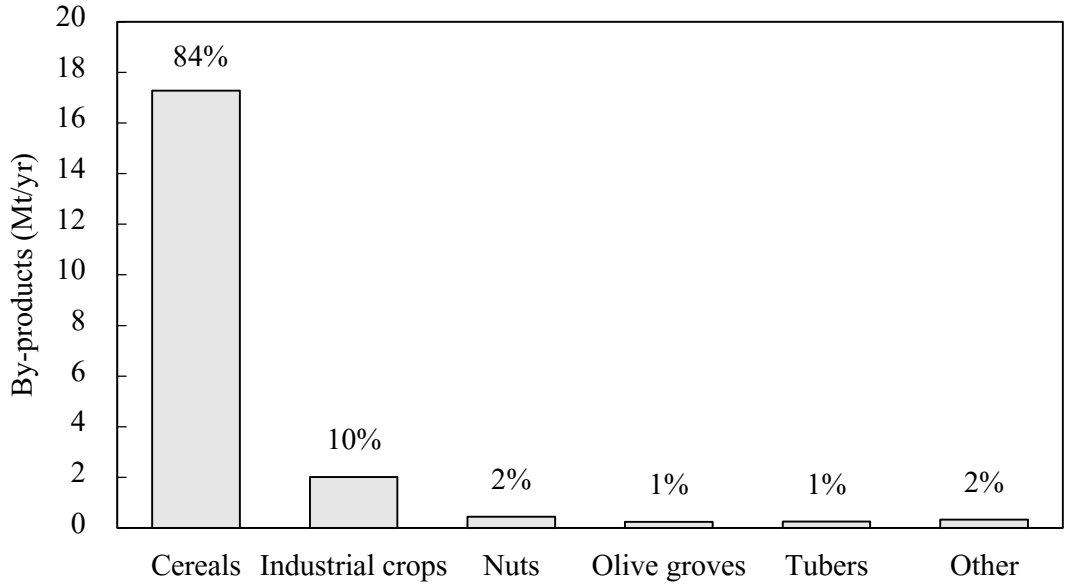

Figure 3.1. Average of the crop by-products yearly produced in Spain (dry basis) for the period 2007-2010. Values taken form Hernandez and elaborated by the author following his methodology.

Due to the rising interest in the energetic use of biomass, a large number of studies exist nowadays that evaluate the availability of agricultural residues at different territorial scales (Jölli and Giljum 2005; Ericsson and Nilsson 2006; Fischer et al. 2007; Copeland et al. 2008; Boyle et al. 2010; Scarlat et al. 2010; Bava et al. 2012). Such evaluation can be statistically based, using crop production or crop surface area as input data, or based on RS and GIS technologies. Long et al (2013) presented a comprehensive review comparing such methodologies. Nevertheless, statistically based methods are the ones most commonly used. In these methods, calculations based on crop production are preferred over those based on crop surface areas, as factors such as crop yields are included in the calculation, which results in a greater accuracy of the estimates. With this methodology, the production of crop by-products (Bt) is estimated from the grain production using Equation (3.1), which takes into account both the residue to product ratio (RPR) and the natural moisture content (MC) of each kind of crop. Some authors also use the harvest index (HI), which correspond to the fraction of the crop that is harvested and is related to the RPR as shown in Equation (3.2).

$$Bt = p \times RPR\,(1 - mc) \qquad (3.1)$$

$$RPR = \left(\frac{1 - HI}{HI} \right) \qquad (3.2)$$

Values of MC and RPR vary from author to author as they are dependent on local factors such as the type of farming practices, the climatic conditions or the kind of soil, which are not easily included in large scale estimations. A review of the different RPR and MC factors used by different authors can be found in Scarlat (Scarlat et al 2010; 2011).

It is important to note the difference between the total crop by-products (Bt) and the available crop by-products (Ba). Bt corresponds to the crop by-products produced yearly in a certain territory while Ba corresponds to the crop by-products that can be exploited. Thus, as it is expressed in Equation (3.3), the difference between Bt and Ba are the unavailable crop by-products that are either allocated for other uses (Bu) or re-incorporated into soils to maintain their productivity (Bf).

$$Ba = Bt - Bu - Bf \qquad (3.3)$$

As was earlier the case, Bu and Bf are difficult to estimate as they depend on local factors. The values of RPR and weighting of Bf, Bu and Ba encountered in literature review are summarised in Tables 3.1 and 3.2. Therefore, it is not surprising that discordances on the evaluation of Ba are higher than in Bt. In fact, Jölli and Giljum (2005) pointed out the scarcity of comprehensive data on crop by-products availability (Ba) despite the large number of published works, a fact that was confirmed from the reviewed literature.

Fischer et al. (2007) using FAOSTAT databases estimated that the production of crop by-products (Bt) in EU-27 between 2000 and 2002 was 457 Mt, 47% of which corresponded to available crop by-products (Ba) and three-quarters of Ba came from cereals. Ericsson and Nilsson (2006) calculated the energy produced from cereal (wheat, barley, rye and oats) and maize residues for EU-15. Data was taken from FAO and average yields between 1998 and 2002 were used for calculation. Bt was calculated from grain production, establishing a ratio straw to grain of 1.3 for cereals and 1 for maize. It was assumed that only 25% of Bt would be harvested

and that a third of the harvested Bt would have already been used in existing activities. In a report realised by the Bloomberg New Energy Finance, BNEF (Boyle et al. 2010), it was assumed that only 17.5% of the total crop by-products is available, which may be considered as a conservative assumption (Kretschmer et al. 2012). Wheat straw, sugar beet residues, barley straw and maize stover were signalled as the main crop by-products available in EU-27, which account for about 156 Mt. Boyle et al. (2010) also estimated that the biomass residue supply for 2020 in Spain will be between 19 and 23 Mt (that is between 15 and 18.4 Mt of crop by-products), which puts this country among the top five biomass producers in Europe. Hernandez and Fuertes (2011) quantified the total biomass production in Spain from 2005 to 2007. It was found that an average of 17.4 Mt of crop by-products was produced yearly. Among these, 83% was cereal straw (about 14.5 Mt). In this case, Ba from cereals was equivalent to 50% of their Bt. Similar results were presented by IDAE (Instituto para la Diversificación y Ahorro de la Energía) in the PER11-20 (IDAE 2011). In this work, crop by-products referred only to cereal straw and corn stalks and Bu was estimated to be 50% of Bt. Neither of these two works considered Bf, although it seems to be a relevant factor, especially in Spain, where more than 50% of the soils are classified as medium-high risk of desertification (Artigas et al. 2011).

Table 3.1. Residue to Product ratio (RPR) values of the different crops used by different authors.

Author	Territory	Straw				Stalks		Husks
		Barley	Wheat	Rice	Others	Maize	Sunflower	Rice
Ericsson and Nilsson 2006	Europe				1.3	1		
Fao 2007	Europe	1.2	1.0		1.3-4.0	2.0		
Fischer et al 2007	Europe	2.5	1.8	2.0		3.5	2.0	
Hernández and Fuertes 2011	Spain	1.1	1.1	1.3	0.7-1.0	0.4	2.0	
Kim and Dale 2004	Wold	1.2	1.3	1.4	1.3	1		
Sahito et al 2012	Pakistan		1	1.1				0.5
Scarlat et al 2010	Romania	1.1-1.8	1.1-1.9		1.1-1.4	1.0-1.5	2.2-3.5	
Wang et al 2013	China		1.3	1.0	2.3	0.9		0.2

Table 3.2. Percentages of the produced crop by-products reincorporated to fields (Bf), currently used (Bu) and available (Ba) according to different authors.

Author	Territory	Bf	Bu	Ba
Copeland and Turley 2008	UK	40.0	12.0	48.0
Scarlat et al 2010	Romania	53.7	6.8	39.6
Ericsson and Nilsson 2006	Europe	75.0	8.3	16.7[a]
BNEF 2010		75.0	7.5	17.5
Hernández and Fuertes 2011	Spain	0.0	50.0	50.0
WWF 2012		-	-	35[b]
Di Blasi et al 1997		0.0	40-60	40-60[c]

[a]For maize is Ba=25; [b] For rice is Ba=30; [c] For rice is Ba=70-85 and for Sunflower Ba=90-100.

In fact, there is an open discussion on what is the amount of by-products that should be retained in the soils in order to ensure a sustainable crop production and, to the author's knowledge, there is no conclusive published work in this regard, probably because it depends to a large extent on specific local conditions (Fischer et al. 2007). In particular, in the case of cereals, it was generally assumed that 50% of the straw could be removed without any significant impact on soil fertility or soil erosion (Fischer et al. 2007; Martinez 2013), but recent studies tend to be more conservative. A report carried out by WWF (Singer and Denruyter 2013) indicated that, generally, an extraction rate between 20% and 40% is recommended, while the International Energy Agency recommends an extraction rate of 25% (Boyle et al. 2010). In Spain, Martinez (2013) estimated that the average loss of humus in fields is 700Kg/ha·year, with a notable variation observed from one field to another. For cereals, it is estimated that roots and stubble (which account for 60-80% of the straw) can provide between 300 and 1000kg/ha·year of humus (Canet and Instituto Valenciano de Investigaciones Agrarias 2014), which leaves a margin for straw exploitation. However, experiments carried out on non-irrigated cereal crops in Andalucía (Lacasta and Meco 2005) showed that humus can increase by about 100% in 20 years when incorporating all the straw, and in general, the more straw that is left, the better. On the other hand, the intensity of current crop production may impede the incorporation of crop by-products in the soil, as degradation cannot take place over such short periods of time. To improve degradation, by-products are triturated and Nitrogen is added or the materials are composted somewhere else

before being incorporated. The speed of degradation depends on several factors, but in Spain, the most restrictive of these is low rainfall during summer periods. Cereal straw, and especially pruning waste, degrade slowly due to their high C/N ratio (Canet and Instituto Valenciano de Investigaciones Agrarias 2014).

3.2. Methodology

3.2.1. Availability of crop by-products

The estimation of the total crop by-products (Bt) produced yearly in Spain was undertaken for the period 2008-2010 with the statistically based method, using baseline data provided by the Spanish *Ministerio de Agricultura, Alimentación y Medioambiente* (MARM). Statistical data from MARM is created from on-site enquires (ESYRCE) and data compiled from regional organisms. Crops are divided into 13 categories and information on production, crop areas and agricultural yield, among several others, is provided yearly. The statistical year-book also includes the volume of harvested straw, that is straw already used, which is usually estimated to represent 50-55% of total straw production (Hernandez and Fuertes 2011; Bava et al. 2012; Martinez 2013). As explained above, the estimation was limited to main crops, which is cereals and sunflower. Bt (dry basis) was calculated from grain production using Equation (3.3). The values of RPR and MC used were those provided by Hernandez except for RPR of rice husk that was set at 0.3. Ba was assumed to be 37% of Bt as it corresponds to the average percentage found in the reviewed literature (see Table 3.2).

3.2.2. Estimation of demand for insulation materials

The results on the availability of crop by-products are contrasted with two different estimations of future demand of crop by-products as raw materials for bio-based thermal insulations. Such estimations are based on two different scenarios.

In the first scenario, the forecast demand corresponds to the volume of insulation that is required in building retrofit if the targets for reducing greenhouse gases (GHG) emissions by the year 2050 posed by the European Commission are to be fulfilled. Such targets urge member countries to reduce the internal GHG emissions by 80% in the year 2050 with respect to their 1990 emissions levels. In Spain,

according to the reports presented by the GTR (Spanish acronym for Working Group on Refurbishment), this only can be achieved by refurbishing about 10 million dwellings between now and the year 2050 (Cuchí and Sweatman 2011; 2012; 2014). These reports provide information on the current situation of the existing building stock and suggest the measures that should be adopted in order to reduce its energy consumption by 80%. From the U values presented in the GTR reports it is possible to estimate the potential demand for thermal insulation materials and, thus, the volume of crop by-products needed to produce them. For the purpose of the calculation, the assumption is made that the density and the thermal conductivity of the thermal insulation materials is constant and equal to the average values of existing bio-based insulation products, as shown in Table 3.3.

Table 3.3. Density and thermal conductivity of existing NFI materials. [1] Data from existing NFI materials. [2] Data from the literature (Pfundstein 2007).

Raw material	Form of supply	Density (kg/m^3)	λ (W/mK)
Cereal Straw[1]	Pellets	110	0.050
Cereal Straw[2]	Bales	100	0.055
Hemp[1]	Board	43	0.042
Hemp[2]	Board	44	0.045
Wood[1]	Board	172	0.042
Wood[2]	Board	150	0.045
Coconut[1]	Board	95	0.045
Coconut[2]	Board	95	0.045
Flax[1]	Board	36	0.039
Flax[2]	Board	50	0.041
Cork[1]	Board	151	0.039
Cellulose[1]	Loose fill	138	0.047
Average		**99**	**0.045**

The second scenario is based on the forecast of the volume of the Spanish insulation market for the period 2013-2018 (Rockwool 2013). While the first scenario takes only housing refurbishment into account, in the second, three different groups of

constructions are considered: housing refurbishment, housing (both refurbishment and new construction) and the whole building sector.

In both scenarios, the demand of food crop by-products (dry basis) is estimated taking into account the following assumptions:

1) Total demand is met exclusively with insulation materials based on crop by-products, that is, their market share corresponds to the whole Spanish insulation market. This assumption over-sizes the results, since the market share of natural insulation materials is much lower, as discussed in Section 1.1.
2) 10% of the insulation materials correspond to binders and additives, which means that only 90% correspond to crop by-products.
3) 20% of the raw materials are lost during transportation and production.

As a result, the demand for food crop by-products ($D_{by\text{-}products}$) is calculated using the following equation:

$$D_{by-products} = V_{ins} \cdot \rho_{ins} \cdot 0.9 \cdot 1.2 \qquad (3.4)$$

where V_{ins} is the volume demand of insulation in m^3 and ρ_{ins} is the average density of existing insulations as shown in Table 3.3. Factor 0.9 refers to assumption 2 and 1.2 refers to assumption 3.

3.3. Results and discussion

3.3.1. Availability of crop by-products in Spain

Barley straw and wheat straw are the most abundant crop by-products, followed by corn stalks and rice straw and husks. Sunflower by-products are also copious, even exceeding some types of cereals such as rye or oats. These top five crop by-products account for 77% of Ba, and their availability is evaluated over a longer period of time (from 2004 to 2011). Results are shown below in Figure 3.2.

On average, the volume of Ba for the top five crops is 6.6 Mt·year-1. Even if the volume tends to be constant over time, important fluctuations are revealed, possibly as a consequence of climatic conditions and other drivers, such as crop policies,

among others. The standard deviation is 1.2 Mt. The distribution of this production throughout the territory is shown in Figure 3.3. The Ba from barley and wheat are distributed throughout the whole country, while Ba from corn and sunflowers are complementary. A large part of the available crop by-products are concentrated in the northern and central areas of Spain and in Seville. Rice Ba are confined to specific areas such as Valencia and the south-west of the country.

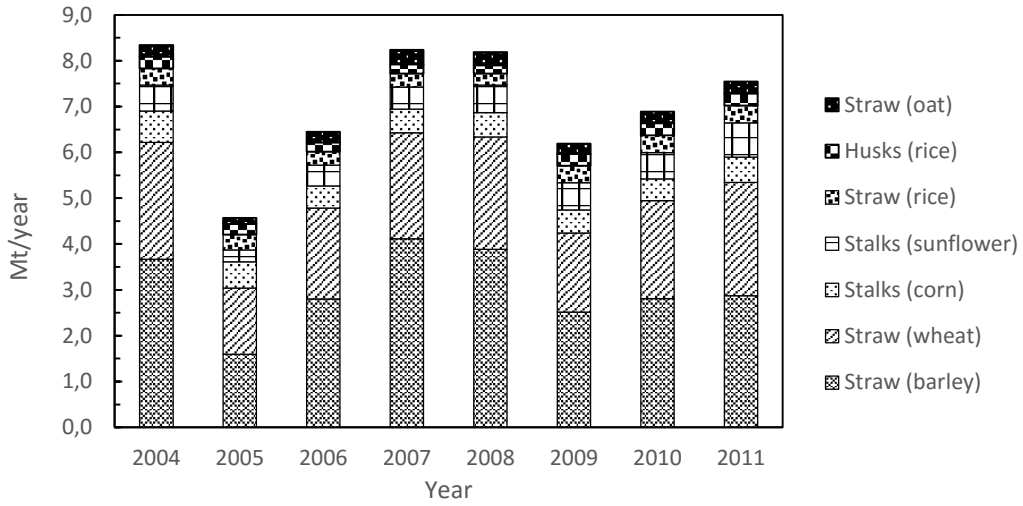

Figure 3.2. Fluctuation over time of the Ba for the top seven crops in Spain.

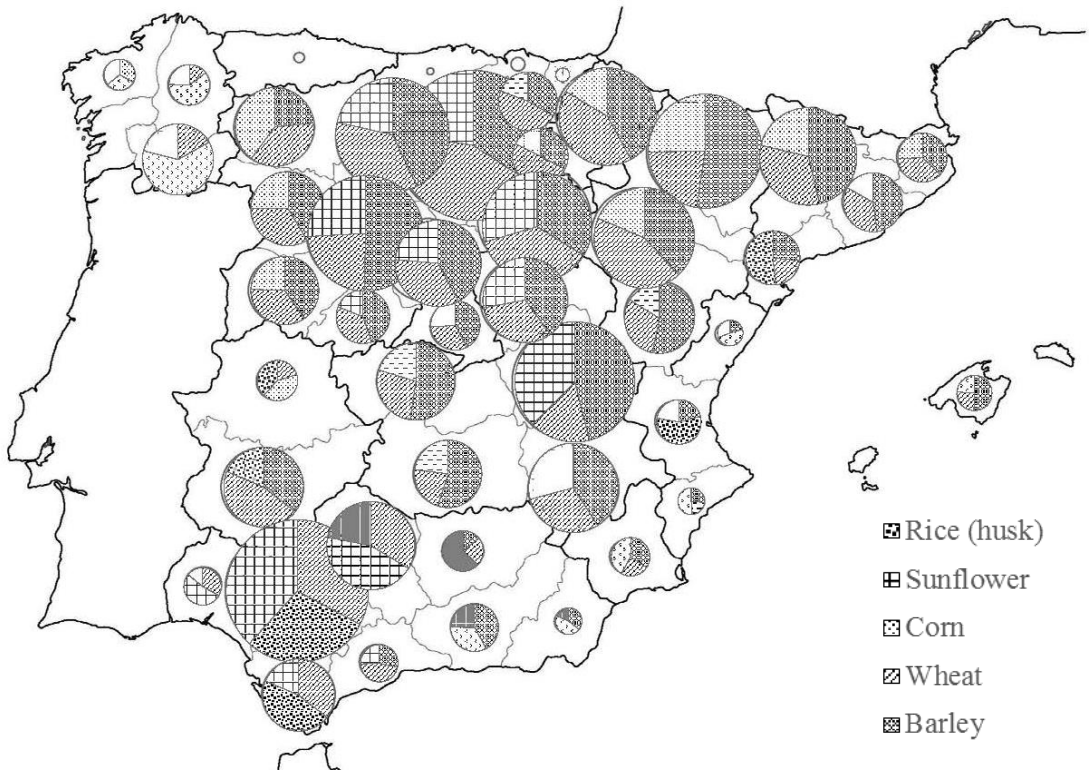

Figure 3.3. Distribution of main crop by-products by province (Data for 2010 from MARM)

3.3.2. Estimation of demand for crop by-products to be used as raw materials for natural thermal insulations

A range for the demand of crop by-products is estimated according to the two different scenarios described in the methodology. Results are shown in Table 3.4. The two chosen scenarios differ widely in their forecasts: the first presumes a break in the trend in order to meet political goals, while the second represents a continuation of the present situation. Thus, in the first scenario, about 0.5 Mt of cop by-products are needed each year to cover the demand for housing refurbishment, while in the second this figure falls to 0.06 Mt. In the latter scenario, 1.1 Mt of crop by-products are needed to meet the whole demand for building insulation materials in Spain.

A crosscheck between demand and availability shows that 16.4% of the top five Ba would satisfy the total annual demand for building insulation materials. Less than 0.5 Mt of crop by-products would be used in housing refurbishment, which corresponds to the availability of corn by-products. These results, therefore, suggest that insulation based on crop by-products could be developed without competing with existing uses or compromising soil fertility, since it would require 5.3% and 12.6% of the total Bt and Ba respectively.

Table 3.4. Estimation of demand for crop by-products under the two scenarios evaluated. Bt5 and Ba5 correspond to the top five crops.

Scenario			Demand			
			Insulation (m3)	Crop by-products (Tn)	Bt5 (%)	Ba5 (%)
GRT	Housing	Refur	4,656,172	497,838	2.8	7.5
RW	Housing	Refur	537,822	57,504	0.3	0.9
		Refur + new constr	3,229,737	345,323	1.9	5.2
	Building	Refur + new constr	10,102,969	1,080,209	6.1	16.4

3.4. Conclusions

The availability of crop by-products to be used as raw materials for building thermal insulations is evaluated. Availability is compared to the demand forecast on the basis of two different scenarios. Although the results vary greatly from one scenario to another, they indicate an order of magnitude from which it is possible to draw some conclusions.

A sustainable production of insulation materials based on crop by-products seems to be feasible. The results show that, by and large, enough crop by-products exist to meet all the estimated demand without compromising other existing uses or soil fertility. Even when demand is greatly over-sized, it would still require less than 17% of the available crop by-products produced every year in Spain. Available corn by-products would be enough to insulate between 250,000 and 450,000 dwellings annually.

Thus, insulation production would not compete with other emerging industries such as energy production in the use of these raw materials.

Future research should explore the technical feasibility and characterization of insulations based on crop by-products, especially from barley, wheat, corn, rice and sunflowers. These top five crop by-products represent 77% of the total available by-products (6.6 Mt·year-1).

Potentially, insulations based on crop by-products constitute an economically viable and sustainable alternative to existing materials, depending on the production process. A similar production process to that implemented for the existing natural thermal insulations would foreseeably be required.

4. LABORATORY TESTS

This section presents the laboratory test methods used in the experimental work of the present thesis. The experimental campaign is divided into four different parts each one aiming at different objectives:

1. Materials' characterization, mainly focused on the thermal and the hygroscopic properties which are relevant to thermal insulation materials.
2. Analysis of the materials' hygrothermal performance.
3. Evaluation and improvement of the materials' behaviour in front two important degradation agents of bio-based materials.
    a. Fire
    b. Fungal attack
4. Evaluation of the materials' durability.

Such test methods were used in evaluating: the raw materials, either the crop by-products or the biopolymers; the preliminary formulations of the six different experimental bio-based thermal insulations tested; the corn pith-alginate boards; and the ETICS systems incorporating the corn pith-alginate boards. Table 4.1 summarises the tests performed on each kind of material.

Table 4.1. Experimental tests methods used at each step of the material development.

	Laboratory test methods	Crop by-products	Biopolymers	Experimental bio-based materials	Corn pith alginate boards	ETICS systems
1	**Physical properties**					
	Gas pycnometry	X		X		
	Scaning Electron Microscopy	X	X		X	
	Mercury porosimetry	X		X		
	Surface area analysis	X				
	Thermal properties					
	Electronic Thermal Analyser	X		X	X	
	Heat Flow Meter				X	
	Hygroscopic properties					
	Water sorption isotherm analysis	X		X	X	
	Water vapour permeability test			X	X	
2	**Hygrothermal performance**					
	Dynamic hygric test: MBV				X	
	Dynamic higrothermal test	X		X	X	X
3a	**Small scale flammability**					
	Pyrolysis Combustion Flow Calorimetry	X	X	X	X	
	Thermogravimetric Analysis	X	X	X	X	
	Medium-scale flammability					
	Ignition time and extinguishability test			X		
	Limiting Oxigen Index test			X		
	Smouldering					
	Smouldering test				X	
3b	**Fungal resistance**					
	Fungal growth				X	
4	**Durability / mechanical**					
	Accelerated ageing test					X
	Cohesion test					X
	Karsten tube					X
	Shrinkage					X

4.1. Characterization

4.1.1. Physical properties

Density and porosity are probably the most relevant physical properties in the assessment of the hygrothermal performance of materials. Characterization of porous materials normally implies the determination of the total volume of porosity and the pore size distribution curve. Moreover, other aspects such as specific surface area, pores' morphology and interconnectivity are also important. Such aspects influence the hygrothermal performance of the materials. In this work, the porosity of the raw materials and the composites is investigated using the different methods described below.

4.1.1.1. Gas pycnometry

The skeletal density of the materials is determined by gas pycnometry. Such method uses the technique of volume displacement to measure the volume of the solid skeleton of any kind of material with high accuracy. Helium gas is usually used as it is inert and able to penetrate pores of up to 2 Angstroms. In this thesis, a Micrometrics AccuPyc 1330 gas pycnometre from the SCTUB is used. Thereafter, the bulk density of the materials is calculated by measuring the dimensions of the samples, and open porosity is determined by taking the ratio between skeletal and bulk density.

4.1.1.2. Scanning Electron Microscopy (SEM)

The porous structure and the surface morphology of the materials was visually analysed using the Scanning Electron Microscopy (SEM). SEM is a type of electron microscope that produces images of a sample by colliding an accelerated electron beam to it. Such collision produces various signals (secondary electrons, back-scattered electrons, characteristic X-rays) providing information about the sample's surface topography and composition. The most common mode of detection is by secondary electrons (SE) emitted by atoms excited by the electron beam. SE provide topographic images, which inform about surface morphology and relief. SEM is characterized by its high resolution (which can be better than 1 nanometre) and its depth of field, which gives three-dimensional images.

In this thesis the device used was the Jeol JSM-7001F Field Emission from the UPC. The observation was made by SE mode. Before the tests, the samples were sectioned using a scalpel, oven-dried at 60ºC for 24 hours and placed in a sticky holder. In order to limit the possible alteration of samples, no further pre-treatment other than metallisation was used (Magniont 2010).

4.1.1.3. Mercury Porosimetry

The pore size distribution of a material can be determined using a mercury porosimetry, a destructive test where the pores are filled with mercury through the effect of a controlled applied pressure, or gas adsorption and where porosity is characterized through sorption isotherms of a gas such as nitrogen. The Mercury Porosimetry is appropriated in a range between 360 microns to 30 angstroms, while gas adsorption gives information of smaller pore sizes, between 0.1 microns and 4.0 angstroms. In this thesis, Mercury Porosimetry was used to determine pore size distribution of the materials as it covers a wider range of pore sizes. Gas adsorption was used to determine the Brunauer-Emmet-Teller (BET) surface area of the materials, as detailed subsequently.

Besides pore size distribution, mercury porosimetry provides information about pore volume, bulk apparent density and specific surface of porous materials. The principle of such technique is based on the fact that mercury behaves like a non-humectant liquid with a wide range of materials which means that it does not penetrate into the voids of a material unless a pressure is applied. This is due to its surface tension and its contact angle, which is higher than 90º. The pressure applied is thereafter mathematically correlated using the Washburn equation (2.1) with the diameter of the pores intruded by mercury:

$$D = -\frac{4\gamma cos\theta}{P} \qquad (4.1)$$

where γ is the surface tension, for mercury 0.480-0.485 N/m; θ corresponds to the contact angle, between 130 and 140º, and P is the required pressure.

It is important to note that the results do not correspond to the real pore structure, but to the pore size distribution of a porous system built on cylindrical pores of equivalent diameter. Moreover, pore walls of weak materials may be destroyed, due

to high pressure during analysis which might lead to erroneous results. Sample pre-treatment is not required and is often not used.

The mercury Porosimetry was performed using a Micrometrics AutoPore IV 9500 at the University of Navarra. The testing parameters are summarised in Table 4.2.

Table 4.2. Testing parameters of the mercury porosimetry test performed.

Pen. Constant (μL/pF)	11.117	Adv. and Rec. Contact Angle (º)	130.000
Stem Volume (mL)	0.3660	Hg Surface Tension (dynes/cm)	485.000
Pen. Volume (mL)	5.9673	Hg Density (g/mL)	13.5335
Pen. Weight (g)	62.8202	Evacuation Pressure (μmHg)	50
Max. Head Pressure (MPa)	0.030682	Evacuation Time (min)	5
Assembly Weight (g)	140.5112	Mercury Filling Pressure (MPa)	0.0017
		Equilibration Time (s)	10

4.1.1.4. Surface area analysis

The specific surface area is the dividing line between a solid and its surroundings. It is expressed in terms of the total surface area of a material per unit of mass (m^2/kg) or per unit of volume (m^2/m^3). This property gives information about the porous structure and the surface interaction of the material, as it expresses the quantity of surface of the material that is available for phenomena, such as water adsorption or adhesion with binders. The BET model is the most common method for determining the surface area of porous materials. In this technique, the surface area of the solid is evaluated from the measured monolayer capacity of the material (w_m) which is the adsorbate content when the adsorbent surface area is covered with a complete unimolecular layer. Gas Adsorption analysis is generally used for such measurement and nitrogen is most commonly used as the adsorbate. Samples are exposed to the gas at its liquefaction temperature (-195ºC for N_2) under relative pressures less than unity (generally in a range between 0.025 and 0.30) which are achieved by creating conditions of partial vacuum. High-precision pressure transducers monitor those pressure changes (in a fixed and known volume) due to the adsorption process. The specific surface area ($A_{BET)}$ is then calculated using the equation:

$$A_{BET} = \sigma_m N \frac{w_m}{M} \qquad (4.2)$$

where A_{BET} is the specific surface area of the adsorbent; σ_m is the diameter of a single adsorbate molecule; N is the Avogadro's number, w_m is the monolayer capacity of the material and M is the molecular weight of adsorbate.

4.1.2. Thermal properties

4.1.2.1. Electronic Thermal Analyser

The thermal conductivity (λ) and thermal diffusivity (α) of the materials can be determined with the electronic thermal analyser Quickline-30 Thermal Properties Analyser, using a surface probe of a needle probe. The measurement is based on the analysis of the temperature response of the material to heat flow impulses induced by electrical heating using a resistor heater having a direct thermal contact with the surface of the materials (ASTM D5930 standard). The advantage of this technique is that it is possible to perform rapid measurements on small samples with accuracy of 5% of reading at temperatures between -20 to 70ºC. Moreover, the device calculates the value of the product of density and specific heat capacity (ρC_p) using the equation:

$$\alpha = \frac{\lambda}{\rho C_p} \qquad (4.3)$$

4.1.2.2. Heat Flow Meter

The Heat Flow Meter (HFM) is a device capable of measuring the thermal conductivity and the heat capacity of materials. To measure thermal conductivity, the HFM must be operated on the principle of the stationary slab method (EN 12664). Samples are placed between an upper and lower plate which are maintained at different temperatures. This generates a heat flux through the sample which is registered during the test by heat flux transducers bonded to the centre of both plates. The thermal conductivity is calculated as soon as the equilibrium is reached using the one-dimensional steady-state Fourier equation. In this work, the tests were performed at three different mean temperatures: 10ºC, 20ºC and 30ºC, being the

temperature gradient between the plates 20ºC in all cases. Temperature equilibrium was set at 0.2ºC, with a minimum number of 25 blocks and 5 calculation blocks.

4.1.3. Hygroscopic properties

4.1.3.1. Water sorption isotherm analysis

As discussed earlier, a porous material can be regarded as a three-phase system in dynamic equilibrium with the environment, as the amount of water and water vapour present in the pores changes with relative humidity and temperature. Such phenomenon is called sorption. The relationship between the water content of a porous material and the relative humidity of its environment at a determined constant temperature and steady-state conditions is represented through its (water) sorption isotherm.

Distinct porous materials present different isotherms with pronounced shape differences. Besides, such isotherms may present hysteresis, whereby the moisture content of the material in desorption is higher than in adsorption. The mechanisms responsible for hysteresis are not completely understood thus far although the related phenomena classically described in literature are capillary condensation, the ink-bottle effect or the difference in contact angle between adsorption and desorption (Collet et al. 2008; Magniont 2010). Moreover, the isotherms of a material measured at different temperatures are similar in shape but displaced: as the temperature increases, the moisture content of the material at a certain relative humidity decreases. The 1985 IUPAC classification distinguishes between six different types of isotherms, with reference to pore size, and four different types of hysteresis loops, related to the pore structure. Characteristically, cellulosic and lignocellulosic materials show a Type II isotherm (sigmoidal shape) and hysteresis. According to BET Theory, it is possible to distinguish between three different zones in the sorption isotherm: monolayer adsorption, where water molecules bond with hydroxyl groups on the material matrix; multilayer adsorption, where the water molecules overlay to those already covering the material surface; and capillary condensation, where the pores begin to fill up with liquid water. Figure 4.1 (Straube 2006) shows the different zones of the sorption isotherms according to BET Theory: monolayer adsorption (A); multilayer adsorption (B) and capillary condensation (C). The zones of capillary suction (D) and of supersaturated regime (E), do not correspond to the adsorption process but to the free capillary water.

The sorption isotherm is generally determined by exposing the material to an environment where the relative humidity is controlled. The moisture content of the material is determined gravimetrically. When the system reaches hygric equilibrium, that is, the weight of the materials is constant, the relative humidity is increased and maintained until the hygric equilibrium is reached again. The relative humidity is increased successively by steps to reach 99% and then decreased again likewise. This procedure is generally performed using the saturated salt solution method or with the aid of a Dynamic Vapour Sorption (DVS) apparatus. In this thesis both methods were used and compared. The DVS is less time consuming but uses small samples which might not be representative of the material. The reproducibility of this method is discussed by Hill et al (2010). Using the saturated salt solution method larger samples can be tested, but the time it takes for stabilisation is longer, of the order of several months (Magniont 2010).

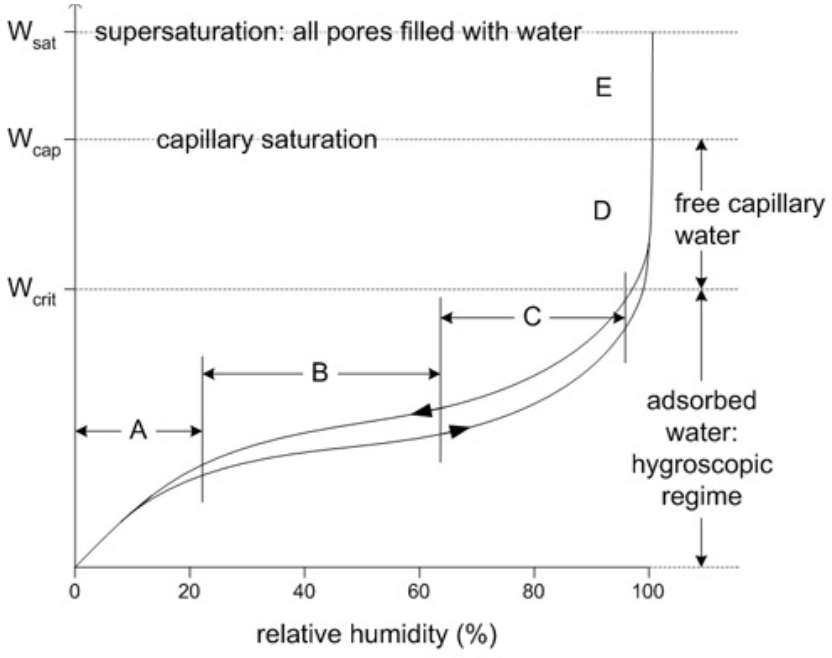

Figure 4.1. Different zones of the sorption isotherms according to the BET Theory. Figure taken from (Straube 2006).

The DVS used in this thesis was a DVSINT-Std from the University of Bath. Tests were performed at a constant temperature of 23ºC on samples weighing between 40 and 100 mg. A typical run (shown in Figure 4.2) started at zero percent relative

humidity and increased by 5% RH steps up to 85% RH and then in steps of 2.5% up to a maximum of 99% RH, before decreasing to 0% RH again with the same steps. The instrument maintained the samples at a constant RH until the weight change per minute (dm/dt) value reached 0.0001%/min or until 360 minutes elapsed.

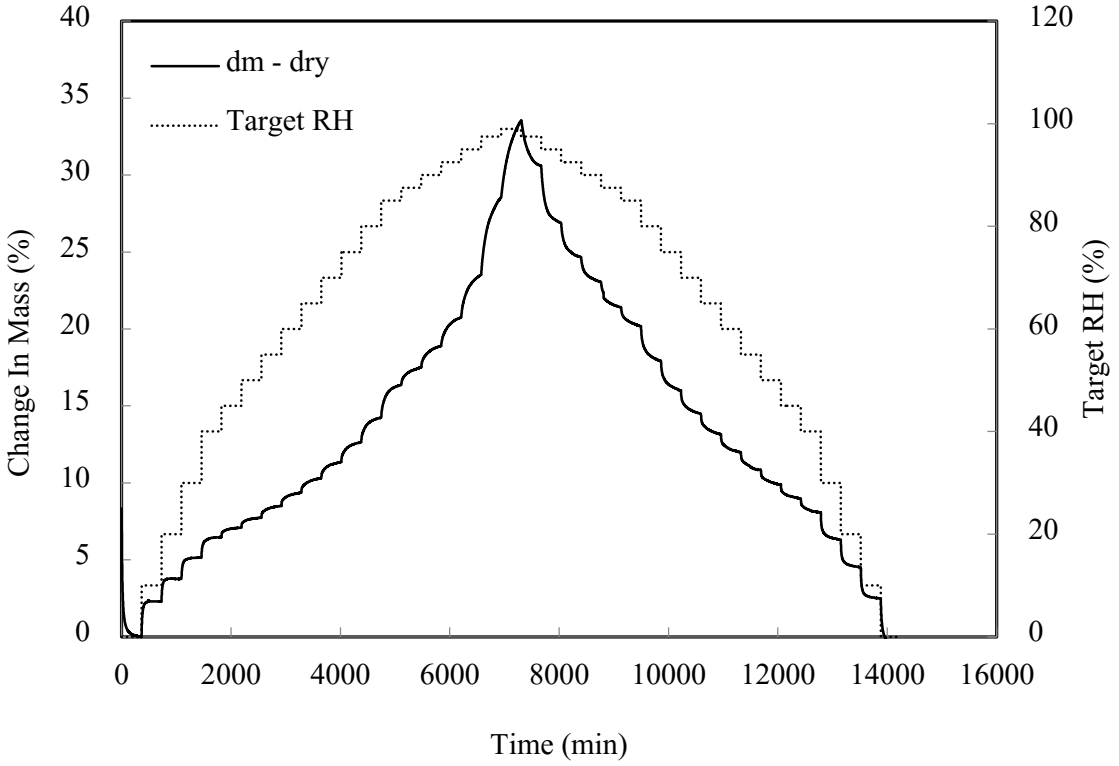

Figure 4.2. Typical run set for the DVS. The dotted line shows the steps of different target relative humidities and the red line the mass change of the sample, in this case Barley straw.

In the saturated salt solution method, samples were placed in sealed capsules containing different saturated salt solutions which maintained a certain relative humidity within the capsules. The temperature was set at 20ºC and maintained constant during the test. The samples were periodically weighed until equilibrium was reached or certain time elapsed (minimum two weeks). The different salts used and the corresponding relative humidities, as well as the corresponding mean RH registered are included in Table 4.3. The fluctuation of the RH was ± 5%.

It should be noted that an accurate determination of the sorption isotherm needs the hygric equilibrium to be completely reached. This is highly time consuming as it

can take several months or even more than a year, especially at high relative humidity (Magniont 2010). In this work, due to time restrictions, the equilibrium is not always completely reached which might affect the results. However, isotherms are used here to qualitatively estimate the hygrothermal performance of the materials in dynamic situations, where the equilibrium is never reached. The method was considered, thus, useful for comparison.

Table 4.3. Salt solutions used and corresponding mean RH.

Salt	RH (%)
Sodium hydroxide (NaOH)	33
Sodium nitrate ($NaNO_3$)	67
Sodium sulphate (Na_2SO_4)	82
Potassium nitrate (KNO_3)	95

4.1.3.2. Water vapour permeability and water vapour resistance factor

The water vapour permeability of a material (δ) is used to describe the rate at which water vapour will diffuse through a material. It is defined as the time rate of water vapour transmission through a unit area of flat material of unit thickness induced by a unit vapour pressure difference between two specific surfaces, under specified temperature and humidity conditions. In this investigation the water vapour permeability of the materials (δ) was determined experimentally following the standard ISO 12571. Samples were placed on top of sealed cases containing a silica gel or a saturated salt solution. The laterals of the samples were sealed so that only their top and their bottom surfaces were exposed. The arrangements were placed in a conditioning chamber at 20ºC and 50% relative humidity respectively, and protected with a cover in order to prevent air movement. Thus, a relative humidity gradient across the samples was created. The difference in partial vapour pressure at each side of the samples creates a vapour flux. Specimens and cases were weighed regularly until a steady-state vapour flux was established. A linear regression was used to determine the water vapour flow rate, G (kg/s). The water vapour permeability was then calculated using the following expression (4.4):

$$\delta = \frac{Gd}{A \cdot \Delta p} \qquad (4.4)$$

where, d (m), is the sample thickness, A (m^2), is the exposed surface area, and Δp (Pa) is the average water vapour pressure difference across the sample during the test.

For comparison, the water vapour diffusion resistance factor (μ) is usually used. It is defined as the ratio of the water vapour permeability of air, δa, (kg/msPa) to the water vapour permeability of the material, δ, (kg/msPa). Thus, it can be calculated from water vapour permeability using the following equation (4.5):

$$\mu = \frac{\delta a}{\delta} \qquad (4.5)$$

The water vapour permeability of hygroscopic materials is dependent on the relative humidity gradient in which the test is performed. At a high relative humidity, the permeability can increase as liquid water forms in the pores and liquid transport takes over diffusion.

4.2. Hygrothermal performance

In order to experimentally analyse the hygrothermal performance of the materials, these were exposed to cyclic changes of humidity and temperature separately. Firstly, the samples were maintained at a certain temperature while the relative humidity was changed between two levels. Thereafter the temperature was changed between two levels, maintaining the absolute humidity.

4.2.1. Moisture Buffering Test

In this investigation the Moisture Buffering Value has been determined following the methodology indicated in ISO 24353. The specimens were exposed to a series of step changes in relative humidity between two levels, in cycles of 24hs (12hs at

a 53% RH and 12hs at 75% RH) and maintaining the temperature at 23ºC. Specimens were prepared measuring 200 x 200 mm and approximately 100 mm thickness. The lateral and bottom surfaces of the samples were sealed with an aluminium foil so that only the top surface was exposed before conditioning them at 20ºC and 60% RH. The samples were placed on top of a scale in order to record the mass change during the test which continued until the amount of adsorbed and desorbed water approached the same value and thus, a dynamic equilibrium. MBV was calculated using the following equation (4.6):

$$MBV = \frac{\Delta m}{A \cdot \Delta \phi} \qquad (4.6)$$

where, Δm is an average of the adsorbed and desorbed mass after the system has reached a dynamic equilibrium (kg), A is the exposed surface area (m^2), and $\Delta\phi$ is the difference in relative humidity (%). Dynamic equilibrium is reached when Δm changes not more than 5% over 3 cycles (Rode et al. 2005).

4.2.2. Dynamic hygrothermal test

4.2.2.1. Protocols used for testing the insulation boards

The hygrothermal behaviour of the corn pith alginate materials was investigated with dynamic tests and compared with that of three commercially available insulation materials, that is, wood wool (WW), mineral wool (MW) and expanded polystyrene (EPS). The tests were carried out at the Fire Laboratory of the EPSEB, Universitat Politècnica de Catalunya and the Institut Català de la Fusta (INCAFUST) laboratories in Lleida.

A first set up was designed where two thermocouples were fixed to each of the specimens, one on the top surface and the other at the middle section of the sample. The samples were placed in a conditioning chamber at 40ºC until thermal equilibrium was reached, after which they were placed on top of a scale in a second conditioning chamber pre-set at a lower temperature (10ºC). The mass change and the temperature change were monitored during the test. Then, when thermal equilibrium was reached again, the process was repeated the other way round. In this set-up, only the temperature was controlled. Relative humidity was registered, but not controlled.

The second set-up was similar to the previous one, although this time around the samples were introduced in a climatic chamber that was pre-set to perform cyclic changes in temperature and relative humidity. Three different runs of three 8-hours-long cycles each were made for the first time. A fourth run of 24-hours-long cycles was also performed.

4.2.2.2. Protocol used for testing the thermal insulation systems (ETICS)

The hygrothermal behaviour of three thermal insulation systems incorporating corn pith alginate boards, wood fibre boards and polystyrene boards respectively, were also analysed. To this aim, three specimens of 700 x 700 mm were built. The specimens consisting of two layers of insulation material and a render system. Further details can be found in Section 8.1. The specimens were fixed at the opening of the climate chamber, so that one side was facing the inside of the chamber and the other facing the laboratory. The runs were designed in order to simulate outside conditions at the inside of the chamber and indoor conditions at the laboratory. Thus, the rendered side of the samples was, in all cases, facing towards the interior of the chamber, as shown in Figure 4.3. Two thermocouples were placed at each side and at the internal section of the samples (6 in total), and a flux metre was placed at the exterior side in order to measure the heat flux.

Figure 4.3. Experimental set-up used for the specimens of different ETIC systems. The specimens were fixed at the opening of the climate chambre (left) and covered with an isolated box (right).

4.3. Fire reaction

4.3.1. Small scale flammability tests

4.3.1.1. Pyrolysis Combustion Flow Calorimetre

Small-scale flammability tests are carried out on a Fire Testing Technology Pyrolysis Combustion Flow Calorimetre (PCFC) at the Fire Laboratory of the Barcelona School of Building Construction (EPSEB) of the UPC. Microscale combustion calorimetry combines thermal analysis and oxygen consumption calorimetry, thus enabling the determination of Heat Release (HR) and Heat Release Rate (HRR) of small samples. Data from the PCFC have been known to correlate well with other established fire tests (Lyon and Walters 2004; Cogen et al. 2009) and it has been approved as an ASTM International Standard for plastics and other solid materials (ASTM D7309:2007). The device incorporates two different chambers, the pyrolyser (where anaerobic thermal degradation takes place) and the combustor (where the products from the anaerobic thermal degradation are combusted). The sample is introduced into the pyrolyser, which is in a nitrogen atmosphere. The pyrolyser is then heated at a controlled rate, which causes the progressive thermal degradation of the sample and thus, the release of gases. The gases are mixed with a stream of oxygen and brought to the combustor for combustion. The Heat Release Rate (HRR) is determined from the oxygen consumption. Total heat release (HR) is calculated as the integral of the HRR all through the duration of the test.

For the tests carried out in this investigation the heating rate at the pyrolyser was set to 60°C/min up to a maximum temperature of 750ºC. Products from the anaerobic thermal degradation were mixed with a 20 cm^3/min stream of oxygen prior to entering the combustion furnace at 900°C. For each experiment a mass of 10.0 mg ± 0.1 mg is used.

4.3.1.2. Thermogravimetric Analysis (TGA)

In the thermogravimetric analysis the weight variation of a sample exposed to a controlled heating process is measured. Such variation is due to the release of gases when the temperature rises. The sample is placed in a furnace in a crucible on top of a scale. Results are generally presented plotting mass against temperature (thermogram). The resulting curve derived can be used to analyse the rate of mass

change with temperature. Differential Scanning Calorimetry is a thermos-analytical technique in which the difference in the amount of heat required to increase the temperature of a sample and the reference is measured as a function of temperature.

A TA Instruments SDT Q600 Simultaneous TGA-DSC was employed in this thesis to measure the heat flow associated with the thermal decomposition of the samples, at the same time than their mass loss. The analysis can be performed in two different atmospheres: air and nitrogen. Measurements were taken with a heating rate of 10°C/min from 30ºC to 600ºC. For each experiment, a mass of 5 mg ± 0.5 mg was used and the flow rate of gas was 50 ml/min.

4.3.2. Medium-scale flammability tests

4.3.2.1. Ignition time and extinguishability

When analysing the fire behaviour of a material, the testing scale has a great impact on the results. Thus, it is not possible to extrapolate the findings from medium-scaled tests to real life behaviour. However, it is possible to have some indications on how the material will behave in case of fire. In particular, the ignition time and extinguishability test indicates the ease with which a material inflames when the temperature rises and its potential contribution to the fire propagation. Early, long-time flaming with dropping indicates a high potential to fire propagation. A radiator device described in the Spanish Standard UNE 23.725-90 was employed to measure the ignition time and the degree of extinguishability of combustion. The samples were placed on a metallic grid 3 cm below a heat source of 500W, which was removed 3 seconds after each ignition and replaced after each extinction, during the 5 minutes of the test. The most important parameters determined were the time of the first ignition, the number of ignitions and the average value of combustion extent during the 5 minutes of the assay.

4.3.2.2. Limiting Oxygen Index (LOI)

The Limiting Oxygen Index is a useful test to determine the ease of combustion of a material. In a fire situation, it is likely that a decrease in the oxygen level occurs due to combustion, which plays against fire propagation. Materials which combust at low oxygen concentrations may constitute a risk in case of fire. The Limiting Oxygen Index was determined using the device and the procedure described in UNE-EN ISO 4589-2.

Samples were placed vertically in a test chimney. A gaseous mixture of nitrogen and oxygen was then blown through the chimney and the sample was ignited. This procedure was repeated a minimum of six times for each material. The oxygen concentration of the gas mixture was changed every time as indicated in the above mentioned standard, in order to determine the concentration at which the sample burned.

4.3.3. Smouldering combustion analysis tests

4.3.3.1. Small scale tests

Small-scale smouldering reaction heat tests are performed by Simultaneous Thermal Analysis (STA) using the TA Instruments SDT Q600 equipment previously mentioned. The difference is that, in this case, experiments are carried out in air, and in a crucible with lid. Due to the lid, the sample is oxidized without flame because of the limitation of air penetration into the crucible. Moreover, not only the mass change and its derivative are obtained, but also the differential heat flow (W/g) resulting from the thermal degradation. Measurements are taken with a heating rate of 10°C/min, from 30ºC to 600ºC. For each experiment a mass of 5 mg ± 0.5 mg is used and the flow rate of gas is 50 ml/min.

4.3.3.2. Medium scale smouldering set-up

An experimental set-up similar to the one described by Hagen et al (2011) was designed to determine the velocity of the smouldering front. In such set-up an elongated specimen was held on top of a hot plate. Five type-K thermocouples were placed every 3 cm along the vertical centerline of the sample and one in direct contact with the hot plate. The described set-up is shown in Figure 4.4.

In experiments, the hotplate was heated until it gets to a pre-determined temperature and it was then allowed to cool to room temperature. If the pre-determined temperature was sufficient, smouldering process initiated and the test continued until the char and ash of the sample had cooled down to less than 100ºC. The set-up was completed placing the ensemble on top of a scale, in order to register the mass loss due to the smouldering process. Moreover, during the experiments, the evolution was visualized with an infrared camera and images were taken each 5 minutes. Smouldering velocity was evaluated based on the temperature recorded by

the thermocouples by determining the times at which each thermocouple position reaches a temperature, here chosen as 250ºC.

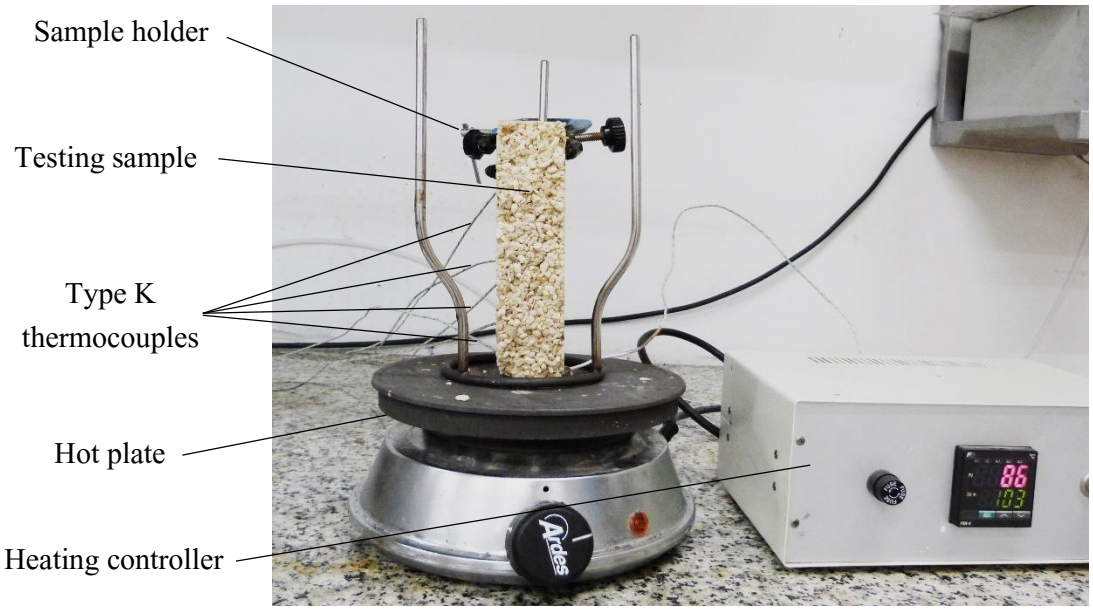

Figure 4.4. Experimental smouldering set-up.

4.4. Mould growth test

In this study, sealed cases were used to monitor mould growth under specified conditions of RH and temperature. The temperature was controlled throughout the experiment by placing the cases within a climate chamber, while relative humidity was regulated placing saturated salt solutions within the cases. The specimens were not sterilised nor inoculated with specific fungal spores to prevent unknown changes to the substrate and to closely reproduce a real exposure situation (Thomson and Walker 2014). Therefore, naturally occurring spores were used to determine the resistance to mould growth of the specimens. Two sets of experiments are performed. On the first, pre-treated aggregates alone are exposed to two different relative humidities (75% and 97%). On the second, corn pith alginate boards including the pre-treatments selected from the first set of tests are

exposed to a total of 10 different environments (5 different relative humidities at two different temperatures). These are presented in Table 4.4.

Table 4.4. Environments at the different sealed growth cases.

Case nº	T (ºC)	RH (%)
1	13	86.1
2	13	90.1
3	13	94.3
4	13	95.3
5	13	96.4
6	27	75.5
7	27	83.5
8	27	89.2
9	27	92.5
10	27	93.5

The total test time was 42 days for the first set of experiments and 63 days for the second. The specimens were inspected at defined intervals for fungal growth. The frequency of the inspections was daily for the first five days and reduced to a weekly inspection for the rest of the test. Fungal growth was qualitatively determined by visual inspection with the aid of a binocular loupe, following the methodology proposed by Johansson et al (2012). Mould growth (both visible to the naked eye and under the microscope) was rated according to a five-point rating scale where:

0 = No growth
1 = Sparse, initial growth with only one or a few hyphae present
2 = Sparse but clearly established growth
3 = Patchy, heavy growth
4 = Growth over most or all of the surface.

An extended description of this method and discussion on its reproducibility can be found in Johansson (2014).

The rating assessment of mould growth can be presented though different means. In this work, the results are presented through figures, where the rating of test specimens is plotted against time. Such figures enable the comparison of mould growth development over time on the same material exposed at different conditions or on different materials exposed to the same conditions.

Moreover, the isopleth traffic-light system described in Section 2.5 (Sedlbauer 2001; Sedlbauer et al. 2011) is adapted with the aim to produce figures that allow a rapid and direct comparison between the untreated and treated materials. Isopleths are graphic representations of situations of similar mould growth. Thus, it is possible to determine those environments at which a similar mould growth (either expressed in terms of growth speed or in terms of total mould growth extension after a certain time of exposure) is expected on a specific material using the isopleth system.

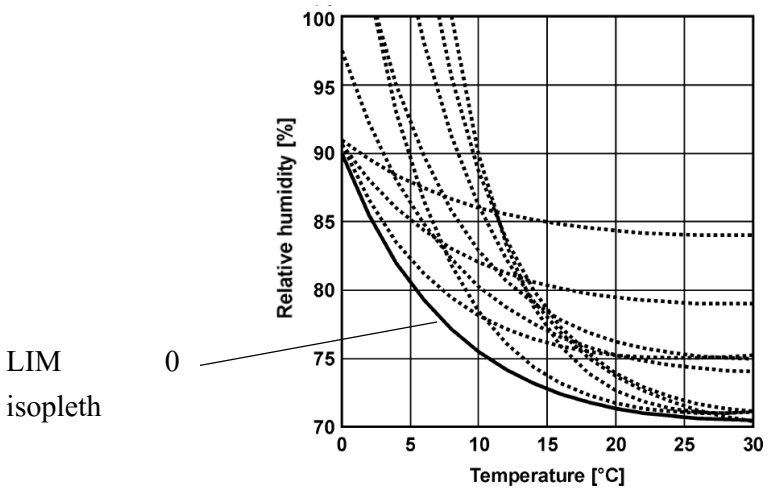

Figure 4.5. Isopleths for mycelium growth of various fungus species and Lowest Isopleth for mould (LIM 0) resulting from that. Figure taken from Sedlbauer (2001).

Sedlbauer (2001) analysed the environmental conditions at which different mould species grow on a cultivation substrate using the isopleth system and determined the Lim 0 isopleth from which no mould growth is expected in any substrate (solid line in Figure 4.5). Nevertheless, to the best knowledge of the author, neither Sedlbauer (2001) nor Hofbauer et al. (2008) published the equations for the isopleth

curves. Thus, the equations proposed by Johansson et al. (2013) are used. The growth limit curves are defined as:

$$\phi = a + c\,(T^2 - 54T)\ [\%] \qquad (4.7)$$

where T is the temperature in ºC and the parameters c and a are estimated using Equation (4.8) and Equation (4.9) respectively, where the data for RH_1 and RH_2 and the corresponding temperatures (T_1 and T_2 respectively) are deduced from the results of the laboratory tests.

$$c = \frac{\phi_1 - \phi_2}{T_1^2 - T_2^2 - 54(T_1 - T_2)} \qquad (4.8)$$

$$a = \phi_1 - c(T_1^2 - 54T_1) \qquad (4.9)$$

Figure 4.6 shows the correlation between the results presented by Sedlbauer et al. (2011) and the curves defined by the equations presented above (dotted lines on the figure). As claimed by Johansson et al. (2013), an acceptable correlation is achieved within the range of temperatures relevant to building environments (between 5 and 30 ºC).

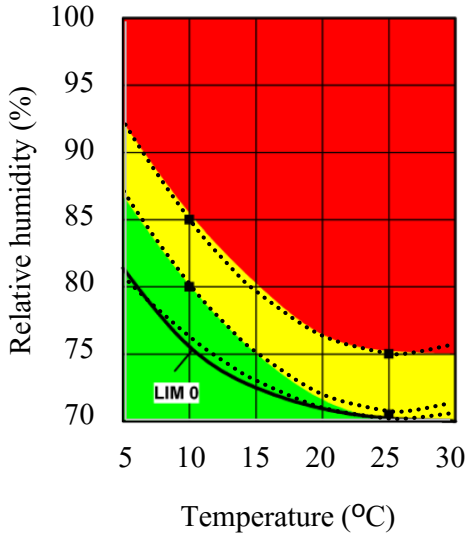

Figure 4.6. Correlation between the results presented by Sedlbauer et al. (2011) for straw and the equations proposed by Johansson et al. (2014).

In this study, the traffic-light colours have been correlated with the rating system used for the mould growth assessment in such a way that:

- Green corresponds to no mould growth: rating 0
- Yellow corresponds to limited mould growth: rating between 0 and 2
- Red corresponds to severe mould growth: with ratings from 2 to 4

4.5. Accelerated ageing with climate simulation

The aim of a climate simulation test is to accelerate weathering processes on building materials in order to determine the sensitivity, the behaviour and the resistance of the material to the environmental conditions. The test consists of exposing the samples to cycles of different extreme conditions, which are determined with regard to the characteristics of the material being tested and the natural exposure conditions.

In this investigation, the climate simulation test was used to study the compatibility of the corn pith-alginate insulation boards with different renders. The response of the render to dimensional variations due to swelling of the insulation board and their effect on the hygroscopic behaviour of the material was analysed. Specimens of 250 x 250 x20 mm were coated on one of their faces with one of the different mortars tested (lime, cement, clay and cork). The specimens were then wrapped with an aluminium foil so that only the coated face was exposed, and conditioned at the laboratory for one week. Specimens of expanded polystyrene (EPS) were prepared for comparison, as EPS is the most commonly used material in ETIC Systems. During the test, the samples were exposed to 10 cycles in which the temperature and the relative humidity were simultaneously changed. A typical cycle lasted 48 hours and included four steps:

1) 8 hours inside the humidity chamber (100% RH and 20ºC)
2) 16 hours under laboratory conditions (50% RH and 20ºC)
3) 8 hours in the laboratory oven (0% RH and 100ºC)
4) 16 hours under laboratory conditions (50% RH and 20ºC)

The response of the testing samples to the ageing cycles was analysed by measuring the mass variations after each part of the cycle and by comparing the results of the water absorption test before and after ageing.

The water absorption test was used to determine the penetration of a water column at a definite time and definite area into a porous material. In this investigation, the water absorption was determined using the Karsten tube test method (RILEM II.4). The Karsten glass tube was fixed on the material's surface using removable putty. Then the pipe was filled with water up to the graduation "0" and the time measurement was started. Thereafter readings on the quantity of water absorbed by the material in function of time are made, generally at 2, 5, 10, 15 and 30 minutes respectively.

5. RAW MATERIALS

5.1. Crop by-products

Among the available raw materials in Spain (see Section 3), three are chosen for the study: barley straw, corn pith and rice husks. Materials are selected for their availability and also because they present remarkable morphological differences which motivate the interest of their analysis and comparison. A picture of each of the crop by-products used in this work is shown in Figure 5.1.

Figure 5.1. Barley straw fibres, corn pith aggregate and rice husks used as raw materials.

5.1.1. General description

5.1.1.1. Barley straw

Straw is the generic word used to designate the dried, yellow stems of crops, especially cereals. Despite the apparent similarity of the straw from different

cereals, there are important differences among them (De Bouter et al. 2009). Such differences were traditionally well known, for instance, oat straw was preferred for basket making and barley straw for animal feeding and bedding. In construction its use in straw bale walls and earth renders is gaining increasing interest (Summers et al. 2003; Lawrence et al. 2009; Pan et al. 2010; Wall et al. 2012). Despite the efforts made towards the industrialization of this kind of construction techniques they remain still rare and are based on artisanal practices. However, some industrialized products such as pre-fabricated strawbale walls, compressed straw wall partitions or straw based particle boards are nowadays commercially available (*Ecoclay, Stramit, Modcell, Okambuva, EcoCocon*, etc.).

In this work, barley straw was chosen as it is the most abundant crop by-product in Spain. It was recovered from a regional organic producer, chopped with a hammer mill at the laboratory and sieved to obtain groups of fibres of similar diameters.

5.1.1.2. Corn pith

The pith is the soft, spongy tissue present at the interior of corn stalks and cobs and other plant and tree parts such as sunflower stalks, miscanthus or cattails. It has a remarkable low density and is mainly constituted by the parenchymal tissue of the plant. In the case of corn, the pith represents about 20% of the by-products (Blanco et al.), while in the case of sunflowers, it accounts for about 35% (Magniont 2010). Corn crops are mainly designed for animal feeding. To this aim, corn is harvested either when the plant is green or when it is ripen. In the first case, the whole plant, including stalks, is collected and chopped on site and designed animal feeding. In the second case, which is the most usual in Spain, the cobs are pulled out of the stalks, which are left in the field. The product obtained by this process is of higher quality than the one previously mentioned. The stalks are balled and used in pellet production or buried in the fields and thus, valuated for their humic and mineral content. Nowadays, there is no industrial use of the corn pith alone, although a patent was found proposing a procedure to separate the different parts of the corn by-products to produce different materials such as paper pulp, alcohol or energy (Blanco et al.). Some attempts have been made to use pith as a construction material. Since some pioneering patents and research from the first decades of the twentieth century (De Long; Hinde 1927; Elmendorf 1929; Sweeney and Emley 1930) to the present, the production of insulation boards from corn pith has been investigated. Pinto et al (2011; 2012) found that similitudes exist between corn cob

and EPS regarding their microstructure, although the thermal conductivity of the experimental corn cob panels developed by the authors presented a higher thermal conductivity than EPS. Similar results were obtained by Dowling et al. (2007). Wang and Sun (2002) made low density boards with a mixture of wheat straw and corn pith with promising properties. Magniont (2010) developed light composites using lime/metakaolin and sunflower pith, to be used for instance in walls as self-bearing blocks with improved insulation properties.

In this work, the corn pith used was provided by a regional organic producer. It was manually removed from the stalk, chopped with a hammer mill and sieved to obtain granulates of three different particle sizes: 2, 1 and 0.5 mm.

5.1.1.3. Rice husk

The husk is the dry outer covering of certain fruits or seeds. Although husks are normally used in feeding, rice husks are a by-product with little applications at the present. Due to their high content in silica (about 20%) and lignin, they degrade slowly, which restricts their reincorporation to the fields. As rice husks present a high calorific power (about 4000 kcal/kg), they are being increasingly revalorised for energy production. However, due to the high silica content, high amounts of ash are produced as residue (Gonçalves and Bergmann 2007).

The rice husks used in this study originated from the agricultural cooperative of the Delta de l'Ebre. As it was the case for straw, probably some of the properties of the husk differ from variety to variety. However, it was not possible to determine this in this work. Rice husks were sieved in order to obtain groups of similar sizes.

5.1.2. Characterization of the crop by-products

5.1.2.1. Physical properties

The skeletal density of the samples was determined as described in Section 4.1.1. The bulk density of the three different materials (barley straw, B; corn pith, C; and rice husk, R) in loose form was determined using a vibrating table. Prior to the test the materials were chopped and sieved into three different particle sizes: 2, 1 and 0.5 mm respectively and oven dried for 24 hours at 60ºC. Thereafter, a 500 ml measuring cylinder was placed on top of the vibrating table and filled with each material. Density was determined before and after tapping for each particle size from the mass and volume. The test was repeated eight times for each sample.

Thereafter, the open porosity within the particles together with the space between particles was calculated as 1- bulk density/apparent skeletal density. The results are presented in Table 5.1.

Table 5.1. Density and porosity of the crop by-products.

Crop by-product	Particle size (mm)	Apparent skeletal density (kg/m^3)	Bulk density (kg/m^3)		Porosity (a.u.)	
			Poured	Tapped	Poured	Tapped
B	2	1404	44.9 ±0.9	58 ±1	0.96	0.96
	1		54 ±2	68 ±2	0.96	0.95
	0,5		64 ±2	80 ±2	0.95	0.94
C	2	1584	37 ±1	42 ±1	0.98	0.97
	1		36 ±1	41 ±1	0.98	0.97
	0,5		37.8 ±0.8	42.9 ±0.7	0.98	0.97
R	2	1539	99 ±5	121 ±5	0.94	0.92
	1		138 ±3	167 ±3	0.91	0.89
	0,5		230 ±4	277 ±4	0.85	0.82

The results clearly show the differences in porosity and particle shapes among the materials: while the skeletal densities are similar, bulk densities are much more variable. The average skeletal density of the materials is 1509 ±105 kg/m^3. Such density corresponds to the matrix, which is similar in all cases, and includes close porosity if any. However, significant differences were found in the bulk density of the materials, which varied more than 4 times from one material to the other. It is important to note that bulk density of the loose materials accounts for the porous structure within the particles together with the spaces between particles. Thus, the shape of the particles has an important role on the final density of the material and resulting composites. In this case, barley straw particles are fibrous, corn pith particles are granular shaped and rice husk have a concave shape, similar to a boat hull. This explains the fact that bulk density is much more affected by particle shape in the case of rice husks than in the other cases. When rice husks are shredded, the concave shape is lost. Small rice husk particles consist on flat flakes which are able to compactly arrange, noticeably increasing the overall bulk density (see Figure 5.2). On the contrary, the shape of barley fibres and corn pith granulates are

maintained. Thus, their density is less dependent on particle size, especially in the case of corn pith, which has an arrangement that is assumed to be more homogeneous due to the isotropy of the particles. Tapped loose materials showed a higher density than poured ones but again, the difference was reduced in the case of corn pith samples. In general, the bulk density of corn pith aggregates is less dependent on particle size and compacting which might be an advantage in composite production. Moreover, corn pith bulk densities are lower than those of barley straw or rice husks. As density is a driving factor of thermal conductivity (Domínguez-Muñoz et al. 2010), this is an important aspect to take into account in the case of the development of insulation materials.

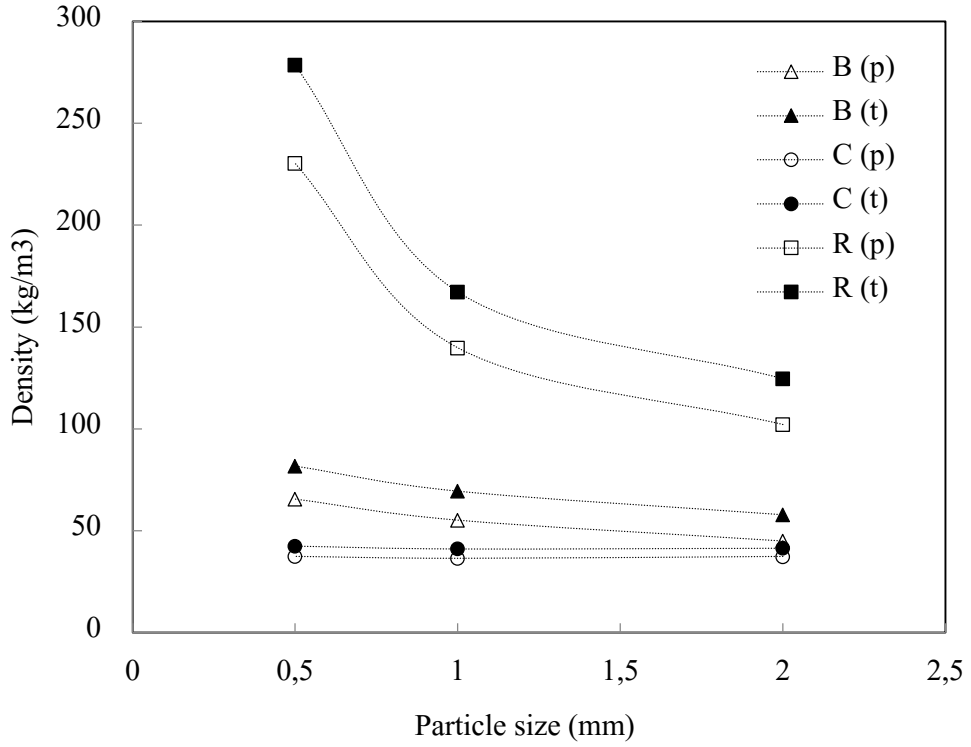

Figure 5.2. Density plotted against particle size for poured (p) and tapped (t) loose materials.

The open porosity of the loose materials was calculated from the bulk and skeletal densities. As discussed earlier, such porosity is highly dependent on the arrangement of the particles and does not explain the differences in the porous structure of the materials. Thus, the porosity within the particles was analysed under a Scanning Electron Microscope (SEM). Such technique is described in Section 4.1.1. The samples were cut with a blade in order to observe their transversal and

longitudinal section. Figure 5.3 shows the porous structure of the raw materials at 500 x, 1,500 x and 15,000 x magnification (left to right).

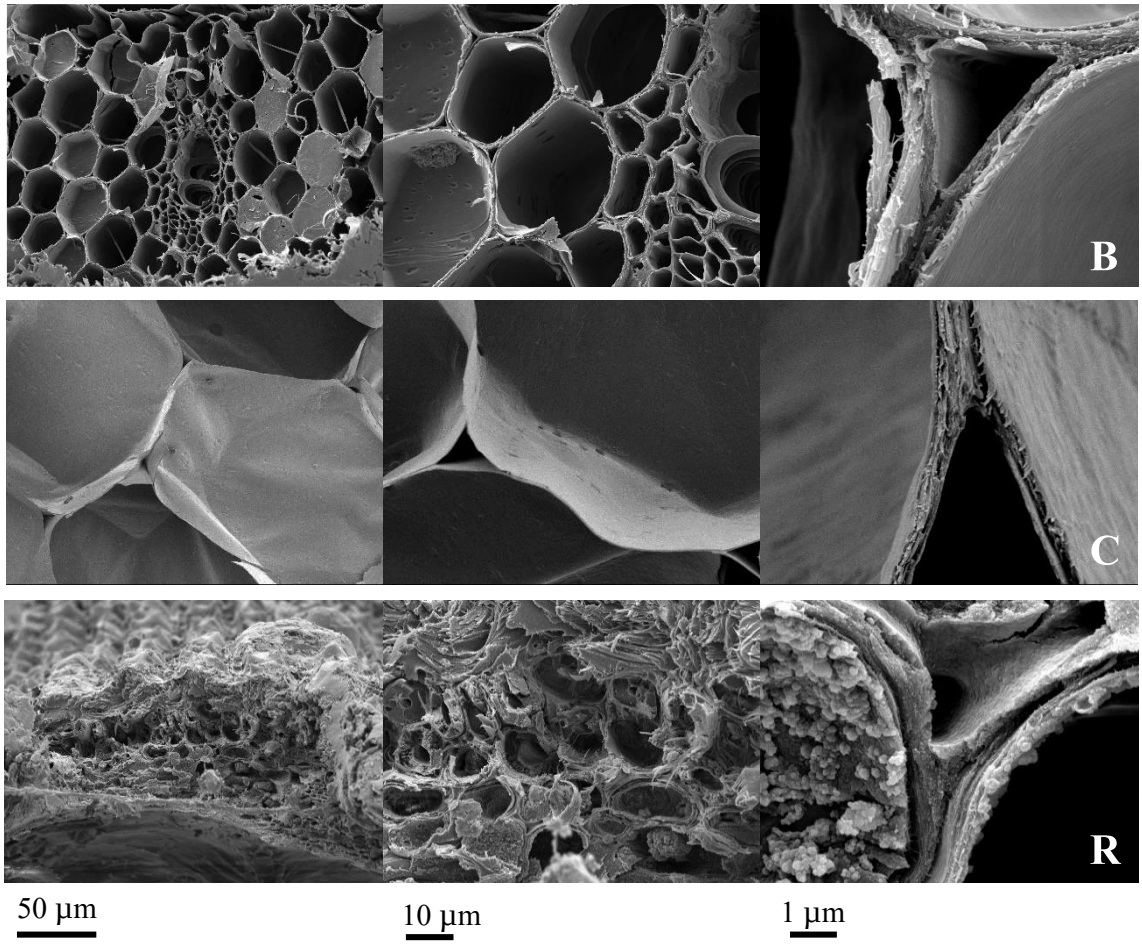

Figure 5.3. SEM images of the tissues present in barley stems (B), corn stems (C) and rice husks (R).

Barley straw is formed by a mixture of stalk and leaf tissues, which are formed by parenchymatic cellules of diameter between 25 to 45 µm and several vascular bundles of fibrous structure. The total thickness of the cellular wall and the plasma membrane of the parenchymatic cellules are about 0.6 µm, with an intercellular space of diameter about 3 µm. On the other hand, corn pith is mainly formed by parenchymatic cellules, as the vascular bundles, which are mainly present at the cortical part of the stalk, are removed by decortication. This fact explains that shredded particles are fibrous shaped in the case of barley and granular in the case of pith. The cellules forming the parenchyma tissue are larger in the case of corn pith (diameter of about 100-140 µm) and cellular walls thinner (width of about 0.4

μm), which indicates a higher macro-porosity of this material. The intercellular spaces are also bigger than that of barley straw, with diameters about 10 μm. The cells are interconnected through plasmodesmata with diameter of about 2 μm. Rice husks present a less porous structure, with cellules of diameter 2 to 5 μm and walls of 3 μm thick. Moreover, the surface of the rice husk's cell walls greatly differ from those of barley straw and corn pith, as they have a great number of protuberances corresponding to silica incrustations.

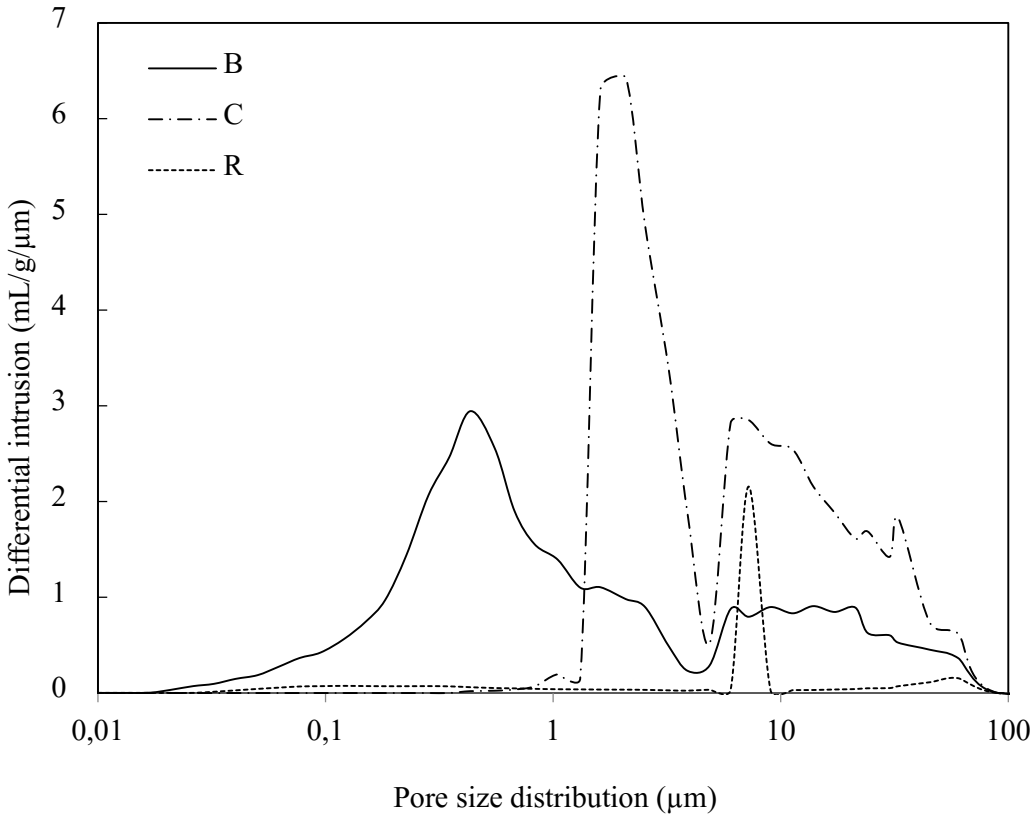

Figure 5.4. Pore size distribution (represented in log scale) for the three raw materials.

The pore size distribution of the materials was determined using the technique of mercury porosimetry as described in Section 4.1.1. The results are presented in Figure 5.4 where the differential intrusion is plotted against pore size distribution. The range of pore size analysed runs from 10 nm to 100 μm. It is important to note that the technique used is based on a simple porous model. The porous structure is assumed to be formed by interconnected spherical pores of different sizes. Thus, the results show the pore size distribution of equivalent spherical pores rather than

the actual pores' size. However, the results are useful for comparison. From the results, it can be observed that rice husks present a lower porosity than the rest of the materials. Rice husk's porosity is unimodal, with a peak at 8 microns, which probably correspond to the diameters of the cellular lumen observed in the SEM images. It is practically non porous at other ranges. On the contrary, barley straw and corn pith are highly porous. Both materials present a bimodal porosity with peaks at about 0.5 and 10 microns in the case of barley and 2 and 10 microns in the case of corn pith. Such peaks correspond to the diameters of the plasmodesmata and the intercellular spaces respectively. The shape of the peaks indicates a more homogeneous porous structure in the case of corn pith than in the case of barley straw, which is in agreement with observations from SEM. Results show that the average pore diameter of corn pith samples is higher than that of barley straw and rice husks which is also in agreement with SEM observations.

The BET Surface Area of the materials was determined using the methodology described in Section 4.1.1. The results are presented in Table 5.2 per mass unit and per volume unit. Despite their distinct porosity, barley straw and rice husks present a similar surface area per mass unit. In contrast, corn pith presents the greatest surface area, which is slightly less than 5 times higher than that of the other two materials. This indicates a possible higher reactivity of the material with binders and a higher hygroscopicity. Results expressed per unit volume show that the surface area of barley straw and corn pith is similar, while that of rice husk is about one-third of the other two materials.

Table 5.2. BET Surface area results.

Crop by-product	BET surface area	
	m^2/g	m^2/m^3
B	0.463	0.034
C	2.211	0.032
R	0.451	0.014

5.1.2.2. Thermal properties

The thermal conductivity and thermal diffusivity of the loose materials was determined with a Quickline-30 Electronic Thermal Analyser, using a surface probe, as described in Section 4.1.2. The materials were tested at room conditions (43 ±11 RH and 26 ±2 ºC) and a minimum of three measurements were done for each sample. The results indicate that all the materials present a low thermal conductivity and thus could be potentially used as thermal insulation materials. Nevertheless, the thermal conductivity of corn pith is lower than that of the other two materials, which is in accordance with previous results on the bulk density of the loose material and porosity. In Figure 5.5, thermal conductivity of the three materials shredded at three particle sizes is plotted against the density of the loose material. Results indicate that, as the nature of the matrix is similar in all cases, the thermal conductivity of the materials is greatly dependent on their bulk density. As discussed earlier, the density of loose rice husks is highly conditioned by the particle size and thus, thermal conductivity too.

Table 5.3. Results for the thermal conductivity measurement made using the electronic thermal analyser for samples shredded at different particle sizes.

Crop by-product	Particle size (mm)	Thermal conductivity (W/mK)	Thermal diffusivity (10^6 m^2/s)	Bulk density (kg/m^3)
B	2.0	0.046 ±0.001	0.114 ±0.001	44.9 ±0.9
	1.0	0.052 ±0.001	0.153 ±0.004	54 ±2
	0.5	0.053 ±0.000	0.174 ±0.003	64 ±2
C	2.0	0.048 ±0.002	0.114 ±0.007	37 ±1
	1.0	0.047 ±0.003	0.107 ±0.001	36 ±1
	0.5	0.048 ±0.001	0.133 ±0.010	37.8 ±0.8
R	2.0	0.055 ±0.000	0.105 ±0.002	99 ±5
	1.0	0.059 ±0.004	0.199 ±0.010	138 ±3
	0.5	0.070 ±0.000	0.228 ±0.001	230 ±4

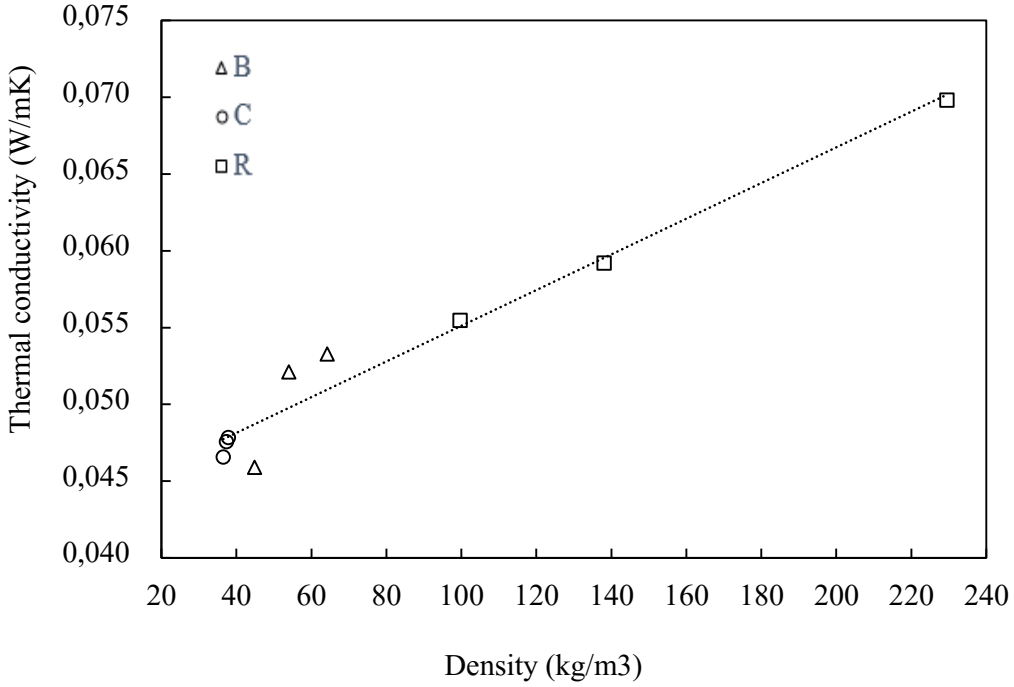

Figure 5.5. Thermal conductivity of the samples shredded at different particle sizes as a function of density.

5.1.2.3. Hygroscopic properties

The hygroscopic properties of the crop by-products were analysed through their sorption isotherms. Water sorption isotherm analysis was performed at a constant temperature of 23ºC using a Dynamic Vapour Sorption apparatus (DVSINT-Std) at the University of Bath. The principle of this method is described in Section 4.1.3. Corn pith and barley samples were 40 mg in weigh while in the case of rice husks their mass was 90 mg. The sorption and desorption isotherm curves of the three materials are presented in Figure 5.6. The materials present a Type II isotherm (IUPAC classification) with hysteresis, which is characteristic of cellulosic and lignocellulosic materials. It was found that the sorption behaviour of the materials was similar to relative humidities of up to 60% and that differences appear when approaching the zone of capillary condensation (see Section 4.1.3). From 60% RH corn pith adsorption is distinctly higher than the rest of the materials, increasing its weight nearly 70%. This might have positive consequences regarding the moisture buffering capacity of the material but also negative implications regarding its fungal resistance and dimensional stability. However, results are given per mass unit

which impedes a direct comparison of the insulation materials due to their different densities.

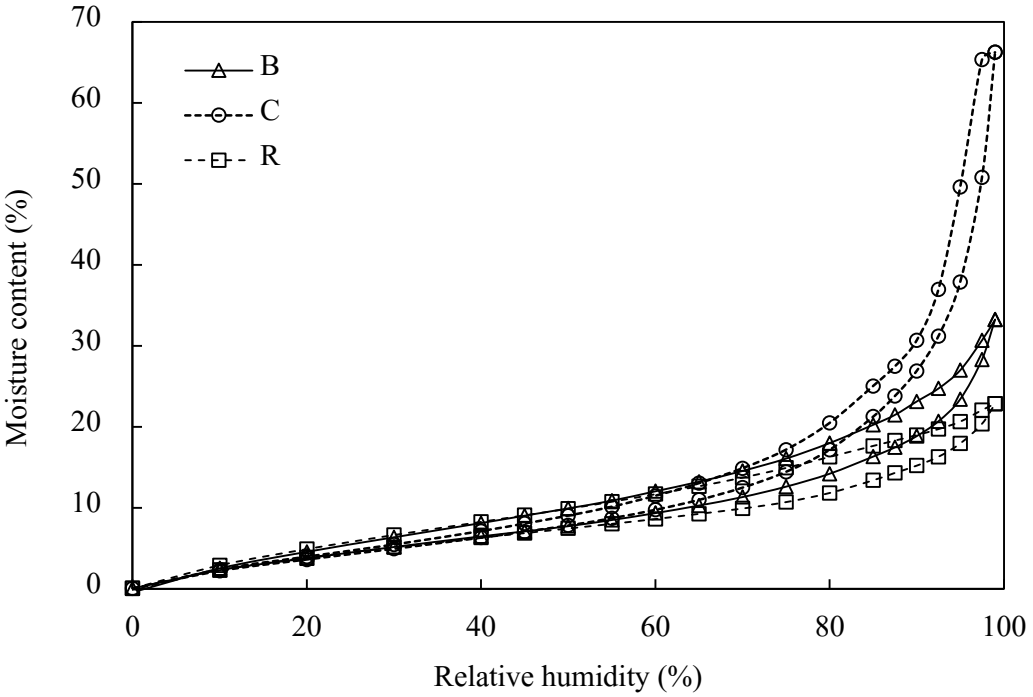

Figure 5.6. Sorption and desorption isotherms of the three materials measured with the DVS.

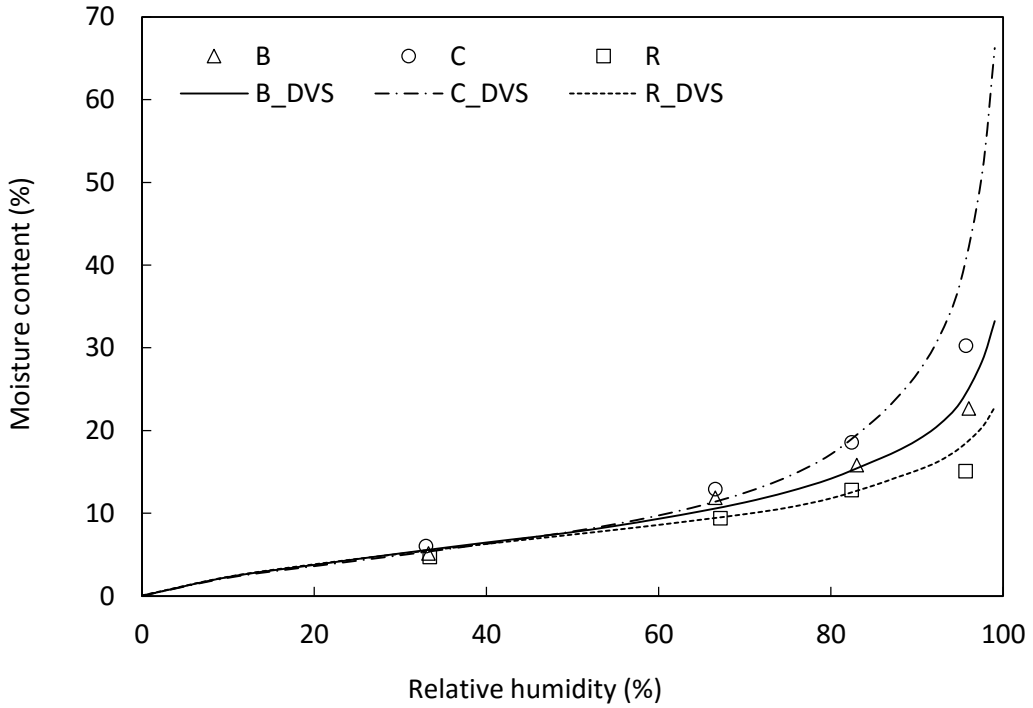

Figure 5.7. Comparison of the results yield by the DVS and those obtained with the salt solution method for the three materials.

In Figure 5.7, the results yielded by the DVS are compared with those obtained from the salt solution method. The loose materials were poured into 100 mm diameter containers and weighed regularly for at least 20 days. Both methods yield equivalent results even if complete equilibrium was not always reached, as discussed in Section 4.1.3. Nevertheless, at high relative humidities the moisture content of the samples obtained with the salt solution method is significantly lower than that obtained with the DVS, as in this zone of the isotherm the method is less accurate. However, for the purpose of this thesis, the method is sufficient for comparison.

5.1.3. Hygrothermal performance of the crop by-products

5.1.3.1. Dynamic thermal behaviour

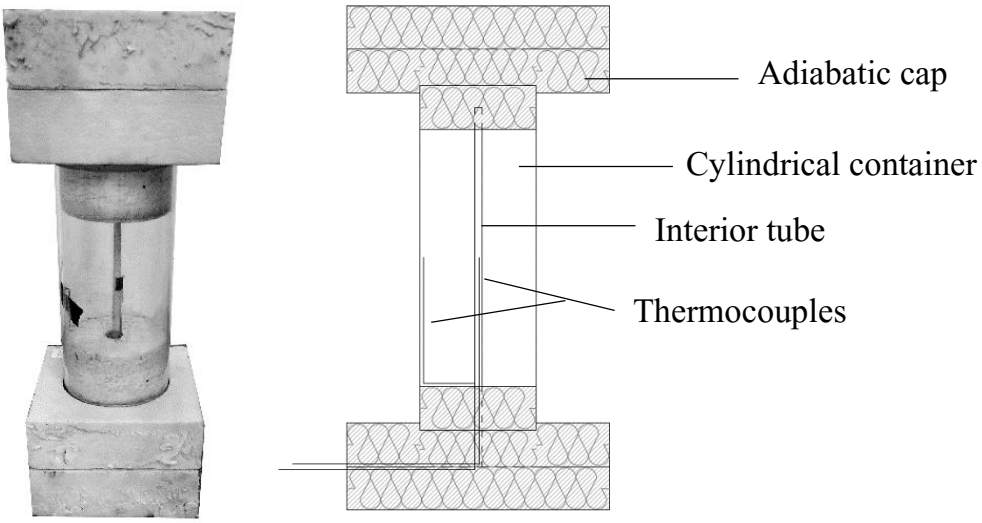

Figure 5.8. Container used in the dynamic thermal tests of the loose materials

The hygrothermal performance of the different loose materials shredded at different particle sizes (2.0, 0.5 and 0.1 mm) was compared using the methodology described in Section 4.2.2. The test was performed twice for each specimen. A special container, similar to the one described in (Pruteanu 2010) was constructed in order to perform the test on the loose materials. The container (shown in Figure 5.8) consisted of a 150 mm diameter, 300 mm length plastic tube with an isolated cap at each of its extremes and a second tube of 5 mm diameter fixed at its centreline. Two thermocouples, one at the inner face of the largest tube and another at the

exterior face of the interior tube were fixed at 150 mm from the edges. The loose materials were poured into the container and placed in a conditioning chamber set at 10ºC, until the temperature registered by the two thermocouples was the same (±0.5ºC). After being conditioned, the samples were subjected to a temperature change of 37ºC by placing them in a second chamber pre-set at 47ºC. Results are shown in Figure 5.9.

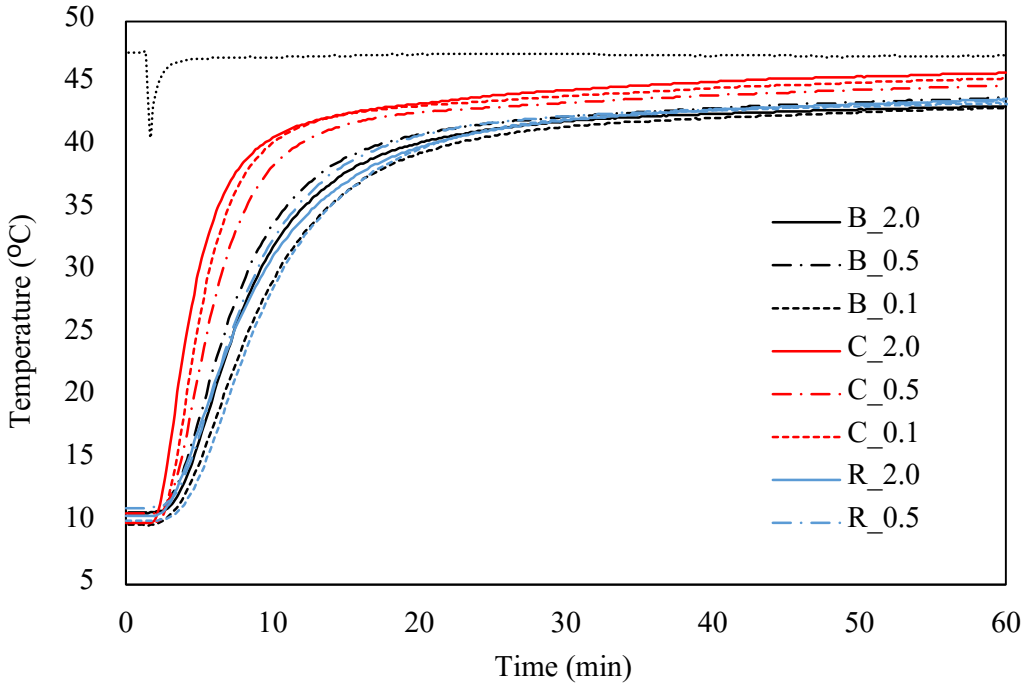

Figure 5.9. Temperature of the inner thermocouple by time of the loose materials subjected to a sudden temperature change of 37ºC.

Results indicate that, although corn pith present the lowest thermal conductivity, its thermal diffusivity is higher than that of barley straw and rice husk, as the initial slope is steeper. As the specific heat capacity of the materials is probably very similar, this difference is mainly due to the low density of the corn pith aggregate. The three materials show an important slowness in the temperature increase between 35ºC and 40ºC, and do not reach the oven temperature at the end of the test. This effect is probably due to moisture desorption within the internal porous structure of the materials which is an endothermic process. The results indicate as well that, despite their low porosity, rice husks present a similar behaviour to barley

straw and corn pith. The particle size does not seem to have any significant impact on the hygrothermal behaviour of the materials.

5.1.4. Thermal decomposition of the crop by-products

The thermal decomposition of the three raw materials was compared at small-scale. Two flammability tests, described in Section 4.3.1, were performed: Pyrolysis Combustion Flow Calorimetre (PCFC) and Thermogravimetric analysis (TGA).

The PCFC test was performed in triplicate at a heating rate of 60ºC/min using small samples of 10±0.05mg. The results obtained for each material are presented in Figure 5.10. The Heat Release Rate (HRR) is represented as a function of temperature, the resulting curves presenting the characteristic shape of lignocellulosic materials. All the samples show a clear peak, mainly as a result of the thermal decomposition of cellulose. This peak is higher in corn pith, which indicates a higher amount of cellulose. In some cases, a 'shoulder' is observed at lower temperatures (under 300ºC), which is commonly associated with the thermal decomposition of hemicellulose (Antal and Varhegyi 1995; Alvarez and Vázquez 2004). This shoulder is quite visible in rice husk and barley straw samples but is not present in corn pith. The high temperature tails that appear in all curves may be associated with lignin, the degradation temperature range of which is wide, from 200ºC to 500ºC (Dorez et al. 2013). Results qualitatively agree with the chemical composition presented in Table 5.4 which summarises the noticeable dispersion in values found in literature.

The main parameters obtained from the PCFC that are associated with flammability and hazard in case of fire are:

- Total heat release (HR), which is the integral of the HRR over the complete time of the test.
- Onset temperature of combustion (T_0), here considered as the temperature when the HRR value is 10 W/g.
- Temperature corresponding to the maximum heat release rate (T_{max})
- Maximum heat release rate (PHRR).
- Mass loss fraction (M_{loss})

Table 5.4. Main chemical composition of vegetable materials.

Crop type	Cellulose (%)	Hemicellulose (%)	Lignin (%)	Ash (%)	Ref.
B	31.0-45.0	24.0-29.0	14.0-15.0	3-7	Rowell and Rowell 1996 Sun 2010
C	43.2-50.5	31.0	14.6-15.0	2.2	Demirbas 2004 Sun 2010
R	24.3	24.3	14.3	15.3	Rowell and Rowell 1996 Di Blasi et al 1999

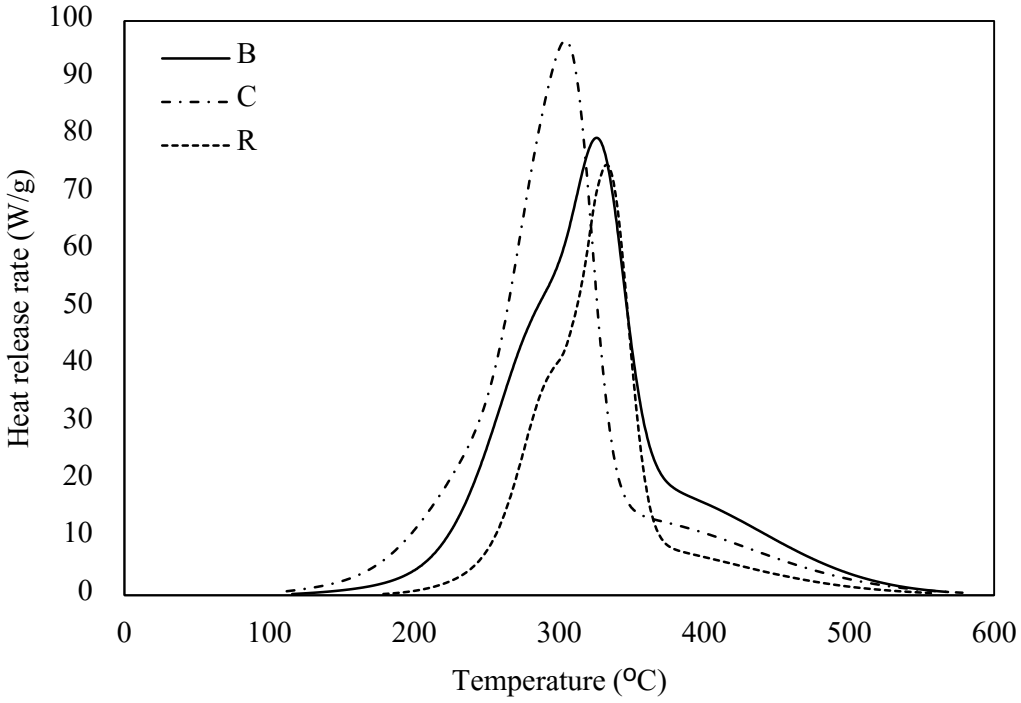

Figure 5.10. Heat release rate as a function of temperature for the different crop by-products.

Table 5.5 summarises the results obtained for the three crop by-products averaged over three samples of each type. In addition to their agreement with Figure 5.10, these results show that rice husks yield the best behaviour in terms of fire protection due to the lowest values of HR, PHRR and M_{loss}. It is well known that rice contains a high content of inorganic silica. During pyrolysis, organic components are decomposed and gasified, leaving a silica layer which can play the role of heat shield (Zhao et al. 2009).

Table 5.5. PCFC results for crop by-products.

Raw material	HR (MJ/kg)	T_{onset} (ºC)	T_{MAX} (ºC)	PHRR (W/g)	Mloss (a.u.)
Rice husk	5.6	268	342	56.4	0.69
Corn pith	8.8	215	312	92.6	0.73
Barley straw	8.0	230	329	68.3	0.75

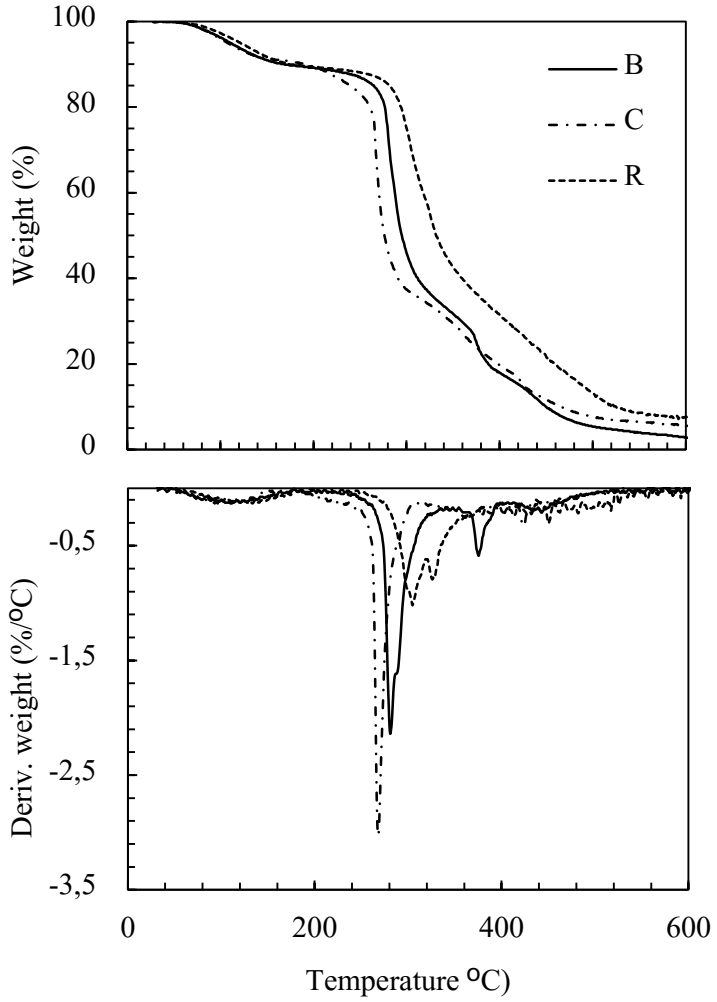

Figure 5.11. TGA and derivative for the three selected crop by-products

Moreover, the three crop by-products have been studied by Thermogravimetric Analysis (TGA). The heating rate was 10ºC/min and the weight of the samples 500±10 mg. Figure 5.11 depicts the results obtained for the mass loss and its derivative. Results qualitatively agree with the PCFC ones shown in Table 5.5, the

rice husk having the lowest weight loss and the lowest peak (more slow decomposition), which appears at the highest temperature. Barley straw and corn pith have similar weight loss, although thermal decomposition occurs earlier and faster in the case of the corn pith.

5.2. Binder materials

Two different biopolymers were used as binders to produce the panels. The two materials were polysaccharides, one obtained from corn (starch) and the other from algae (sodium alginate). These two different biopolymers were chosen because they are biodegradable and non-toxic materials, usually used in the food industry and are inexpensive. Both were commercially available products provided by *Cargill Haubourdin SAS.*.

5.2.1. Corn starch

5.2.1.1. General description

Corn starch is a polysaccharide produced by plants as a metabolic reserve. Industrially it is mainly obtained from corn (maize), cassava (tapioca), wheat and potato, although in Europe, corn is the main source of starch with a yearly production of 5.55Mt (Anderson et al. 2010). Due to its low-cost it has a wide range of applications. It is widely used in the food industry where it is classified by the FDA (USA) and the European Community as suitable and safe food ingredients, as a major ingredient in biodegradable plastics and as substitute for polyolefins in various packaging applications. The industry of starch is continuously increasing with new market applications such as the production of bio-ethanol, which may potentially influence the demand, the price and the availability of starch.

The starch used in this investigation is a corn starch commercially available and provided by *Cargill Haubourdin SAS*. It is present in the form of a free flowing white powder under the commercial name *C*Gum NC 03432*. The product is used to prepare corrugating adhesives, particularly Minocar and No-carrier glue preparation systems but may be also used for preparing Stein Hall adhesives. The main properties of the product declared by the manufacturer are listed below:

Moisture content: 10-13 %

Ash content: 0.1 %

Bulk density of the loose material: 500 g/l

Self-ignition temperature ≥170 °C

pH slurry (20g + 100 ml): 4-7

Viscosity alkaline Brab: 4-7 min

Viscosity cold slurry (44%, 25ºC): 250 mPa·s

5.2.1.2. Chemical structure

Starch is a long polymer of α-linked d-glucopyranoses. The most common linkages between units are the α-1,4 linkage, which forms helical structures, and the α-1,6 linkage, which creates a branching point where new chains can be formed. Such combinations generate two main structures that make up starch: amyloses and amylopectines. Amyloses are mainly linear structures with few side chains formed by 500 to 2,000 units whilst amylopectines are much more highly branched structures containing from 10,000 to 100,000 glucose units (Anderson et al. 2010; Jensen 2015).

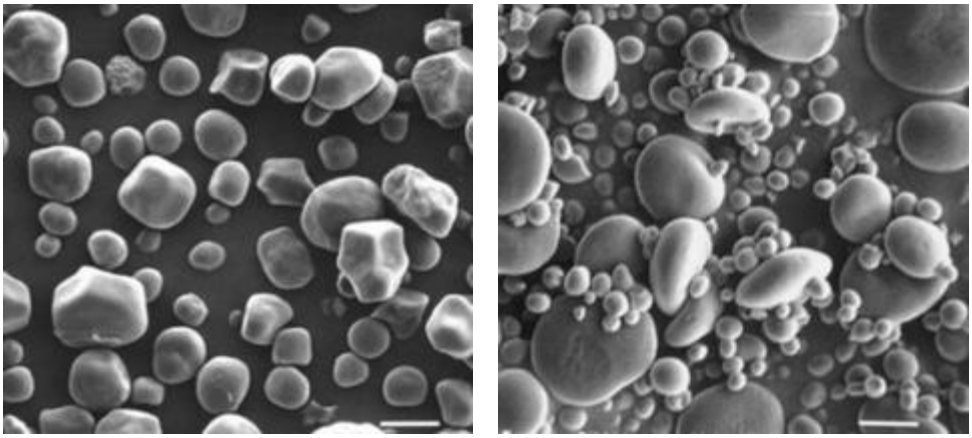

Figure 5.12. SEM images (x 100) of corn (left) and wheat (right) starch granules (Jensen 2015).

In plants, amyloses and amylopectines are packed together forming granules. Such granules may also contain other residual components including proteins, fats or salts. The size and shape of such granules depend on the ratio of amyloses and amylopectines which varies depending on the source of origin (see Figure 5.12).

This ratio, together with the degree of polymerisation, that is, the number of glucose units present in each chain, and the ratio between highly polymerised and lowly polymerised chains within the amylopectin macromolecules are the main characteristics that determine the different functional properties of the different starches (Anderson et al. 2010; Vissac et al. 2013; Jensen 2015). Table 5.6 summarises some of the properties of the most commonly used starches.

Table 5.6. Differences between the amylose and amylopectin contents of starch from different sources. Data from (Anderson et al. 2010; Vissac et al. 2013; Jensen 2015).

	Volume Europe	Amylose (%)	Amylopectin (%)	Granular size (μm)	Granular shape	T_{gel} (ºC)
Corn	5.55	25-28	72-75	75-80	Polygonal round	75-80
Waxy corn		<1	>99	63-72	Polygonal round	63-72
Wheat	3.57	25-26	74-75	1-40	Round lenticular	80-85
Potato	1.99	19-21	79-81	5-100	Oval, spherical	56-69
Waxy potato		<1	>99	5-100	Oval, spherical	56-69

Moreover, besides naturally occurring starches, chemically, physically, enzymatically or genetically modified starches have been introduced in order to achieve specific properties adapted for intended uses. Further information on starch modification can be found in (Anderson et al. 2010).

5.2.1.3. Gelling process

When hydrated and heated, starch undergoes a physical change called gelatinization. This process is composed of different phases. As starch is insoluble in water, in a fist stage, the starch granules are suspended in the liquid. When the system reaches a certain temperature hydrogen bonds in the starch granules break and allow water to enter into the granules. Starch forms hydrogen bonds with water and the granules swell due to water absorption. Once swelling is completed, the granules burst and the amylose and amylopectin polymers are released into the solution and are free to create associative networks, adsorb great amounts of water

and form a gel. The range of temperatures at which gelatinization occurs is characteristic of the type of starch. Starches with high amylose content (such as corn starch) tend to set back and gel more than those with lower amylose content. The conditions influencing gelatinization are numerous, including temperature, speed of cooling, type and concentration of starch and the presence of other substances such as acids. More details can be found in (Vissac et al. 2013).

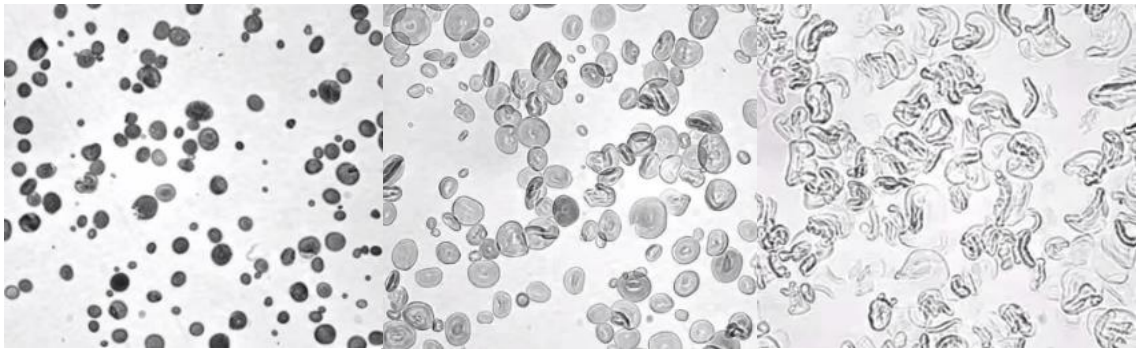

Figure 5.13. Microscopic images of heat gelation of wheat starch granules (Jensen 2015).

5.2.2. Sodium alginate

5.2.2.1. General description

Sodium alginate is the name given to one of the alginic acid salts present both in cell walls and intercellular spaces of brown algae tissues. Their function in nature is to provide flexibility and strength to the tissues, similar to cellulose in plants. Alginates are nowadays extracted from wild species of brown algae as cultivation is expensive. However, an economically competitive cultivation of brown algae exists in China (Anderson et al. 2010) suggesting the possibility of a growing production practice in the future. There are several species of brown algae that are harvested to produce different kinds of alginate, the most important ones being Laminaria, Macrocystis and Ascophyllum (McHugh 1987; McHugh 2003). In Figure 5.14, the harvesting areas in Europe are indicated in orange.

As for corn starch, there is also a wide range of industrial applications for alginates. Nowadays, they are mainly used in cosmetic and food industries as thickeners, stabilizers and for gel or film forming. Besides, they are also used in the pharmaceutical and medical industries where they are used in making pills and

toothpaste, as inhibitors of intestinal absorption of radiative isotopes or as cellular support in immunotherapy. In agriculture, alginates are used as suspension agents for plant treatments and as humectant substrates in transplants. Algae products have been used for centuries in construction as stabilizers in clay renders and binders. During the last restoration of the Antoni Gaudi's Palau Güell it was discovered that a substance similar to alginate was used to adhere the ceramic finishes to the walls. More recently, sodium alginate was used in the formulation of clay bricks presenting enhanced mechanical properties (Galán-Marín et al. 2010). It is estimated that the consumption of alginate in the OCDE is about 12 Mt, close to half of which is consumed by the food industry. The cost of alginates vary depending on the degree of purity: low-purity alginate might cost 1€/kg while ultra-pure alginate typically costs around 5€/g (Kurt).

Figure 5.14. Industrially used Brown seaweeds. Adapted from (Anderson et al. 2010)

The alginate used in this thesis is a commercially available sodium alginate provided by Cargill. It has alimentary grade (E401) and consists of a mixture of sodium alginate and sunflower oil (<1%). It is marked in the form of a creamy-white to light-brown powder, of neutral odour and flavour of 200 microns particle size. The rheological information provided in the technical sheet indicates a break strength of a gel in water of 500 – 700 g and a viscosity in a 1% aqueous solution of 150– 300 cps. The pH at 1% aqueous solution is between 6 to 8.5.

5.2.2.2. Chemical structure

Alginates are copolymers formed by blocks of β-d-mannuronic acid (M) and its C-5 epimer, α-l-guluronic acid (G), linked together to form a linear polysaccharide with (1,4)-glycosidic bonds and with a high degree of polymerization. Such blocks are arranged in sections consisting of homopolymeric M or G blocks (MMMMMM or GGGGGG) or heteropolymeric blocks where M and G alternates (MGMGMG). The arrangement of the blocks and the ratio of M and G polymers, which vary depending on the seaweed from which alginates are obtained, determine the properties of the alginates. For instance, MG blocks are the most flexible conformations while GG are the most rigid ones (Anderson et al. 2010). Table 5.7 summarises the chemical composition of alginates obtained from different sources.

Table 5.7. Typical composition of alginates obtained from different species (Anderson et al. 2010).

Alginate source	F_G	F_{GG}	F_{MM}	F_{MG}
Laminaria hyperborea (stem)	0.68	0.56	0.20	0.12
Laminaria digitata	0.41	0.25	0.43	0.16
Laminaria japonica	0.35	0.18	0.48	0.17
Ascophyllum nodosum	0.36	0.16	0.44	0.20
Macrocystis pyrifera	0.39	0.16	0.38	0.23
Lessonia nigrescens	0.38	0.19	0.43	0.19
Durvillea antarctica	0.29	0.15	0.57	0.14
Lessonia trabeculata (stem)	0.62	0.47	0.23	0.15

5.2.2.3. Gel formation

Alginates have the advantage of forming cold soluble, freeze-thaw and heat stable gels which can set at room temperatures. The gel formation mechanism is based on the selective ion-binding characteristics of the G blocks. In the presence of acids or any multivalent cations except magnesium, the G blocks within the alginate molecules link together through chain-cation-chain interactions forming the gel network. This process is usually illustrated through the simple “egg box” model, although more accurate steric arrangement have been suggested (Draget et al. 2005; Anderson et al. 2010). The structural void of the alginate chain is fitted by calcium

ions, like eggs in an egg box (Figure 5.15). The number and length of junction zones, the molecular weight of the chain and the level of available cations influence the strength of the gel. The MM and the MG blocks give elasticity to the gel. Moreover, the composition of the aqueous system or the presence of impurities will determine its intrinsic viscosity. The cation most commonly used for alginate gelation is Ca^{2+} the release of which must be controlled in order to avoid the formation of lumps and get homogenous gels. This can be achieved by using low soluble substances or with the use of a calcium sequestrant such as a phosphate or citrate (Anderson et al. 2010).

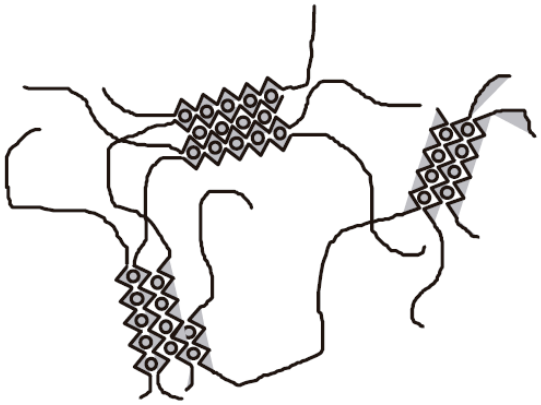

Figure 5.15. Schema of the gel structure of alginate (Anderson et al. 2010).

5.2.2.4. Durability and stability of the gel

As in many biopolymer gel systems, alginate gels may suffer a synerisis effect (the process in which the gel network contracts and loses water), however, it can be avoided by using a balanced formulation regarding the cation to alginate ratio. On the other hand, there is a direct relationship between the degree of polymerization (DP) and the molecular weight and the viscosity of alginate solutions. Alginates with low DP tend to be more stable than those with high DP. Alginates are susceptible to being depolymerized both at low and high pH, being stable only at nearly neutral pH. However, they are quite resistant to temperature. If attacked by microorganisms, alginate gels might become depolymerized and lose viscosity. Therefore, preservatives such as sorbic acid, potassium sorbate and benzoic acid, among others can be added in order to prevent such degradation.

5.2.3. Thermal decomposition of the binder materials

As for the crop by-products, two small-scale flammability tests were performed, PCFC and TGA, described in Section 4.3.1, in order to determine the thermal decomposition of the materials. Samples of 10 mg (±0.05mg) in mass were tested in the PCFC. Results are shown in Figure 5.16, where the Heat Release Rate (HRR) is represented as a function of temperature, and Table 5.8, which includes the main parameters obtained from the test averaged over three samples of each type.

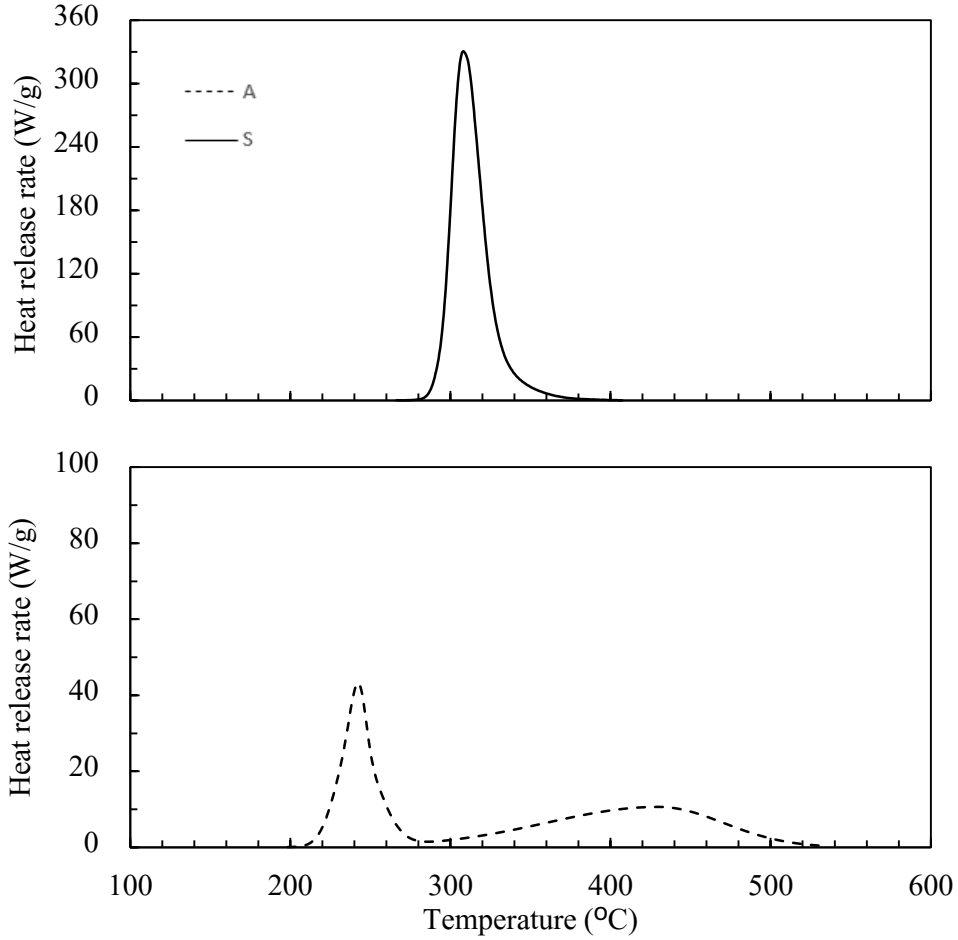

Figure 5.16. Heat release rate as a function of temperature for the different binders.

The differences between these two binders are remarkable: whereas sodium alginate presents two peaks of a lower magnitude than the peaks observed in the crop materials, starch has a sharp and much higher peak around 300ºC (the different scales may be observed in the figure).

Table 5.8. PCFC results for the two binders.

Raw material	HR (MJ/kg)	T_{onset} (ºC)	T_{MAX} (ºC)	PHRR (W/g)	Mloss (a.u.)
Starch	9.2	288	308	330.5	0.80
Alginate	2.5	213	232	27.2	0.68

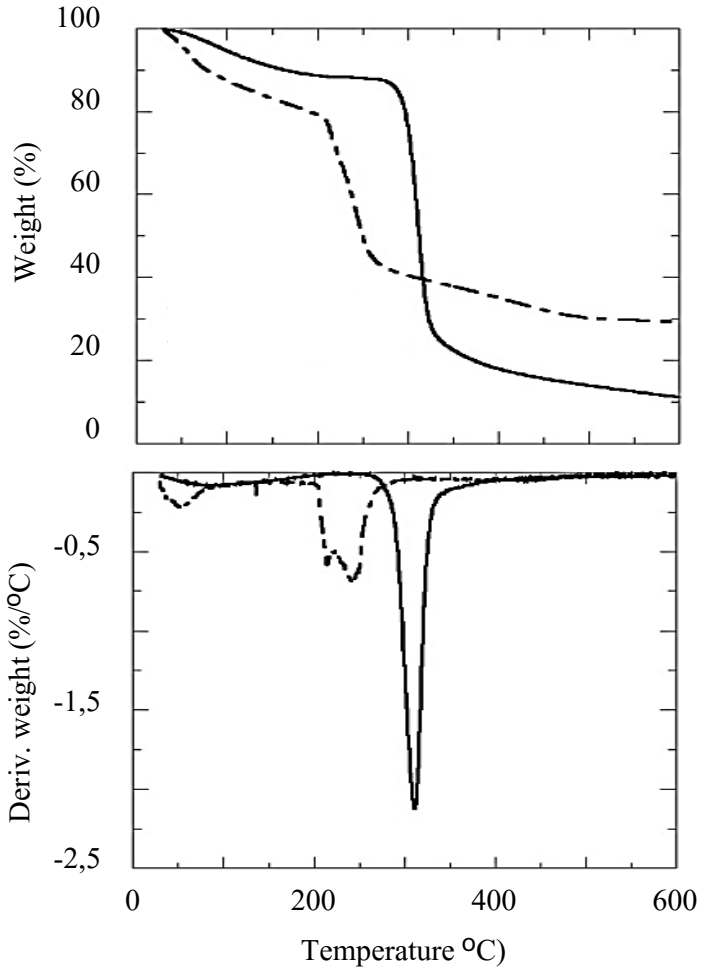

Figure 5.17. TGA and derivative for the two selected binders.

Figure 5.17 shows the results obtained for the mass loss and its derivative. An appreciably different behaviour is observed between the two binders. Starch weight is reduced by 90% and the derivative presents a sharp peak with a magnitude approximately three times higher than that obtained for the alginate and the crop by-products (the different scale may be observed in the figure). This higher peak indicates a faster thermal decomposition.

6. EXPERIMENTAL BIO-BASED THERMAL INSULATION BOARDS

In this section, the physical properties, hygrothermal properties and fire reaction of six different experimental composites are analysed. Barley straw, corn pith and rice husk are used as aggregates, while the matrixes are corn starch and sodium alginate. The main objective of the work presented here is to compare relevant properties of the composites in order to select the one that present an overall most suitable performance for its use as insulation material in buildings. The first section of this chapter deals with the characterization of the experimental boards, focusing on the analysis of the porous structure and density of the materials and on the basic hygrothermal properties such as thermal conductivity and diffusivity, moisture permeability and moisture content at different relative humidities. The second part relates to the fire reaction of the materials, analysing their flaming combustion with a PCFC analysis, together with extinguishability test and Limiting Oxygen Index (LOI) test.

6.1. Board formation

In order to analyse the above mentioned aspects of the experimental insulation boards, six different formulations were made. The crop by-products were prepared as described in section 5.1: the raw materials were shredded and sieved to obtain groups of particles of similar size. The ratio of the organic matrices with respect to the crop materials was adjusted in each case to obtain specimens with low density, but also enough cohesion to maintain their integrity during handling. It was

observed that the particle size of the aggregates highly influenced the amount of binder needed to obtain cohesive composites. After some preliminary work the chosen formulations were those depicted in Table 6.1. Composites based on rice husk required the greatest amount of blender per volume unit, especially when the particles were large (2 mm). This was probably due to the shape of the particles: the rice husk particles having a concave shape and being randomly arranged would have less contact points than the straw fibres or the pith spherical particles. The lowest ratio was achieved by corn pith granulates as the granules are highly flexible and squashed under pressure, which increase the contact surface between the particles.

Table 6.1. Formulations of natural thermal insulations and their corresponding densities.

Thermal insulation	Code	Particle size (mm)	Aggregate (%)	Matrix (%)
BSarley straw + starch	BS	0.5	83	17
Barley straw + alginate	BA	0.5	94	6
Corn pith + starch	CS	2.0	91	9
Corn pith + alginate	CA	2.0	97	3
Rice husk + starch	RS	1.0	71	29
Rice husk + alginate	RA	1.0	89	11

Figure 6.1. Image of the specimens based on barley straw (left), corn pith (centre) and rice husk (right)

The matrixes were mixed with the aggregates in their gelled state. In order to achieve the gelatinization, the starch was mixed with water and heated on a hot plate, while the alginate was gelatinised with the addition of calcium sulphate di-

hydrate ($CaSO_4 \cdot 2H_2O$) and a solution of sodium citrate which was used to control the speed of gelatinisation. The mixture was then introduced in a mould and cold-pressed until desired density. Pressure was maintained for 10 minutes and then the boards were oven-dried at 60ºC for 24-48 hours. The outcome of the resulting specimens is illustrated in Figure 6.1.

6.2. Characterization of the different bio-based composites

6.2.1. Physical properties

The skeletal and bulk density of the samples are determined as described in Section 4.1.1. To obtain the bulk density, the dimensions of 100 mm diameter samples are measured using a calliper with 0.5 mm accuracy. Thereafter, the total porosity of the materials was calculated as 1 – bulk density / skeletal apparent density. The results are presented in Table 6.2. The skeletal apparent densities of the composites are slightly higher than those of the crop by-products alone, especially after the addition of alginate. However, this is not reflected in the bulk densities of the materials being that the porosities are similar between the two binders. In general, the addition of binders have little impact on the porosity of the composites, when compared with the loose materials alone (see Table 5.1 in Section 5.1.2).

Table 6.2. Physical properties of the six experimental bio-based insulation boards.

Code	Skeletal aparent density (kg/m^3)	Bulk density (kg/m^3)	Porosity (%)
BS	1512	145.35	0.90
BA	1607	125.32	0.92
CS	1585	58.17	0.96
CA	1618	55.24	0.97
RS	1629	203.08	0.88
RA	1682	219.45	0.87

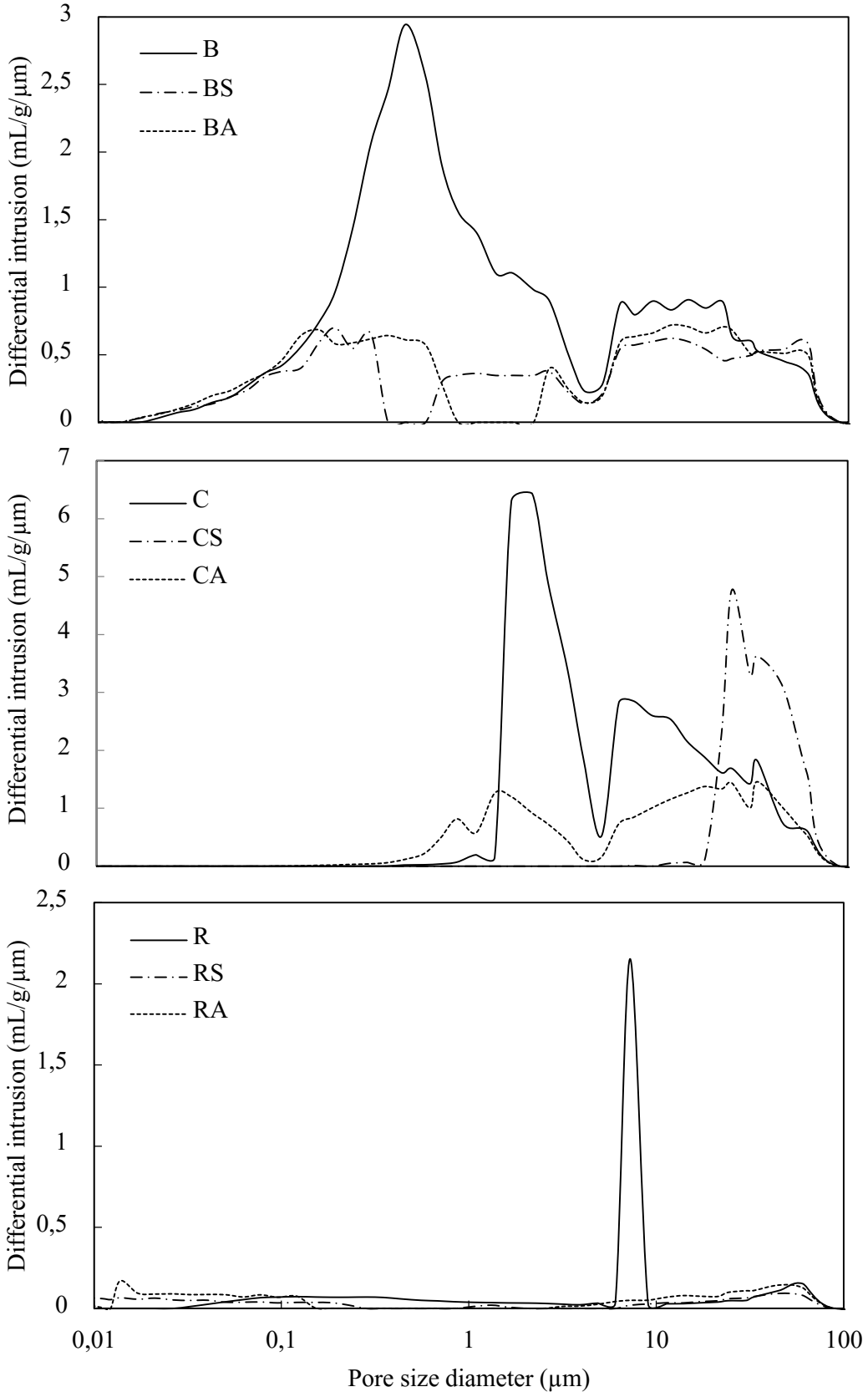

Figure 6.2. Results of the Mercury Porosimetry of the different composites compared to the raw materials. The pore size diameter is plotted in log scale. Note the different scales in the y axis.

The porosity of the composites was also investigated through mercury porosimetry. The description of the principles and procedures used for this technique is discussed in Section 4.1.1. The pore size distribution obtained from the formulations is compared with that of the crop by products alone in Figure 6.2, where the pore size diameter is plotted against the differential intrusion. The results indicate an important variation in the porosity of the materials due to the incorporation of the binders, generally showing a reduction in the porosity and thus, a good compaction. In the case of barley straw and rice husks materials, little differences are observed between composites incorporating corn starch and those incorporating sodium alginate which is not the case for the corn pith specimens. In barley straw materials, the results indicate an important reduction in the peak at 0.5 microns, probably due to obstruction of the interstitial spaces between fibres. However, the peak at 10 microns is maintained as this is the characteristic porous size of the internal structure of the straw particles. Corn pith alginate specimens yield good compaction results. The composite presents a bimodal distribution with peaks at 2 and 24 microns, but the intrusion at the peaks is reduced 5 and 2 times respectively. Corn pith starch specimens also show a good compaction although a new peak is formed between 20 and 30 microns. Finally, in rice based composites compaction is very clear as porosity is reduced almost entirely.

6.2.2. Thermal properties

Thermal conductivity and thermal diffusivity of the six composites are determined with a Quickline-30 Thermal Properties Analyser using a surface probe. The principles and methodology of this test is discussed in Section 4.1.2. The measurements are made on specimens of 95 mm diameter at room conditions (20ºC; 50%) in triplicate. The mean values obtained are shown in Table 6.3, together with those obtained from other commercial insulation materials. Mixtures containing rice husks present the highest thermal conductivity and the ones containing corn pith the lowest, regardless of the binder used. These results are consistent with the measured densities of the formulations, as rice products are four times denser than corn products. Regarding the binders, alginate mixtures tend to be less dense and thus, present a lower thermal conductivity, while starch seems to increase the thermal conductivity of the mixtures. The best result obtained was for corn pith based boards (0.044 W/mK). The results can be compared to those obtained from

wood wool boards, even though they are higher than other commercially available insulation materials.

The thermal diffusivity of corn pith and rice husk boards is similar to that of wood wool materials. Barley composites present a lower thermal diffusivity, similar to that of wood fibre boards, which indicates a higher thermal inertia.

Table 6.3. Thermal properties of the six composites. Density and thermal conductivity of conventional insulation materials are also included for comparison.

Code	Thermal conductivity (W/mK)	Thermal diffusivity (10^{-6} m^2/s)	Bulk density (kg/m^3)
BS	0.054 ±0.0010	0.381 ±0.010	145.35
BA	0.052 ±0.0003	0.393 ±0.001	125.32
CS	0.044 ±0.0010	0.750 ±0.080	58.17
CA	0.044 ±0.0010	0.823 ±0.030	55.24
RS	0.068 ±0.0003	0.708 ±0.010	219.45
RA	0.060 ±0.0010	0.455 ±0.010	203.08
WW	0.049 ±0.0020	0.613 ±0.010	56.10
WF	0.072 ±0.0001	0.316 ±0.001	235.30
MW	0.039 ±0.0001	0.970 ±0.003	43.00

6.2.3. Hygroscopic properties

The hygroscopicity of the composites was analysed through two important aspects concerning moisture transport and storage within a material: the equilibrium moisture content of the samples, and the water vapour permeability (δ). The equilibrium moisture content gives information about the amount of moisture adsorbed in the porous structure of the material under certain conditions. On the other hand, the water vapour permeability indicates how the moisture migrates from one side of the material to the other. In both cases the values refer to stationary conditions. The equilibrium moisture content was determined using the saturated salt solution method exposing the specimens to three different relative humidities

and at constant temperature (20ºC). The water vapour permeability of the materials was determined experimentally by creating a relative humidity gradient across the samples. Both methods are further described in Section 4.1.3.

Table 6.4 depicts the results of the moisture content test, expressed per unit mass (left) and per unit volume (right).

Table 6.4. Results of the equilibrium moisture content and water vapour permeability tests of the six composites.

Code	Moisture content w/w (%)			Moisture content w/vol (g/cm^3)		
	36%	67%	94%	36%	67%	94%
BS	3.0	10.1	20.3	3.3	11.5	22.2
BA	2.8	10.4	23.1	2.6	9.0	19.7
CS	2.5	9.4	41.7	1.3	4.7	18.0
CA	2.3	13.3	48.9	1.0	4.8	15.6
RS	3.2	8.7	14.9	5.0	11.5	22.5
RA	2.7	8.9	18.0	4.0	10.1	21.2

These results are compared in Figure 6.3 with those obtained from the raw materials by applying the same method and with those obtained using the DVS. As discussed in section 2.3, the moisture content of the materials increases with relative humidity following a certain curve that is common for bio-based materials. From Figure 6.3 it is possible to conclude that the behaviour of the composites is similar to that of the crop by-products alone. Nevertheless, at low relative humidities the composites tend to adsorb a lower amount of water vapour than the crop by-products alone. Moreover, despite no significant differences exist between samples incorporating corn starch and those incorporating sodium alginate, the latter present a slight tendency to adsorb higher amounts of moisture at high relative humidities.

The results of the water vapour permeability test are presented in Table 6.5, and expressed using the water vapour resistance factor μ. The water vapour permeability of air was assumed to be $1.95 \cdot 10^{-10}$ kg/msPa and the barometric pressure of the air 1013 hPa.

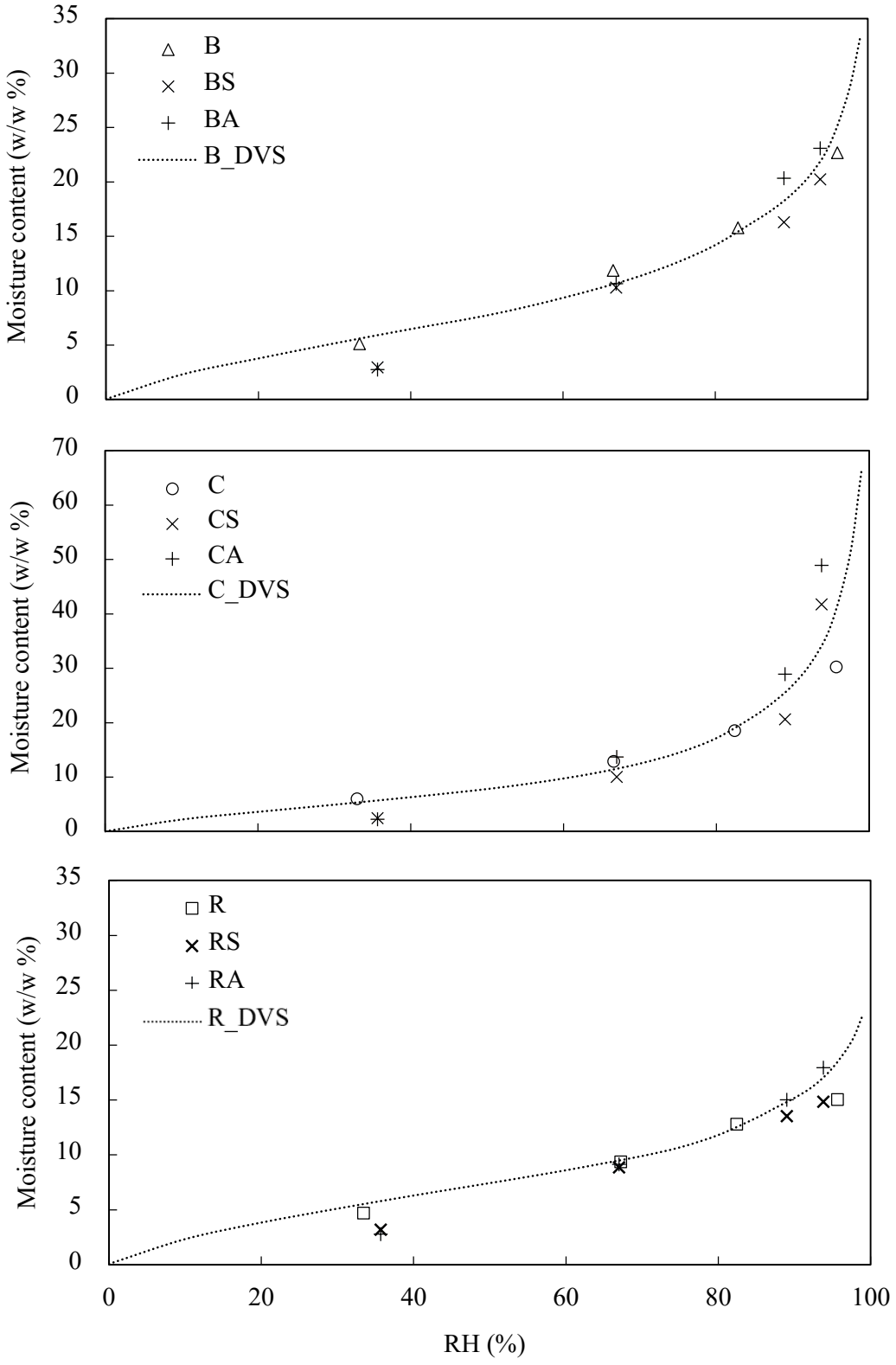

Figure 6.3. Equilibrium moisture content of the six experimental composites and the raw materials.

Table 6.5. Water vapour permeability of the materials.

Code	DRY (50% mean RH)		WET (80% mean RH)	
	δ (10^{-11} Kg/msPa)	μ	δ (10^{-11} Kg/msPa)	μ
BS	4.0 ±0.6	5.1	5.1 ±0.2	3.8
BA	3.6 ±0.7	5.2	4.9 ±0.2	4.0
CS	4.2 ±0.6	4.8	6.5 ±0.1	3.0
CA	4.4 ±0.4	4.4	6.7 ±0.6	2.9
RS	-	-	4.3 ±0.2	4.6
RA	4.5 ±0.6	4.3	3.8 ±0.5	4.7

6.3. Fire reaction of the different bio-based composites

6.3.1. Small scale flammability tests

The six bio-based thermal insulation materials are analysed with PCFC and TGA methods, as described in Section 4.3.1. The results are compared with those obtained for other commercial organic foams (polystyrene and polyurethane), thereby confirming that insulations based on crop by-products present a better fire behaviour than organic foams. Table 6.6 summarises the results obtained averaged over three samples of each type.

The results obtained from the composites are compared with the raw materials in Figures 6.4-6.6. In each figure, the heat release rate of the composite is compared with that obtained for each of the two components (binder and crop by-product) separately. HRR curves for each component alone (discontinuous lines, obtained from Figure 5.10 and Figure 5.16 in Section 5.2.3) are adjusted according to their percentage in the composite as shown in Table 6.1.

Table 6.6. Pyrolysis Combustion Flow Microcalorimetre results for the natural insulators.

Code	HR (MJ/kg)	T_{onset} (ºC)	T_{MAX} (ºC)	PHRR (W/g)	Mloss (a.u.)
BS	7.1	229	313	68.4	0.76
BA	6.2	227	310	56.4	0.73
CS	7.0	199	313	61.7	0.77
CA	6.0	184	309	61.4	0.70
RS	6.5	264	317	67.7	0.71
RA	5.8	250	335	58.0	0.66
EPS	38.7	339	434	631.0	0.99
PUR	13.5	200	335	85.0	0.78

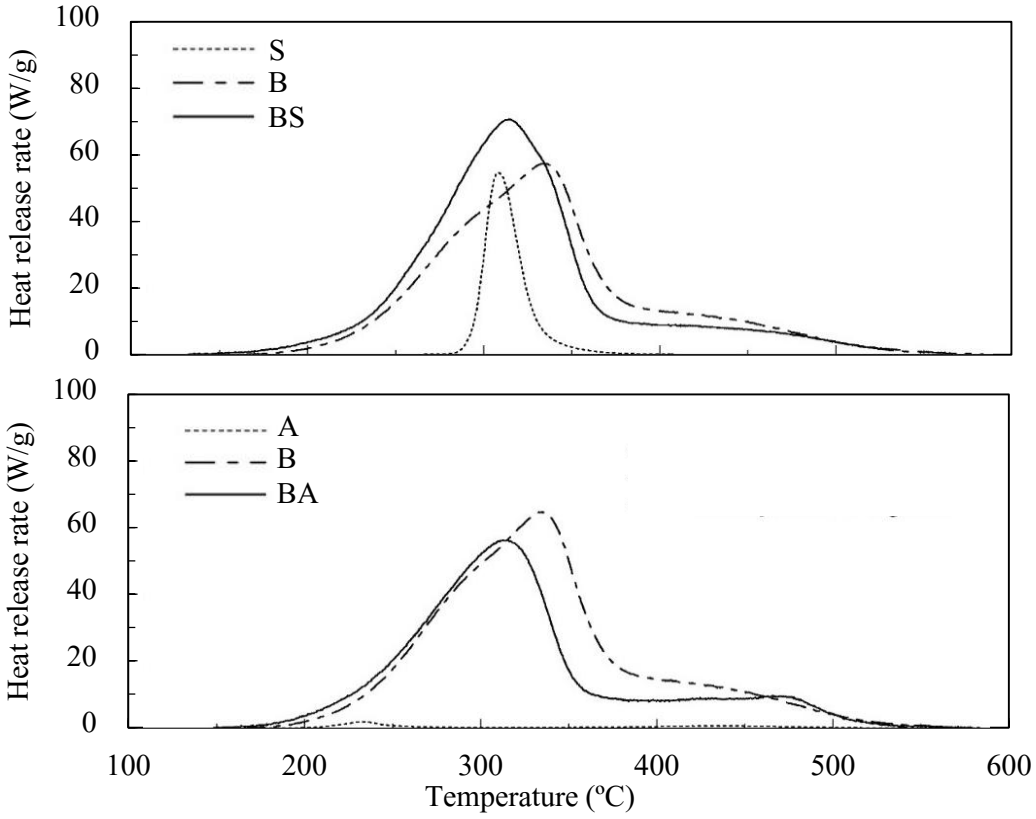

Figure 6.4. Heat release rate as a function of temperature for the components alone (discontinuous lines) and the thermal insulations (solid lines) formulated with barley straw and the two binders: corn starch (top panel) and sodium alginate (bottom panel).

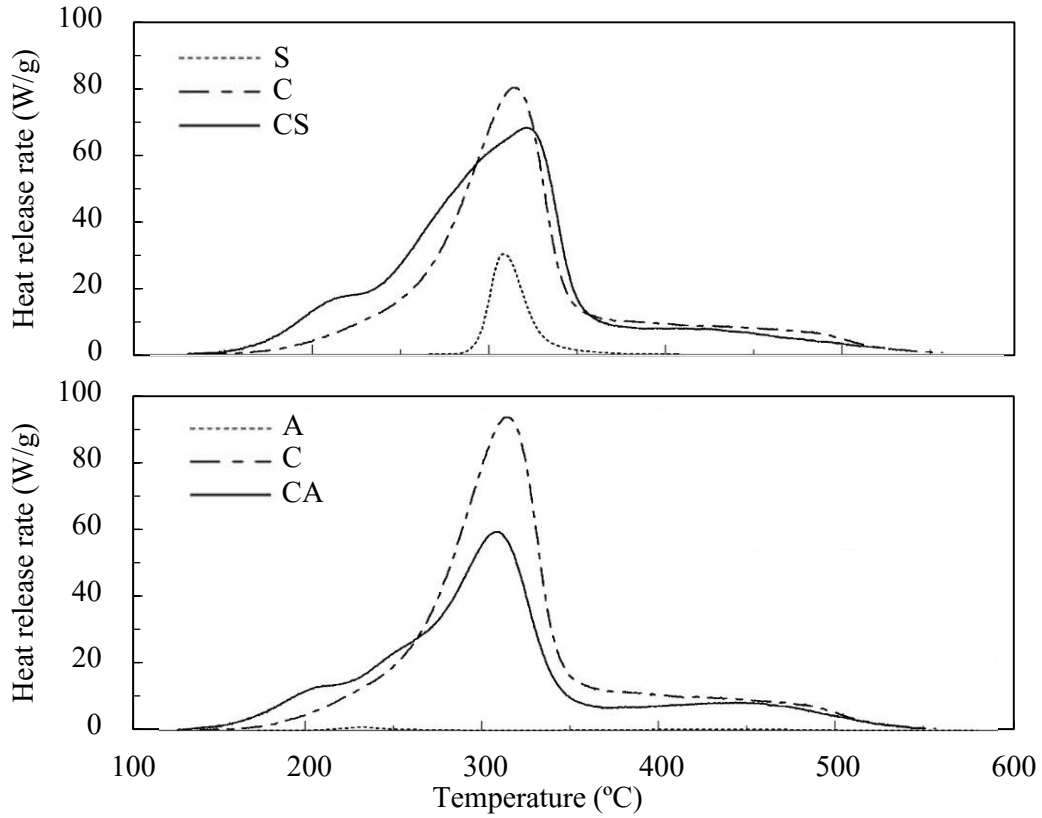

Figure 6.5. The same as Figure 6.4 for insulations formulated with corn pith and the two binders.

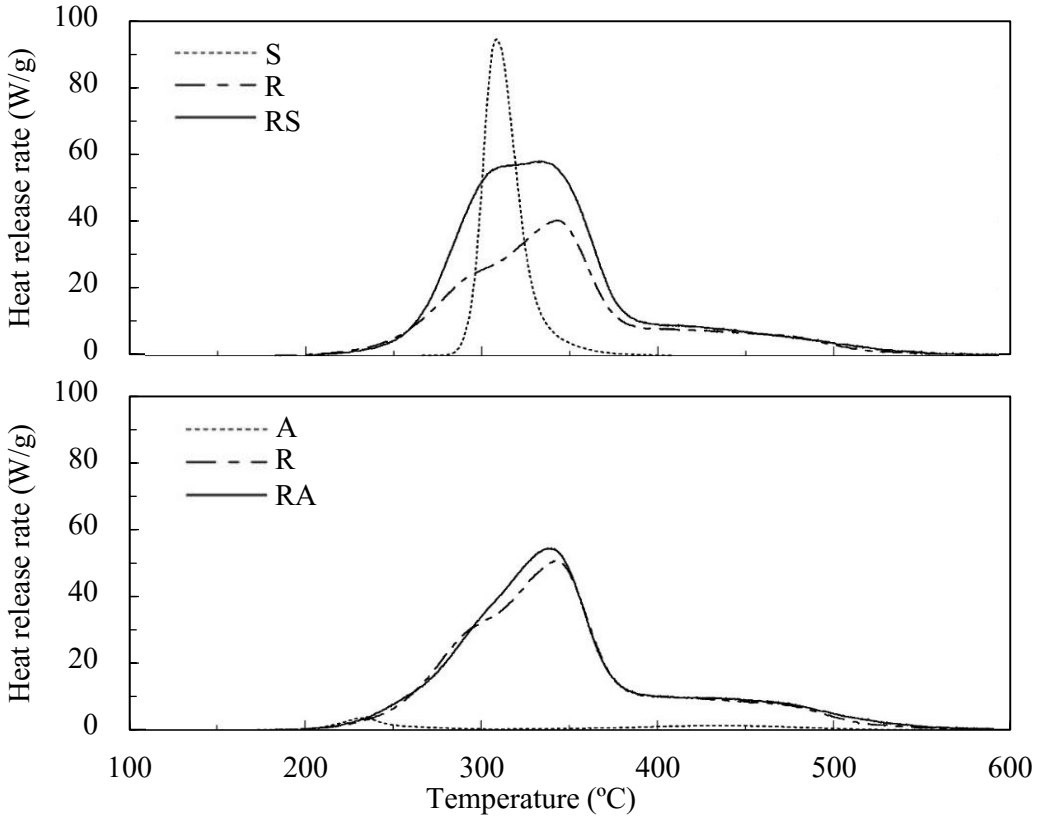

Figure 6.6. The same as Figure 6.4 for insulations formulated with rice husk and the two binders.

The higher percentages of starch, in comparison with alginate, together with its high HRR give, as a consequence that, in general, the composites incorporating starch show a higher HRR, and thus a worse fire behaviour than the corresponding crop by-product alone. This occurs especially in the case of the rice husk, where starch is about 30% of the mixture. On the other hand, alginate has little contribution to the heat release and, in general, significantly improves the fire behaviour of the crop by-products. The results were compared to that of existing organic foam insulation materials. The HR of these foams is found to be between 2 and 6 times higher. In particular, polystyrene presents a remarkably high PHRR (about 10 times higher than bio-based insulations), which however appears later (at approximately 430ºC).

TGA was performed in air, with a heating rate of 10 ºC/min from 30 ºC to 900 ºC. For each experiment a mass of 500 mg ± 10 mg was used. The results are presented in Figures 6.7-6.9.

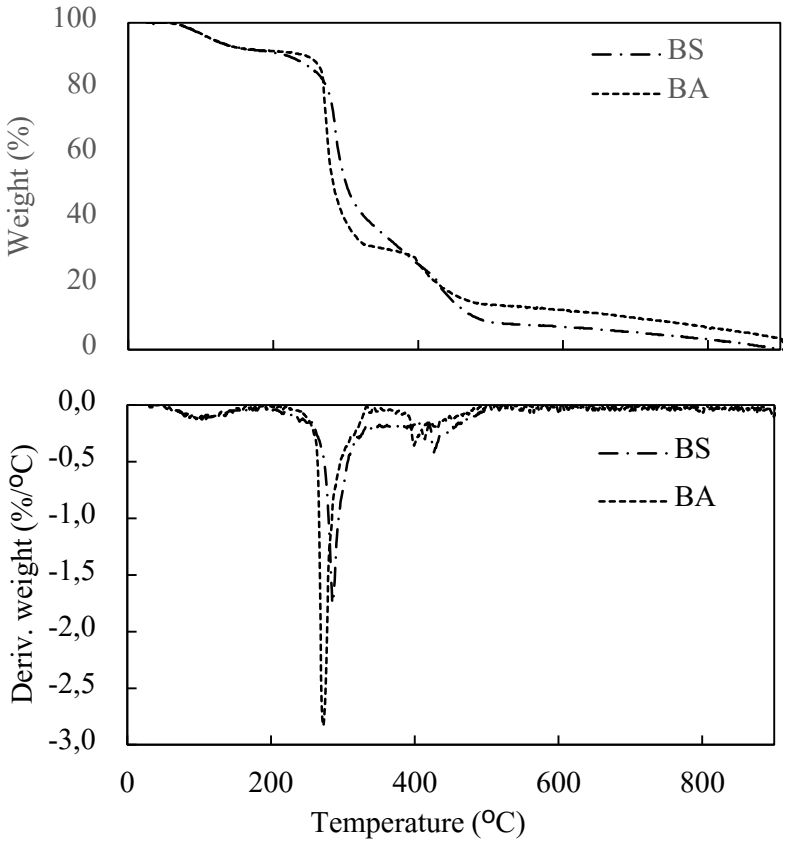

Figure 6.7. Mass loss and derivative plotted against temperature for corn pith samples.

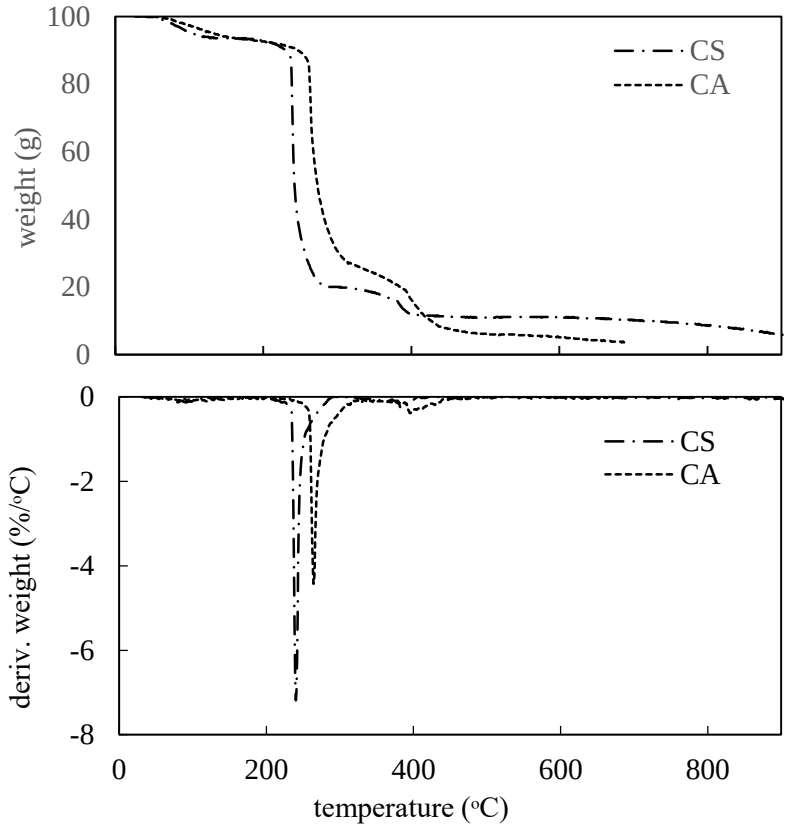

Figure 6.8. Mass loss and derivative plotted against temperature for corn pith samples.

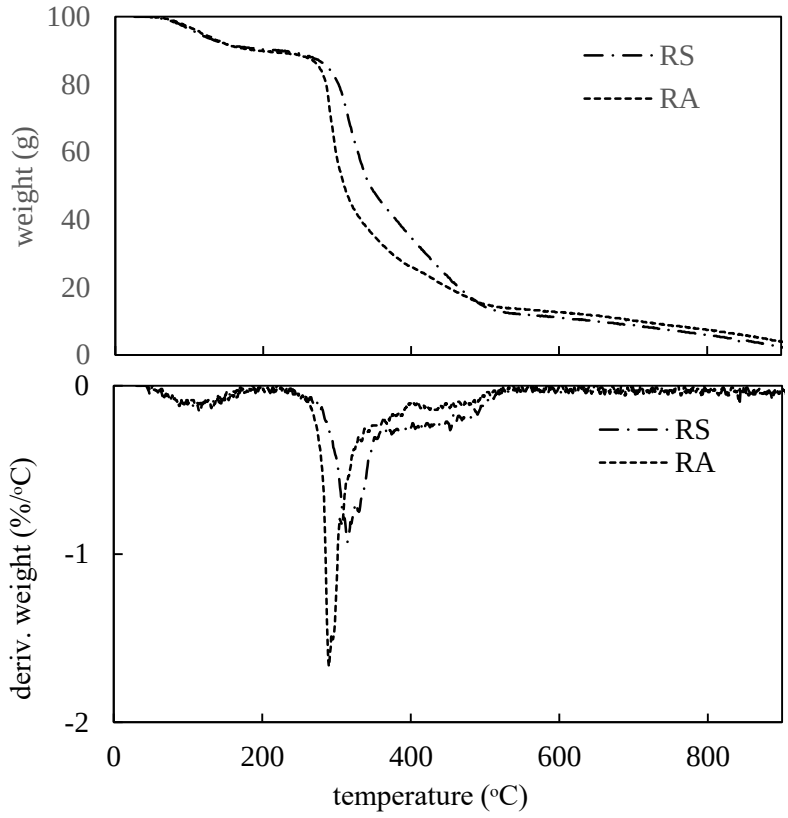

Figure 6.9. Mass loss and derivative plotted against temperature for rice samples.

The first peak that can be observed in the bottom panels of the figures is due to the loss of the water present in the materials. The second peak, which is much more important, is related to the thermal decomposition of the cellulose, while the tail may be due to the decomposition of the lignin. The results are in qualitative agreement with those obtained with the PCFC. Corn pith composites decompose faster than barley straw and rice husks (note the different scales on the y axis in panels showing the derivative mass loss of the samples). Moreover, it can be observed that mixtures containing alginate present worse behaviour (faster and sooner decomposition) than those incorporating starch, with an exception of corn composites whose behaviour can be improved with the addition of alginate.

6.3.2. Medium scale flammability tests

The flammability of the samples was analysed by the ignition time and extinguishability and the limiting oxygen index.

A radiator device was employed to measure the ignition time and the degree of extinguishability of combustion for the six composites following the procedure indicated in Section 4.3.2. Samples of surface 70 x 70 mm^2 and variable thickness were placed on a metallic grid 3 cm below a heat source of 500 W, which was removed and replaced after each ignition and extinction, respectively during the 5 minutes of the assay. The thickness of each sample was selected in order to obtain a similar mass of 10 g (± 1 g) for all samples. Therefore, due to the large difference in densities (Table 6.2), the thicknesses ranged from 1.0 cm for the rice husk based materials to 3.3 cm for the corn pith based materials (see Table 6.7).

The parameters obtained from the test, as shown in Table 6.7 are:

- First ignition time (t_0)
- Number of ignitions in 5 minutes (N_{ig})
- Average duration of the ignitions (Δt_{ig})
- Mass loss fraction (M_{loss})

amongst which the number of ignitions and the average value of combustion extent are the most important.

On the application of the radiator, the first ignition occurred within seconds, the specimens made with rice husks taking longer. The radiator was removed 3 seconds after the ignition and, once the flame was extinguished, a progressive smouldering was observed, with the exception of the rice husk samples. Since this test assesses the occurrence of flame, the radiator was replaced after each extinction until the 5 minutes of the assay were completed.

Table 6.7. Ignition and extinguishability test results

Sample	t_1 (s)	N_{ig}	Δt_{ig} (s)	Mloss (a.u.)	Thickness (mm)	Smouldering
BS	5	9	14	0.89	15	Yes
BA	5	3	6	0.83	18	Yes
CS	2	3	15	0.92	25	Yes
CA	2	1	7	0.90	33	Yes
RS	6	12	17	0.65	10	No
RA	9	10	9	0.83	10	No

The results for Δt_{ig} show that the natural insulations formulated with starch have ignitions of longer duration than those formulated with alginate, and therefore a worse behaviour might be expected in case of fire. After five minutes of the assay, and without additional application of the radiator, smouldering is observed to continue until the samples formulated with corn pith or barley straw are almost completely consumed. The mass loss fraction M_{loss} shown in Table 6.7 is calculated once smouldering is finished. Although the rice husk samples have a greater number of long ignitions, this accounts for the reason why their mass loss is smaller. Especially remarkable is the case of corn pith with alginate, which undergoes only one flaming ignition of short duration, but its mass is reduced by 90% because of smouldering.

The Limiting Oxygen Index was determined using the device described in Section 4.3.2. Samples of 70 x 2 x 0.5 mm were placed vertically in a test chimney. A gas mixture of nitrogen and oxygen was then blown through the chimney and the sample was ignited. This procedure was repeated a minimum of six times for each

composite, the oxygen concentration of the gas mixture being changed every time in order to determine the concentration at which the sample burned.

In general, the results for LOI (Table 6.8) are in concordance with those previously recorded with the microcalorimetre and the ignition and extinguishability test. In this case, samples of the same size were compared (that is, with different mass) in order to determine when consumption occurs, either with or without flame (smouldering). Rice husk composites burn at a clearly higher oxygen index than barley and corn ones, and corn, as expected from the ignition and extinguishabililty test, present smouldering. Nevertheless, only slight differences are observed between the binders, indicating that this test may not be sufficient to reveal such differences.

Table 6.8. Oxygen Index test results

Code	OI
BS	20.3
BA	20.9
CS	18.8
CA	18.0
RS	26.8
RA	30.4

Although the LOI test is useful for comparison, the results are hardly indicative of the flammability of the materials in real fire situations, as factors such as air velocity or temperature, can affect the LOI of a material. Moreover, LOI results do not show a clear correlation with the heat release rate or other fire properties of the materials (Chapple and Anandjiwala 2010). The LOI of the corn composites is in the range of those of polystyrene and polypropylene, which are highly flammable materials. Barley straw composites present a slightly lower flammability, with LOI values comparable with those of vinyl esters. Rice husk composites present LOI values between 27 and 30, similar to those of polyamides and considered suitable from a flammability point of view (Chapple and Anandjiwala 2010).

6.4. Conclusions

Six experimental bio-based insulation materials based on crop by-products (rice husk, barley straw and corn pith) and natural binders (corn starch and sodium alginate) were characterized based on their physical, thermal and hygroscopic properties. It was found that the properties of corn pith alginate (CA) composites were favourable for its use as thermal insulation in buildings. The amount of binder needed to conform the composite was lower than in the rest of the cases (only 3% of the binder was needed), probably due to the granular and spongy nature of the material which would allow a good contact surface between the particles. This aspect presents an advantage in terms of cost of production and environmental impact. The evaluation of such factors is beyond the scope of this thesis and further research is needed in this regard. Moreover, CA presented the least bulk density among the tested materials (about 55 kg/m^3), twice lower than that of barley straw composites and four times lower than that of rice husk. Low bulk density represents an advantage in terms of transportation and ease of handling. It is also a driving factor for the thermal conductivity of the material which is minimum at densities between 30 and 100 kg/m^3 (Domínguez-Muñoz et al. 2010). Thus, the thermal conductivity of CA boards was also lower than the rest of the materials (0.044 W/mK at room conditions). This value is lower than those obtained from the existing wood based insulation materials. It was discovered that the incorporation of the blenders do not significantly affect the porosity of the crop by-products. However, from Mercury Porosimetry, a reduction in the smallest pores is observed, which may be explained by the obstruction of these pores after the incorporation of the binders. This is in agreement with the results from the equilibrium moisture content test, which indicate that the moisture content of the crop by-products is slightly reduced by the addition of the blenders, especially in composites blended with starch.

The viability of the six experimental insulation materials is evaluated in terms of their reaction in case of fire. PCFC results indicate that, in general, the use of alginate as a binder improves the properties of the crop by-product alone, especially in the case of corn pith, where both the total heat release HR and the peak of heat release rate PHRR are reduced by 30%. It should be noticed that such improvement is achieved with a small amount of alginate (3% w/w), the lowest among the composites.

By contrast, the results are not so positive when starch is used, especially in the case of rice husks. Since rice husk is the crop by-product with the least heat release, the addition of starch worsens its behaviour. PCFC results show similar behaviour for materials incorporating the same binder, regardless of the crop by-product used, which indicates that binders, even in small portions, have a strong influence on the thermal degradation of the composites. In any case, the fire properties of the six experimental insulation materials are very favorable when compared with other organic foamy materials commonly used in building insulation, such as polystyrene and polyurethane. The corn pith materials show a faster thermal degradation than the other materials when tested at the TGA. It is interesting to note that the addition of alginate seems to have a negative effect on barley straw and rice husk materials, but improves the behaviour of the corn pith. CA composites decompose more slowly and later than CS materials.

Fire reaction tests on a larger scale agree qualitatively with the microgram scale PCFC results. From the ignition and extinguishability test, fewer ignitions with significantly shorter duration are observed for the materials with alginate in comparison with those containing starch. In particular, the CA mixture yields an extremely good result, with only one ignition with duration of only 7 seconds. However, this result refers only to flaming combustion, and a smouldering process is also observed, which slowly burns the specimens. Such smouldering, also observed in the LOI experiments, constitute an important problem that is yet to be solved, and further research is needed to minimise this negative point.

The fire behaviour of the bio-based insulation materials analysed is a positive aspect to be added to the other benefits that, in terms of environmental impact, these materials have in front of other commercial insulations. Although the six formulations could satisfy the necessities of their application as building insulation, the results point to the one consisting of corn pith and alginate as highly promising. It is worth pointing out that PHRR provides the results per unit of mass, but insulations made from corn pith have densities approximately 3 times lower than the others. This means that, as thermal conductivity is similar in all the cases, in a real situation the insulation made with corn pith would contain a lower mass, and therefore a lower fire load than the others. Thus, it was decided to further analyse the properties and performance of the corn pith alginate formulations. The results of such work are presented in the following section.

7. CORN PITH ALGINATE THERMAL INSULATION BOARDS

7.1. Introduction

In section 6 it was discovered that the corn pith alginate formulation (CA) was the material having the most promising properties for its use in building thermal insulation. Low density, low thermal conductivity and low fire contribution are some of the favourable properties detected. The material presented significant moisture adsorption which may have positive consequences, such as high moisture buffering, but also undesired ones such as low mould growth resistance or poor durability due to shrinkage. Therefore, it was decided that this experimental material would be subjected for further investigation. The results of this work are presented in this section. The performance of the corn pith board is analysed in three main areas: hygrothermal performance, fire reaction and resistance to mould growth. The dependence of the main thermal and hygroscopic properties of the material to moisture content is analysed together with its moisture buffering capacity and its hygrothermal performance. Thereafter, the fire behaviour of the material is investigated and improved upon. In light of the results presented in Section 6.3, the analysis is focused on the smouldering process. Different fire retardants are added in order to reduce the speed of propagation and increase the combustion onset temperature of the material. Similarly, the mould growth resistance of the composite is analysed and improved by subjecting the corn pith aggregate to different pre-treatments.

The results are compared with two kinds of wood fibre insulation boards (WW and WF) and two conventional insulation materials: expanded polystyrene (EPS) and mineral wool (MW). The main characteristics of these materials are presented in Table 7.1.

Table 7.1. Main characteristics of the thermal insulations used for comparison.

Material	Code	Product	Nature	Density (kg/m^3)
Corn pith alginate	CA	Board	Cellular	60
Wood wool	WW	Mat	Fibrous	55
Wood fibre	WF	Board	Fibrous	230
Expanded Polystyrene	EPS	Board	Cellular	30
Mineral wool	MW	Mat	Fibrous	30

7.2. Hygrothermal performance

The basic hygrothermal properties of the raw materials and the composite proposed in this thesis have been determined in Section 5.1.2 and Section 6.2 respectively. However, most of these properties are dependent on the temperature and the relative humidity of the surrounding environment. In this section, the variation of thermal conductivity, thermal diffusivity, moisture content and water vapour permeability of the corn pith alginate composite with relative humidity and/or temperature is investigated. The results are compared with other commercially available bio-based insulation materials, that is, wood wool (WW) and wood fibre (WF). Moreover, the hygrothermal performance of the material is evaluated through dynamic tests where the relative humidity or/and temperature are cyclically changed.

7.2.1. Thermal properties: dependence on relative humidity and temperature

With the aim to determine the influence of moisture content on thermal conductivity and thermal diffusivity of the materials, samples of 200 x 200 mm were prepared. They were conditioned at 20 ºC and different relative humidities in sealed capsules containing saturated salt solutions for at least two weeks. Their

thermal conductivity and thermal diffusivity were then determined with the Quickline-30 Electronic Thermal Analyser using a surface probe (see Section 4.1.2). In order to maintain the environmental conditions during the test, the surface probe was introduced into the capsules for testing. After each measurement the moisture content of the samples was gravimetrically determined with an accuracy of 0.01 g. At the end of the assay the samples were oven dried at 100 ºC for 24 hours and weighed again in order to quantify the dry mass. From thermal conductivity (λ) and thermal diffusivity (α), the value of the product of density and the specific heat capacity (ρCp) was determined using Equation (4.3), presented in Section 4.1.2.

The variation of thermal conductivity with temperature was analysed using a Heat Flow Meter and operating on the principle of the stationary slab method for three different temperature ranges (BS EN 12664). The mean temperatures were 10, 20 and 30ºC, being 20ºC the temperature gradient in all cases. For this test, specimens of 600 x 600 mm were prepared. Measurements were taken both on dry specimens and on specimens conditioned at 80% relative humidity. In order to maintain and control the moisture content of the specimens during the test, they were wrapped with a plastic film and weight before and after the test. After the test, the specimens were oven dried at 100 ºC for 24 h and weighed again in order to quantify the dry mass.

The variation of λ and ρCp with relative humidity is shown in Figures 7.1 and 7.2. A linear regression was used to fit the experimental data ($\lambda = \lambda_0 + \lambda_1 \phi$ and $\rho Cp = \rho Cp_0 + \rho Cp_1 \phi$ respectively). The values of the fitted factors are presented in Table 7.2. In all cases the thermal conductivity and the product of density and specific heat capacity increase with moisture content which is an expected result. Results also indicate a clear dependence of the thermal conductivity with density, which is in accordance with the literature (Domínguez-Muñoz et al. 2010), as the CA and WW specimens present a lower thermal conductivity than the WF ones. For the commercially available materials the results are in agreement with declared values although important deviations were found on measurements made under the same conditions on consecutive days. This might be due to errors generated from the experimental method used, such as moist migration through the material when the sealed capsules were opened to introduce the probe and to weigh the samples or to inaccuracies in the weight measurements taken. Another factor explaining such

variability is the measurement device, which only analyses a part of the material near the surface of the probe through electric impulses that might also cause moisture migration.

Table 7.2. Values of the fitted factors for the λ and the ρCp variation with relative humidity.

	λ_0	λ_1	R^2	ρC_{p0}	ρC_{p1}	R^2
CA	0.029	0.019	0.95	38,400	62,500	0.95
WW	0.033	0.015	0.96	53,400	66,700	0.96
WF	0.052	0.019	0.98	161,200	116,400	0.98

The results indicate that the behaviour of the three materials present, in general, similar rates in which thermal conductivity and the product of density and specific heat capacity increase with relative humidity. This can be observed from the slopes of the fitting equations presented in Table 7.2 and implies a similar sensitivity to moisture changes of the three materials. These results do not explain the different hygroscopic behaviour of the materials. Although CA is the composite that adsorbs the highest amount of moisture per mass unit when the relative humidity is increased (see Figure 7.4a), the change rate of its thermal properties seem to be similar to the wood based materials. Similarly, when the water content of the materials is expressed in terms of mass per volume unit, which can be considered more appropriate for comparison (see Figure 7.4b), the higher moisture content of the WF material is not translated in a more pronounced variation of its thermal properties. The correspondence between moisture content and the variation of thermal properties of different materials is difficult to determine experimentally and is subjected to the proportion of matrix, air and water present in the composite as well as to complex changes in the internal structure of the materials which are not completely understood to the date. The devices measuring the thermal properties of the materials generate a heat flux through the sample which produces a moisture migration and thus affect the final results. Moreover, in the case of the materials analysed here, their low density and heterogeneity are important sources of error. Larger samples might provide more reliable results, but the conditioning time would exponentially multiply.

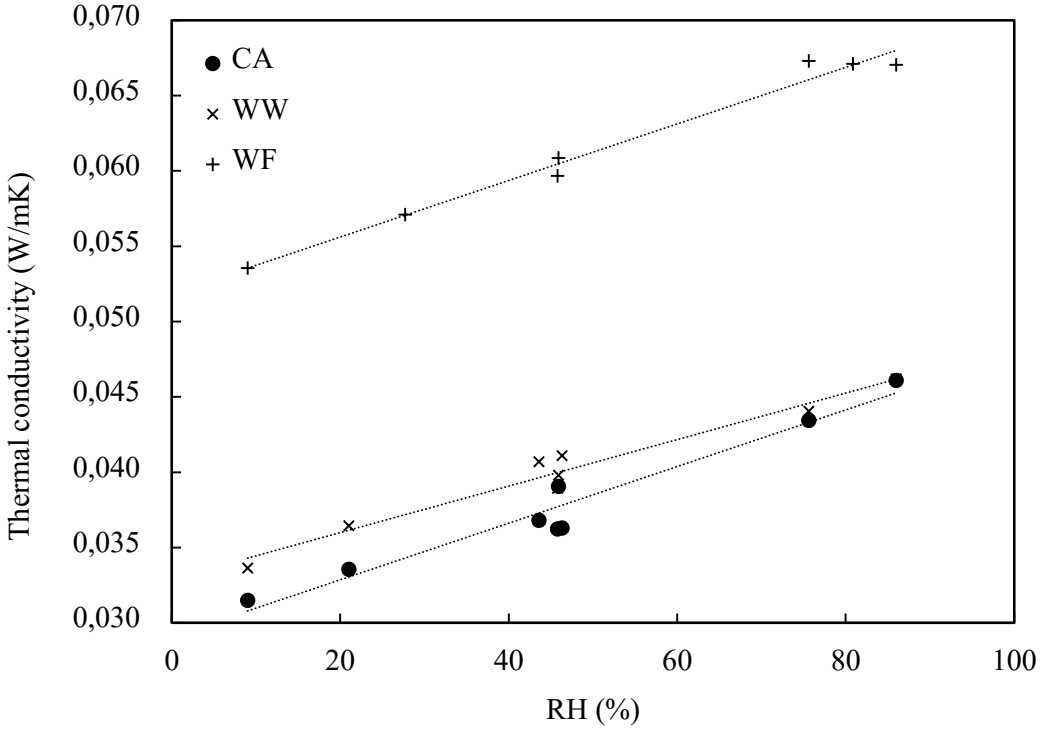

Figure 7.1. Variation of thermal conductivity (λ) with relative humidity for the three samples. Experimental results are linearly fitted.

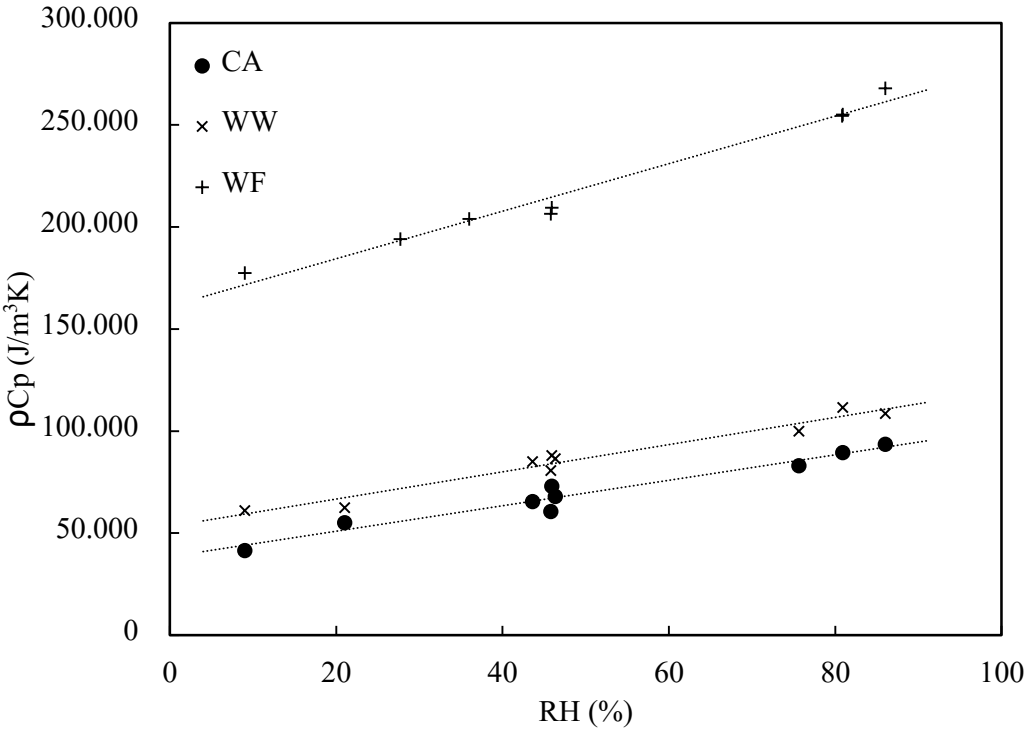

Figure 7.2. Variation of the product density and specific heat capacity (ρCp) with relative humidity for the three samples. Experimental results are linearly fitted.

Nevertheless the WF material presents an absolute higher thermal conductivity, which plays against thermal inertia, and a higher product of density and specific heat capacity, which plays in favour of thermal inertia. As explained above, the variation rate of thermal conductivity with relative humidity on WF specimens is similar to the other two materials, however, the variation rate of the product of density and specific heat capacity (ρCp) is about twice that of the CA and WW composites. This indicates a higher increase in the thermal inertia at high relative humidities due to water adsorption. This can be explained by the fact that the density of the air is so low compared with that of the water or the lignocellulosic matrix that has a negligible contribution to the total ρCp of the composite. Thus, the increase in this factor is more closely related to the increase in moisture content. Being the moisture adsorption per volume unit higher in the case of the WF composite it is not surprising that the variation of the product of density and specific heat capacity is greater in this case.

The influence of moisture content on thermal conductivity has also been tested using the Heat Flow Meter as indicated in Section 4.1.2. To achieve this aim, the samples were wrapped with a plastic film after conditioning in order to prevent moisture migration. However it is manifested in the results obtained that the plastic film sealing did not succeed in preventing moisture migration. Samples are weighed before and after being tested at the HFM, showing a variation in mass between 0.02 and 3.6 %, which correspond to a variation range in relative humidity of up to 36.6 % at low RH. Moreover, only slight variations in thermal conductivity are registered in samples conditioned at different air humidities. It is possible that a better sealing of the samples might have yielded more accurate results for a wider range of moisture contents. However, the electronic thermal analyser seems to be more appropriate for this test, as the thermal properties of the samples can be directly tested in the conditioning chamber.

Nevertheless, the HFM yielded satisfactory results when the influence of temperature on the thermal properties of the materials was investigated. For comparison, the variation of thermal conductivity with temperature and with relative humidity of CA and WF samples are plotted together in

Figure 7.3. The range of the primary and secondary X-axis correspond to the relative humidity and the temperature amplitude respectively registered in a typical year under a moderate climate. Results, show a limited rise in the thermal

conductivity when the temperature is increased. This is in agreement with literature, where the dependence of thermal conductivity with temperature is reported to be less important than with relative humidity (Ochs et al. 2008; Jerman and Cerny 2012; Abdou and Budaiwi 2013). Indeed, the thermal conductivity of CA samples increases by 0.004 W/mK from the minimal to the maximal temperatures registered during a year, while it increases by 0.014 W/mK due to yearly variations of relative humidity. The results support the usual practice of neglecting the effect of temperature on the thermal conductivity in models and calculations, as its effect is limited in the normal range of temperatures for building materials. However, these ranges of temperature are characteristic of a moderate climate and do not take into account the effect of direct radiation. In extreme climates or façades directly exposed to solar radiation, the temperature changes will have a more important role in the hygrothermal performance of the materials.

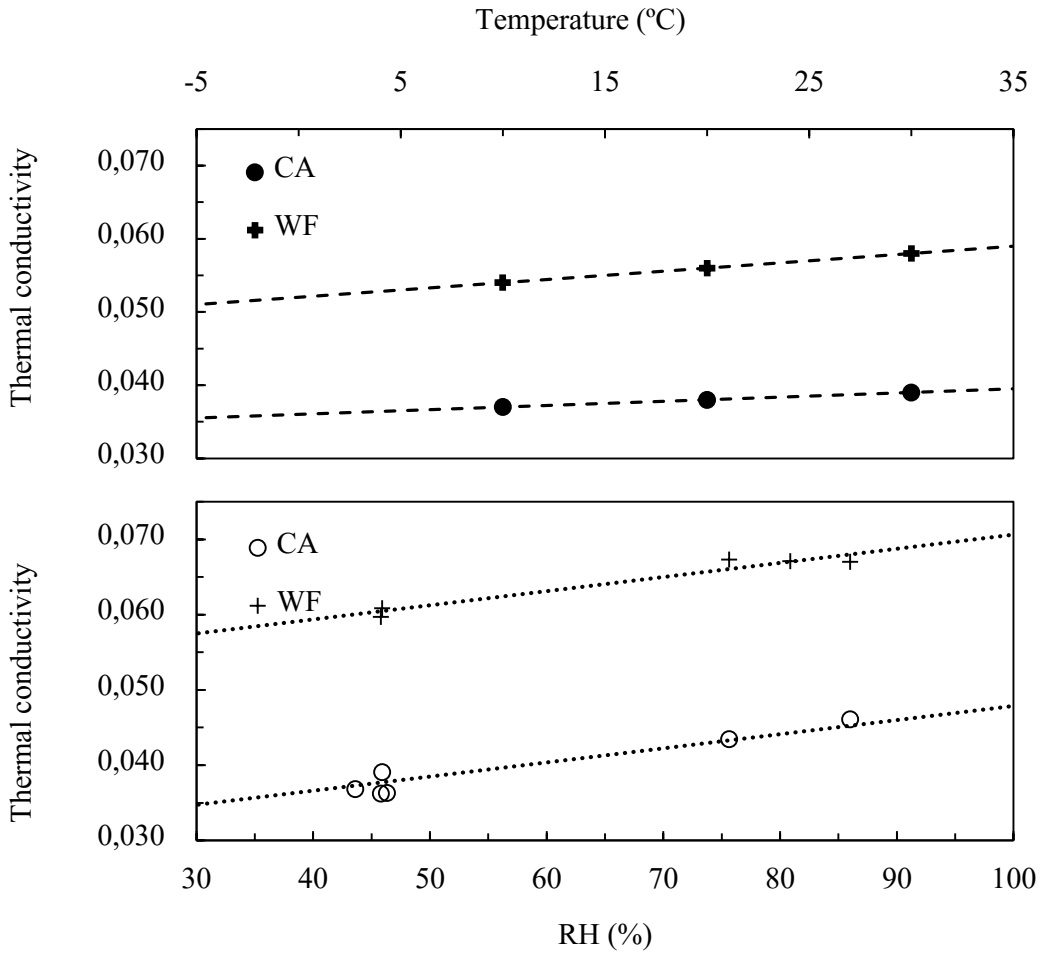

Figure 7.3. Effect of temperature (top panel) and relative humidity (bottom panel) on the thermal conductivity of the CA and WF samples.

7.2.2. Hygroscopic properties: dependence on relative humidity and temperature

The moisture content of the materials at different relative humidities was determined using the saturated salt solution method, described in Section 4.1.3. The results are presented in Figure 7.4, where the moisture content of each material expressed per mass unit (top panel) and volume unit (bottom panel), is plotted against relative humidity. For the CA sample, the results obtained with the DVS are also included for comparison. Such plot corresponds to the isotherm curve. The experimental data was fitted using the Oswin model, which establishes a relationship between moisture content (u) and relative humidity (ϕ) through the equation:

$$u = A\left[\frac{\phi}{1-\phi}\right]^{B} \qquad (7.1)$$

where A and B are the fitting parameters specific to each material, presented in Table 7.3. The Oswin model has been reported to provide a satisfactory fitting in several works (Aviara et al. 2006; Gálvez et al. 2006; Arabhosseini et al. 2010; Rosa et al. 2010) and has the advantage of being a simplified model with only two fitting parameters.

Figure 7.4 shows a good correspondence between the results obtained by the two experimental methods (the salt solution method and the DVS) although it is clear that the deviation is greater with the salt solution method. The curves obtained with the Oswin model present a good adjustment to the experimental data. The moisture content of the materials is usually expressed per mass unit (top panel in Figure 7.4),

Table 7.3. Values of the fitted factors for the moisture content (A, B) and water vapour permeability (δ_0, δ_1) with relative humidity.

	A	B	δ_0	δ_1
CA	0.110	0.52	0.8	7.4
WW	0.057	0.60	0.9	6.4
WF	0.082	0.34	1.3	4.9

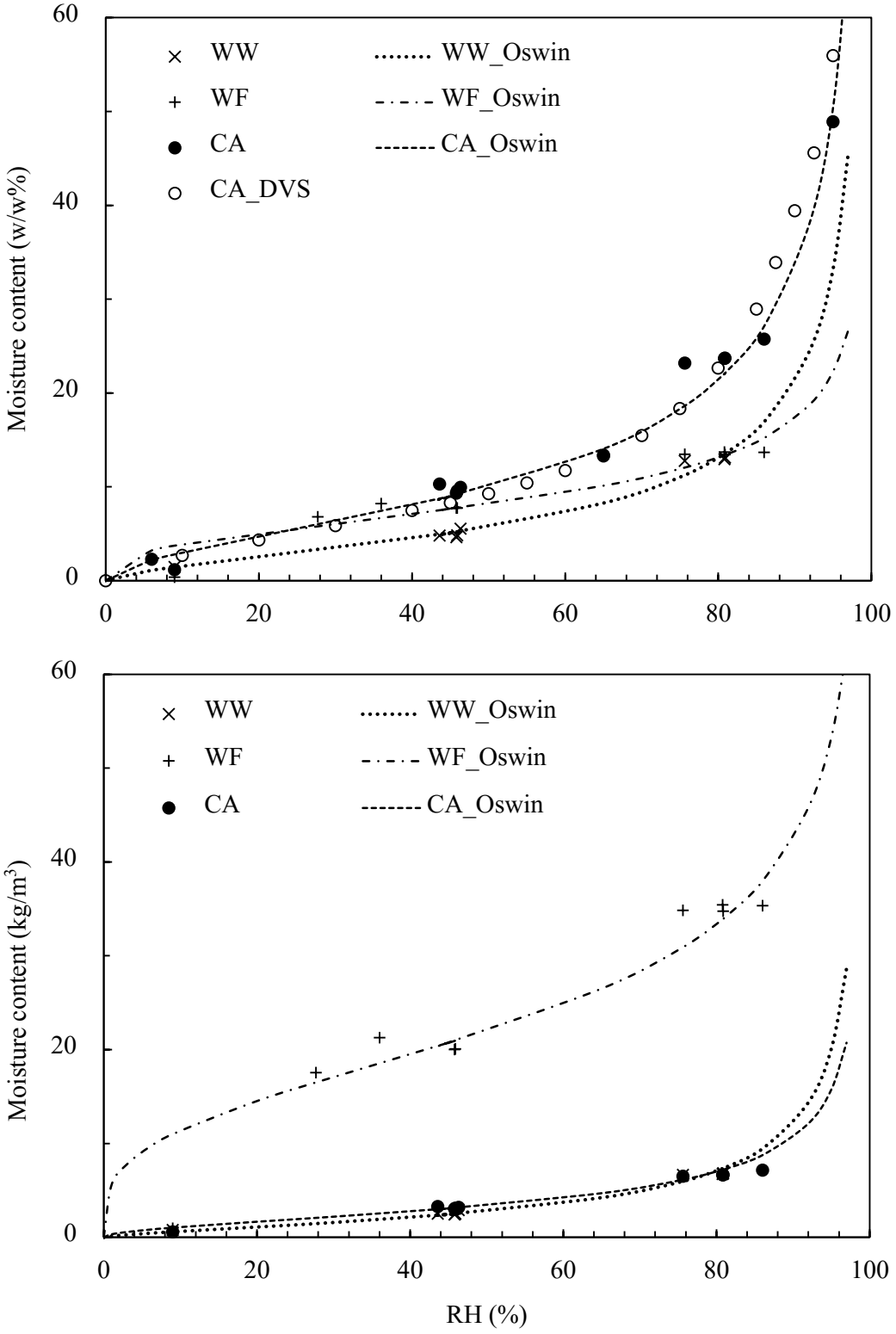

Figure 7.4. Moisture content of the materials at different relative humidities. Experimental results (dots) and fitting curves (lines) presented per mass unit (top panel) and volume unit (bottom panel).

but in the case of building insulation materials, the moisture content per volume unit (bottom panel in Figure 7.4), or better, per functional unit is more appropriate as expresses the amount of water adsorbed by a surface unit of wall.

In the case of the corn pith alginate, the DVS was used to draw the sorption isotherms at 23ºC and 40ºC. Typically, the moisture content of a material decreases with temperature. However, in the case of CA, results indicated that, at the ranges tested, temperature have little effect on the moisture content below 80% RH. Only the capillary condensation zone of the isotherm is affected by temperature.

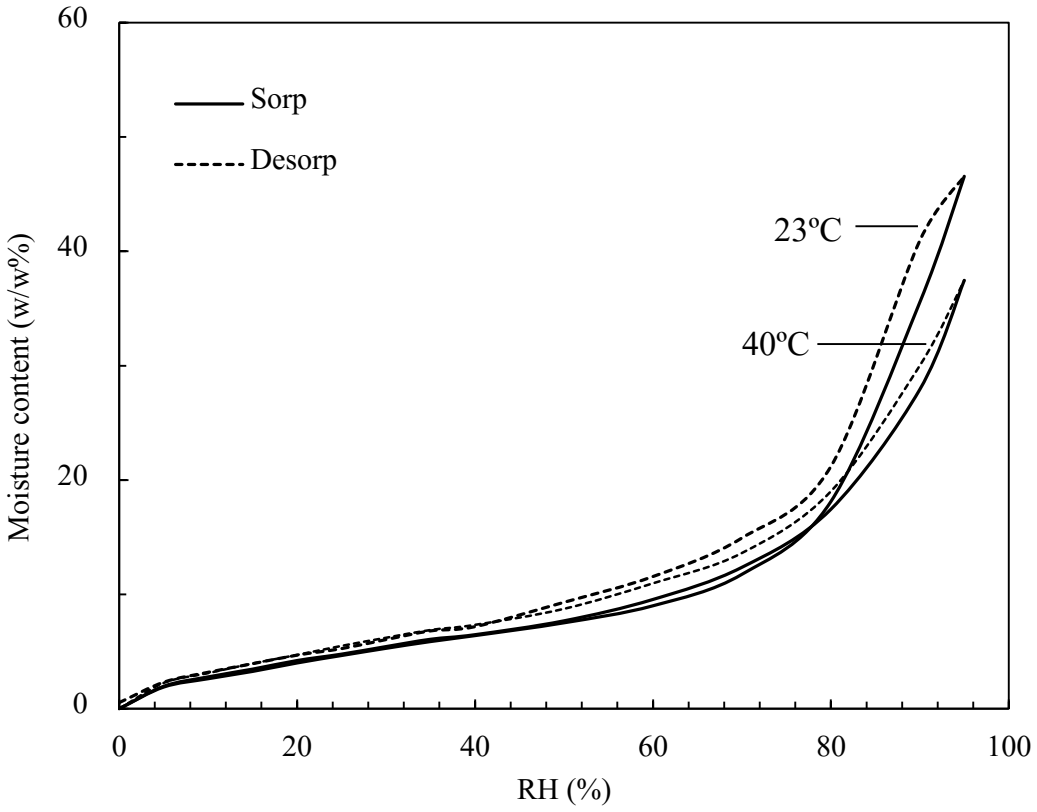

Figure 7.5. Moisture content of the CA specimen at different relative humidities for two different temperatures: 23ºC and 40ºC.

The water vapour permeability (δ) of the materials was determined experimentally using the cup method, by creating a relative humidity gradient across the samples (see Section 4.1.3). In order to determine the influence of relative humidity on water vapour permeability, at least two tests were performed, one at a lower mean relative

humidity (dry cup), and the other at higher relative humidity (wet cup). In the case of the CA sample, the test was performed at two more mean relative humidities (already presented in Section 6.2.3 and included in Figure 7.6).

The results of the water vapour diffusion resistance test are shown in Figure 7.6 and in Table 7.4. Since the water vapour permeability was determined experimentally for only two mean water vapour pressures, the fitting equation has been simplified to a linear fitting ($\delta = \delta_0 + \delta_1\phi$), assuming that such approximation is valid only to relative humidities up to 70%. The fitting parameters are shown in Table 7.3. Results show that the two wood based materials present a similar variation of their water vapour permeability with relative humidity. The variation in the case of the corn pith alginate sample is about 50% higher than of the other two specimens. This variation is associated to an increase in the surface diffusion, which becomes noticeable at higher humidities (Krus 1996).

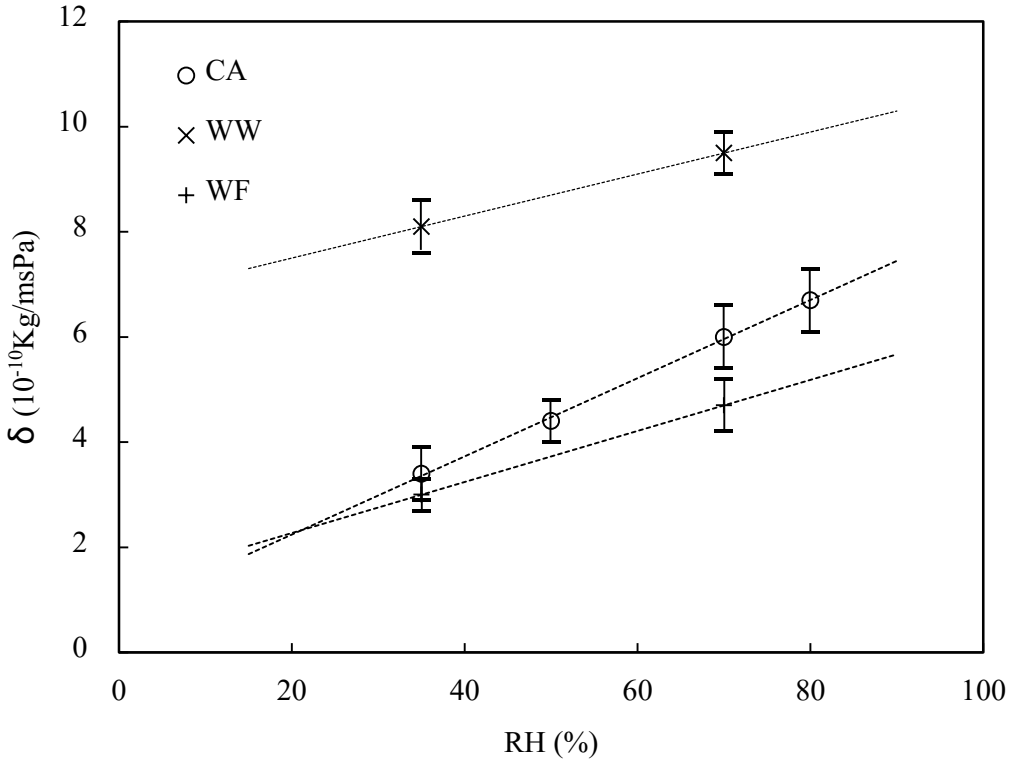

Figure 7.6. Effect of relative humidity on the water vapour permeability of the three specimens. Experimental data and corresponding linear fittings. Error bars indicate extreme values measured.

Table 7.4. Water vapour permeability for each sample, measured by the dry and wet cup method.

Sample	DRY (35% mean RH)		WET (70% mean RH)	
	δ (10^{-11} Kg/msPa)	μ	δ (10^{-11} Kg/msPa)	μ
CA	3.4 ± 0.5	5.7	6.0 ± 0.6	3.2
WW	8.1 ± 0.5	2.4	9.5 ± 0.4	2.1
WF	3.0 ± 0.3	6.5	4.7 ± 0.5	4.2

7.2.3. Hygrothermal performance: Moisture buffering Value.

The MBV is determined using the methodology indicated in Section 4.2.1. Table 7.5 shows the results of the moisture uptake and the moisture buffering values of the different specimens calculated once the dynamic equilibrium was reached. The results show significant differences in the MBV of the materials. Moreover, the mass change of the samples with time at dynamic equilibrium is graphed in Figure 7.7. CA was found to be the material having a higher moisture buffering capacity (2.9 g/m2·ΔRH), followed by the WW specimen, and the WF one, which present the lowest MBV. Despite the differences, the tree materials can be considered excellent moisture buffers as their MBV is higher than 2.0 g/m2·ΔRH (Collet and Pretot 2012). It is interesting to notice that although the WF sample presented the highest moisture content at equilibrium conditions, in a dynamic situation the adsorbed moisture is lower, which is indicative of the time that the material takes to adsorb and desorb moisture.

Table 7.5. Moisture buffering values of the insulation of the samples.

Sample	Width (mm)	Moisture uptake (g)	MBV ($g/m^{2}\cdot\cdot\Delta RH$)
CA	75	2.76	2.86
WW	125	2.50	2.59
WF	80	2.00	2.07

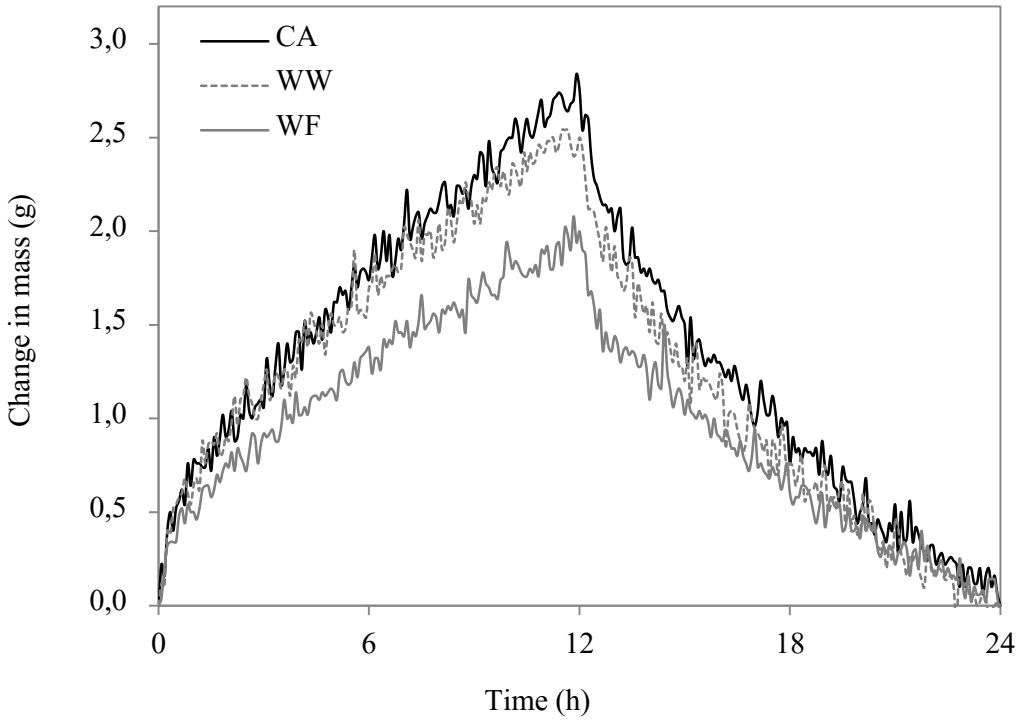

Figure 7.7. Moisture content of the three insulation materials over one cycle once the dynamic equilibrium is reached.

7.2.4. Hygrothermal performance: Dynamic hygrothermal test

A dynamic hygrothermal test was carried out in order to analyse the hygrothermal performance of the material. Such test was conducted using the two experimental set-ups described in Section 4.2.2. The hygrothermal performance of the developed material was compared with that of commercial insulations: wood wool, mineral wool and expanded polystyrene.

In the first set-up samples of size 150 x 200 x 80 mm were subjected to sudden variations in temperature (from 40ºC to 10ºC and from 10ºC to 40ºC). Two thermocouples were fixed to the specimens, one on the top surface and the other at the middle section of the samples. First, the samples were placed in an oven at 40ºC. After 24 hours of conditioning, after when the thermal equilibrium was reached, the samples were placed in a test chamber set at 10ºC. The mass change and the temperatures were monitored for about 6 hours. Then, once the thermal equilibrium was reached again, the samples were placed again in the oven at 40ºC, and the mass change and temperatures were recorded for 6 more hours.

Figures 7.8 and 7.9 show the mass change and the temperature recorded by the thermocouple located at the centre of the samples respectively. When the temperature is reduced, an increase in the mass adsorbed by the material is observed. Otherwise, when temperature increases, adsorbed water vapour is released, leading to a decrease in the mass. For the three materials, the mass increase is lower than the subsequent decrease. However, the three materials present a remarkable different behaviour.

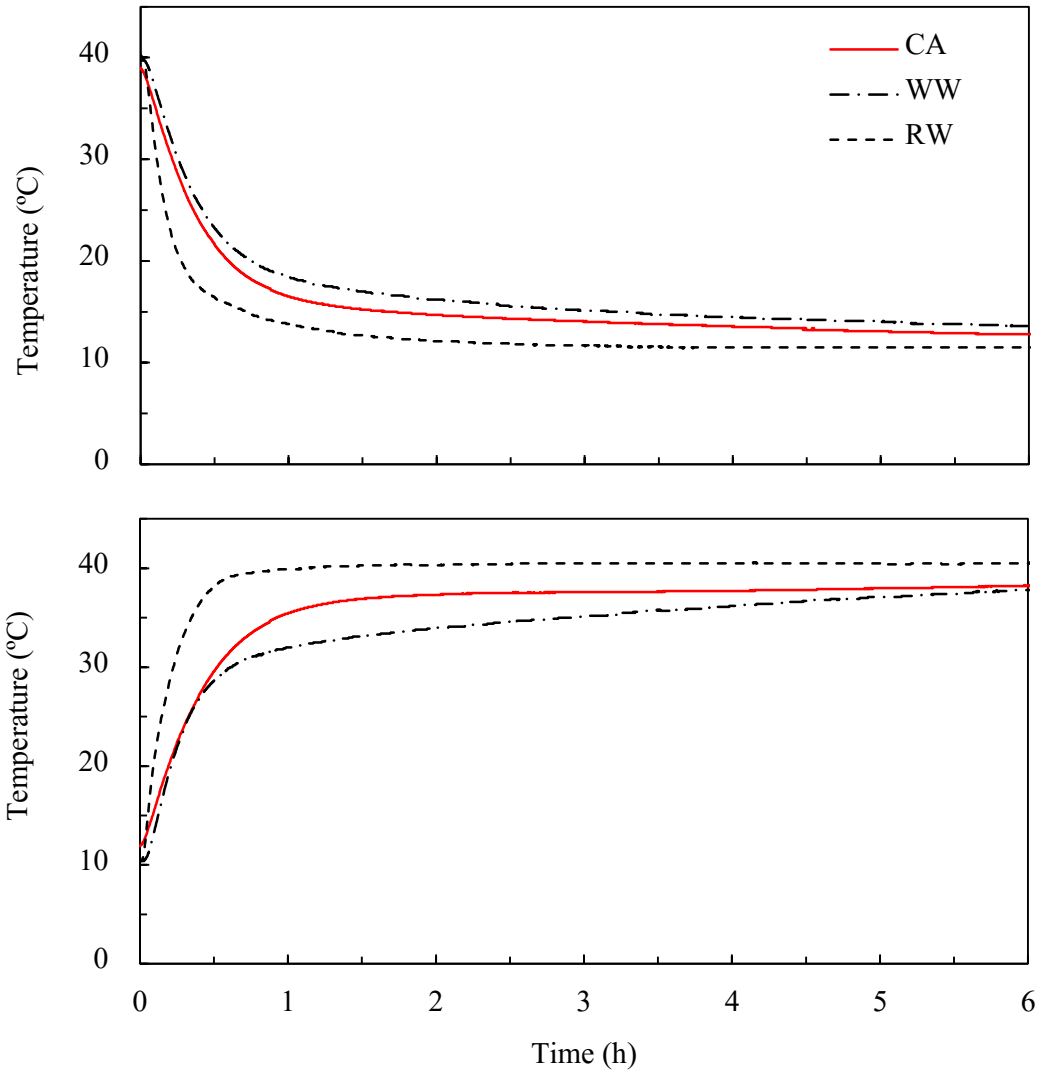

Figure 7.8. Temperature in the middle of the samples when environmental temperature is suddenly decreased (top panel) and increased (bottom panel).

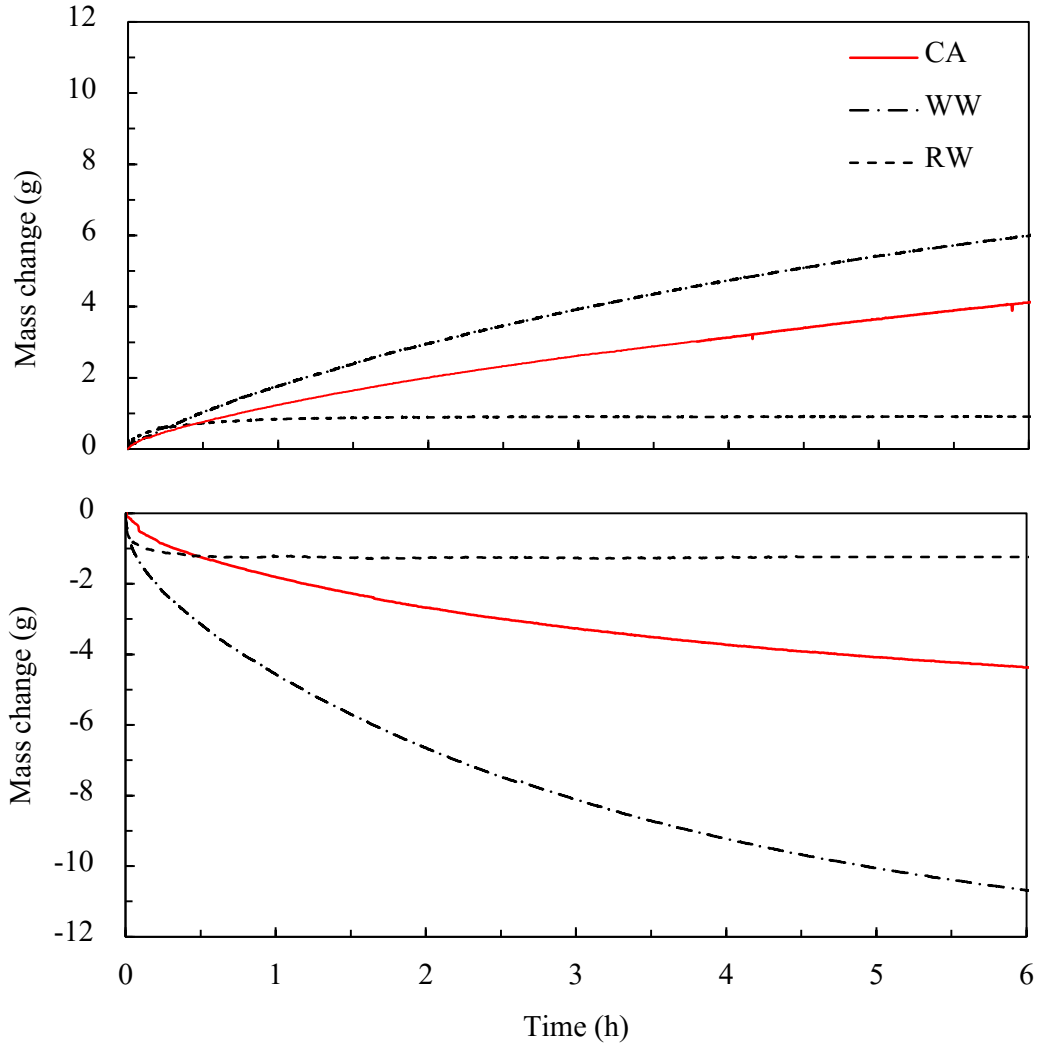

Figure 7.9. Mass changes when environmental temperature is suddenly decreased (top panel) and increased (bottom panel).

In Figure 7.8, it is possible to observe that the two bio-based materials (CA and WW) suffer a temperature change that is remarkably slow, needing longer time to reach the environmental conditions. On the contrary, mineral wool shows a quick response to the external temperature variations. Taking into account that the thermal diffusivity of the three materials is quite similar, it is believed that the differences in the thermal evolution are mainly related to the differences in the hygroscopic characteristics of both kinds of materials. Indeed, the variations in mass for the bio-based materials are much higher than those measured for the mineral wool, as it is depicted in Figure 7.9. Mineral wool seems to absorb a smaller

quantity of water vapour at a higher rate, and no changes in mass are observed after 30 minutes of assay. Nevertheless, bio-based materials are still increasing in mass after the 6 hours displayed in Figure 7.9.

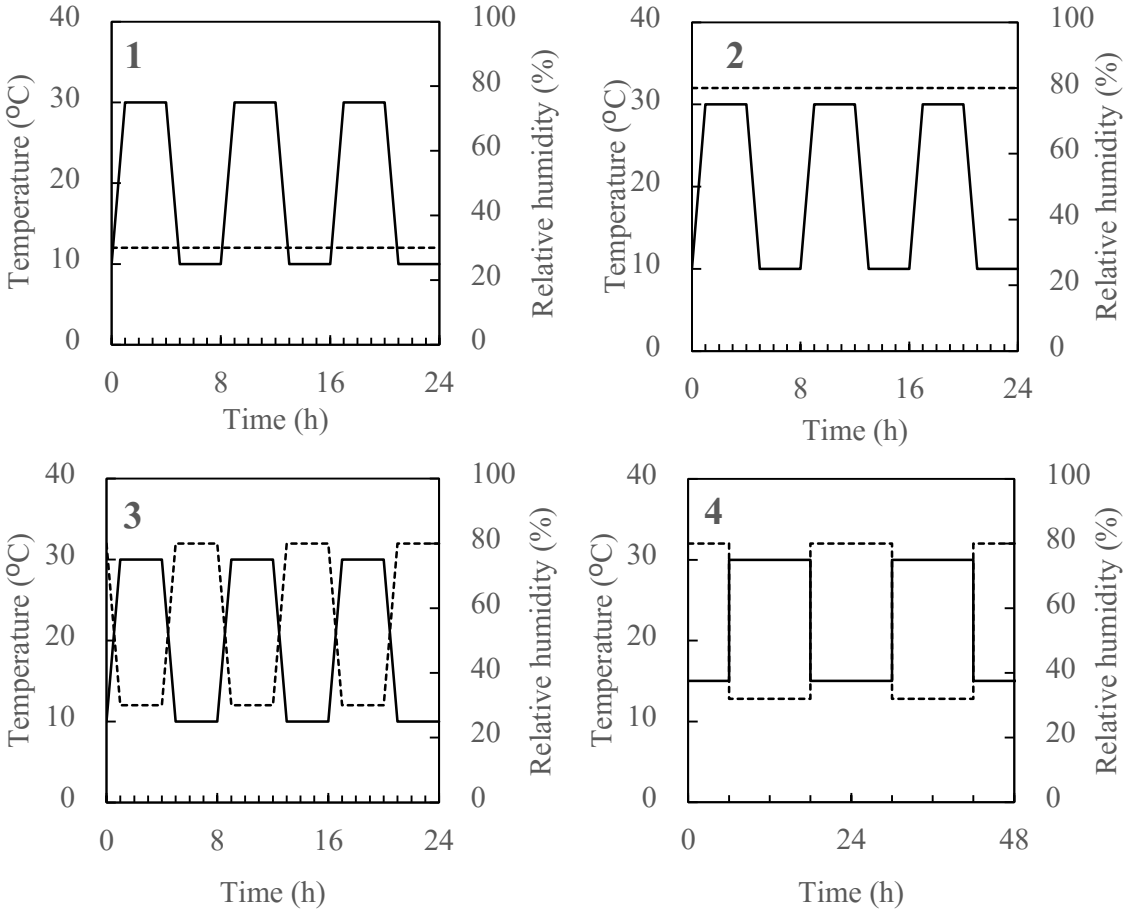

Figure 7.10. Schema of the four different runs performed (1-4). Solid lines correspond to temperature and dotted lines to relative humidity.

A second setup has been used to analyse the hygrothermal performance of the samples, using a climate chambre and following the methodology described in Section 4.2.2. Four specimens, one of each material (corn pith alginate CA, wood wool WW, mineral wool RW and polystyrene EPS) were tested in a climate chambre at the same time. Four different runs were performed. In the first two runs, the temperature was cyclically shifted between two levels (10 and 30ºC), while maintaining the relative humidity constant (at 30% RH in the first run and 80% in the second) and therefore changing the absolute humidity of air. On the third run,

the relative humidity changed with temperature so that the absolute humidity was maintained nearly constant during the test. Finally, a fourth run was performed where the cycles lasted longer (24h). The different runs are shown in Figure 7.10. Before being tested, the samples were maintained for 24h on the initial conditions of the run. The temperature changes at the surface and middle section of the samples were registered by the thermocouples every minute. Results are shown in Figures 7.11-7.13.

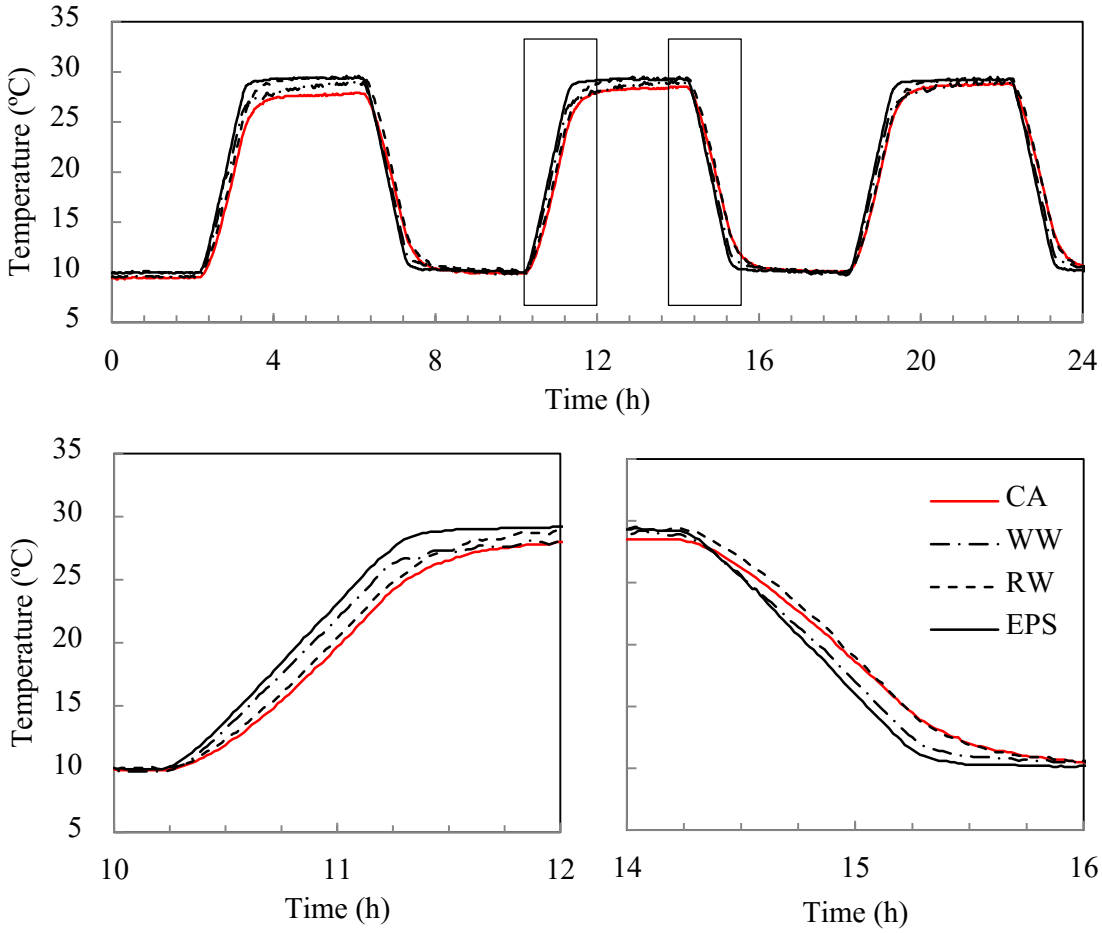

Figure 7.11. Temperature registered by the thermocouple placed at the centre of the samples. Run 1 (Temperature shift from 10 to 30ºC and constant RH at 30%).

Figures 7.11 and 7.12 correspond to runs 1 and 2 (see Figure 7.10). For these cases, the external temperature is periodically changed between 10ºC and 30ºC, but the external relative humidity is fixed at 30% and 80% (run 1, Figure 7.11 and run 2, Figure 7.12 respectively). This means that on the first run the amount water vapour

of the environment is artificially forced to increase while temperature (and therefore pression of saturation P_{sat}) increases, while on the second run, the water vapour content is decreased when temperature (and therefore P_{sat}) decreases. Thus, in both cases, the variations in water vapour have an opposite effect, regarding the adsoption-desorption processes, than that of the temperature variation and, for this reason, no important differences between the various materials are observed.

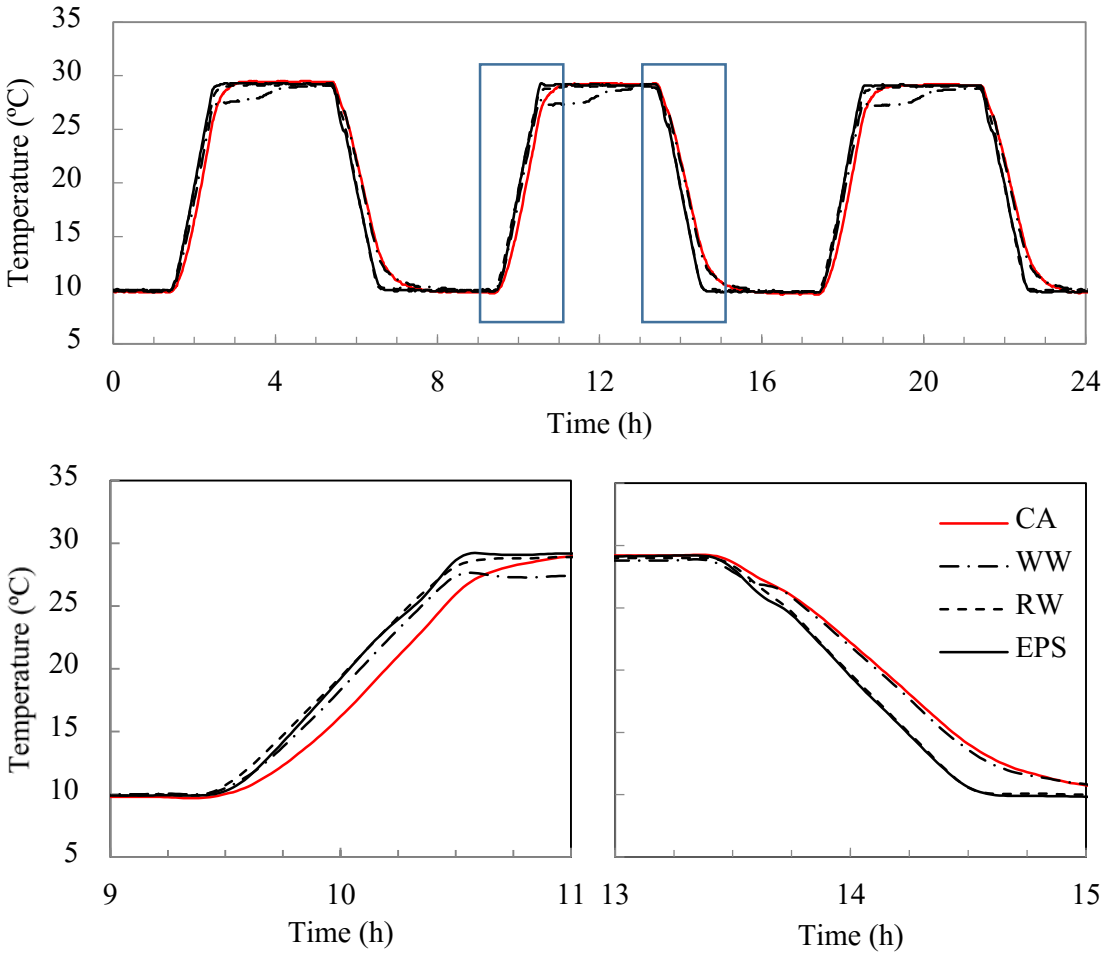

Figure 7.12. Temperature registered by the thermocouple placed at the centre of the samples. Run 2 (Temperature shift from 10 to 30ºC and constant RH at 80%).

Much more significant differences are observed when run 3 is carried out (Figure 7.13). This run consists in a simultaneous variation of temperature (between 10ºC and 30ºC) and relative humidity (between 80% and 30%), as depicted in Figure 7.10. This situation better fits the variations naturally occurring in the environment.

As expected, the EPS sample responds fast to the external variations, therefore, reaching the final values in a short time. RW is just a bit slower. However, the hygroscopic characteristics of the two bio-based materials led to an important slowdown in their thermal dynamics. It is interesting to observe the differences between both bio-based materials. The internal temperature in the WW sample shows small plateaus at about 22ºC during the heating processes and 15ºC during the cooling ones. After that, slopes of 1.7ºC/min and -0.87ºC/min respectively are observed. Despite the CA sample does not exhibit plateaus, the slopes are much lower (about ±0.13ºC/min).

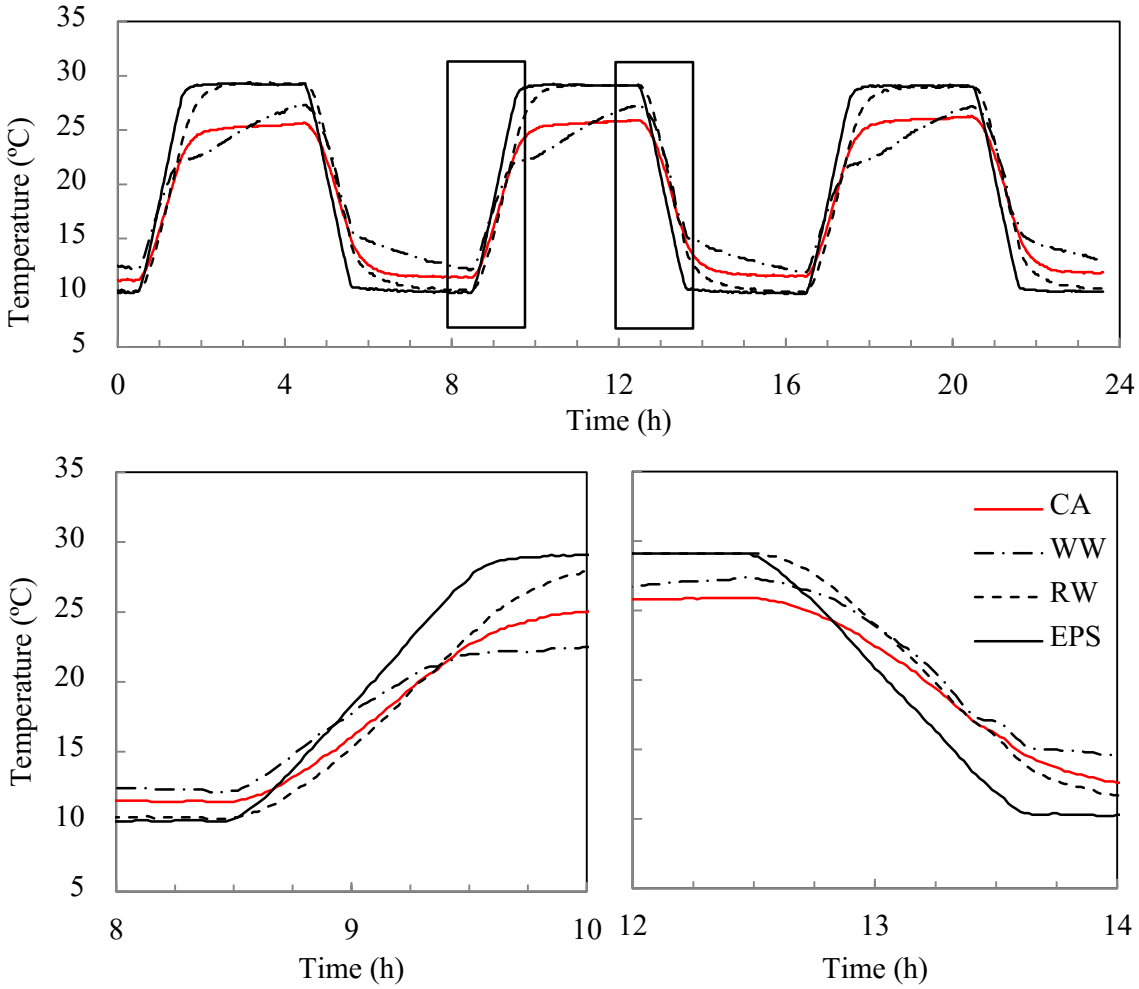

Figure 7.13. Temperature registered by the thermocouple placed at the centre of the samples. Run 3 (Temperature shift from 10 to 30ºC and RH from 80% to 30%).

Similar results are obtained for run 4 (Figure 7.14) where the temperature is varied, abruptly, between 15ºC and 30ºC and, simultaneously, in the relative humidity between 80% and 32%. Each condition in maintained for 12 hours. Run 4 shows, more clearly, the above described trends.

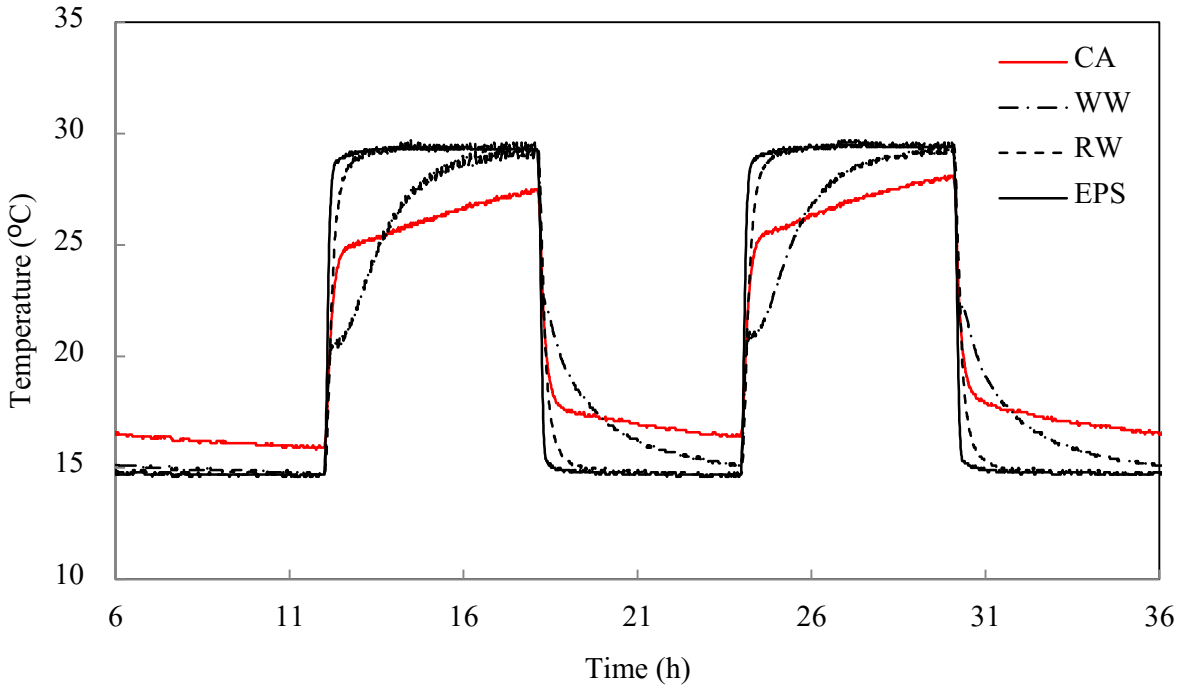

Figure 7.14. Temperature registered by the thermocouple placed at the centre of the samples. Run 4 (Temperature shift from 15 to 30ºC and RH from 80% to 32%).

The results show a remarkably improved thermal behaviour of the bio-based materials when the relative humidity is changed with temperature (runs 3 and 4) so that the absolute air humidity is maintained. This will be further analysed in Section 8.3 using specimens incorporating a render material commonly employed in ETIC Systems, in order to assess the impact that such rendering has on the hygrothermal behaviour of the insulation materials.

7.3. Fire behaviour

7.3.1. Introduction

In section 6, it was concluded that despite the favourable fire behaviour of the corn pith alginate composites as compared with organic foams such as polystyrene or polyurethane, it presents a smouldering combustion which had to be better analysed and improved. In this part of the thesis the smouldering combustion of the corn pith alginate boards treated with different fire retardants is analysed using small-scale and medium scale laboratory tests. Results are compared to wood based insulation boards.

7.3.2. Materials and treatments

Corn pith granulate of 2 mm diameter was used for the fire tests. For the treated specimens, a water solution of boric acid, aluminium hydroxide or ammonium polyphosphate was added to the mixture of corn pith aggregate and sodium alginate. In section 6.3, it was discovered that alginate had a positive effect on the fire reaction of the corn pith composites and thus, a water solution of alginate was also used as treatment.

Table 7.6. Formulations of the different tested specimens.

Code	Corn pith (%)	Alginate (%)	$CaSO_4 \cdot 2H_2O$ (%)	Boric acid (%)	Additive (%)	Additive name
CA	96.0	2.9	1.1	0.0	0.0	-
BAC	88.4	2.6	1.0	0.0	8.0	Boric acid
AH						Aluminium hydroxide
AG						Sodium alginate
APP						Ammonium polyphosphate
BAH	88.4	2.6	1.0	2.7	5.3	Aluminium hydroxide
BAG						Sodium alginate
BAPP						Ammonium polyphosphate

Calcium sulphate dihydrate ($CaSO_4 \cdot 2H_2O$) was added as a source of Ca^{2+} ions to achieve alginate gelation. The blend was energetically stirred and was thereafter poured into a mould and hot pressed at 60ºC for 10 minutes to a target density of 50 kg/m^3. Afterwards, the specimens were dried at 60ºC for 24h and unmoulded. The formulations used for the different specimens are shown in Table 7.6. Plain samples (CA) are also produced for control.

7.3.3. Flaming combustion analysis

Small-scale flammability tests are carried out on a Pyrolysis Combustion Flow Calorimetre (PCFC) following the procedure described in Section 4.3.1. The formulations presented in Table 7.6 are analysed and compared. In this kind of microcalorimeter, the sample is heated in an inert atmosphere, and the pyrolysed gases are mixed with a stream of oxygen to combust completely, at the combustion furnace. Therefore, the measured heat release rate (obtained from the oxygen consumption) corresponds, strictly, to flaming combustion.

Table 7.7. PCFC results for the insulation materials incorporating different additives.

	HR (KJ/g)	T_{onset} (ºC)	TPHRR (ºC)	PHRR (W/g)	Mloss (mg)
CA	7.2	191.0	320.6	70.5	0.73
BAC	3.1	266.2	327.7	25.8	0.59
AH	5.8	218.2	337.8	73.5	0.67
AG	5.9	205.6	319.8	54.8	0.68
APP	6.4	224.9	334.9	51.8	0.69
BAH	7.3	236.6	332.8	50.0	0.72
BAG	4.9	243.2	325.5	46.4	0.70
BAPP	6.3	230.2	328.7	66.2	0.66
WW	9.1	214.2	250.8 460.6	34.3 94.9	0.74
EPS	38.7	339	434	631.0	0.99

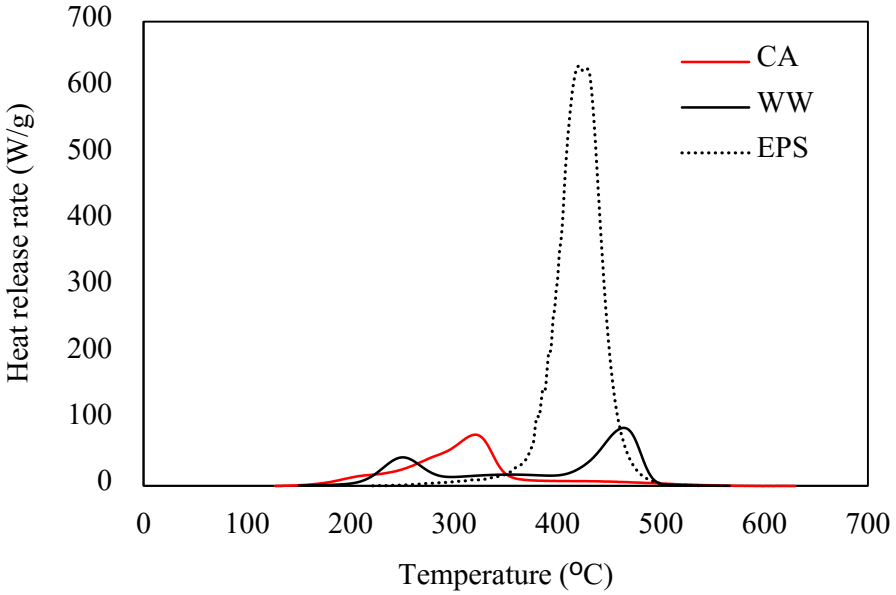

Figure 7.15. Heat release rate as a function of temperature of plain corn pith samples and two commercially available materials: wood wool and expanded polystyrene.

Results show how the heat release rate (HRR) curves draw a characteristic shape having a main peak around 320ºC, which is related to cellulose, a shoulder at smaller temperatures related with hemicelluloses and a tail that some authors relate with lignin and other extractives (Yao et al. 2008). Results show that the total heat release and peak heat release of lignocellulosic materials (CA and WW) is four and eight times lower respectively than that of EPS as shown in Table 7.7 and Figure 7.15. However, the onset temperature was 140ºC higher. WW presented two different peaks, a small one at 250 ºC and the other at 460ºC, probably as a result of the addition of some kind of fire retardant.

The effect of each additive on the fire behaviour of the corn pith-alginate boards is compared in Figure 7.16. Results show that specimens incorporating boric acid present a remarkably better fire behaviour than the rest of the samples. The onset temperature T_{onset} (defined here as the temperature at which HRR reaches 10 W/g) is almost 80ºC higher than non-treated boards as the initial shoulder is displaced to the right, the PHRR is reduced more than three times and the mass loss is lower. Alginate show a significant improvement, in agreement with the results previously found in section 6.3 (Palumbo et al. 2015), although it is moderate compared with

boric acid. Aluminium hydroxide does not seem to have an important effect on the fire behaviour of the material despite the peak temperature (TPHRR) is slightly higher. In the light of the results further specimens are made incorporating mixtures of 3% of boric acid and 6% of one of the other additives to determine whether there is a coupled effect. Results are also shown in Figure 7.16 and Table 7.7. Results are compared with plain specimens (CA) and with boards containing only boric acid (BAC). As expected all the specimens show a better behaviour than untreated samples. The fire behaviour of the different specimens is similar although APP samples present a higher HR. In all cases the first shoulder is prevented and thus T_{onset} is 40ºC higher than untreated samples.

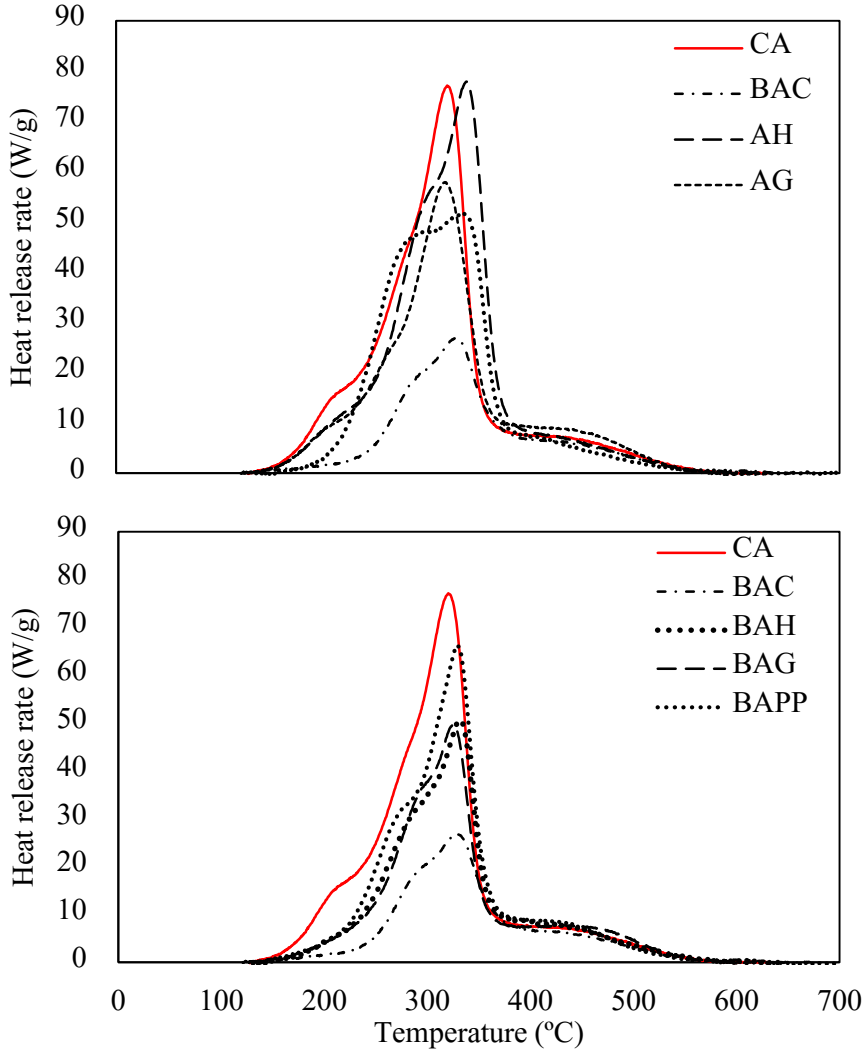

Figure 7.16. Heat release rate as a function of temperature for specimens incorporating each of the tested substances (upper) and boric acid and one of the other additives (bottom).

7.3.4. Smouldering combustion analysis

In section 6.3, it was found that corn pith-alginate composites presented a remarkable propensity to smouldering combustion (Palumbo et al. 2015). Although fire reaction tests yielded good results, even for non-treated specimens, as they showed self-extinguishing behaviour, after flame extinction a slow smouldering process proceeded until the complete consumption of the specimens. In order to analyse these phenomena and their possible improvement by flame retardants, two kind of test are done: a small-scale test (STA) and a medium-scale smouldering set-up.

7.3.4.1. Small scale tests

Small-scale smouldering reaction heat tests are performed using a Simultaneous Thermal Analysis (STA) and the protocol described in Section 4.3.3. In order to analyse smouldering combustion, the tests were performed in air using a crucible with lid. Due to the lid, the sample is oxidized without flame because of the limitation of air penetration into the crucible. The test was performed on plain samples and samples incorporating boric acid, being boric acid the fire retardant that yield better results in the flaming combustion tests. Besides the measurement of the weight change, the differential heat flow was also obtained.

Figure 7.17 shows the results yielded by this test. The DSC curves for the untreated sample (CA) along with the boric acid treated sample (BAC) are shown in the top panel. Both curves present an endothermic peak, at low temperatures, associated with water release, being a bit higher for the BAC sample. The untreated sample CA has a first exothermic peak at 315ºC associated with oxidative polymer degradation, and a second peak at 444ºC associated with char oxidation. The addition of boric acid delays and decreases the exothermic peaks. The first one appears at 335ºC and is reduced by about 14%. The second one appears at 515ºC and is reduced by about 15%. The results are in a qualitative agreement with the results reported by Ohlemiller for a cellulosic insulation, although in this case the addition of boric acid caused a higher reduction in the second peak (Ohlemiller 1990). The curve for the untreated sample is quite similar to that obtained by He et al (2009) for corn stalk.

The derivative weight (DTG) curves are shown also in Figure 7.17 for the same samples as earlier (bottom panel). It is possible to observe that the shape of the DSC and DTG curves are similar, but the peaks do not occur at the same temperatures. For example, in the untreated sample the first exothermic peak (oxidative pyrolysis) for DSC appears at 314ºC while the corresponding DTG peak appears at 273ºC. Similarly, the second exothermic peak (char oxidation) occurs at 444ºC for DSC and at 423ºC for DTG. These differences were also observed by He et al (2009). The delay caused by the addition of boric acid is also clearly seen in the DTG curves, as well as the reduction in the magnitude of the first exothermic peak. However, the char oxidation peak can only be delayed, but not reduced.

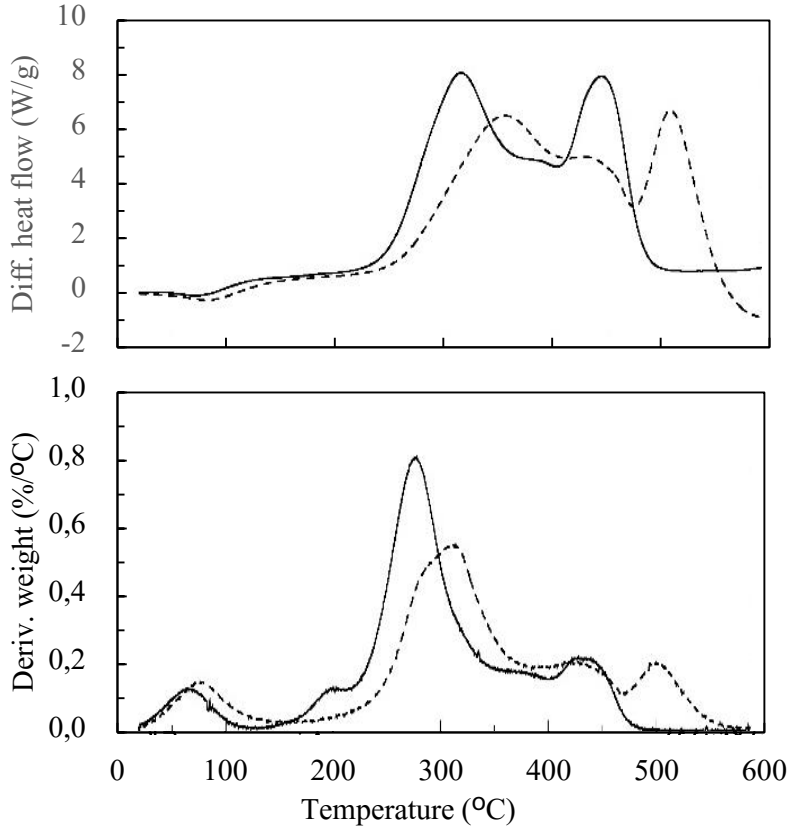

Figure 7.17. DSC curves (top) and DTG curves (bottom) for untreated sample (continuous line) and sample with boric acid (dashed line).

7.3.4.2. Medium-scale smouldering set-up

Medium-scale smouldering tests are performed on an experimental set-up similar to the one described by Hagen et al (2011). The set-up is designed to determine the velocity of the smouldering front. Elongated specimens of 40 x 40 x 160 mm are prepared for the untreated (CA) and retarded samples (BAC, AH, AG and APP). Wood wool (WW) specimens are also tested for comparison. During the experiments, the evolution is visualized with an infrared camera. The resulting images are presented in Figure 7.18. The images are presented in a sequence of six pictures taken every 5 minutes (from minute 25 to minute 50). White colour represents the region where combustion is occurring. Red edges correspond to temperatures around 200-300ºC. A delay in the origin of smouldering in all retarded samples can be observed. Indeed, the high temperature region seems to be smaller in extension than non-treated samples (CA) in all cases, with the exception of AG samples.

Figure 7.19 shows the temperature recorded by the thermocouples on samples tested to a pre-set temperature of 280ºC. The dashed lines correspond to the temperatures measured at the hotplate surface. From this data, smouldering velocity can be evaluated by determining the times at which each thermocouple position reaches a certain temperature, here it is chosen as 250ºC. In all the cases analysed, position and time exhibit a linear behaviour, as shown in Figure 7.20. The slopes (smouldering velocities) are shown in the inset of the figure. The velocities for the untreated samples and for samples with added alginate are very similar, but it is interesting to note that aluminium hydroxide reduces the velocity by about 27%, and boric acid does in 34% while the addition of APP prevented the combustion of the sample. The WW sample used for comparison did not combust either.

As the best results are obtained for the APP and BA samples, further samples are tested containing a lower amount of ammonium polyphosphate (APP-3) and a mixture of ammonium polyphosphate and boric acid (APPB) which are added in 5.3% and 2.7% of the total weight. It is found that in both cases the combustion at 280ºC is still prevented. Thus, further tests at higher pre-set temperatures are performed in order to find the lowest temperature at which combustion occurs in each case (Tonset) and the speed of propagation of the smouldering front at such temperature (speed at Tonset). The results are presented in Table 7.8. The APP sample presented the lowest speed of propagation. Moreover, a positive coupled

effect is observed in APPB samples, in which combustion begins at 30ºC higher than untreated samples, but 20ºC lower than the WW samples.

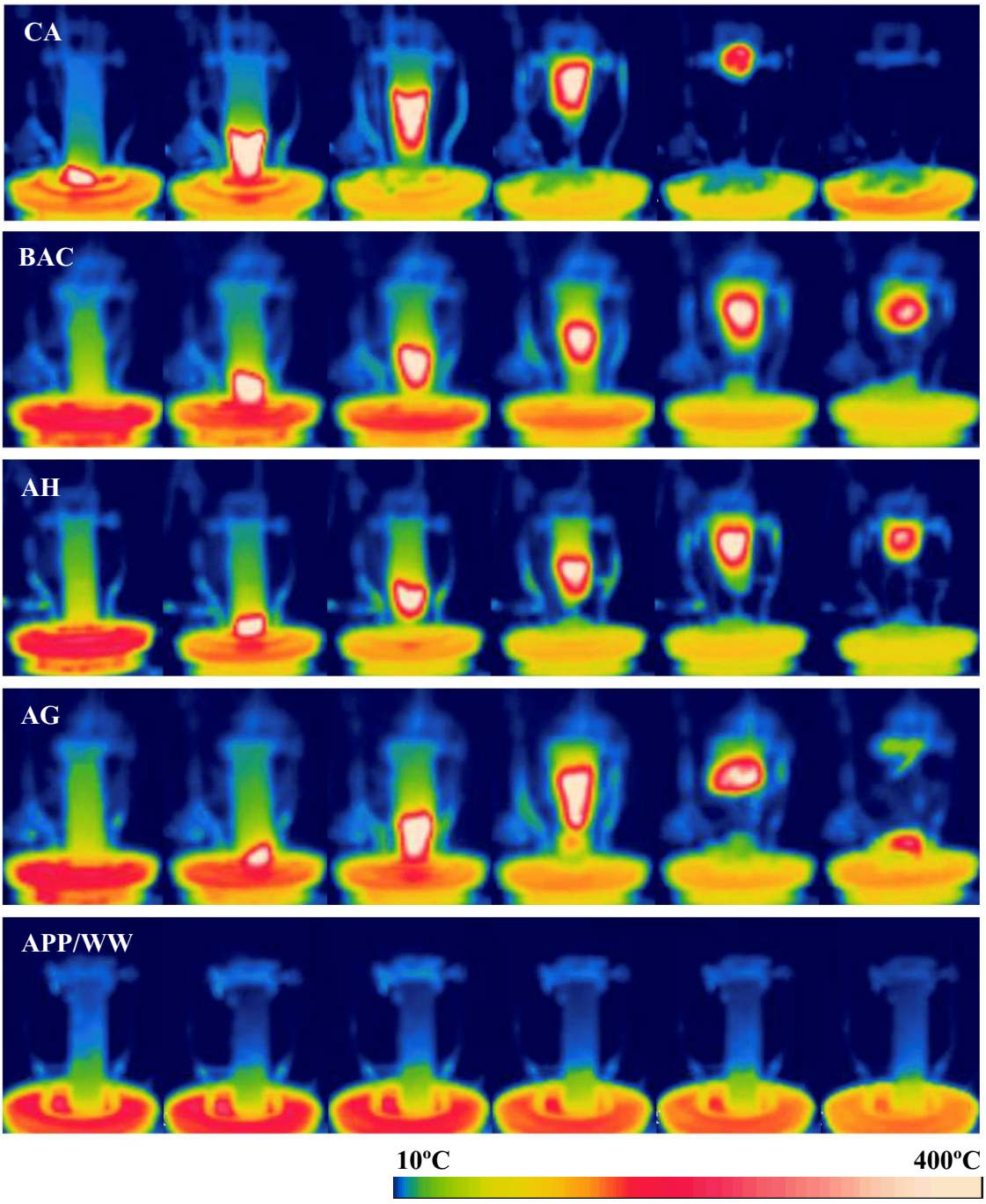

Figure 7.18. Infrared images of untreated (top) and treated samples at times t=25, 30, 35, 40, 45 and 50 min. From top to bottom: CA, BAC, AH, AG and APP samples. Pre-set temperature of the hot plate: 280ºC.

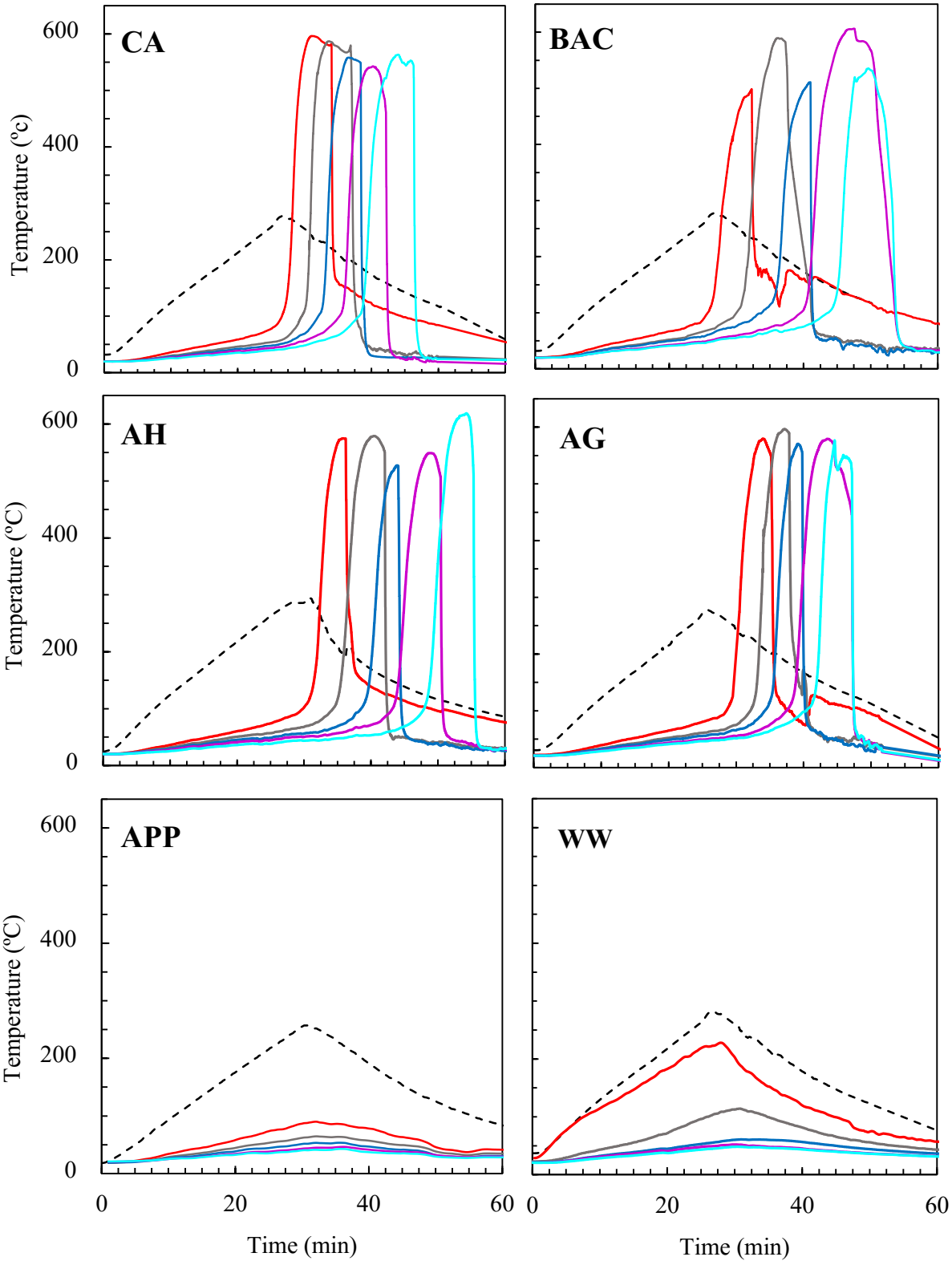

Figure 7.19. Temperature evolutions for thermocouples located each 3 cm along the samples. Pre-set temperature of the hot plate: 280 ºC. Corn pith samples treated with ammonium phosphate do no experience smouldering.

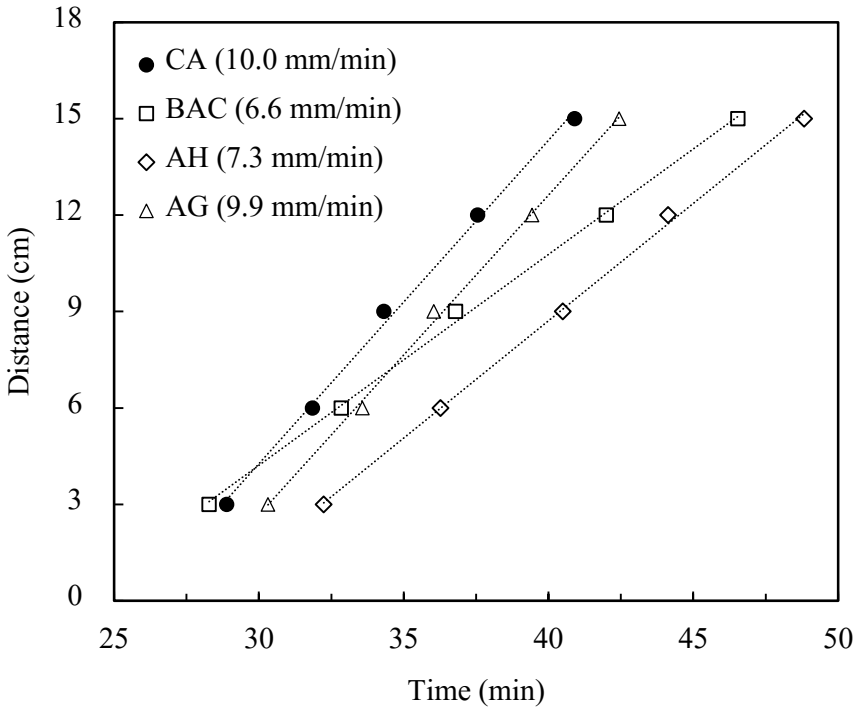

Figure 7.20. Thermocouple position versus time at which temperature reaches 250ºC for the different samples analysed. APP and WW did not burnt. Pre-set temperature of the hot plate: 280 ºC.

Table 7.8. Effect of the treatments on the lowest combustion temperature and speed of propagation of the smouldering front.

Sample	T_{onset} (ºC)	Speed at T_{onset} (mm/min)	R^2 (a.u.)
CA	< 280	10.0	0.997
BA	< 280	6.6	0.999
AH	< 280	7.3	0.999
AG	< 280	9.9	0.998
APP	300	3.6	0.983
APP-3	290	9.7	1.000
BAPP	310	5.9	0.981
WW	330	10.7	0.998

7.4. Mould growth resistance

One of the main drawbacks of bio-based materials in terms of durability is their low resistance to mould growth. As discussed in Section 2.5, bio-based materials represent a source of nutrients for fungi and bacteria and, in general, are easily colonised by microorganisms when the conditions of temperature and relative humidity are favourable. Sedlbauer et al. (2011) suggested that building materials can be classified into three categories regarding their mould growth resistance: Class I, II and III from less to more resistant. Assuming that corn pith alginate boards present a low mould growth resistance (comparable to that of straw and other Class I materials), different pre-treatments are used which are susceptible to improve such resistance. The aim of this part of the study is to evaluate the effect of the different pre-treatments on the mould growth resistance of the material. A first test is performed, intending to carry out the evaluation of the effect of a wide range of pre-treatments on the aggregates alone. Then, a second test is run on boards including selected pre-treated aggregates. The materials are exposed to diverse environmental conditions during a certain period of time in which mould growth is periodically monitored. The experimental set-up and the testing protocols used for mould growth assessment is further explained in Section 4.4. Untreated and wood fibre based samples are used for comparison and control. The mould growth on the pre-treated aggregates alone is monitored at two different relative humidities within 42 days. Six different pre-treatments are used at different concentrations resulting in a total of 13 different formulations. From this first experiment three of the formulations are selected to form boards that are tested within 63 days under 10 different environmental conditions. The mould growth resistance of these materials are compared using the isopleth traffic light system (Sedlbauer et al. 2011).

7.4.1. Pre-treatments used in the corn pith aggregates

For the first test, performed on pre-treated granulates alone, samples of 2 g of corn pith granulates are used. The different pre-treatments used are chosen for their low toxicity and environmental impact and are listed in Table 7.9.

In general, the substances chosen are commonly used in wood and are considered of low toxicity. Boric acid and its salts are effective wood treatments against fungi and insects in aboveground exterior applications. They are also widely used in cellulose insulation. They present low toxicity to mammals. Mimosa tannin is used

in combination to boric acid to reduce leaching. Acetylation, together with furfurylation is one of the main chemical modifications performed on wood with the aim to reduce its moisture retention. It involves bonding a simple chemical (in this case acetic anhydride) in the reactive part of a cell wall polymer (Calkins 2008). Besides, lime has been traditionally used as an antiseptic agent in buildings due to its basic nature. Stearates are widely used as waterproofing agents in several applications and are often used in combination to fungicides, and lauryl gallate grafting has been reported to be effective in reducing the water uptake of paper (Garcia-Ubasart et al. 2011; Cusola et al. 2013).

Table 7.9. Treatments and treatment methods used to improve the mould growth resistance of the corn pith aggregates.

Code	Treatment method	Additive name	% to granulate
C	none	-	
A	none	-	
CA	none	-	
BAC-5	mixing	Boric acid	5
BAC-10	mixing	Boric acid	10
L-5	immersion	Lime (5% solution)	-
L-10	immersion	Lime (10% solution)	-
L-20	immersion	Lime (20% solution)	-
ST-2	mixing	Stearate	2
ST-10	mixing	Stearate	10
MT-2	mixing	Mimosa tannin	2
MT-10	mixing	Mimosa tannin	10
MT-50	mixing	Mimosa tannin	50
AT_V	vapour phase	Acetic anhydride	
AT_I	immersion	Acetic anhydride	
LG	grafting	Lauryl Gallate	

Pre-treatments are performed on oven-dried corn pith (60ºC/24h) using four different methods:

- Mixing the aggregate with a 2 ml solution of the reagent.

  The additive is diluted at different concentrations in 2 ml of distilled water before being mixed with the corn pith aggregate. The mixture is stirred for about 5 minutes and left to settle for 12 hours, after which the aggregate is oven-dried at 60ºC for 24h.

- Immersion of the aggregate in 50 ml of the reagent and draining.

  This method is used for lime and acetic anhydride. Lime is diluted in distilled water at different concentrations while acetic anhydride is used pure. The corn pith aggregate is immersed in the reagent and left to settle for 12 hours. It is then filtered in order to eliminate the residual reagent and oven-dried at 60ºC for 24hs. Samples treated with lime are introduced into a carbonation chambre until complete carbonation before drying.

- Vapour phase acetylation.

  The corn pith is also treated with acetic anhydride by vapour phase acetylation. To this aim, an experimental set-up similar to the one described in (Karr and Sun 2000) is used. The process flow diagram is presented in Figure 7.21. Firstly air is dried by passing it through driedrite and the flow rate is regulated with a flow meter to 500cc/min. Then, the dry air is bubbled through two saturated bottles of acetic anhydride and mixed with the corn pith into a reactor vessel. Finally, the air is conducted through a by pass to a sodium hydroxide solution for neutralization. Both the saturated bottles and the reactor vessel are maintained at 80 ºC by placing them in a preheated laboratory oven. After treatment, which lasted for 1.5 and 3 hours, in order to remove the excess reagent, the air flow continues through the by-pass line for a further 12 hours, the temperature of the oven dropped to 50ºC.

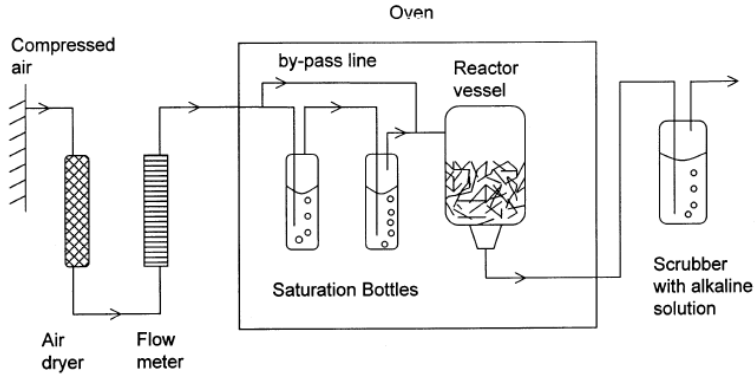

Figure 7.21. Schema of the set-up used for the vapour phase acetylation process (Karr and Sun 2000).

- Laccase-mediated grafting.

The method used for this treatment is the one presented by Dong et al. (2014). Laccase enzymes (from Pleurotus Ostreatus) are used as catalyst. The reagent used is lauryl gallate. For 2 g of aggregate, 0.17 g of lauryl gallate and 1000 enzyme units (U) of laccases are used. The reaction is made with 100 ml of sodium acetate tampon solution (pH 3) at 50ºC and at constant agitation for 4 hours. After this time, the aggregate is washed with distilled water at 80ºC and filtered before a final washing with acetone.

Figure 7.22 correspond to the SEM images of untreated samples (CA) and samples subjected to some of the pre-treatments (BAC, L and LG). No important physical changes are observed on boric acid treated samples. However, it is possible to clearly identify the lime crystals covering the whole surface of the cell walls. By the other hand, the lauryl gallate grafting produces and important wrinkling of the cell wall surface.

7.4.2. Selection of pre-treatments

Samples of two grams of corn pith aggregate pre-treated with each of the different reagents presented above are prepared for this test. Plain corn pith and sodium alginate gel are also tested for control. The specimens are oven

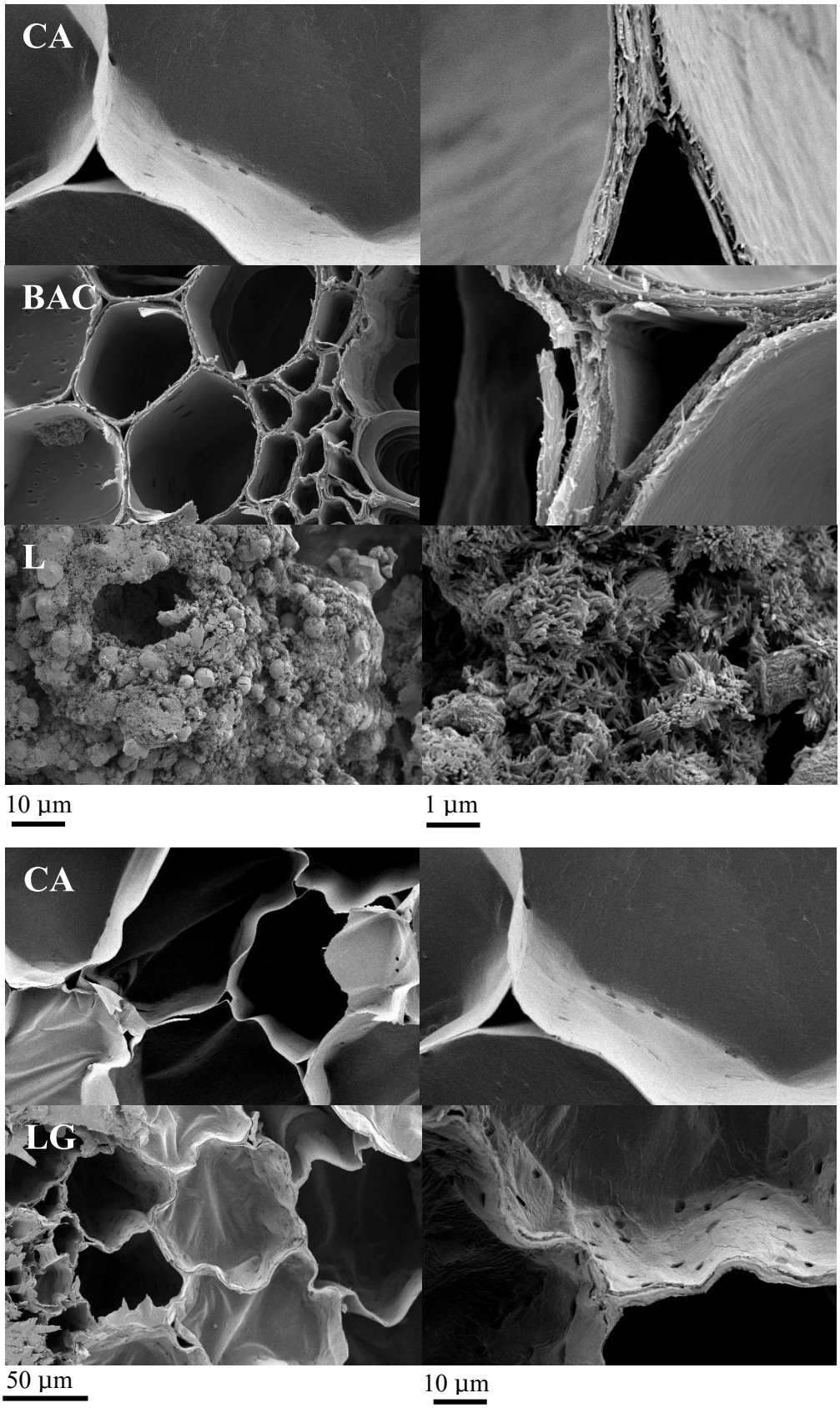

Figure 7.22. SEM images of untreated (CA) and boric acid (BAC), lime (L) and lauryl gallate (LG) treated samples.

dried and weighed before being placed in sealed growth cases, where they are exposed to two different environments: 97% (±2%) and 75% (±2%) RH at a constant temperature of 23ºC (±0.3ºC). The mould growth is weekly determined by visual inspection with the aid of a binocular loupe. A more detailed description of the methodology used is presented in Section 4.4. Results are summarised in Figures 7.23-7.27.

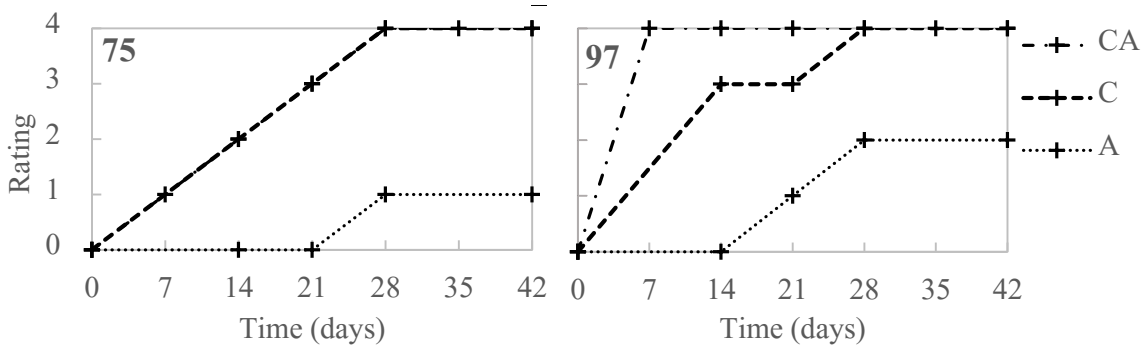

Figure 7.23. Mould growth by time on the raw materials –corn pith (C) and alginate (A)– and untreated samples (CA)

As mentioned in section 4.4, fungal growth is determined qualitatively following the methodology proposed by Johansson et al (2012). Qualitative assessment is based on a five grade rating system (from 0 to 4) where 0 correspond to no mould growth and 4 to heavy growth over more or less the entire surface (Johansson et al. 2012; Johansson et al. 2014). This method is fast and effective but, as signalled by Johansson, it is somewhat subjective. In order to reduce measurement uncertainty, five people independently evaluated all the test specimens.

Results show that corn pith is more sensitive to mould growth than sodium alginate (see Figure 7.23). All the analysed pre-treatments succeeded in improving the mould growth resistance of corn pith at low relative humidities. Pre-treated samples showed an improved resistance to mould growth when exposed to 75% RH. None of the pre-treated specimens showed important mould growth and were rated 2 or less after the 42 days of the test if the concentrations used were sufficient. However pre-treated aggregates were highly affected at more severe conditions with the exception of BAC-5, BAC-10, L-20 and ST-10. Indeed, for boric acid and lime at

20% concentration pre-treatments were found to be the most effective ones. Both were rated 0 or 1 at the end of the test at 97% RH. Acetylation (both by immersion and by vapour phase treatment) and the addition of the stearate also showed remarkable improvement at 97% RH.

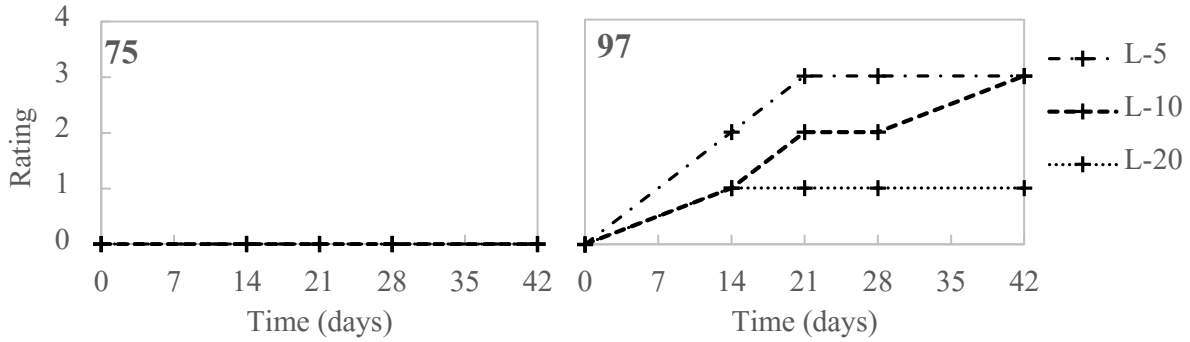

Figure 7.24. Mould growth by time on the lime treated aggregates.

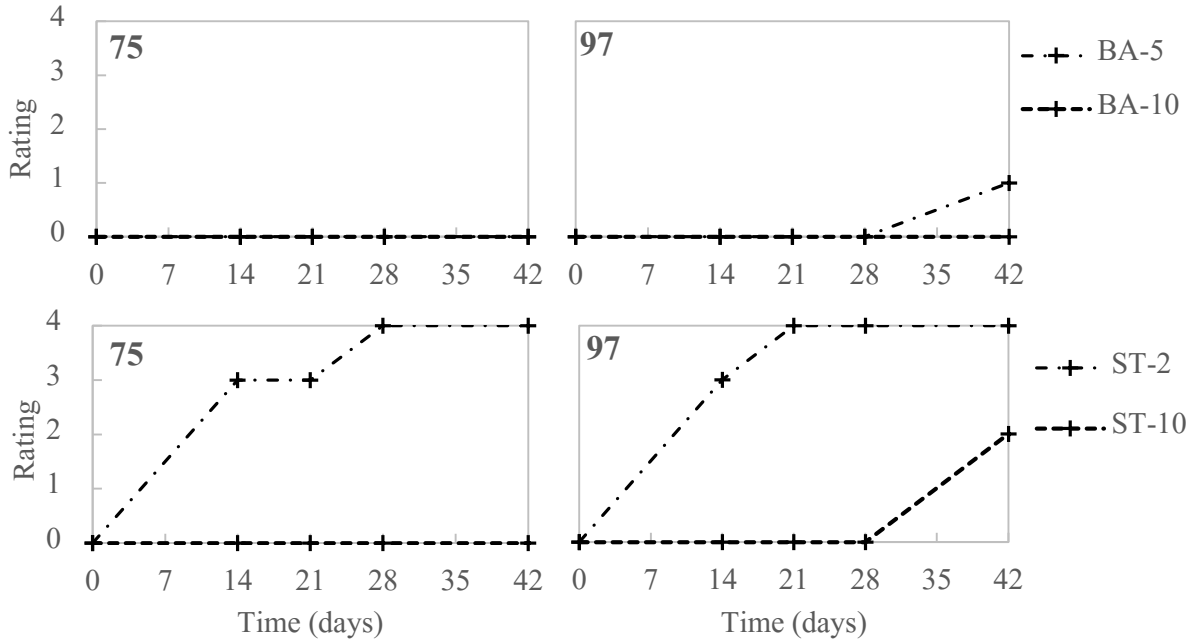

Figure 7.25. Mould growth by time on the boric acid (BAC) and stearate (ST) treated aggregates.

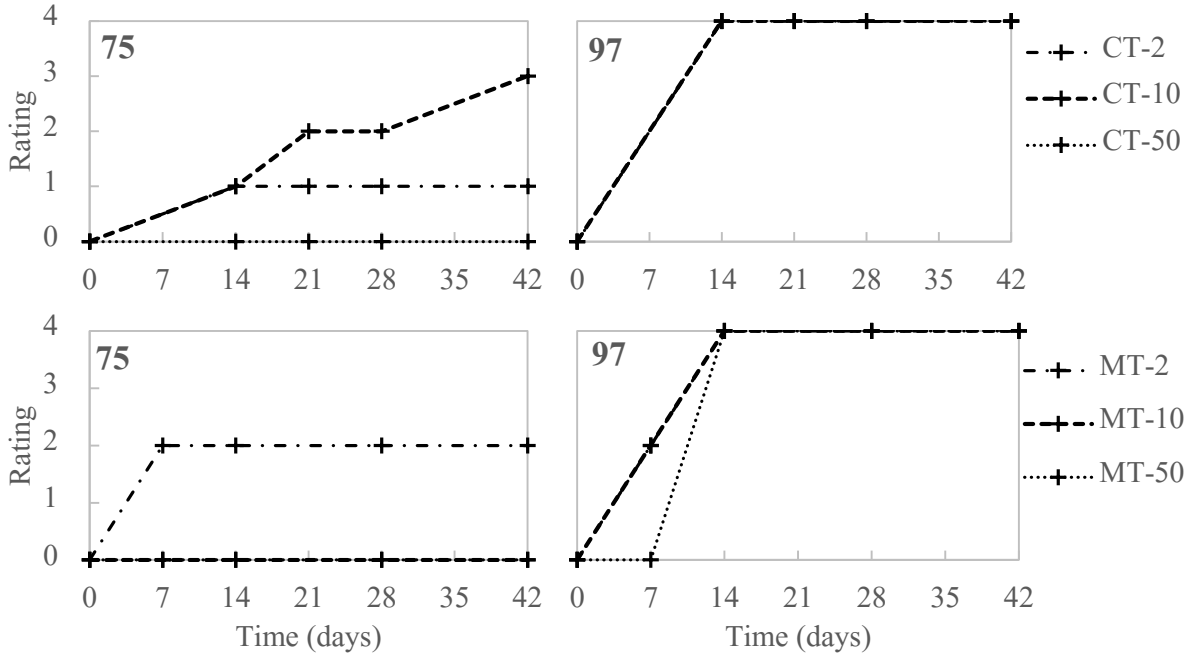

Figure 7.26. Mould growth by time on chestnut tannin (CT) and mimosa tannin (MT) treated aggregates.

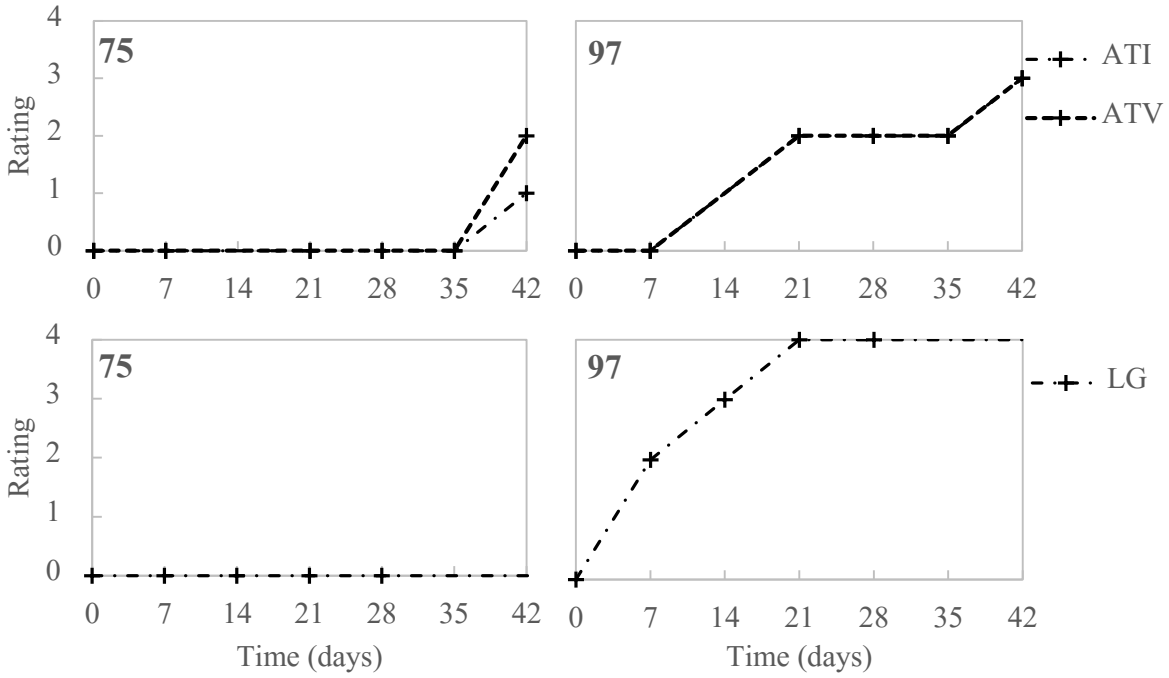

Figure 7.27. Mould growth by time on acetylated (A_{TI} and A_{TV}) and grafted (LG) aggregates.

It is important to note that the comparison of the treatments are made at early stages of the mould growth development (only for 6 weeks after the start of the test). For a more accurate assessment of the effectiveness of the pre-treatments, samples should be evaluated for longer periods of time, typically 12 to 14 weeks (Sedlauber 2001; Humar and Lesar 2013; Johansson et al. 2013). Here, the period of the tests was reduced due to time constraints. However, the results are useful for comparison and to determine the vulnerability of the different samples to mould growth. The mould growth profiles of the tested materials are similar with those presented by Johansson for other wood based building materials such as pine sapwood and pine plywood.

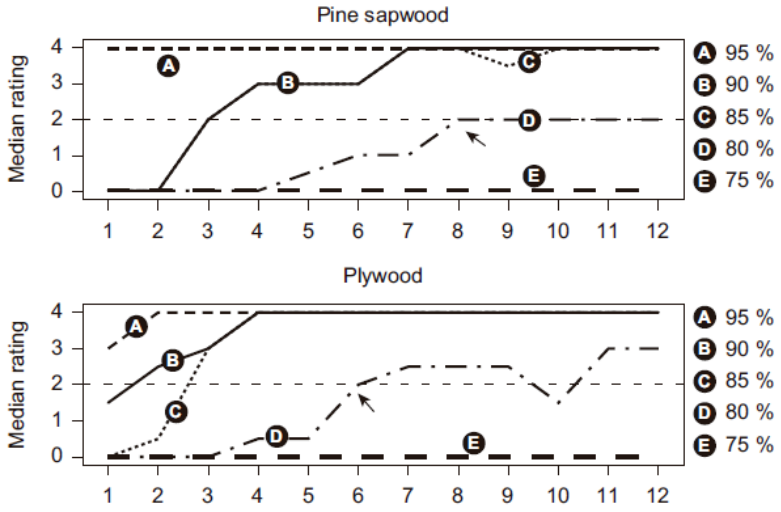

Figure 7.28. Mould growth by time on pine sapwood and plywood. Results presented by Johansson et al. (2012)

7.4.3. Mould growth profiles of selected materials

A second test was performed on boards that incorporated three of the pre-treatments under study: L-20, AT_V and LG. Although BAC-5, BAC-10 and ST-10 presented also good results, they were discarded due to poor compatibility with the binder, which produced the disintegration of the samples after drying. Such undesired phenomenon was also observed in lime treated samples, although to a lower extent. The aggregates were treated before board formation as described in Section 7.4.1.

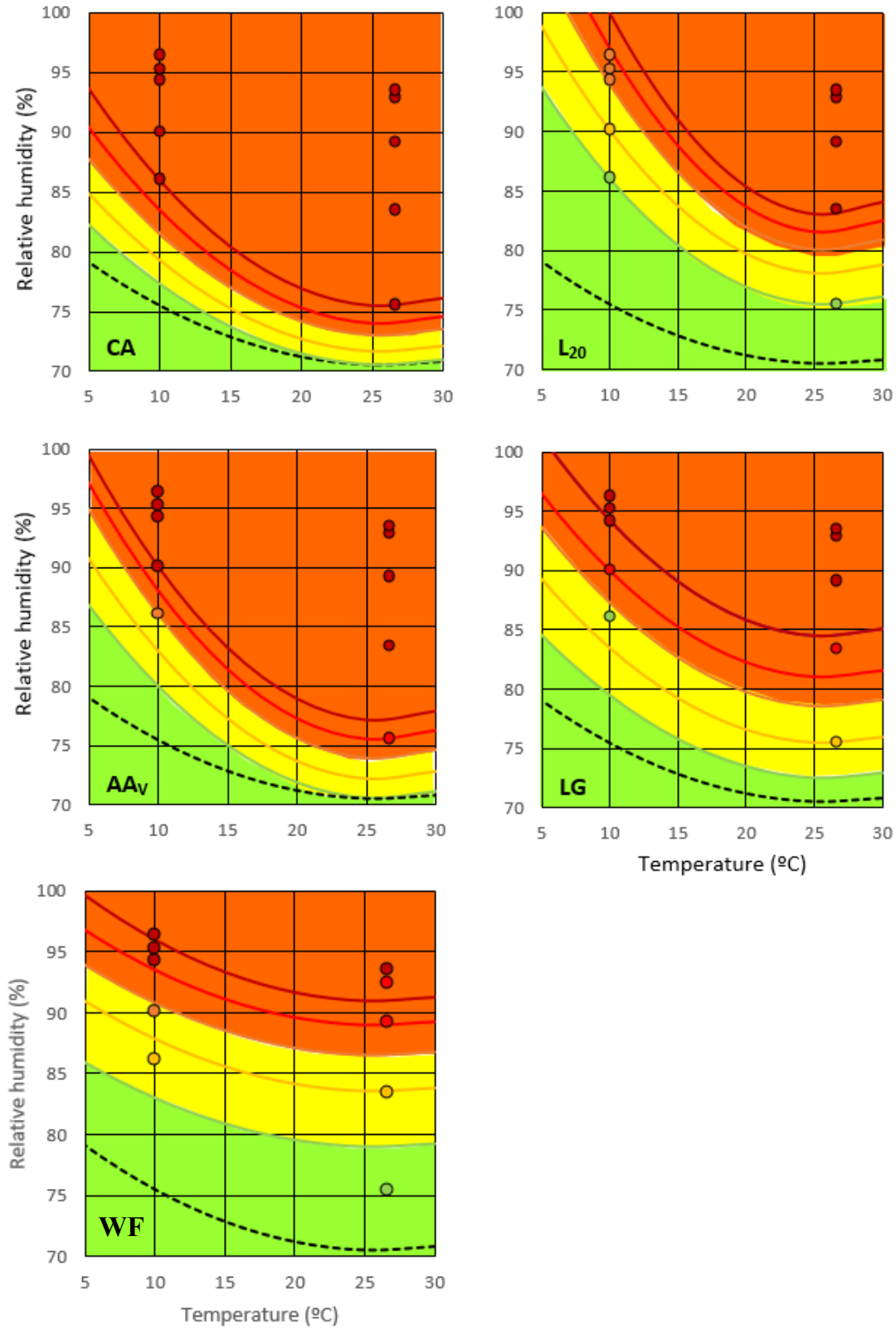

Figure 7.29. Mould growth resistance profiles of untreated (CA) samples, samples treated with lime (L20), acetylated (AA_V) and graphed (LG) and control sample (WW).

Plain samples and commercially available wood fibre samples were used for control. Samples of 250 x 160 x 10 mm were made following the procedure indicated in Section 6.1. Ten test specimens of 50 x 80 x 10 mm were cut from these samples and exposed to 10 different environments for 8 weeks. The environments of the different sealed growth cases are presented in Section 4.4.

The mould growth was monitored daily for the first five days and afterwards, once a week up to 63 days. The mould growth at the end of the test is presented in Figure 7.29 using the material specific "isopleth traffic-light system" proposed by Hofbauer et al. (2008). The use of this system allows for a straightforward comparison between the mould growth resistances of different materials at different environmental conditions. In the present work, the traffic-light colours have been correlated with the rating system used for the mould growth assessment in such a way that green, yellow and red colours correspond to rating 0, rating 0 to 2 and ratings 2 to 4 respectively. The way how this system is adapted for the purposes of this work is further explained in Section 4.4.

The results show that both untreated and treated specimens present a Class I profile and thus, are highly vulnerable to mould growth. The pre-treatment that showed the best results was L-20, with a significant improvement of the mould growth resistance of the materials. The control sample (WF), however, show a better profile which can be included in the Class II materials, probably due to a fungicide treatment.

7.5. Conclusions

The dependence of the main hygrothermal properties of the corn pith alginate material with moisture content was analysed and compared with wood based insulation boards. The material proposed in this thesis showed similar hygrothermal properties than wood wool insulations. Its thermal conductivity at room conditions (20ºC and 50% RH) was found to be 0.038 W/mK, which increased by about 20% when the RH approached the dew point. Similar trends were found in wood materials. Moreover, the moisture buffering capacity of the experimental materials was higher than the wood based boards, indicating a higher capacity to regulate

indoor moisture levels. The hygrothermal performance of the materials is clearly affected by the moisture adsorption and desorption processes. Both CA and WW materials showed remarkably more favourable results when both the temperature and the RH were changed than when only the temperature or RH was changed. This is probably due to the fact that, in these last two cases, in order to maintain the pre-set environmental conditions, the climatic chamber was forced to continuously supply or remove moisture to the environment, which was consequently adsorbed or desorbed by the hygroscopic materials.

The effect of different substances on the fire reaction and the fungal growth resistance of the experimental insulation board made with corn pith and alginate is evaluated. Regarding flaming combustion, the best results are obtained with specimens treated with 8% of boric acid. All the studied parameters related to flaming combustion were improved with the addition of boric acid. HR was reduced by about 50%, the PHRR by about 60% and mass loss after combustion was 20% lower. Taking into account these results and the fact that the use of boric acid is restricted to 5.5% (w/w) of the final product at the European Union (ECHA 2010), samples containing mixtures of 2.7% of boric acid and 5.3% of one of the other substances were also tested. These materials still showed an improved fire behaviour. However, this improvement was attributed mainly to boric acid, which is supported by the fact that the PCFC results were similar for all the specimens. Nevertheless this trend changes when the smouldering combustion is analysed. In this case, samples incorporating ammonium polyphosphate showed better results, as the onset temperature was increased. Boric acid did not have the effect of increasing the onset temperature, but still reduced the speed of propagation by almost 40%.

The resistance against mould growth of the CA composite was also investigated and compared to wood based insulation materials. Different pre-treatments were also proposed with the aim of increasing the mould growth resistance of the plain material. Results indicated that the pre-treatments were effective, especially at moderately favourable environmental conditions. At extreme conditions mould growth could not be prevented although it was retarded.

The mould growth resistance of corn pith aggregates pre-treated with different additives at different concentrations was evaluated. After 6 weeks of monitoring, most of the treatments showed a remarkable improvement at low RH, but a

moderate improvement at high RH. The pre-treated aggregates showing the best results were used to form corn pith alginate insulation boards which were exposed to 10 different environments in sealed growth cases and monitored for 8 weeks. The mould growth resistance profile of all the materials can be classified as Class I which indicates a high vulnerability to mould growth. Although none of the treatments resulted in a Class II or III material, the L-20 specimen showed important improvement. This material showed a profile close to that of commercially available wood fibre insulation boards. Thus, such materials can be used as thermal insulation boards in construction only in controlled environments.

In general most of the treatments showed efficacy and it would be interesting to continue investigating their possible beneficial effects. In the case of the tannins, for instance, it would be interesting to determine if higher concentrations of the additives would raise better results. Moreover, a positive coupled effect has been reported between mimosa tannin and boric acid that was not investigated in this work but that might be conducted in future work. Moreover, the method used for the pre-treatment might have an impact on the final results which is another field for further research. It was also observed in some cases an undesired interaction between the additives and the binder which significantly reduced its binding properties resulting in the disaggregation of materials. This aspect should be analysed for deeper comprehension.

Further work is needed to analyse how the pre-treatments are affecting the other properties of the material presented in this work, that is, hygroscopic properties, thermal properties and fire behaviour. Acetylation or lauryl gallate grafting are known to efficiently reduce liquid water absorption. However, fungi use the water adsorbed by the substrate to grow before liquid water occurs. Thus, pre-treatments capable of reducing the water adsorption at high RH without changing the MBV at lower RH would be an interesting field of study. In this regard, it might be interesting to work on the modification of the crystalline structure of the cell wall polymers or on the possibility of incorporating crystalline structured coatings.

8. CORN PITH ALGINATE THERMAL INSULATION CONSTRUCTION SYSTEMS

As mentioned in Section 7, corn pith insulation boards have shown several promising results indicating its suitability as a new thermal insulation building material. In this section, the material is evaluated in the context of a specific thermal insulation system in order to evaluate its behaviour in a situation similar to a real case. To this aim an ETIC System was chosen.

8.1. Construction of the insulation systems

The construction of the prototypes was made following the details of an experimental wood based ETIC System proposed by INCAFUST in previous work (INCAFUST 2012). The elements conforming the system are sketched in Figure 8.1. The proposed system consists of two layers of thermal insulation material coated with a cement based adhesive mortar system. The two layers of insulation are composed of a 50 mm thick, low density, wood wool mat (3) built into a wooden frame (2) and a 20 mm thick high density wood fibre board (4) mechanically anchored on top of the frame (5). The cement based adhesive mortar system consists of three different layers: a first 2 to 3 mm thick layer of mortar incorporating an imbedded glass fibre reinforcement mesh (6-7), a primer coat (8) and a 1 to 2 mm thick render (9). The main characteristics of each layer are presented in Table 8.1.

Table 8.1. Main characteristics of the different layers composing the ETIC System.

ETICS Prototype	Layer	Product	d (mm)	ρ (kg/m^3)	λ (W/mK)	α (10^{-6} m^2/s)
WF	3	Mat	50	55	0.053	0.60
	4	Board	20	230	0.074	0.34
CA	3	Board	50	60	0.042	0.70
	4	Board	18	100	0.048	0.61
EPS	3	Board	50	30	0.039	1.42
	4	Board	20	30	0.039	1.42
ALL	6	Adhesive mortar	2-3	1400*	0.800*	-
	7	Mesh	-	-	-	-
	8	Primer	-	-	-	-
	9	Render	1-2	1800*	0.700*	-

*Values declared by the manufacturer

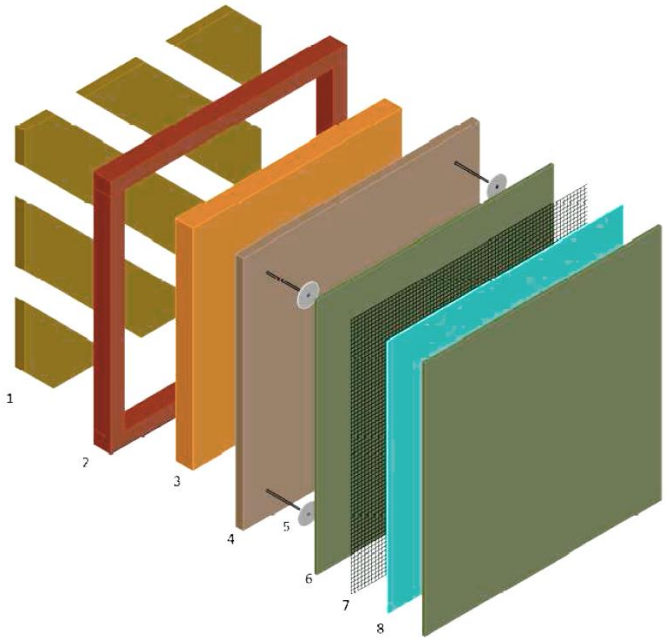

Figure 8.1. Schema of the ETIC System used. Drawing taken from

The U-values of the systems (calculated assuming that the thermal resistances of the interior and the exterior surfaces are 0.13 m^2K/W and 0.04 m^2K/W respectively) are:

WF: 0.719 W/m^2K

CA: 0.561 W/m^2K

EPS: 0.507 W/m^2K

Specimens of 700 x 700 mm were built for the dynamic tests evaluating the hygrothermal performance of the systems. Moreover, smaller specimens of 200 x 200 mm were made incorporating only the external insulation layer (4), which was coated with four different rendering systems (layers 5 to 9) in order to evaluate the interaction between the insulation materials and the coatings. The coatings evaluated were a lime based render, a clay based render and a cork based render, apart from the above mentioned cement based adhesive mortar. The other side and laterals of the samples were wrapped with an aluminium foil in order to impede the moisture migration through them.

8.2. Accelerated ageing test of the ETIC Systems

An accelerated ageing test was performed on samples of 200 x 200 mm following the protocol described in Section 4.5. Ten 48-hours length cycles were performed in which both the temperature and the relative humidity were shifted to extreme conditions. During the test the mass change was gravimetrically monitored between each change in the environmental conditions.

The specimens tested were corn alginate and expanded polystyrene coated with four different renders: cement based mortar, lime based mortar, clay based mortar and cork based mortar.

The mass change of the different specimens, expressed as the difference between the mass after each conditioning period and the initial mass, is presented in Figures 8.2 and 8.3.

In Figure 8.2 the change in mass during the ten cycles for the CA and EPS samples is compared. The plot evidences how, on the EPS specimens, the moisture uptake and loss is similar in all cases (about 30 g) and tends to remain constant throughout

the experiment. In contrast, the CA specimens present a remarkably different behaviour depending on the coating material used. In all cases, these specimens experience more acute changes in mass within a cycle than the EPS ones (up to about 160 g). Moreover, clay and cement rendered CA specimens present a remarkable cumulative mass increase, which is far more significant in the case of the latter. These results are not surprising in the case of the cement rendered specimens as it has been previously reported that low vapour permeable renders tend to increase humidity levels ambient conditions (Lawrence 2009). In this case, the cement render has a water vapour resistance factor (μ) of about 15, which is two times higher than that of the lime or the clay renders. By the other hand, the cumulative increase of mass can be indicative that an internal condensation has occurred. As it is discussed later, both the cement and the clay renders show a low water uptake which would impede the materials from drying out.

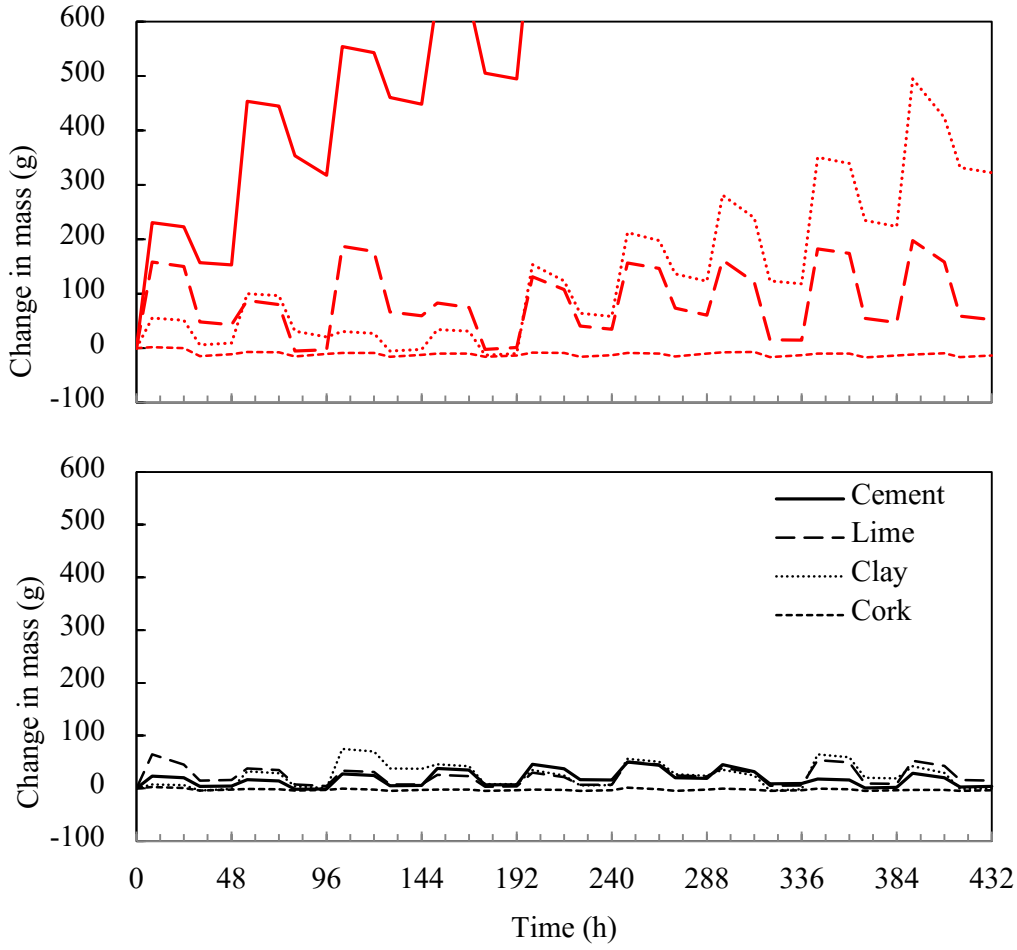

Figure 8.2. Change in mass during the ten cycles of the accelerated ageing test for CA (top panel, red lines) and EPS (bottom panel, black lines) coated with the different materials.

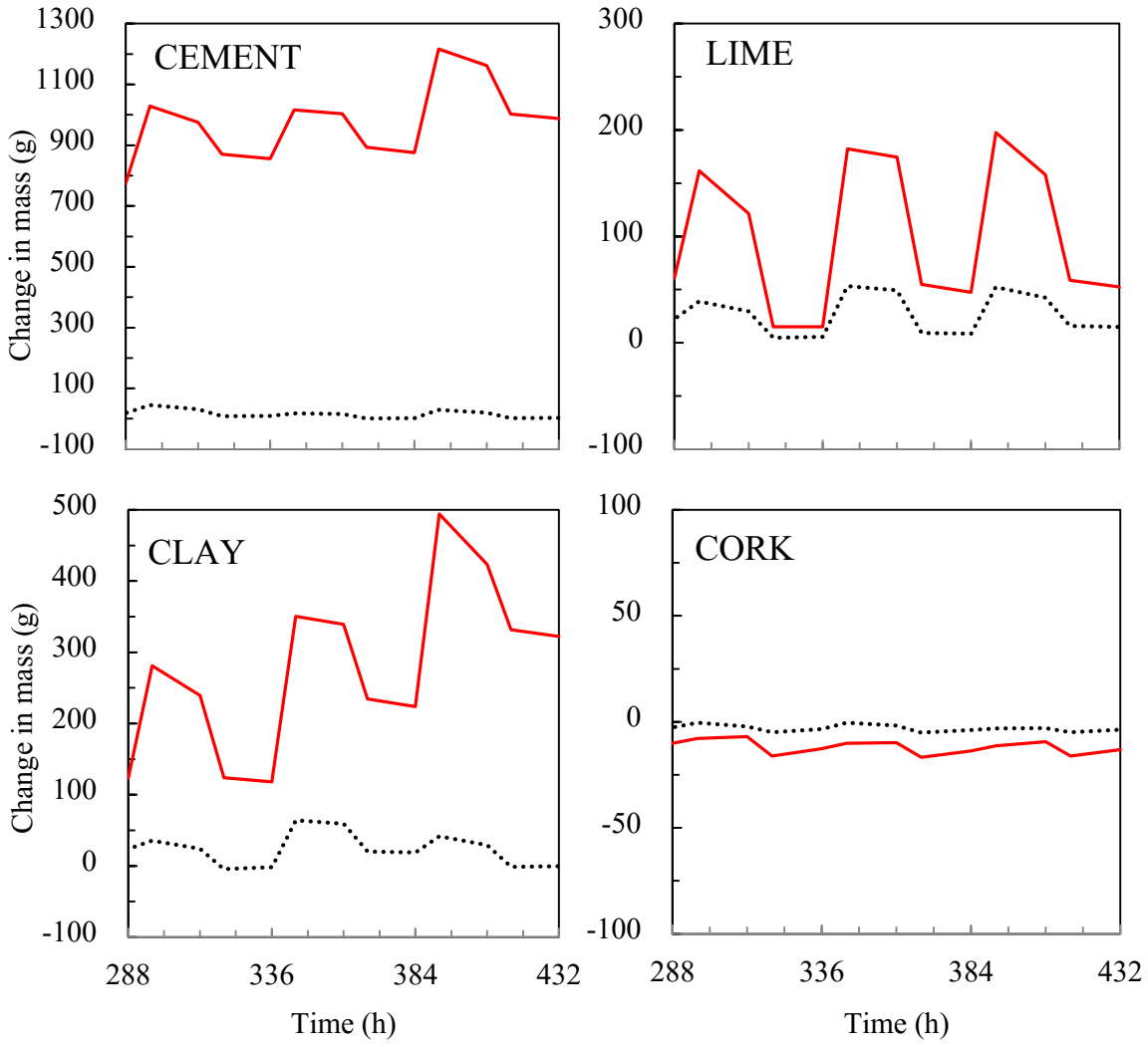

Figure 8.3. Change in mass during the three last cycles of the accelerated ageing test for CA (red lines) and EPS (black lines) coated with the different materials.

The average, maximum and minimum change in mass experienced by the materials is presented in Table 8.2. It is noticeable how in EPS and CA specimens coated with the cork render the change in mass within a cycle is reduced to an average amplitude of about 5 g. This is probably due to the higher water vapour permeability of this render which allows the moisture migration through the insulation system. All these trends are presented in more detail in Figure 8.3, where the three last cycles are compared. Due to the above mentioned cumulative mass increase, the CA cement-rendered materials present a moisture uptake of almost 1 kg at the end of the test, which sharply contrast to the only 4 g soaked up by the EPS samples.

Similarly, the moisture uptake of the CA clay-rendered sample is about 300 g, while the EPS sample present almost the same moisture content than at the beginning of the test. Moreover, the average amplitude of mass variations are 6 times and 2 times higher respectively.

Table 8.2. Change in mass of the different ETIC Systems tested.

		Change in mass (g)		
		Average	Max	Min
Lime	CA	116	146	85
	EPS	33	49	22
Cement	CA	156	229	106
	EPS	26	36	17
Clay	CA	66	96	36
	EPS	34	45	11
Cork	CA	5	8	1
	EPS	4	7	1

The liquid water uptake before and after the accelerated ageing test was measured with a Karsten tube following the methodology described in Section 4.5. The results are presented in Figure 8.4. The results for cork coated samples after ageing are not presented as the water uptake was too high for the measures. The results show that the initial water uptake is distinct for all the materials. In all cases, the water uptake is higher for CA samples, especially in the case of clay and cork mortars. Cork coated samples present an important absorption of water which is dramatically increased after ageing. A singular effect was observed during the test in which the water absorbed by the material was immediately expulsed nearby the tested area. Cement mortar samples show an impermeable behaviour.

Regarding the effect of the ageing process, the results show that the water uptake is increased in all cases after the ageing process indicating the possible presence of micro fissures due to the dimensional variations. The only exception is lime coated CA. In this case, the water uptake is slightly reduced after ageing. In general EPS samples present greater increase in water uptake than CA samples. Clay rendered

CA samples, for instance, showed no significant differences before and after ageing.

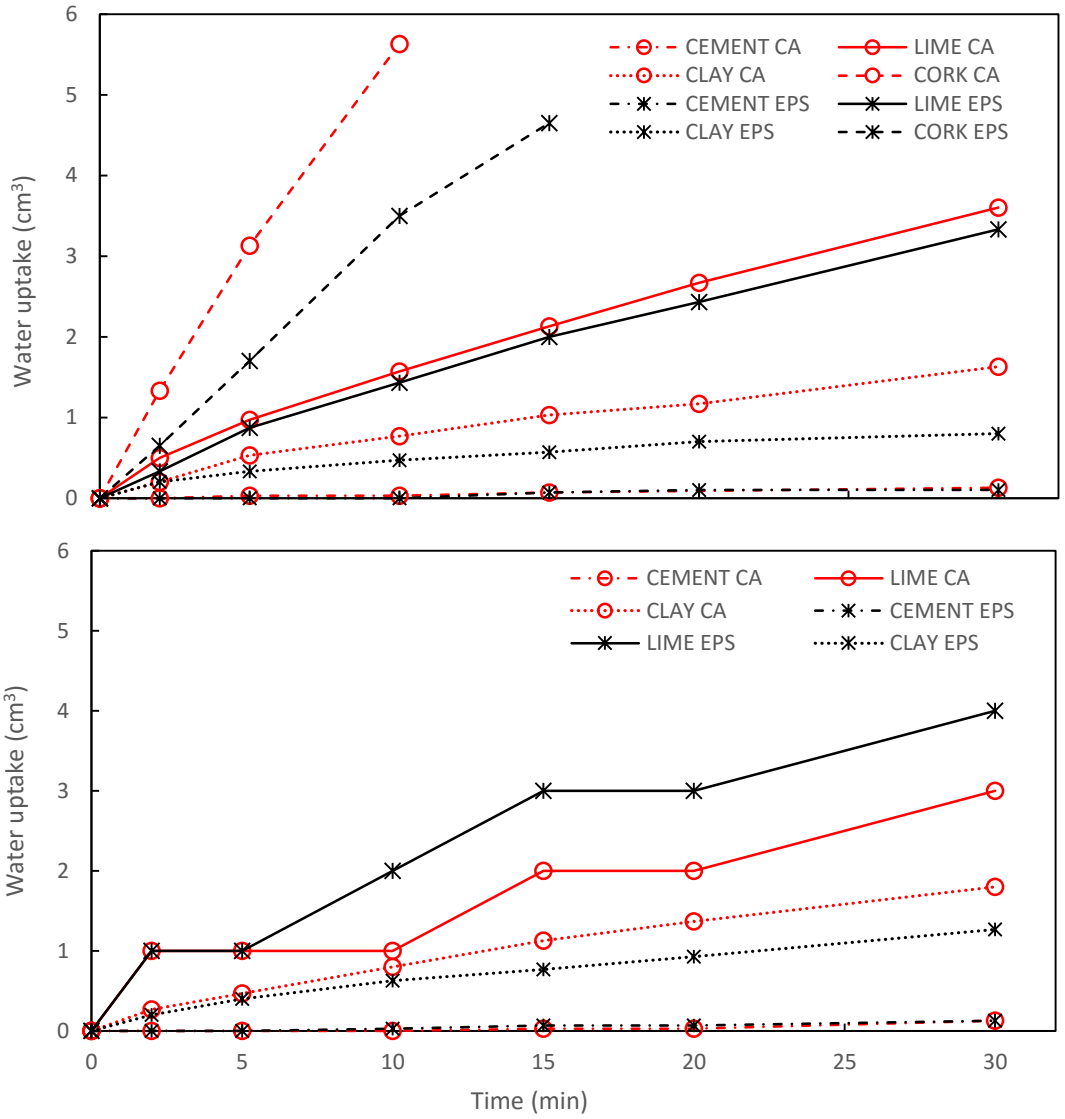

Figure 8.4. Water uptake of the different samples before (top) and after (bottom) the accelerated ageing test.

8.3. Hygrothermal performance of the ETIC Systems

The ETIC system prototypes of dimensions 700 x 700 mm were tested in a climatic chamber, following the setup and protocol described in section 4.2.2. The sample was fixed at the opening of the climate chamber, so that one side was facing the

inside of the chamber and the other the laboratory. A typical run consisted of six cycles of 24h which were designed similar to a typical spring day in a moderate climate. Each cycle consists in a daily variation of temperature (between 15 and 30ºC) and RH (between 80 and 32%), simulating a real evolution of environmental conditions on a typical spring day in Lleida (Figure 8.5). Hence, air conditions within the chamber correspond to the exterior of a building while laboratory air conditions correspond to the indoor environment. During the test, temperatures at different points were recorded and the heat flux measured.

Moreover, three more cycles were performed in which the climatic chamber was turned off and the external insulated box removed in order to evaluate the performance of the systems at the laboratory conditions. These "free" cycles were monitored equally with the previous ones for three days.

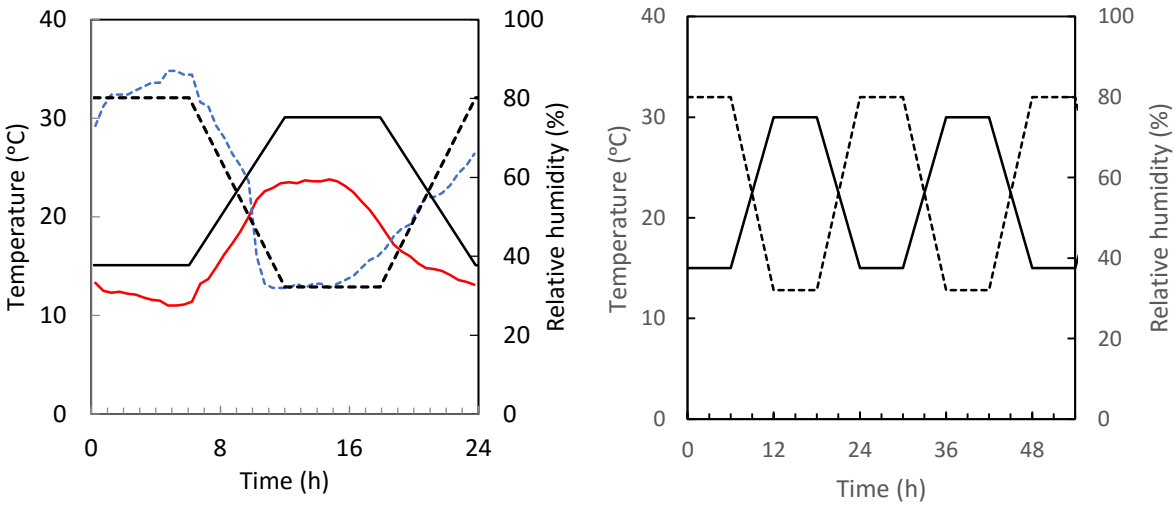

Figure 8.5. Temperature and relative humidity registered on the 31st of March 2015 in Lleida (red and blue lines respectively) and registered in the climate chamber during one cycle. Solid lines correspond to temperature and dotted lines to relative humidity.

The results of the tests performed under controlled cycles are presented in Figures 8.6, 8.7 and 8.8 for WF, CA and EPS based ETIC Systems respectively. The curves correspond to:

- Tac: Air temperature inside the chamber.

- Tsc: Surface temperature at the prototype's surface facing inside the chamber (average of measurements at two points).
- Tint: Temperature within the panel, at the interface between the two material layers, of high and low densities (average of measurements at two points).
- Tsl: Surface temperature at the prototype's surface facing outside the chamber).
- Tal: Air temperature at the laboratory.

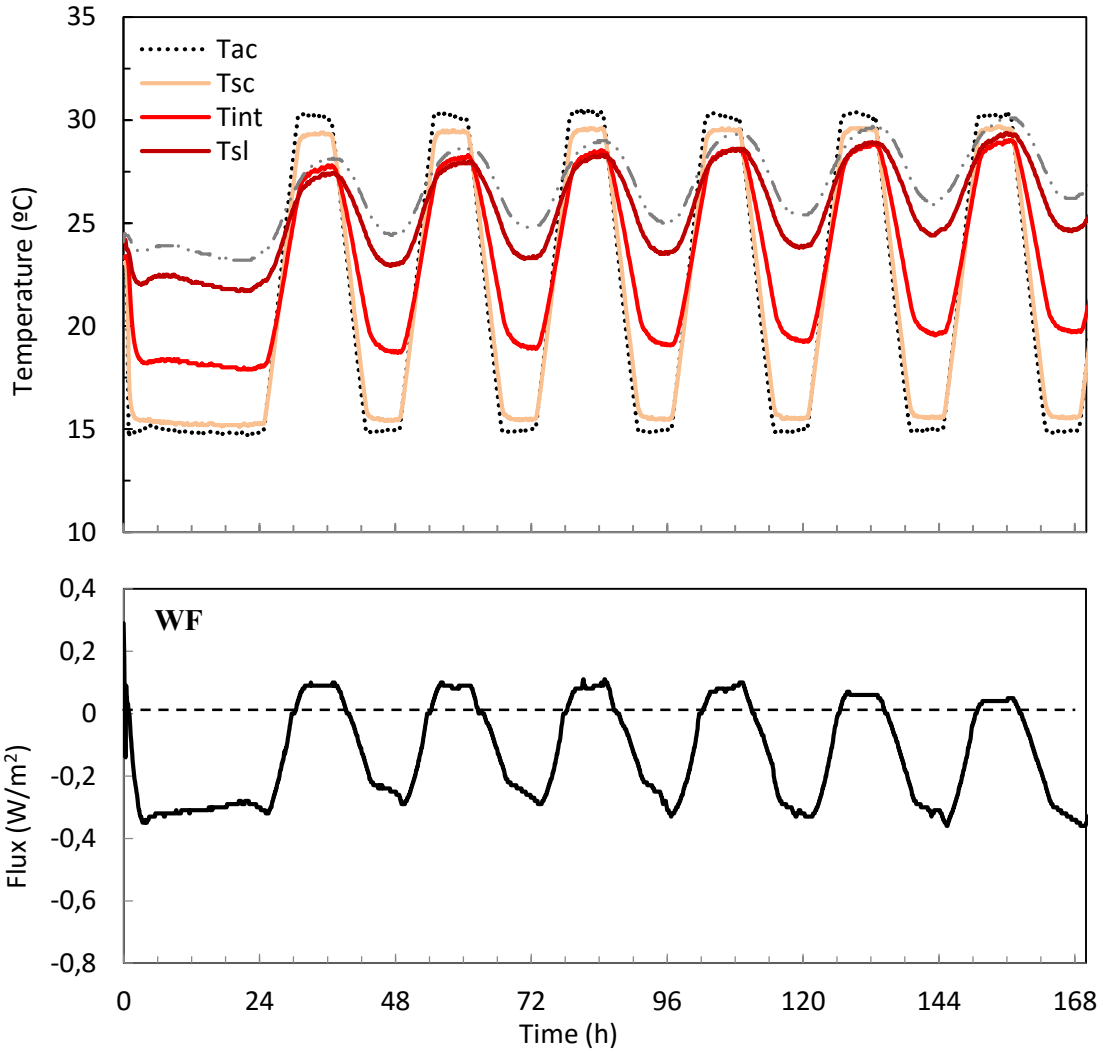

Figure 8.6. Temperatures (top) and heat flux (bottom) for the cycles performed on the WF based insulation system.

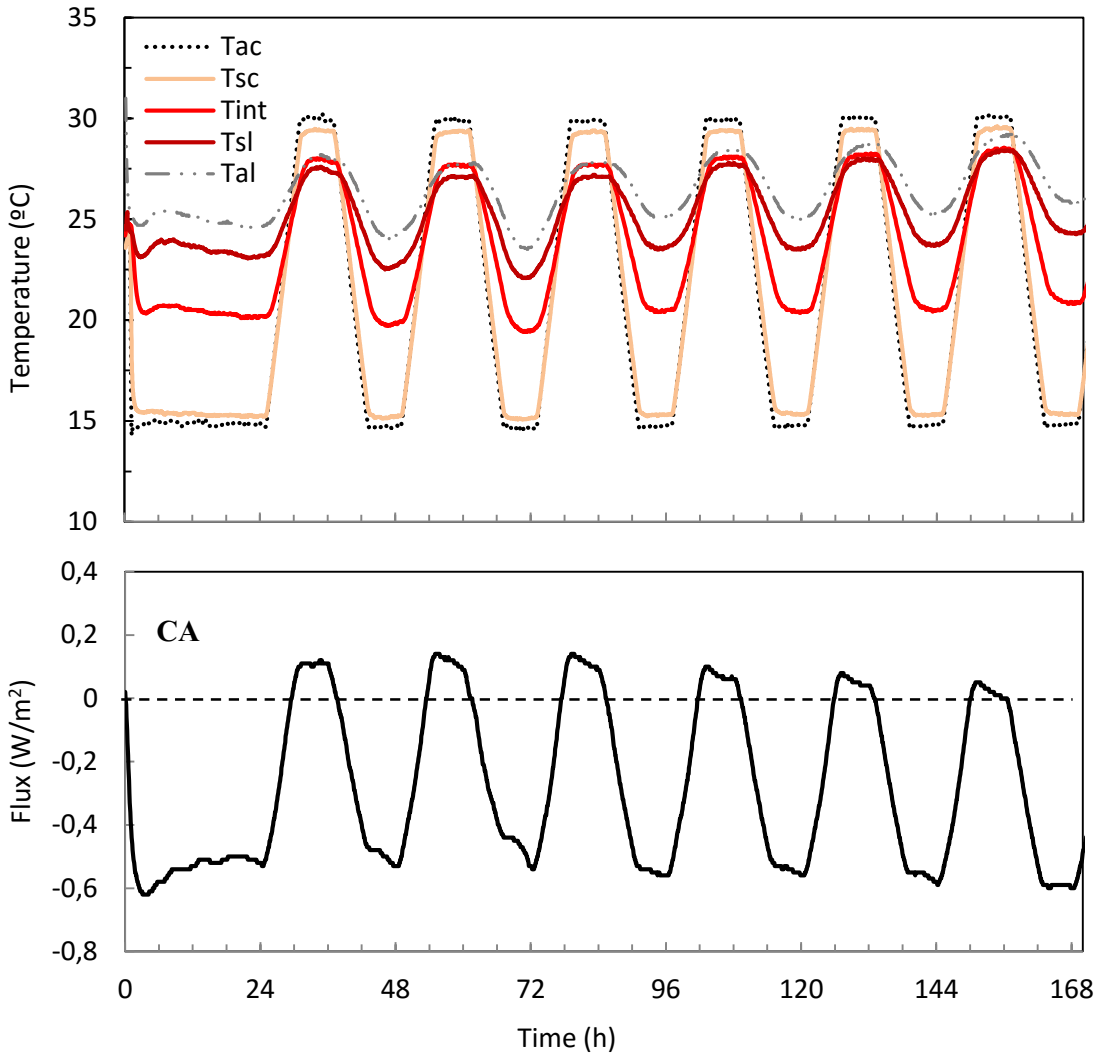

Figure 8.7. Temperatures (top) and heat flux (bottom) for the cycles performed on the CA based insulation system.

The results show similar behaviour of the three insulation systems in terms of temperature changes along their section. However, slight differences can be observed. Although being the system with the highest total U-value, the WF ETIC System presents a lower temperature change in the Tsl, which indicates a better performance. As observed in previous tests for WF boards alone (see Section 7.2.4), in WF ETIC System the sinusoidal shape of the curves is flattened, showing an abrupt slowdown in temperature change when the temperature in the climate chamber is maintained.

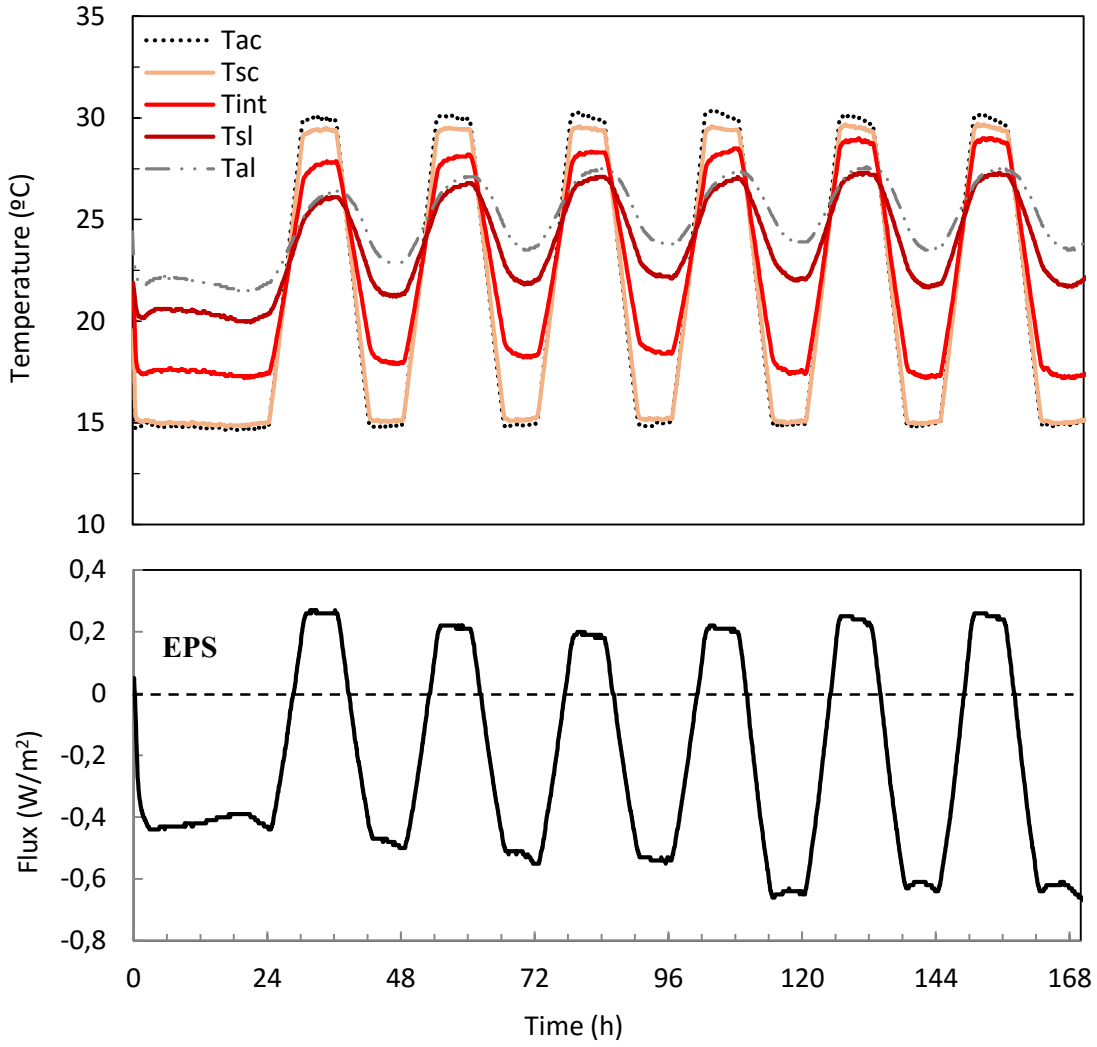

Figure 8.8. Temperatures (top) and heat flux (bottom) for the cycles performed on the EPS based insulation system.

Furthermore, the results show clear differences in the heat flux through the different specimens subjected to the test conditions. The maximum heat flux measured in the WF ETIC system is about 37% lower than in the CA ETIC System in both directions. Despite its lower thermal conductivity, the EPS ETIC System is the one that allows the passage of a higher amount of energy through it: the maximum heat flux is 5% higher towards the laboratory and up to 46% higher in the climate chamber.

The thermal inertia of the insulation systems can be quantified by two main parameters:

- The attenuation factor (μ_{TI}), which is the ratio of the temperature amplitudes at the internal and external surfaces.

- The thermal lag ($\varphi_{MAX;}\ \varphi_{MIN}$), that is the time it takes the heat wave to propagate from the external surface to the inner one. It is evaluated here as the difference of t_{MAX} and t_{MIN} respectively, for both surface temperatures.

The values for the temperature amplitudes and the attenuation factors at each of the 6 cycles is given for WF, CA and EPS in Tables 8.3, 8.4 and 8.5 respectively.

Table 8.3. Temperature amplitudes and attenuation factors of the WF ETIC Systems for each cycle.

WF	n1	n2	n3	n4	n5	n6
ΔTac	15.7	15.5	15.5	15.3	15.4	15.4
ΔTsc	14.9	14.8	14.8	14.9	14.8	14.7
ΔTint	9.1	9.3	9.0	9.3	9.1	8.6
ΔTsl	4.8	5.0	5.1	5.0	4.9	4.9
ΔTal	3.5	4.0	4.0	4.2	4.1	4.1
μ_{TI}	0.32	0.34	0.34	0.34	0.33	0.33

Table 8.4. Temperature amplitudes and attenuation factors of the CA ETIC Systems for each cycle.

CA	n1	n2	n3	n4	n5	n6
ΔTac	15.1	15.0	14.7	14.9	14,7	14.9
ΔTsc	14.2	14.3	14.2	14.0	14.0	14.2
ΔTint	7.8	7.8	7.3	7.4	7.6	7.4
ΔTsl	4.9	5.0	4.9	4.4	4.2	4.2
ΔTal	3.5	4.1	3.2	3.4	3.7	3.6
μ_{TI}	0.35	0.35	0.35	0.31	0.30	0.30

Table 8.5. Temperature amplitudes and attenuation factors of the EPS ETIC Systems for each cycle.

EPS	n1	n2	n3	n4	n5	n6
ΔTac	15.5	15.4	15.3	15.3	16.4	15.1
ΔTsc	14.6	14.5	14.4	14.3	14.7	14.7
ΔTint	10.5	10.2	10.1	9.9	11.4	11.8
ΔTsl	6.2	5.4	5.2	4.7	5.0	5.5
ΔTal	4.8	4.1	3.7	3.6	3.6	4.0
μ_{TI}	0.42	0.37	0.36	0.33	0.34	0.37

The results of the "free" cycles are shown in Figure 8.9. The thermal lag shown in Table 8.5 is calculated from these cycles. The results reveal a considerable thermal inertia of the WF ETIC System, which is manifested in a high attenuation of the amplitude of the thermal variation, as well as a delay in the time when the temperature peaks occur. Table 8.6 shows the temperature amplitude (ΔT), the corresponding attenuation factor and the thermal lag for each of the three cycles and the three insulation systems.

Table 8.6. Temperature amplitude, attenuation factor and thermal lag of the ETIC Systems for each "free" cycle.

	WF			CA			EPS		
	n1	n2	n3	n1	n2	n3	n1	n2	n3
ΔTsl	2.0	3.0	3.0	1.9	2.1	2.2	2.5	2.8	2.7
ΔTsc	0.6	0.9	1.0	0.8	0.6	0.9	1.1	1.0	0.9
μ_{TI}	0.30	0.30	0.33	0.42	0.29	0.41	0.44	0.36	0.33
φ_{MAX}	5.4	5.3	5.0	4.4	3.7	4.1	3.5	3.5	4.4
φ_{MIN}	4.5	2.9	4.0	2.4	4.1	3.7	1.7	2.7	2.5

The values for the attenuation factor and the thermal lag indicate the higher thermal inertia for the WF insulation system. This explains why the heat flux is lower in this case and the good results yielded by this system. The mean values of these factors calculated from all the test cycles are presented in Table 8.7.

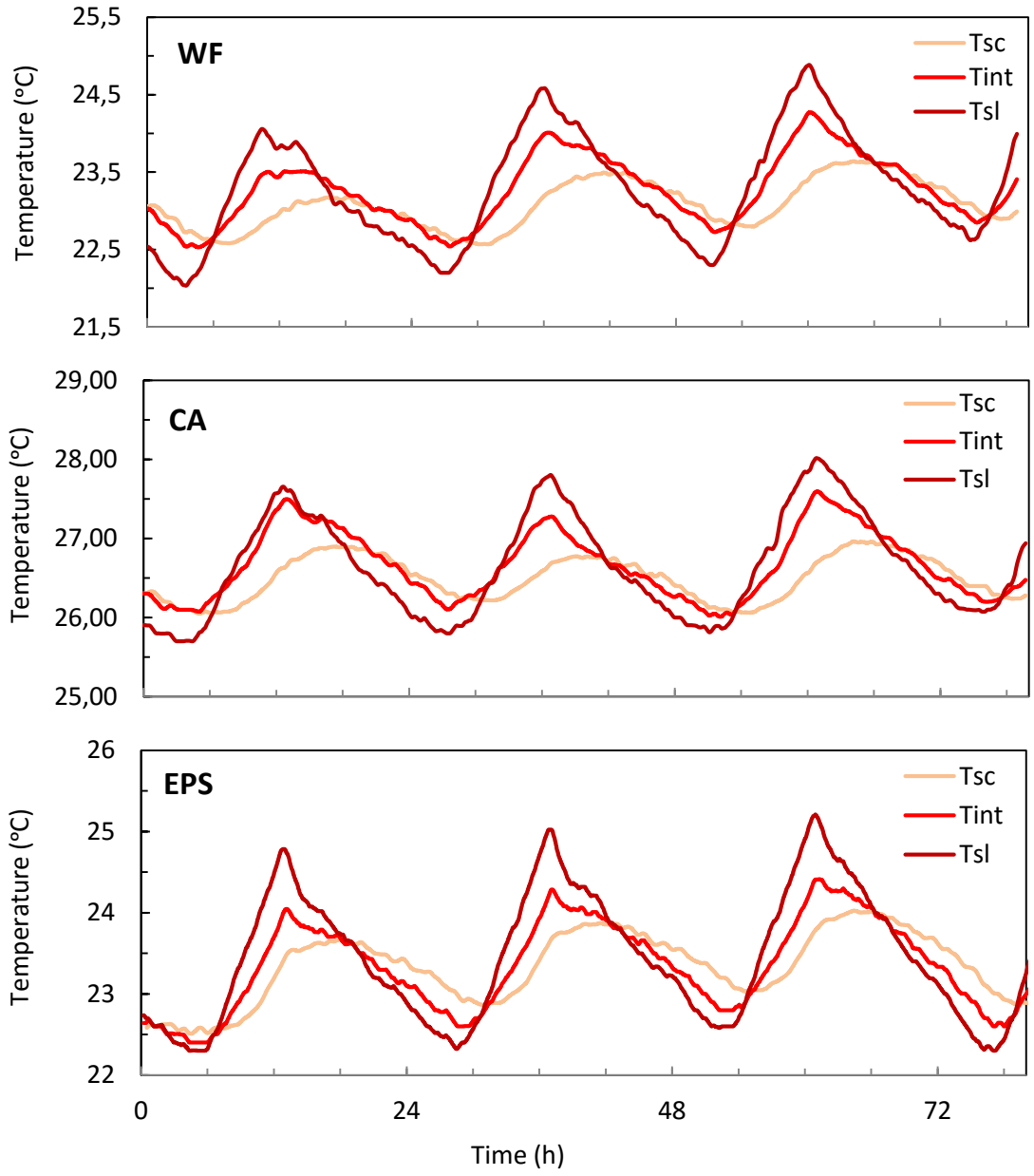

Figure 8.9. Temperature registered during the "free" cycles at the surfaces and centre section of the insulation systems.

Table 8.7. Mean attenuation factor and thermal lag of the insulation systems.

	μ_{TI}	φMAX	φMIN
WW	0.32	5.2	3.8
CA	0.35	4.1	3.4
EPS	0.37	3.8	2.3

8.4. Conclusions

The corn pith alginate thermal insulation material proposed in this thesis is integrated into an External Thermal Insulation System in order to evaluate its behaviour in a situation similar to a real case. To this aim an accelerated ageing test and a dynamic hygrothermal test including two testing protocols are performed. The ETIC System incorporating the CA boards is compared with systems incorporating wood based insulation materials on one hand and expanded polystyrene boards on the other.

The accelerated ageing test showed remarkable differences in water migration through the system when the coating material was changed. The cement based coating prevented the CA systems from drying, which caused an accumulative moisture uptake along the test which indicates a poor interaction between these materials. Clay based renders and especially lime based renders showed better behaviour. The cork based render showed a remarkably good behaviour in the moisture migration but it also presented a high water uptake which might compromise the durability of the system especially in the case of external insulation systems. However, such renders may fit humid indoor applications. The obtained results indicate that the insulation systems incorporating the CA insulation boards do not present problems of durability when exposed to extreme temperature conditions. However, if the hygroscopic performance of the render is not carefully analysed, an increasing moisture uptake together with problems of condensation may occur.

Regarding its hygrothermal behaviour, the CA ETIC System was found to present a similar performance to the other two systems. Under the tested protocols, the hygrothermal performance of this system was better than that shown by the EPS, but not as good as the behaviour presented by the wood based system. It was found that under the chosen protocols (which simulate a typical sprint day in a moderate climate region), the thermal inertia plays an important role in the overall performance of the systems. The attenuation factor and the thermal lag indicated that the WF system presents a higher thermal inertia than the CA system. However, the U-value of the CA system was lower than that of the WF system and similar to that of the EPS system which can be an advantage in other environmental situations such as persistent cold periods where the thermal inertia is a less decisive factor.

9. CONCLUSIONS AND FURTHER WORK

The main objective of this thesis was to develop a new thermal insulation building material formulated from crop by-products and biopolymers that present competitive hygrothermal performance, controlled fire reaction and enhanced mould resistance. This material presents the advantage of being based on available renewable materials, being completely compostable.

To this end, the availability of the different crop by-products in Spain is analysed under the hypothesis that it is relevant to the construction industry and that the exploitation of such raw materials can be made in a sustainable way without compromising the productivity of soils or food production. Due to the complexity in the establishment of reliable values for the analysis, a rather conservative approach was assumed where the available crop by-products correspond only to 37% of the yearly produced by-products. Barley, wheat, corn, rice and sunflowers by-products were found to be the most abundant ones, representing 77% of the total available crop by-products in Spain (6.6 Mt·year-1). The analysis indicates that a sustainable production of insulation materials based on crop by-products seems to be feasible as the amount of crop by-products yearly available is above 5 times higher the amount of the crop by-products needed to produce the insulation for all the current demand of the building sector in Spain. The available corn by-products alone would be sufficient to produce the insulation required for the thermal refurbishment of between 250,000 and 450,000 dwellings annually which would allow for the fulfilment of the European requirements of 80% reduction in CO_2 emissions by the year 2050.

Three of the most abundant crop by products (barley straw, corn pith and rice husks) were chosen for their distinct morphologies and were experimentally characterised under the hypothesis that such materials naturally present advantageous hygrothermal properties for their use in building thermal insulation materials. It was discovered that the thermal conductivity of the crop by-products ranges between 0.070 and 0.047 W/mK, which are considered acceptable values to insulation materials but are slightly higher than the typical values of commercially available products (0.040 W/mK). Corn pith is the raw material that presented the lowest thermal conductivity, with less dependence on the particle size. However, in the dynamic hygrothermal tests, a rapid change in temperature was observed, indicating a lower thermal inertia, which was attributed to its remarkably lower density. Regarding the fire behaviour of the materials, rice husk presented better results on the PCFC and TGA, which can be explained by its high silica content.

The crop by-products were then used in the form of bundles of fibres and granulates to produce experimental insulation materials agglomerated with two different biopolymers. A total of six different formulations were obtained. The resulting materials were evaluated and compared in terms of their physical, thermal and hygroscopic properties and their fire reaction, under the hypothesis that it is possible to produce highly performant thermal insulation materials from crop by-products by incorporating a low ratio of binder materials and using low tech manufacturing systems. It was found that this hypothesis was true especially for the corn pith alginate composites (CA). The amount of binder needed in this formulation was between 3 and 5 % in weight, probably due to the granular and spongy nature of the material which would allow a good surface contact between the particles. Moreover, CA presented the lowest bulk density among the tested materials (about 55 kg/m^3), and thus a lower thermal conductivity (0.044 W/mK) and lower fire load, even if the overall fire behaviour of rice husk was better than that of the corn pith. On the other hand, through the PCFC and TGA, it was discovered that alginate has a positive impact on the fire behaviour of the corn pith. PCFC results indicated that the addition of 3% alginate results in a 30% reduction in the total heat release HR and the peak heat release rate due to thermal decomposition. Moreover, the CA composites show remarkably good results on larger scale flaming combustion test as shorter combustions are observed. However, a smouldering process is also observed which represents a negative aspect. In any case, the fire properties of all the experimental insulation materials

are found to be better than those of the organic foamy materials commonly used in building insulation, such as polystyrene and polyurethane.

On the basis of the above mentioned outcomes, the technical feasibility of the CA composites was further analysed. The tests indicated that the hygrothermal performance of the CA composites is similar than that of commercially available wood based insulation boards. Its thermal conductivity at room conditions (20ºC and 50% RH) was found to be 0.038 W/mK, slightly lower than that of the wood fibre materials. However, similar to other bio-based materials, this value is increased by about 20% when the RH approaches the 100%. The moisture buffer capacity of the experimental materials is also slightly better than the wood based boards, indicating a higher capacity to regulate indoor moisture levels. Dynamic hygrothermal tests indicated that the hygrothermal performance of the materials are clearly affected by the moisture adsorption and desorption processes, which can be an advantage in terms of a certain thermal inertia resulting from this process. Both CA and WW materials showed remarkably more favourable results than EPS samples when subjected to sudden temperature changes in the range of 10 to 40 ºC. The water adsorption and desorption within the materials was gravimetrically monitored during the tests indicating a greater moisture migration in the case of WW composites. It was observed that the temperature change within both samples was significantly increased when the RH was artificially maintained during the test indicating the relevance of the adsorption phenomenon in the hygrothermal performance of the materials. Moreover, it was noted that the evolution of the temperature change in WW and CA samples was significantly different which resulted in a lower temperature change in the WW samples at the end of the cycles and thus, results in a better performance. The results indicated that the adsorption kinetics and extent differ depending on the materials, affecting its overall hygrothermal performance. Further work is needed in order to deeply understand the causes of these differences.

Under the hypothesis that the main drawbacks of bio-based insulation materials are fire reaction and mould growth resistance, relevant tests are performed in order to evaluate such aspects. The results are compared with wood fibre insulation boards and with conventional insulation materials such as expanded polystyrene and mineral wool insulations. This hypothesis is confirmed in the case of mould growth, but is not as clear in the case of fire reaction, as it is confirmed that the bio-based materials present better behaviour than the existing organic foamy materials.

Moreover, under the hypothesis that it is possible to improve the major negative aspects of the materials (fire reaction and mould growth resistance) using harmless fibre pre-treatments and additives further tests were performed on treated samples. In the case of fire, different fire retardants are added in order to reduce the speed of propagation and increase the combustion onset temperature of the smouldering process. Similarly, the mould growth resistance of the plain board is improved using different pre-treatments of the raw materials.

Regarding flaming combustion, the best results are obtained with specimens treated with 8% of boric acid. Indeed, all the studied parameters related to flaming combustion were improved by the addition of boric acid which is however a substance classified as possibly toxic. Indeed its use has been restricted to 5.5% (w/w) of the final product at the European Union (ECHA 2010). None of the harmless substances was capable of yielding comparable results regarding flaming combustion. Nevertheless, in the case of smouldering combustion samples incorporating ammonium polyphosphate showed remarkably improved behaviour, thereby increasing the onset temperature for smouldering to occur and reducing the propagation speed of the smouldering front.

Regarding the mould growth resistance, although none of the treatments resulted in a Class II or Class III material, the L-20 specimen showed important improvement, with a profile close to that of commercially available wood fibre insulation boards. Thus, it is possible to estimate that such materials can be used as thermal insulation boards in construction, but only in controlled environments, where the RH is maintained below 75%. For the use of the material in ETIC Systems the render materials are of great importance.

In general the tests performed in this thesis regarding the incorporation of both fire retardants and mould growth inhibitors represent an initial stage that opens the possibility of several areas of investigations. Other additives and pre-treatments, as well as other proportions and application methods should be tested. Further awareness of the underlying principles affecting the efficacy of the treatments and the effects that such treatments have on the thermal and the hygroscopic properties of the material should be investigated in future work. Moreover, the interactions between the treatments and the binder material might be another interesting area of analysis.

Finally, the corn pith alginate thermal insulation material proposed in this thesis is integrated into an External Thermal Insulation System in order to evaluate its behaviour on a larger scale, similar to a real case. To this aim an accelerated ageing test and a dynamic hygrothermal test are performed. The ETIC System incorporating the CA boards is compared with one incorporating an EPS material. It was found that the durability of the system is highly dependent on the coating material. In the case of CA ETIC Systems, the cement mortar coating is the cause of an accumulative moisture uptake, indicating a poor moisture desorption process. Clay and lime renders showed the best overall results, with equilibrated moisture migration and moderate liquid water uptake. Moreover, in the case of the lime-coated samples little differences in the overall behaviour were observed after ageing.

On the other hand, the hygrothermal performance of the CA ETICS was evaluated in contrast to a WF and an EPS ETICS. It was found that the three systems presented a similar behaviour. Under the chosen protocols (which simulate a typical sprint day in a moderate climate region), the thermal inertia plays an important role in the overall performance of the systems. The attenuation factor and the thermal lag indicated that the WF system presents a higher thermal inertia than the CA system. However, the U-value of the CA system was lower than that of the WF system and similar to that of the EPS system which can be an advantage in other environmental situations such as persistent cold periods where the thermal inertia is a less decisive factor.

According to the results presented in this work, it is possible to conclude that the corn pith alginate insulation board proposed present positive aspects that satisfactorily fulfils the technical requirements of the building thermal insulation industry. However, further work is needed in order to further improve the overall behaviour of the material and to investigate other important aspects such as mechanical behaviour or resistance in front of other biotic and abiotic agents. The CA boards present the advantage of being rigid and light at the same time, feature that no commercially available bio-based insulation material exhibit till date. Such features can be an advantage in certain applications such as suspended ceiling systems or ETIC Systems similar to the one analysed in this thesis. Each specific application will demand specific requirements that should be carefully analysed in the context of construction systems integrating the material.

In the present work it was assumed that the CA formulations needing a lower ratio of binder, as a matter of fact, was advantageous with respect to the other experimental materials analysed in terms of cost of production and environmental impact, as it is usually the case of composite materials. However, further work should be done in order to confirm this hypothesis and quantify the environmental impact of the proposed formulation. To achieve this aim, it is necessary to determine the most efficient manufacturing processes of the boards. The mechanisation of the decortication process, which was handmade and highly time consuming in the context of this thesis, and the reduction in the use of water during the manufacturing process are two important areas of improvement.

10. LIST OF PAPERS

Journal papers

Palumbo M, Formosa J, Lacasta AM. 2015. Thermal degradation and fire behaviour of thermal insulation materials based on food crop by-products. *Construction and Building Materials* 79:34–39.

Palumbo M, Avellaneda J, Lacasta AM. 2015. Availability of crop by-products in Spain: new raw materials for natural thermal insulation. *Resources, Conservation and Recycling* 99: 1–6.

Palumbo M, Lacasta AM, Holcroft N, Shea A and Walker P. 2015. Determination of hygrothermal parameters of experimental and commercial bio-based insulation materials. (Pre-print).

Conference proceedings

Palumbo M, Navarro A, Avellaneda J, Lacasta AM. 2014. Characterization of thermal insulation materials developed with crop wastes and natural binders. In: WSB14 World Sustainable Building Conference (GBC). Barcelona, 28-30 Oct. p 1–10.

Palumbo M, Navarro A, Giraldo P, Lesar B and Lacasta AM. 2015. Performance of a bio-based insulation board from crop by-products and natural gums. In: First International Conference on Bio-based Building Materials. Clermont-Ferrand, 22-24 Jun.

Other related publications

Navarro MA, Lacasta AM, Palumbo M, Garcia D, Milla L. 2013. Revestimientos con tierra y fibras vegetales: metodología de estudio". In: X CIATTI Congreso Internacional de Arquitectura con Tierra: tradición e innovación. Cuenca de Campos, 27-29 Sep. Universidad de Valladolid. p. 1-10.

Navarro A, Palumbo M, Gonzalez B and Lacasta AM. 2015. Performance of clay-straw plasters containing natural additives. In: First International Conference on Bio-based Building Materials. Clermont-Ferrand, 22-24 Jun.

Godoy A, Palumbo M, Sánchez N, Vilajoana A. 2012. (e)co, equilibrium through cooperation. In: I Congreso EECN Edificios Energía Casi Nula: libro de comunicaciones. Madrid, 7-8 May. p. 333-338.

11. REFERENCES

Abadie MO, Mendonça KC. 2009. Moisture performance of building materials: from material characterization to building simulation using the Moisture Buffer Value concept. *Building and Environment* 44(2):388–401.

Abdou A, Budaiwi I. 2013. The variation of thermal conductivity of fibrous insulation materials under different levels of moisture content. *Construction and Building Materials* 43:533–544.

Al-Homoud MS. 2005. Performance characteristics and practical applications of common building thermal insulation materials. *Building and Environment* 40(3):353–366.

Alvarez VA, Vázquez A. 2004. Thermal degradation of cellulose derivatives/starch blends and sisal fibre biocomposites. *Polymer Degradation and Stability* 84:13–21.

Anderson P, Gaserod O, Blakemore WR, et al. 2010. Food Stabilizers, Thickeners and Gelling Agents. Imerson A, FMC BioPolymer, editors. John Wiley & Sons, Ltd.

Antal MJJ, Varhegyi G. 1995. Cellulose pyrolysis kinetics: the current state of knowledge. *Industrial & Engineering Chemistry Research* 34(3):703–717.

Arabhosseini A, Huisman W, Müller J. 2010. Modeling of the equilibrium moisture content (EMC) of Miscanthus (Miscanthus × giganteus). *Biomass and Bioenergy* 34(4):411–416.

Artigas J, Garcia L, Cabrera M, et al. 2011. Evaluación del potencial de energía de la biomasa. Estudio técnico PER 2011-2020. Instituto para la Diversificación y Ahorro de la Energía.

Aviara NA, Ajibola OO, Aregbesola OA, et al. 2006. Moisture sorption isotherms of sorghum malt at 40 and 50°C. *Journal of Stored Products Research* 42(3):290–301.

Bava F, Zegers J, Vieillefont V, et al. 2012. L'oservatoire national des ressources en biomasse. Évaluation des ressources disponibles en France. FranceAgrimer, établissement national des produits de l'agriculture et de la mer.

Blanco JL, Blanco RJM, Canovas BC, et al. Universitat Politècnica de Catalunya. 2011 Des 07. Procedimiento para el aprovechamiento industrial de los rastrojos de las plantas ricas en médula. EP 11727710 A2.

Di Blasi C, Signorelli G, Di Russo C, et al. 1999. Product distribution from pyrolysis of wood and agricultural residues. *Industrial & Engineering Chemistry Research* 38(6):2216–2224.

Di Blasi C, Tanzi V, Lanzetta M. 1997. A study on the production of agricultural residues in Italy. *Biomass and Bioenergy* 12(5):321–331.

Bledzki AK, Mamun AA, Lucka-Gabor M, et al. 2008. The effects of acetylation on properties of flax fibre and its polypropylene composites. *Express Polymer Letters* 2(6):413–422.

De Bouter A, King B, Achte C, et al. 2009. Concevoir des batiments en bottes de paille. La Maison en Paille Editions.

Boyle H, Ezekiel U-H, Herold I, et al. 2010. Next-generation ethanol and biochemicals: what's in it for Europe? Bloomberg New Energy Finance.

Bozsaky D. 2010. The historical development of thermal insulation materials. *Periodica Polytechnica. Architecture* 41(2):49–56.

Branca G, Cacchiarelli L, Cardona C, et al. 2007. Agricultural residues component. Crop residues and livestock residues. In: BEFS RA User manual volumes. Food and Agriculture Organization of the United Nations (FAO).

Cadena C, Bula A. 2002. Estudio de la variación en la conductividad térmica de la cascarilla de arroz aglomerada con fibras vegetales. *Ingeniería & Desarrollo.* 12:8–9.

Calkins M. 2008. Materials for sustainable sites: a complete guide to the evaluation, selection, and use of sustainable construction materials. John Wiley & Sons.

Canet R, Instituto Valenciano de Investigaciones Agrarias. 2014. Uso de materia orgánica en Agricultura. [accessed 2014 Jul 8]. http://www.ivia.es/rcanet/descargas/MO enAgricultura.pdf

Carmeliet J, Hens H, Roels S, et al. 2004. Determination of the liquid water diffusivity from transient moisture transfer experiments. *Journal of Building Physics* 27(4):277–305.

Chapple S, Anandjiwala R. 2010. Flammability of natural fiber-reinforced composites and strategies for fire retardancy: a review. *Journal of Thermoplastic Composite Materials* 23:871–893.

Claramunt J. 2011. Utilització de fibres vegetals per a l'elaboració de morters de ciment d'altes prestacions (SHCC). Doctoral Disertation. Universitat Politècnica de Catalunya.

Cogen JM, Lin TS, Lyon RE. 2009. Correlations between pyrolysis combustion flow calorimetry and conventional flammability tests with halogen-free flame retardant polyolefin compounds. *Fire and Materials* 33(1):33–50.

Collet F, Bart M, Serres L, et al. 2008. Porous structure and water vapour sorption of hemp-based materials. *Construction and Building Materials* 22(6):1271–1280.

Collet F, Chamoin J, Pretot S, et al. 2013. Comparison of the hygric behaviour of three hemp concretes. *Energy and Buildings* 62:294–303.

Collet F, Pretot S. 2012. Variation de la capacité hydrique tampon de bétons de chanvre en fonction de la formulation. In: Ecobat Sciences et techniques 1ère édition. Paris, France.

Collet F, Pretot S. 2014. Thermal conductivity of hemp concretes: variation with formulation, density and water content. *Construction and Building Materials* 65:612–619.

Copeland J, Turley D, Agri-Environment and Land Use Strategy Team. 2008. National and regional supply/demand balance for agricultural straw in Great Britain. Central Science Laboratory.

Cuchí A, Sweatman P. 2011. Una visión-país para el sector de la edificación en españa.

Cuchí A, Sweatman P. 2012. Informe GTR 2012. Una visión-país para el sector de la edificación en españa. Plan de acción para un nuevo sector de la vivienda.

Cuchí A, Sweatman P. 2014. Informe GTR 2014. Estrategia para la rehabilitación. Claves para transformar el sector de la edificación en España. Green Building Council España and Fundación Conama.

Cusola O, Valls C, Vidal T, et al. 2013. Application of surface enzyme treatments using laccase and a hydrophobic compound to paper-based media. *Bioresource Technology* 131:521–526.

Demirbas A. 2004. Combustion characteristics of different biomass fuels. *Progress in Energy and Combustion Science* 30(2):219–230.

Dittenber DB, GangaRao HVS. 2012. Critical review of recent publications on use of natural composites in infrastructure. *Composites Part A: Applied Science and Manufacturing* 43(8):1419–1429.

Domínguez-Muñoz F, Anderson B, Cejudo-López JM, et al. 2010. Uncertainty in the thermal conductivity of insulation materials. *Energy and Buildings* 42(11):2159–2168.

Dong A, Yu Y, Yuan J, et al. 2014. Hydrophobic modification of jute fiber used for composite reinforcement via laccase-mediated grafting. *Applied Surface Science* 301:418–427.

Dorez G, Taguet A, Ferry L, et al. 2013. Thermal and fire behavior of natural fibers/PBS biocomposites. *Polymer Degradation and Stability* 98(1):87–95.

Dowling A, Mathias JA. 2007. Experimental determination of the insulating ability of corn by-products. *Journal of Sustainable Agriculture* 30(2):15–27.

Draget K, Smidsrød O, Skjåk-Bræk G. 2005. Alginates from algae. In: Steinbuchel A, Rhee S, editors. Polysaccharides and polyamides in the food industry. Properties, productions and patents. Willey-VCH Verlag GmbH & Co. KGaA. p. 1–30.

Drysdale D. 1998. An introduction to Fire dynamics. John Wiley & Sons Ltd œ.

Ebnesajjad S, editor. 2008. Adhesives technology handbook. 2nd edition. William Andrew Inc.

ECHA (European Chemicals Agency). 2010. Member state committee draft support document for identification of boric acid as a substance of very high concern because of its CMR properties.

Elmendorf A. 1929. Insulating building material and method of making the same.

Ericsson K, Nilsson LJ. 2006. Assessment of the potential biomass supply in Europe using a resource-focused approach. *Biomass and Bioenergy* 30(1):1–15.

Evrard A. 2008. Transient hygrothermal behaviour of lime-hemp materials. Doctoral Dissertation. Universite Catholique de Louvain.

Fischer G, Hizsnyik E, Prieler S, et al. 2007. Assessment of biomass potentials for bio-fuel feedstock production in Europe: methodology and results. Land Use Change and Agriculture Program Assessment.

Galán-Marín C, Rivera-Gómez C, Petric J. 2010. Clay-based composite stabilized with natural polymer and fibre. *Construction and Building Materials* 24(8):1462–1468.

Gálvez AV, Aravena EL, Mondaca RL. 2006. Isotermas de adsorción en harina de maíz (Zea mays L.). *Ciência e Tecnologia de Alimentos* 26(4):821–827.

Garcia-Ubasart J, Esteban A, Vila C, et al. 2011. Enzymatic treatments of pulp using laccase and hydrophobic compounds. *Bioresource Technology* 102(3):2799–2803.

Glé P, Gourdon E, Arnaud L. 2011. Acoustical properties of materials made of vegetable particles with several scales of porosity. *Applied Acoustics* 72(5):249–259.

Gonçalves MRF, Bergmann CP. 2007. Thermal insulators made with rice husk ashes: Production and correlation between properties and microstructure. *Construction and Building Materials* 21(12):2059–2065.

Hagen BC. 2013. Onset of smoldering and transition to flaming fire. Doctoral Dissertation. University of Bergen.

Hagen BC, Frette V, Kleppe G, et al. 2011. Onset of smoldering in cotton: Effects of density. *Fire Safety Journal* 46(3):73–80.

Hagen BC, Frette V, Kleppe G, et al. 2015. Transition from smoldering to flaming fire in short cotton samples with asymmetrical boundary conditions. *Fire Safety Journal* 71:69–78.

Halvarsson S, Edlund H, Norgren M. 2010. Wheat straw as raw material for manufacture of medium density fiberboard (MDF). *BioResources* 5(Lowgren 1986):1215–1231.

He F, Yi W, Zha J. 2009. Measurement of the heat of smoldering combustion in straws and stalks by means of simultaneous thermal analysis. *Biomass and Bioenergy* 33:130–136.

Hernandez CG, Fuertes A. 2011. Biomasa vegetal no alimentaria producida en España con posibilidad de uso energético. *ITEA Informacion Tecnica Economica Agraria* 107(3):209–225.

Hill CAS, Norton AJ, Newman G. 2010. The water vapour sorption properties of Sitka spruce determined using a dynamic vapour sorption apparatus. *Wood Science and Technology* 44(3):497–514.

Hinde JJ. 1927. 1924 Nov 17. Process of manufacturing insulating and plster board from cornstalks. US 1623184.

Hofbauer W, Krueger N, Breuer K, et al. 2008. Mould resistance assessment of building materials - Material specific isopleth-systems for practical application. In: Proceedings of Indoor Air 2008. Copenhgen, 17-22 Aug. Fraunhofer- Publica.

Humar M, Lesar B. 2013. Efficacy of linseed- and tung-oil-treated wood against wood-decay fungi and water uptake. *International Biodeterioration and Biodegradation* 85:223–227.

IDAE. 2011. Plan de acción nacional de energías renovables de españa (PANER) 2011 - 2020. Instituto para la Diversificación y Ahorro de la Energía. Ministerio de Industria, Turismo y Comercio.

INCAFUST. 2012. Assessorament tècnic de l'activitat pilot IA3.1. Informe del sistema constructiu. Projecte MARIE.

Jelle BP. 2011. Traditional, state-of-the-art and future thermal building insulation materials and solutions - Properties, requirements and possibilities. *Energy and Buildings* 43(10):2549–2563.

Jensen L. 2015. Structure of starches. Eberly College of Science. The Pennsylvania State University. [accessed 2015 Feb 3]. https://online.science.psu.edu/chem005_wd/node/7882]

Jerman M, Cerny R. 2012. Effect of moisture content on heat and moisture transport and storage properties of thermal insulation materials. *Energy and Buildings* 53:39–46.

Jerman M, Keppert M, Výborný J, et al. 2013. Hygric, thermal and durability properties of autoclaved aerated concrete. *Construction and Building Materials* 41:352–359.

Johansson P. 2014. Determination of the critical moisture level for mould growth on building materials. Doctoral Dissertation. Lund University.

Johansson P, Ekstrand-Tobin A, Bok G. 2014. An innovative test method for evaluating the critical moisture level for mould growth on building materials. *Building & Environment* 81:404–409.

Johansson P, Ekstrand-Tobin A, Svensson T, et al. 2012. Laboratory study to determine the critical moisture level for mould growth on building materials. *International Biodeterioration and Biodegradation* 73:23–32.

Jölli D, Giljum S. 2005. Unused biomass extraction in agriculture, forestry and fishery. Sustainable Europe Research Institute (SERI).

Karamanos a., Hadiarakou S, Papadopoulos a. M. 2008. The impact of temperature and moisture on the thermal performance of stone wool. *Energy and Buildings* 40(8):1402–1411.

Karr GS, Sun XS. 2000. Strawboard from vapor phase acetylation of wheat straw. *Industrial Crops and Products* 11(99):31–41.

Kim S, Dale BE. 2004. Global potential bioethanol production from wasted crops and crop residues. *Biomass and Bioenergy* 26(4):361–375.

Korjenic A, Petránek V, Zach J, et al. 2011. Development and performance evaluation of natural thermal-insulation materials composed of renewable resources. *Energy and Buildings* 43(9):2518–2523.

Kretschmer B, Allen B, Hart K. 2012. Mobilising cereal straw in the EU to feed advanced biofuel production. Institute for European Environmental Policy.

Krus M. 1996. Moisture transport and storage coefficients of porous mineral building materials. Theoretical principles and new test methods. Fraunhofer-Institut für Bauphysik IBP.

Krus M, Theuerkorn W, Großkinsky T, et al. 2014. New sustainable and insulating building material made of cattail (typha). In: Proceedings of the 10th Nordic Symposium on Building Physics. Lund, 15-19 Jun. Fraunhofer- Publica.

Lacasta C, Meco R. 2005. Efecto de la incorporación de la paja del cereal sobre la productividad de la cebada y sobre algunos parámetros químicos y bioquímicos del suelo. In: Congreso Internacional sobre Agricultura de Conservación. Córdoba, 9-11 Nov. Digital CSIC.

Latif E, Wijeyesekera D, Newport D. 2010. Potential for research on hemp insulation in the UK construction sector. In: Proceedings of Advances in Computing and Technology, (AC&T) The School of Computing and Technology 5th Annual Conference, University of East London. p. 143–150.

Laurent A, Gourlay E. 2012. Experimental study of parameters influencing mechanical properties of hemp concretes. *Construction and Building Materials* 28(1):50–56.

Lawrence M, Heath A, Walker P. 2009. Determining moisture levels in straw bale construction. *Construction and Building Materials* 23(8):2763–2768.

Leisewitz A, Kruse H, Schramm E. 2001. Substituting environmentally relevant flame retardants: assessment fundamentals. Results and summary overview. Federal Environmental Agency (Unweltbundesamt).

Lesar B, Straže A, Humar M. 2011. Sorption properties of wood impregnated with aqueous solution of boric acid and montan wax emulsion. *Journal of Applied Polymer Science* 120(3):1337–1345.

Lewin M. 2005. Unsolved problems and unanswered questions in flame retardance of polymers. *Polymer Degradation and Stability* 88:13–19.

Liibert L, Treu A, Meier P. 2011. The fixation of new alternative wood protection systems by means of oil treatment. *Materials Science (Medziagotyra)* 17(4):402–406.

Liu DT, Xia KF, Yang RD, et al. 2012. Manufacturing of a biocomposite with both thermal and acoustic properties. *Journal of Composite Materials*(January).

Long H, Li X, Wang H, et al. 2013. Biomass resources and their bioenergy potential estimation: A review. *Renewable and Sustainable Energy Reviews* 26:344–352.

De Long J. 1923 Jan 16. Insulating material. US 1442325 A.

Lubbeke I, Anderson J. 2012. Smart use of residues - Exploring the factors affecting the sustainable extraction rate of agricultural residues for advanced biofuels. WWF - World Wide Fund For Nature.

Lyon RE, Walters RN. 2004. Pyrolysis combustion flow calorimetry. *Journal of Analytical and Applied Pyrolysis* 71:27–46.

Madurwar M, Ralegaonkar R, Mandavgane S. 2013. Application of agro-waste for sustainable construction materials: A review. *Construction and Building Materials* 38:872–878.

Magniont C. 2010. Contribution à la formulation et à la caractérisation d'un écomatériau de construction à base d'agroressources. Doctoral Disertation. Université de Toulouse.

Martinez FX. 2013. Gestión y tratamiento de residuos agrícolas. [accessed 2013 Feb 22]. http://www.infoagro.com/hortalizas/residuos_agricolas2.htm

McDonough W, Braungart M. 2010. Cradle to cradle: Remaking the way we make things. MacMillan.

McHugh DJ, editor. 1987. Production and utilization of products from commercial seaweeds. FAO Fisheries Technical Paper 288:189 p.

McHugh DJ. 2003. A guide to the seaweed industry. FOA Fisheries Technical Paper 441: 105 p.

Mendes N, Winkelmann FC, Lamberts R, et al. 2003. Moisture effects on conduction loads. *Energy and Buildings* 35(7):631–644.

Moussa NA, Toong TY, Garris CA. 1977. Mechanism of smouldering of cellulosic materials. *Symposium (International) on Combustion* 16(1):1447–1456.

Norford L, Glicksman L, Harvey H, et al. 1999. Development of low-cost wheat-straw insulation board. *HVAC&R Research* 5(3):249–263.

Ochs F, Heidemann W, Müller-Steinhagen H. 2008. Effective thermal conductivity of moistened insulation materials as a function of temperature. *International Journal of Heat and Mass Transfer* 51(3):539–552.

Ohlemiller T, Lucca D. 1983. An experimental comparison of forward and reverse smolder propagation in permeable fuel beds. *Combustion and Flame* 54:131–147.

Ohlemiller TJ. 1990. Smoldering combustion propagation through a permeable horizontal fuel layer. *Combustion and Flame* 81:341–353.

Osanyintola OF. 2005. Transient moisture characteristics of spruce plywood. Master Thesis. University of Saskatchewan.

Osanyintola OF, Simonson CJ. 2006. Moisture buffering capacity of hygroscopic building materials: Experimental facilities and energy impact. *Energy and Buildings* 38(10):1270–1282.

Palumbo M, Formosa J, Lacasta AM. 2015. Thermal degradation and fire behaviour of thermal insulation materials based on food crop by-products. *Consturcion and Building Materials* 79:34–39.

Pan M, Zhou D, Ding T. 2010. Water resistance and some mechanical properties of rice straw fiberboards affected by thermal modification. *BioResources* 5:758–769.

Panoutsou C, Eleftheriadis J, Nikolaou A. 2009. Biomass supply in EU27 from 2010 to 2030. *Energy Policy* 37(12):5675–5686.

Papadopoulos a. M. 2005. State of the art in thermal insulation materials and aims for future developments. *Energy and Buildings* 37(1):77–86.

Papadopoulos A. 2007. Environmental performance evaluation of thermal insulation materials and its impact on the building. *Building and environment* 42:2178–2187.

Patel P, Hull TR, Lyon RE, et al. 2011. Investigation of the thermal decomposition and flammability of PEEK and its carbon and glass-fibre composites. *Polymer Degradation and Stability* 96(0):12–22.

Pfundstein M, Gellert R, Spitzner M, et al. 2007. Insulating materials: principles, materials, applications. Schulz C, editor. Institut für Internationale Architektur-Dokumentation GmbH & Co.

Pinto J, Paiva A, Varum H, et al. 2011. Corn's cob as a potential ecological thermal insulation material. *Energy and Buildings* 43(8):1985–1990.

Pinto J, Vieira B, Pereira H, et al. 2012. Corn cob lightweight concrete for non-structural applications. *Construction and Building Materials* 34:346–351.

Pruteanu M. 2010. Investigations regarding the thermal conductivity of straw. *Bulletin of the Polytechnic Institute of Jassy - Constructions. Architecture Section* 3(LVI (LX)):9–16.

Qin M, Belarbi R, Aït-Mokhtar A, et al. 2009. Simulation of coupled heat and moisture transfer in air-conditioned buildings. *Automation in Construction* 18(5):624–631.

Qin M, Walton G, Belarbi R, et al. 2011. Simulation of whole building coupled hygrothermal-airflow transfer in different climates. *Energy Conversion and Management* 52(2):1470–1478.

Rana a K, Basak RK, Mitra BC, et al. 1996. Studies of Acetylation of Jute Using Simplified Procedure and Its Characterization. :1517–1523.

Rockwool. 2013. Spain total insulation market. Market sizes and market shares 2010-2018. Focus year 2013 (Internal document).

Rode C, Peuhkuri R, Hansen KK, et al. 2005. Nordest project on moisture buffer value of materials. In: AIVC Conference Energy Performance Regulation. Brussels, 21-23 Sept.

Rosa GS, Moraes M a., Pinto L a a. 2010. Moisture sorption properties of chitosan. *LWT - Food Science and Technology* 43(3):415–420.

Rowell RM, Rowell J. 1996. Paper and composites from agro-based resources. CRC press.

Sahito AR, Mahar RB, Memon MA, et al. 2012. Assessment of waste agricultural biomass for prevailing management, quantification and energy potential at sanghar pakistan. *Waste and Biomass Valorization* 3(3):275–284.

Scarlat N, Blujdea V, Dallemand JF. 2011. Assessment of the availability of agricultural and forest residues for bioenergy production in Romania. *Biomass and Bioenergy* 35(5):1995–2005.

Scarlat N, Martinov M, Dallemand JF. 2010. Assessment of the availability of agricultural crop residues in the European Union: Potential and limitations for bioenergy use. *Waste Management* 30(10):1889–1897.

Sedlbauer K. 2001. Prediction of mould fungus formation on the surface of/and inside building components. Fraunhofer Institute for Building Physics.

Sedlbauer K, Hofbauer W, Krueger N, et al. 2011. Material specific isopleth-systems as valuable tools for the assessment of the durability of building materials against mould infestation - The 'isopleth-traffic light'. In: XIIth International Conference on Durability of Building Materials and Components. Oporto, 12-15 Apr. Fraunhofer- Publica.

Shafizadeh F, Bradbury AGW. 1979. Smoldering Combustion of Cellulosic Materials. *Journal of Building Physics* 2(3):141–152.

Shea A, Lawrence M, Walker P. 2012. Hygrothermal performance of an experimental hemp-lime building. *Construction and Building Materials* 36:270–275.

Simonson CJ, Salaonvaara M, Ojanen T. 2004. Heat and Mass Transfer between Indoor Air and a Permeable and Hygroscopic Building Envelope: Part II - Verification and Numerical Studies. *Journal of Building Physics* 28(2):161–185.

Singer S, Denruyter J, editors. 2013. The energy report. 100% Renewable energy by 2050. WWF - World Wide Fund For Nature.

Sobral HS, editor. 2004. Vegetable plants and their fibres as building materials: Proceedings of the Second International RILEM Symposium. Routledge.

Straube JF. 2006. Moisture and materials. *Building Science Digest* 138:1–7.

Suardana NPG, Ku MS, Lim JK. 2011. Effects of diammonium phosphate on the flammability and mechanical properties of bio-composites. *Materials & Design* 32(4):1990–1999.

Summers MD, Blunk SL, Jenkins BM. 2003. How straw decomposes: Implications for straw bale construction. EBNet Straw Bale Test Program.

Sun R. 2010. Cereal straw as a resource for sustainable biomaterials and biofuels: chemistry, extractives, lignins, hemicelluloses and cellulose. Elsevier.

Superficies y producciones anuales de cultivos. Estadísticas agrarias: Agricultura. Ministerio de Agricultura Alimentación y Medio Ambiente (MARM). [accessed 2014 Jul 8]. http://www.magrama.gob.es/es/estadistica/temas/estadisticas-agrarias/agricultura/superficies-producciones-anuales-cultivos/

Sweeney OR, Emley WE. 1930. Manufacture of insulating board from cornstalks. US Government Printing Office.

Thevenon MF, Tondi G, Pizzi A. 2010. Friendly wood preservative system based on polymerized tannin resin-boric acid for outdoor applications. *Maderas. Ciencia y tecnología* 12(3):253–257.

Thomson A, Walker P. 2014. Durability characteristics of straw bales in building envelopes. *Construction and Building Materials* 68:135–141.

Tondi G, Wieland S, Wimmer T, et al. 2012. Tannin-boron preservatives for wood buildings: Mechanical and fire properties. *European Journal of Wood and Wood Products* 70(5):689–696.

Tran Le AD, Maalouf C, Mai TH, et al. 2010. Transient hygrothermal behaviour of a hemp concrete building envelope. *Energy and Buildings* 42(10):1797–1806.

Vejeliene J, Gailius A, Vejelis S, et al. 2011a. Evaluation of Structure Influence on Thermal Conductivity of Thermal Insulating Materials from Renewable Resources. *Materials Science* 17(2).

Vejeliene J, Gailius A, Vejelis S, et al. 2011b. Development of thermal insulation from local agricultural. In: Environmental Engineering. he 8th International Conference. Vilnius, 19-20 May. p. 437–440.

Vissac A, Couvreur L, Moevus M, et al. 2013. Description des molécules des stabilisants organiques et description de la nature des interactions physico-chimiques entre ces molécules naturelles et les argiles. PaTerre+ Project. Laboratoire CRAterre-ENSAG.

Wall K, Walker P, Gross C, et al. 2012. Development and testing of a prototype straw bale house. *Construction Materials* 165(CM6):377–384.

Wang D, Sun XS. 2002. Low density particleboard from wheat straw and corn pith. *Industrial Crops and Products* 15(1):43–50.

Wang X, Yang L, Steinberger Y, et al. 2013. Field crop residue estimate and availability for biofuel production in China. *Renewable and Sustainable Energy Reviews* 27(2):864–875.

Yang CQ, He Q. 2011. Applications of micro-scale combustion calorimetry to the studies of cotton and nylon fabrics treated with organophosphorus flame retardants. *Journal of Analytical and Applied Pyrolysis* 91(1):125–133.

Yao F, Wu Q, Lei Y, et al. 2008. Thermal decomposition kinetics of natural fibers: Activation energy with dynamic thermogravimetric analysis. *Polymer Degradation and Stability* 93(1):90–98.

Yates T. 2006. The use of non‐food crops in the UK construction industry. *Journal of the Science of Food and Agriculture* 86(12):1790–1796.

Zhao Q, Zhang B, Quan H, et al. 2009. Flame retardancy of rice husk-filled high-density polyethylene ecocomposites. *Composites Science and Technology* 69(15-16):2675–2681.